Aus der Professur für Bodenphysik

der Agrar- und Umweltwissenschaftlichen Fakultät

Soil physical properties of peatlands:

Implications for rewetting

Kumulative Dissertation

zur Erlangung des akademischen Grades

Doktor der Agrarwissenschaften (doctor agriculturae)

an der Agrar- und Umweltwissenschaftlichen Fakultät

der Universität Rostock

Vorgelegt von

Miaorun Wang, geb. am 06.12.1992 in Luoyang, Henan, V.R. China

M.Sc. Pflanzenproduktion und Umwelt

Matrikel-Nummer: 217100069

Rostock, Juni 2023

Erster Gutachter:

        Prof. Dr. agr. habil. Bernd Lennartz

        Professur für Bodenphysik

        Agrar- und Umweltwissenschaftliche Fakultät

        Universität Rostock

Zweiter Gutachter:

        Prof. Dipl.-Geogr. Dr. sc. agr. Stephan Glatzel

        Professur für Geoökologie

        Institut für Geographie und Regionalforschung

        Universität Wien

Dritter Gutachter:

        Dr. -Ing. Bärbel Tiemeyer

        Institut für Agrarklimaschutz

        Johann Heinrich von Thünen-Institut

Datum der Einreichung: 26. Juni 2023

Datum der Verteidigung: 20. Dezember 2023

"知者乐水，仁者乐山"

"The wise take pleasure in water; the benevolent find joy in mountains."

——《论语 • 雍也》

The Analects of Confucius · Yong Ye

CONTENT

List of Figures

List of Supplemental Figures

List of Tables

List of Abbreviations

A	Range (m)
A_{cs}	Cross-section area of a soil sample (cm²)
AIC	Akaike information criterion
AICc	Corrected Akaike information criterion
$A_i(x_i)$	A measured soil property value (*e.g.*, bulk density) at spatial location i
$A_i(x_i+h)$	A measured soil property value at spatial location $i+h$
BD	Bulk density (g cm^{-3})
BTCs	Breakthrough curves
C	Partial sill (*e.g.*, m²)
$C0$	Nugget (*e.g.*, m²)
$C0+C$	Sill (*e.g.*, m²)
C_e	Effluent concentration (mg L^{-1})
C_i	Influent concentration (mg L^{-1})
CDE	Convection-dispersion equation
CDOM	Colored dissolved organic matter
CEC	Cation exchange capacity (mmol kg^{-1})
CH_4	Methane (-)
C_{im}	Effluent concentration in the immobile region (mg L^{-1})
C_m	Effluent concentration in the mobile region (mg L^{-1})
C:N	Ratio of the mass of carbon to the mass of nitrogen (-)
CO_2	Carbon dioxide (-)
CV	Coefficient of variation (%)
d_i	Distance between the unsampled point and the sampled point (m)
D	Effective dispersion coefficient (L² T^{-1})
D_{im}	Effective dispersion coefficient of the immobile region (L² T^{-1})
D_m	Effective dispersion coefficient of the mobile region (L² T^{-1})
DF	Degrees of freedom (-)
DOC	Dissolved organic carbon (mg L^{-1})
dyn	A unit of force, "dyne"
EC	Electrical conductivity (mS cm^{-1})
e.g.	*exempli gratia*, "for example"
etc.	*et cetera,* "and so on"
FTR	Flow-through reactor
g	Acceleration of gravity (980 cm s^{-2})

h	Lag distance (m)
H	Water pressure head (–cm H_2O)
H_2O	Water (-)
H_2O_2	Hydrogen peroxide (-)
H_2SO_4	Sulfuric acid (-)
i.e.	*id est*, "in other words"
j	Number of the closest sampled points within the neighborhood searching
k	Number of estimated parameters in AICc equation
K	Hydraulic conductivity (cm d^{-1} or m s^{-1})
KBr	Potassium bromide (-)
K_s	Saturated hydraulic conductivity (cm d^{-1} or m s^{-1})
K_{sv}	Saturated hydraulic conductivity of vertical sample (cm h^{-1})
K_{sh}	Saturated hydraulic conductivity of horizontal sample (cm h^{-1})
L	Length of the flow path (also the length of soil samples, cm) or only refers to the unit of length
LMEMs	Linear mixed-effect models
LOI	Loss on ignition (%)
MIM	Mobile-immobile model
MP	Macroporosity (vol%)
MSE	Mean squared error
n	Empirical parameter (as well as m = 1 - 1/n) of van Genuchten model
N	Number of samples or observed data
NaCl	Sodium chloride (-)
N(h)	Number of available observation pairs (-)
NH_4	Ammonium (-)
Pe	Péclet number (-)
pH	Potential of hydrogen (-)
PTFs	Pedotransfer functions
PV	Pore volume (-)
q	Water flux (cm h^{-1})
Q	Rate of water flow (cm^3 h^{-1})
r	Pore radius (cm)
R	Retardation factor (-)
R^2	Fitting criterion (-)
RSE	Residual standard error
RSS	Residual sum of squares
RTK	Real time kinematic (GPS)
SD	Standard deviation

SE	Standard error
SOM	Soil organic matter (wt%)
SSD	Sum of the squared deviations
SSE	Sum of squared error between observed and predicted values in AICc equation
SWRCs	Soil water retention curves
t	Time or period (h)
T	Dimensionless time (refers to the unit of time)
TiO_2	Titanium oxide (-)
v	Fluid average velocity ($L\ T^{-1}$)
V	Outflow volume (mL)
V_o	Water-filled pore volume under fully water saturated conditions (mL)
VG	van Genuchten (model)
v_m	Pore water velocity in the mobile zone ($L\ T^{-1}$)
V_{water}	Volume of water (mL)
w	Gravimetric water content (wt%)
wt%	Weight percentage (-)
X	Space coordinate (-)
x_i	Spatial location or coordinate of measured soil property (m or °)
$Z^*(x_o)$	Predicted value at the unsampled point x_o
$Z(x_i)$	Observed value at the sampled point x_i
α	Empirical parameter in van Genuchten model, represents the inverse of the air entry pressure head (cm^{-1})
β	Fraction of the mobile water content (-)
$\gamma(h)$	Semivariance, which is the variance (γ) between two spatial locations (m^2)
ΔH	Hydraulic head (cm)
θ	Volumetric water content ($cm^3\ cm^{-3}$)
θ_{im}	Immobile water content ($cm^3\ cm^{-3}$)
θ_m	Mobile water content ($cm^3\ cm^{-3}$)
θ_r	Residual volumetric water contents ($cm^3\ cm^{-3}$)
θ_s	Saturated volumetric water contents ($cm^3\ cm^{-3}$)
ϑ	Soil liquid contact angle (°)
λ	Dispersivity (cm)
λ_i	Weighting coefficient from x_i to x_o in ordinary kriging method
ρ	Density of water (1.0 $g\ cm^{-3}$),
ρ_b	Bulk density ($g\ cm^{-3}$)
σ	Surface tension of water ($dyn\ cm^{-1}$)
ψ	Suction pressure heads ($cm\ H_2O$ or in pF unit)
ω	Exchange coefficient between mobile and immobile regions (-)

XVI

Summary

Peatlands are highly valuable terrestrial wetlands characterized by their significant organic matter content. Despite covering only 3% of the Earth's land surface, peatlands astonishingly store approximately one-third of the global soil carbon. These ecosystems provide essential benefits such as carbon sequestration and water regulation and serve as habitats for unique flora and fauna. However, human activities, such as drainage, extraction, and land use, have led to peatland degradation and carbon mineralization, significantly enhancing climate change. Consequently, restoring peatland ecological functions has become a top priority at both governmental and scientific levels. Peat soils are anisotropic and heterogeneous porous media. Understanding the physical and hydraulic characteristics of peat and their anisotropic and heterogeneous nature at various spatial scales (cm to km) is crucial, as it not only helps reveal the impacts of peatland degradation and rewetting but also guides site-specific management effectively. The thesis consists of three experimental investigations, involving different peat soils sampled from two inland drained fens, an inland restored (previously drained) fen, an inland pristine bog, and a recently rewetted coastal fen in the Federal State of Mecklenburg-Western Pomerania in Germany. The specific objectives are as follows: 1) to assess how peatland degradation affects spatial heterogeneity of hydro-physical properties in different inland peatlands, 2) to investigate the influence of soil anisotropy on water movement and solute transport in a drained and a restored peatland (with the same degradation stage), and 3) to explore the potential impacts of microtopography and salinity on a rewetted coastal peatland and its adjacent environment.

Direct measurements of soil properties of peat (*e.g.*, saturated hydraulic conductivity, K_s; soil water retention curves) are time-consuming and costly. In this thesis, new pedotransfer functions (PTFs) have been developed to estimate the soil hydro-physical properties of intact and degraded peat soils from easily available soil parameters. Macroporosity was highly correlated with K_s and van Genuchten (VG) model parameters derived from the soil water retention curves, indicating that the inclusion of macroporosity in PTFs significantly improves the predictions of VG model parameter values, especially for degraded peat soils. Additionally, site heterogeneity and small-scale spatial variability of soil properties were analyzed by geostatistical models. The hydro-physical properties of peat were weakly to strongly auto-correlated according to the nugget/sill ratio. A strong spatial dependence of the soil organic matter (SOM) content was found only in highly degraded peat. The results suggested that the spatial distribution pattern of soil properties depended on the considered properties and land management; from this we conclude that accurate spatial information should be considered in peatland restoration practices.

SUMMARY

The "hotspot" of biogeochemistry cycles is significantly influenced by the anisotropic and heterogeneous properties of peat soils. In both inland drained and restored fens, the difference in K_s of peat soil samples taken in two directions confirmed the influence of anisotropy on water movement in degraded peat soils (vertical K_{sv} > horizontal K_{sh}). The mobile-immobile model of solute transport successfully described the experimental breakthrough curve. Pronounced preferential flow occurred in the vertical direction with a higher pore water velocity of the mobile zone (v_m). The 5% arrival time of bromide mass, as a proxy for the strength of preferential flow, was related to K_s and solute transport model parameters and was also orientation-dependent and associated with land management, which provided the first evidence of the anisotropic nature of solute transport in peat soils. Additionally, only one vertical sample collected from the drained site showed very high phosphate release (~50 mg L^{-1}), which might be related to phosphorus accumulation in preferential flow pathways. The results implied that the anisotropic structure of peat could facilitate the phosphate transport from drained peatlands under agricultural use to the surrounding environment along the direction of preferential flow. Nevertheless, phosphate release was observed from drained peat only, suggesting that the impact of land use on phosphate release was more significant than soil anisotropy.

At a landscape scale, it was found that the heterogeneous properties of peat soils were largely impacted by microtopography. In a coastal peatland located on the Baltic Sea coast, SOM content and carbon:nitrogen (C:N) ratios were negatively correlated with sampling elevation. These three parameters had varying degrees of spatial dependence, among which SOM and C:N of topsoil were strongly spatially dependent. According to the soil samples taken at different elevations, nutrient leaching experiments using alternating freshwater and brackish water confirmed that low elevation samples released more dissolved organic carbon (DOC) and ammonium (NH$_4^+$) than high elevation samples. This indicated that the low-lying areas of the study site were hotspots for compound cycling and release under a rewetting scenario. Moreover, the leaching of DOC and NH$_4^+$ responded differently to brackish water and freshwater. Increased DOC concentrations were observed when freshwater was reflushed, while transiently increased NH$_4^+$ concentrations occurred when brackish water intruded. The results indicated that heavy precipitation might lead to the export of DOC to the Baltic Sea, while future sea level rise might result in the export of NH$_4^+$ to adjacent water bodies, particularly from low-lying areas. These processes could have significant impacts on marine ecosystems.

This cumulative dissertation underlines the intricate interplay between soil hydro-physical and chemical properties and the surrounding environment. A comprehensive understanding of their dynamics is required to manage peatlands effectively. Ultimately, these insights contribute to the foundational knowledge base for conservation, sustainable use, and restoration of peatland ecosystems.

Zusammenfassung

Moore sind wertvolle terrestrische Feuchtgebiete, die sich durch ihren hohen Gehalt an organischer Substanz auszeichnen. Obwohl sie nur 3% der Erdoberfläche bedecken, speichern Moore erstaunlicherweise ein Drittel des globalen Bodenkohlenstoffs. Diese Ökosysteme erbringen wesentliche Leistungen wie die Kohlenstoffsequestrierung und die Wasserregulierung und dienen als Lebensraum für eine einzigartige Flora und Fauna. Allerdings haben menschliche Aktivitäten wie Entwässerung, Abtorfung und Landnutzung zur Degradation von Mooren geführt, die mit der Kohlenstoffmineralierung einhergeht und den Klimawandel verstärkt. Im Ergebnis hat die Wiederherstellung der ökologischen Funktionen der Moore oberste Priorität sowohl auf Regierungs- als auch auf wissenschaftlicher Ebene erlangt. Torfböden sind anisotrope und heterogene poröse Medien. Das Verständnis der physikalischen und hydraulischen Eigenschaften von Torfböden und ihrer anisotropen und heterogenen Eigenschaften auf verschiedenen räumlichen Skala (cm bis km) ist entscheidend, da es nicht nur hilft, die Auswirkungen der Degradierung und Wiedervernässung von Mooren aufzudecken, sondern auch eine effektive standortspezifische Bewirtschaftung ermöglicht. Die Dissertation besteht aus drei experimentellen Untersuchungen, die verschiedene Torfböden umfassen, die aus zwei entwässerten Niedermooren, einem restaurierten (zuvor entwässerten) Niedermoor, einem unberührten Hochmoor und einem kürzlich wiedervernässten Küstenmoor im Bundesland Mecklenburg-Vorpommern in Deutschland entnommen wurden. Die spezifischen Ziele sind wie folgt: 1) den Einfluss der Bodenanisotropie auf den Stofftransport in einem entwässerten und einem restaurierten Niedermoor (mit dem gleichen Degradationsgrad) zu untersuchen, 2) die Beeinflussung der Degradierung des Moores auf die räumliche Heterogenität der hydro-physikalischen Eigenschaften in verschiedenen Niedermooren zu bewerten, und 3) die potenziellen Auswirkungen von Mikrotopographie und Salinität auf ein wiedervernässtes Küstenmoor und seine angrenzende Umgebung zu erforschen.

Direkte Messungen von Bodeneigenschaften des Torfs (z.B. gesättigte hydraulische Leitfähigkeit, K_s; Bodenwasserrtentionskurven) sind zeitaufwändig und kostenintensiv. In dieser Arbeit wurden neue Pedotransfer-Funktionen (PTFs) entwickelt, um die bodenphysikalische Eigenschaften intakter und degradierter Torfböden anhand leicht verfügbarer Bodenparameter abzuschätzen. Die Makroporosität korrelierte stark mit der K_s und den aus den Bodenwasserrtentionskurven abgeleiteten Parametern des van Genuchten Modellparametern, was darauf hindeutet, dass die Einbeziehung der Makroporosität in PTFs die Vorhersagen von (Modell-)Parameterwerten signifikant verbessert, insbesondere für degradierte Torfböden. Zusätzlich wurde die Standortheterogenität und die räumliche Variabilität der Bodeneigenschaften mithilfe geostatistischer Modelle analysiert. Die hydro-physikalischen Eigenschaften der Torfböden

waren schwach bis stark autokorreliert gemäß des Nugget/Sill-Verhältnisses. Eine starke räumliche Abhängigkeit des Gehalts an organischer Bodensubstanz wurde nur in stark degradiertem Torf festgestellt. Dies deutet darauf hin, dass das räumliche Verteilungsmuster der Bodeneigenschaften von den betrachteten Eigenschaften und der Landbewirtschaftung abhängt, was wiederum für Moorrenaturierungsmaßnahmen von Bedeutung sein kann.

Der „Hotspot" des biogeochemischen Kreislaufs wird maßgeblich von den anisotropen und heterogenen Eigenschaften der Torfböden beeinflusst. In sowohl drainierten als auch renaturierten Mooren bestätigte der Unterschied in der K_s von Torfbodenproben, die aus zwei Richtungen entnommen wurden (vertikal K_{sv} > horizontal K_{sh}), den Einfluss der Anisotropie auf die Wasserbewegung in degradierten Torfböden. Das mobile-immobile Modell des Stofftransports beschrieb erfolgreich die experimentellen Durchbruchskurven. In der vertikalen Richtung trat ein deutlicher präferenzieller Fluss mit einer höheren Porenwassergeschwindigkeit der mobilen Zone (v_m) auf. Die Ankunftszeit von 5 % der Bromidmasse, als Proxy für die Stärke des präferenziellen Stofftransports, war mit K_s und den Modellparametern für den Stofftransport verknüpft und war auch richtungsabhängig und mit der Landbewirtschaftung assoziiert, was den ersten Nachweis für die anisotrope Natur des Stofftransports in Torfböden lieferte. Nur eine, in vertikaler Richtung entnommene Probe, zeigte eine sehr hohe Phosphatfreisetzung (~50 mg L^{-1}), die möglicherweise mit der Phosphorakkumulation in präferenziellen Fließwegen zusammenhing. Dies deutete darauf hin, dass die anisotrope Struktur des Torfes den Transport von Phosphat aus landwirtschaftlich genutzten Torfböden in die Umgebung entlang der Richtung mit stärkerem präferenziellen Fluss erleichtern könnte. Die Phosphatfreisetzung wurde nur bei drainiertem Torf beobachtet, also mit der Landnutzung des Moors einhergeht.

Auf landschaftlicher Skala wurde festgestellt, dass die heterogenen Eigenschaften von Torfböden in hohem Maße von der Mikrotopographie beeinflusst werden. In einem Küstenmoor an der Ostseeküste waren der Gehalt an organischer Bodensubstanz (SOM) und das Kohlenstoff-Stickstoff-Verhältnis (C:N-Verhältnis) negativ mit der geodätischen Höhe der Probenentnahme korreliert. Diese drei Parameter hatten unterschiedliche Grade der räumlichen Abhängigkeit, wobei SOM und C:N des Oberbodens stark autokorreliert waren. Unterschungen zur Nährstoffauswaschung mit abwechselndem Süß- und Brackwasser belegten, dass Proben aus niedrigeren Höhen mehr gelösten organischen Kohlenstoff (DOC) und Ammonium (NH_4^+) freisetzten als Proben aus höheren Lagen. Dies deutet darauf hin, dass die tiefer gelegenen Gebiete der Untersuchungsfläche Hotspots für die Freisetzung von gelösten Verbindungen waren, welches bei Wiedervernässungsmaßnahmen berücksichtigt werden sollte. Außerdem reagierte die Freisetzung von DOC und NH_4^+ unterschiedlich auf Süß- und Brackwasser. Bei erneuter Spülung mit Süßwasser wurden erhöhte DOC-Konzentrationen beobachtet, während vorübergehend erhöhte NH_4^+-Konzentrationen auftraten, wenn Brackwasser in die Bodenroben eindrang. Dies

lässt vermuten, dass starke Niederschläge zu einem Export von DOC in die Ostsee führen könnten, während der künftige Anstieg des Meeresspiegels einem Export von NH_4^+ in Küstengewässer als Folge haben könnte. Die untersuchten Prozesse können erhebliche Auswirkungen auf angrenzende marine Ökosysteme haben.

Diese kumulative Dissertation betont das komplexe Zusammenspiel zwischen hydro-physikalischen und chemischen Bodeneigenschaften und der umgebenden Umwelt, und ein umfassendes Verständnis ihrer Dynamik ist erforderlich, um Moore effektiv zu bewirtschaften. Letztendlich tragen diese Erkenntnisse zur grundlegenden, aber breiten Wissensbasis für die Konservierung, nachhaltige Nutzung und Wiederherstellung von Moorökosystemen bei.

1

General Introduction

Peatland, a distinctive type of wetland, is one of the most valuable natural ecosystems in the world, characterized by the accumulation of organic matter that forms peat layers (Charman, 2009). Peatlands cover only 3% of the global land area, and approximately 80% of them are mainly distributed in the Northern Hemisphere's temperate regions and tropical parts of South Asia (Joosten and Clarke, 2002). A wide range of ecological, economic, and social benefits can be provided by peatlands, including water filtration and regulation, carbon sequestration and storage, habitat for various plant and animal species, growing media, and soil improver (Clarke and Rieley, 2019; Harenda et al., 2018). Nevertheless, long-term environmental changes (*e.g.*, drainage for agriculture, forest clearance, and peat extraction) and short-term ecological disturbances (*e.g.*, flooding and fire) have historically posed threats to peatlands, leading to their degradation and carbon loss. Therefore, the ecological services of peatlands, especially their role in mitigating climate change, have attracted increasing attention in this century. Internationally, "2013 Supplement to the 2006 IPCC Guidelines" has also offered fresh advice and focused on estimating and reporting greenhouse gas emissions and the emission factors from soils in various wetland types (IPCC, 2014).

The north-easternmost Federal State in Germany, Mecklenburg-Western Pomerania (MV), borders the Baltic Sea and has approximately 287,900 hectares of peatlands (Greifswald Moor Centrum, 2019), including coastal peatlands, inland peatland/terrestrialisation mire, transitional peatlands, and raised bog, *etc.*, which are classified by geographic locations and hydrogenetic peatland/mire types (HGMTs; Succow and Joosten, 2001; **Figure 1.1**). Over the period 1960 to 1990, however, most of the peatlands in MV were subjected to drainage for agricultural use, leading to the degradation and mineralization of peat. Greifswald Moor Centrum has reported that peatlands in MV, which cover about 12.5% of the State's land, could emit 6-million-ton carbon dioxide (CO_2) equivalents annually (Hirschelmann et al., 2020). These reports have triggered a growing number of conceptual, operational, and scientific research initiatives in recent years, drawing increased attention to peatlands. The restoration of peatlands, which has been advocated by peatland scientists led by Hans Joosten, has also received attention from various sectors of society (Joosten, 2009). However, developing effective management strategies for

peatland ecosystems, both at a global and local scale, is a challenging task due to the diverse degrees of site heterogeneity and spatial variability exhibited by environmental variables.

Legend of peatland distribution in MV

Küstenüberflutungsmoore allgemein
Coastal flood mires/peatlands (general)

Küstenüberflutungsmoore, flachgründig
Shallow coastal flood mires/peatlands

Küstenüberflutungsmoore, tiefgründig
Deep coastal flood mires/peatlands

Durchströmungsmoore allgemein
percolation mire/peatlands (general)

Durchströmungsmoore, flachgründig
Shallow percolation mire/peatlands

Durchströmungsmoore, tiefgründig
Deep percolation mire/peatlands

Riegen auf dem Neudarß
A specific peatland system (old beach ridges) located in the Neudarß

Moore ohne nährer Information allgemein
Peatlands without further information (general)

Moore ohne nährer Information, flachgründig
Shallow peatlands without recent information

Moore ohne nährer Information, tiefgründig
Deep peatlands without recent information

Hochmoore
Raised bogs

Übergangsmoore
Transitional peatlands (bogs) between fens and raised bogs

Festland
Mainland

Ostsee
Baltic Sea

© 2006 LUNG

Figure 1.1 The distribution of different peatland types in the Federal State of Mecklenburg-Western Pomerania (MV), Germany. In the legend, each type is labeled in German (above) and English (below). (data from LUNG M-V: https://www.umweltkarten.mv-regierung.de).

This thesis is the terrestrial study part (H2) of the interdisciplinary research project "BalticTRANSCOAST", which is oriented towards peatland hydrology, biogeochemistry, and biology to focus on the water and matter fluxes on the terrestrial-marine interface along the German Baltic Sea coast. This thesis aims to investigate the soil physical and hydraulic properties of inland and coastal peatlands in MV, with a focus on the anisotropic and heterogenous nature of soil characteristics in peatlands. The findings of this thesis can contribute to developing site-specific solutions for peatland management and conservation.

1.1 Wetland and Peatland

1.1.1 Definition and classification of wetlands and peatlands

Wetlands, along with oceans and forests, are one of the Earth's three primary ecosystems, each of which is a valuable natural resource and an essential ecological foundation (Whittaker and Likens, 1973). As one of the largest carbon reservoirs in the world, wetlands occupy only 5 ~ 8% of the Earth's surface, but they store 20 ~ 30% of the carbon in terrestrial ecosystems (Lal et al., 2018; Mitsch and Gosselink, 2007). A common feature of all wetlands is that the water table (the groundwater level) is relatively close to the ground's surface, or the surface is covered by shallow water for at least part of the year. The fundamental characteristics of wetlands are

determined by a combination of factors such as soil type, the salinity of water bodies, and the flora and fauna that inhabit the area.

In the past, agreeing on a single and commonly used wetland definition has proved challenging due to the heterogeneity of wetland ecosystems at different scales. Over the years, scientists have used various approaches to inventory and classify wetlands and have reached some acceptable agreements on the definition and classification of wetlands at the national or international level. For instance, Cowardin et al. (1979) established one of the most universally used wetland categorization systems, detailed in "Classification of Wetlands and Deepwater Habitats of the United States". The five principal wetland types in Cowardin's system are marine, tidal, lacustrine, palustrine, and riverine wetlands, which are classified based on their location in the terrain, hydrological regime, and vegetation. Internationally, the most broadly accepted definition and classification of the wetland is the one provided by the "Convention's List of Wetlands of International Importance" that wetlands can be categorized as marine/coastal wetlands, such as mangroves, seagrass formations, salt marshes, *etc.*; inland wetlands, such as lakes/rivers, marshes, peatlands, *etc.*; and artificial wetlands, such as reservoirs, wastewater treatment ponds, *etc.* (Ramsar, 1971). The global review article by Scott and Jones (1995) highly commended Ramsar's definition and classification of wetlands. It advocates that more specific regional and national wetland classifications should be compatible with the Ramsar hierarchy. **Figure 1.2** outlines the main wetland types, including categories and definitions (Adam, 2016; Alongi, 2016; Craft, 2022; Joosten et al., 2017; Lindsay, 2018; Parish et al., 2008; Ramsar, 1971; Short et al., 2007; Vitt, 2013).

Peatland systems (mires and peatlands) are distinguished from other wetland types by their net organic matter accumulation (peat) through partially decomposed plant residues in humid anaerobic environments and microbial action over prolonged periods (IPS, n.d.). However, different countries and organizations may have different criteria for defining "peatland", such as the minimum thickness, the organic matter content, and the origin of peat (Craft, 2022). For instance, peat soils are categorized in organic soils (Histosols) and are defined by International Peat Society (IPS) as "sedentarily accumulated material consisting of at least 30% (dry mass) of dead organic material" with a minimum thickness of 30 cm (IPS, n.d.; Joosten et al., 2017; Joosten and Clarke, 2002). However, Histosols are defined by the United States Department of Agriculture as having a minimum organic carbon content of 12% and thickness of 40 cm, while (undrained) organic soils are, in turn, classified as "hydric soils" (*i.e.*, wetland soils) (USDA, 1999; USDA and NRCS, 2003).
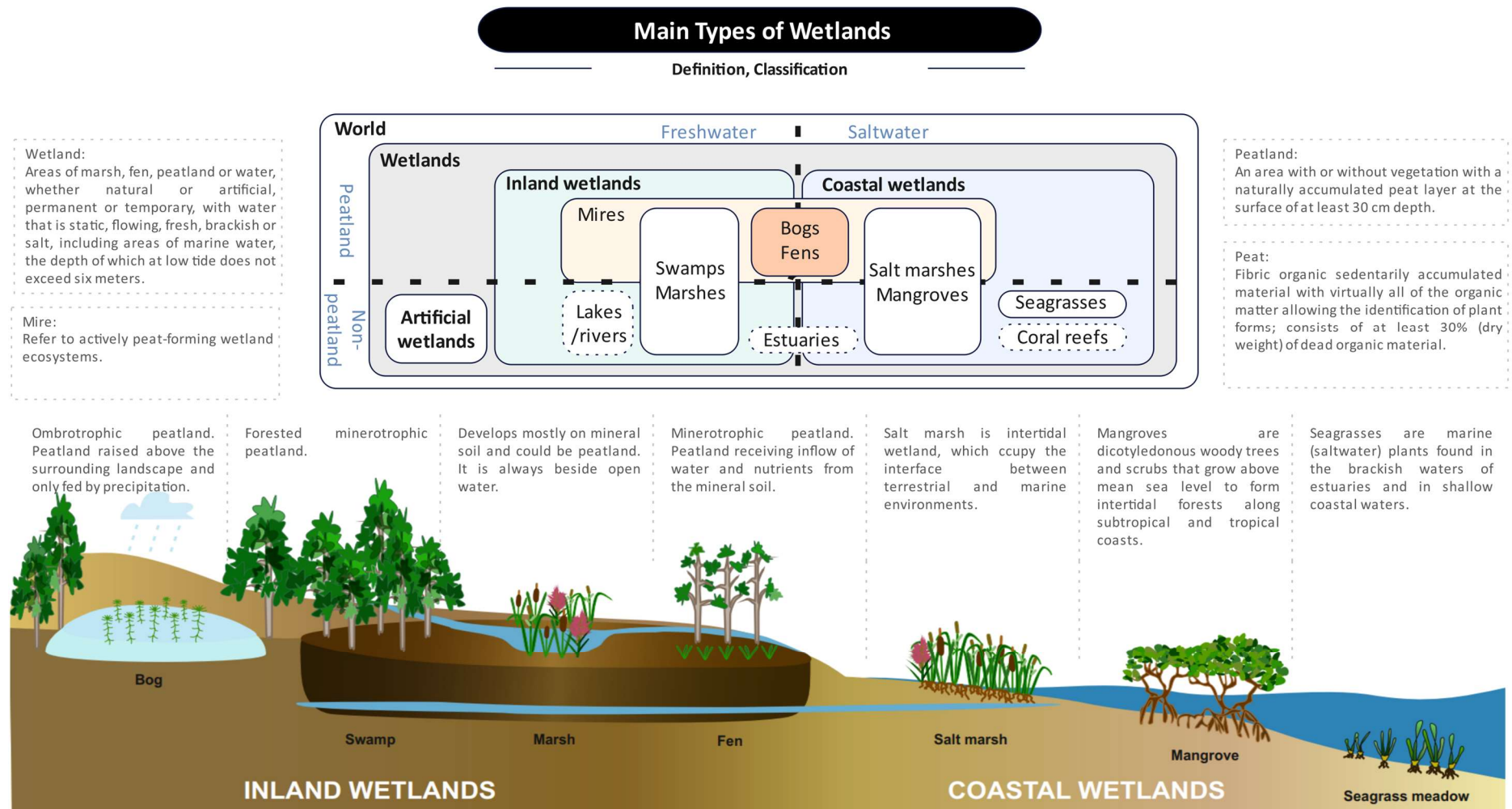
Figure 1.2 The main types of wetlands. (adapted from Joosten et al., 2017; references: Adam, 2016; Alongi, 2016; Craft, 2022; Lindsay, 2018; Parish et al., 2008; Ramsar, 1971; Short et al., 2007; Vitt, 2013).

Peatland terminology is complex and variable, with different terms starting with "T", "P", "M", and "S" used across languages and disciplines, such as "Torf", "peat", "peatland" "mire", "Moor", and "swamp" (**Figure 1.3**). "Peatlands" and "mires" are sometimes used synonymously, but they also have some distinctions (**Figure 1.2**). The former is a more general concept referring to the areas where peat has accumulated with greater than a certain thickness or organic matter content (*e.g.*, Joosten et al., 2017), while the latter is a more specific term that refers to wetland ecosystems, typically dominated by living peat-forming plants (*e.g.*, *Sphagnum* mosses; Parish et al., 2008).

Peatlands can be classified according to various criteria. Lindsay (2018) provided a detailed overview based on existing literature and summarized the main classification systems. These include: 1) classification of water source, which distinguishes minerotrophic peatland (fens) from ombrotrophic mires (bogs), 2) ecosystem classification approaches, which rely on vegetation classification or hydromorphological classification (including hydrogenetic typology), and 3) hierarchical classification, which encompasses six spatial scales: vegetation stand, nanotope, microtope, mesotope, macrotope, and supertope. The most common peatland classification is based on the water source that influences the water and nutrient chemistry of the peat system (Craft, 2022; Joosten and Clarke, 2002; Vitt, 2013). In Germany, this approach to differentiate peatland types can date back to Dau (1823) (Du Rietz, 1954). Subsequently, Niedermoor (fen), Hochmoor (raised bog), and a mixed type between the two, *i.e.*, Übergangsmoor, were identified by Weber (1907) as the three main peatland types in northern Germany. In recent years, Joosten et al. (2017) further detailed the various English terms (*e.g.*, mire, marsh, swamp, fen, and bog) and the corresponding characteristics of European mires and peatlands. Among these terms, bogs refer to the peatlands that depend solely on precipitation for water supply and have low nutrient availability and acidity, while fens are influenced by surface water and groundwater, which are richer in nutrients and have higher pH, productivity, and biodiversity compared to bogs (Craft, 2022; Joosten et al., 2017; Vitt, 2013).

Peatland science has a long tradition of research that spans across various disciplines and regions (**Figure 1.3**). The earliest monographs on peat appeared in Europe as early as the middle of the 17th century (Phragmites peat, n.d.; Schoock, 1658). Over the next two centuries, peat formation and origin were gradually studied by scientists (Degner, 1729; Phragmites peat, n.d.; Rennie, 1810). During this period, peat soil was widely used as fuel for heating and biomass energy. Since then, numerous scientists, mainly in Europe and North America, began to study peatlands in more detail as part of their focus on earth sciences (*e.g.*, Dau, 1823). Meanwhile, intensive peatland drainage started for agriculture (Succow and Joosten, 2001). From the 20th
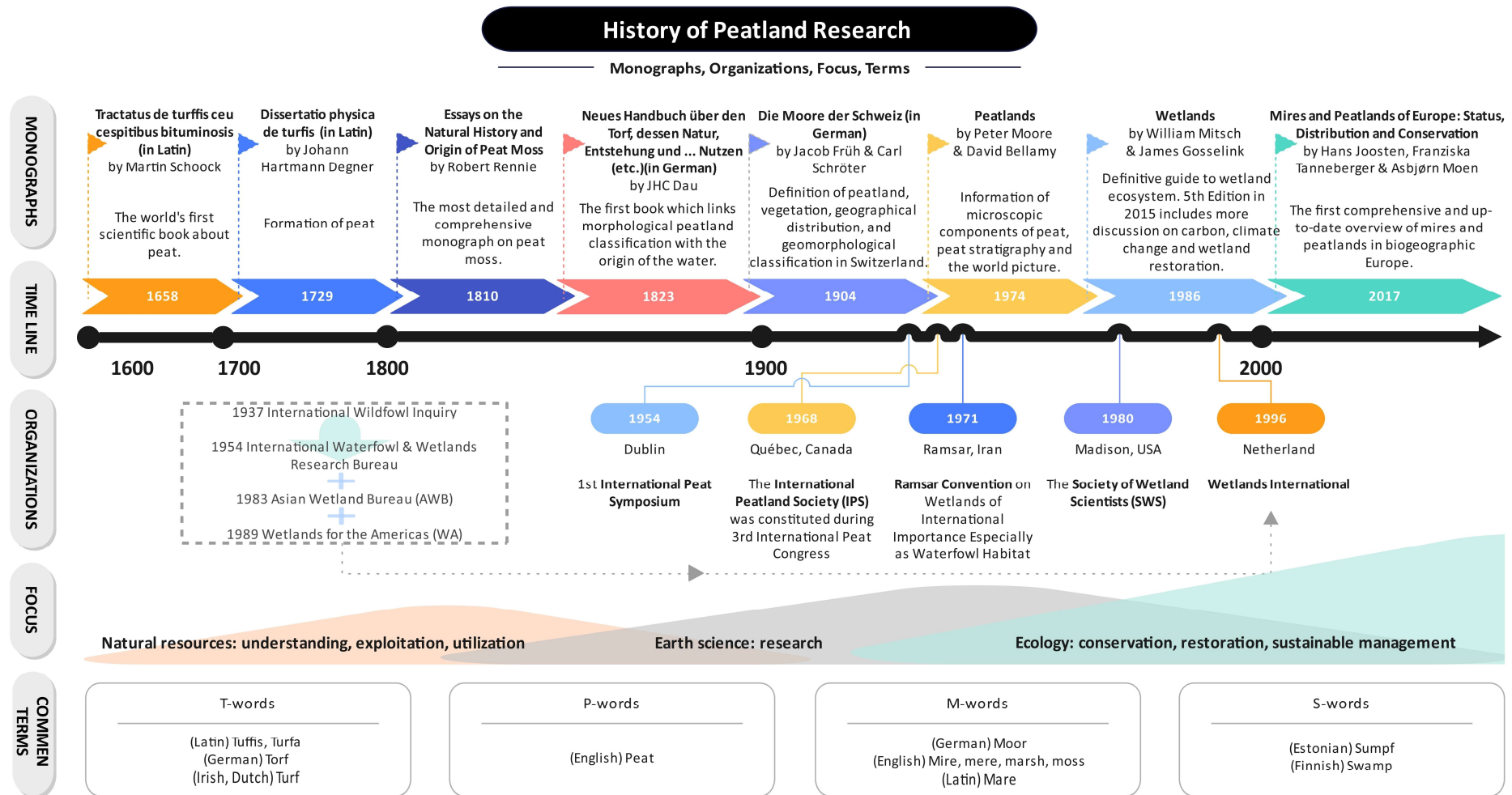
Figure 1.3 History of peatland study.

century onwards, international wetland and peatland organizations have also played an essential role in scientific research and communication. With the signing of the "Ramsar Convention" in 1971 and the explicit acknowledgement to peatlands in 1996, more research has been devoted to the conservation and sustainable use of wetlands and peatlands. Since this century, peatlands have been recognized as important factors in climate change mitigation, and peatland scientists have advocated for their restoration and rewetting as part of the "Kyoto Protocol" (Joosten, 2009; Tanneberger et al., 2011). It is, therefore, essential to understand the extent to which peatlands have been historically affected by anthropogenic activities to assess the success of restoration effectively and efficiently (Schumann and Joosten, 2008).

1.1.2 Ecological importance of peatlands and peatland degradation

Peatlands are exceptional habitats, home to a wide range of animal and plant species, and provide outstanding natural beauty. The naturally accumulated organic layers and incompletely decomposed dead plant material of peatlands make them important carbon sinks (Joosten and Clarke, 2002; Sjörs, 1980). One-third of the global soil carbon is stored in peatlands; thus, protecting peatlands through conservation, rewetting, and sustainable use is of worldwide relevance for the ongoing climate change mitigation (Harenda et al., 2018; Joosten et al., 2016; Tanneberger et al., 2011). Regarding greenhouse gas emissions, northern peatlands are a double-edged sword, *i.e.*, they sequester CO_2 but emit methane (CH_4), although methane emissions and carbon sequestration are currently likely to be negative (net cooling; Frolking et al., 2006). Pristine peatlands can also help regulate the water balance of the landscape. Lennartz et al. (2021) reported how connected peatlands are involved in the water cycle by storing and cleaning water, buffering rainfall, and regulating water quality. They also described how the connection between lowland peatlands and upland mineral soils is influenced by the hydraulic conductivity of the soils, which determines the water and solute movement and the peatland functions. As such, peatlands can act as filters to prevent eutrophication by retaining and removing compounds, diminishing harmful effects on adjacent ecosystems (Parish et al., 2008). Research into the buffering function of peatlands has mainly targeted the reduction of sediment and nitrogen/phosphorus loads in forest peatlands (Nieminen et al., 2005; Väänänen et al., 2008; Vikman et al., 2010). Compared to bogs, fens play a more prominent role in safeguarding water quality due to higher nutrient and solute inputs from lateral inflow and surrounding sources. They can actively mitigate the downstream water quality by means of denitrification, nutrient assimilation, or sediment trapping, particularly in the presence of nutrient-enriched agricultural runoff (Price et al., 2016).

Peatlands have been increasingly recognized as globally valuable ecosystems. However, peatlands in northern Central Europe have been severely disturbed by anthropogenic activities since

the last century, as the ecological functions of peatlands have been overlooked in favor of their economic benefits (Bragg and Lindsay, 2003). Most peatlands have been artificially drained for agriculture, forestry, and extraction for fuel. Overgrazing has also led to heavy trampling of peatlands by livestock. Apart from the direct losses and damages, the stable ecosystem, natural hydrological, and biogeochemical processes of the peatlands were disrupted by the low water table due to the drainage of the peatland. In addition, pollution from other sources, such as agricultural runoff and industrial discharges, has further contributed to peatland degradation. Joosten et al. (2017) investigated that over 40% of European peatlands have been artificially altered by intensive agricultural management (also see **Figure1.4**). For instance, in the United Kingdom (geographically belongs to Europe), historical drainage and subsequent management strategies have caused subsidence, degradation, and loss of peatland areas, while peat decomposition and pedogenic alterations have significantly influenced the physical and hydraulic properties of peat soils (Dawson et al., 2010; Kechavarzi et al., 2010).
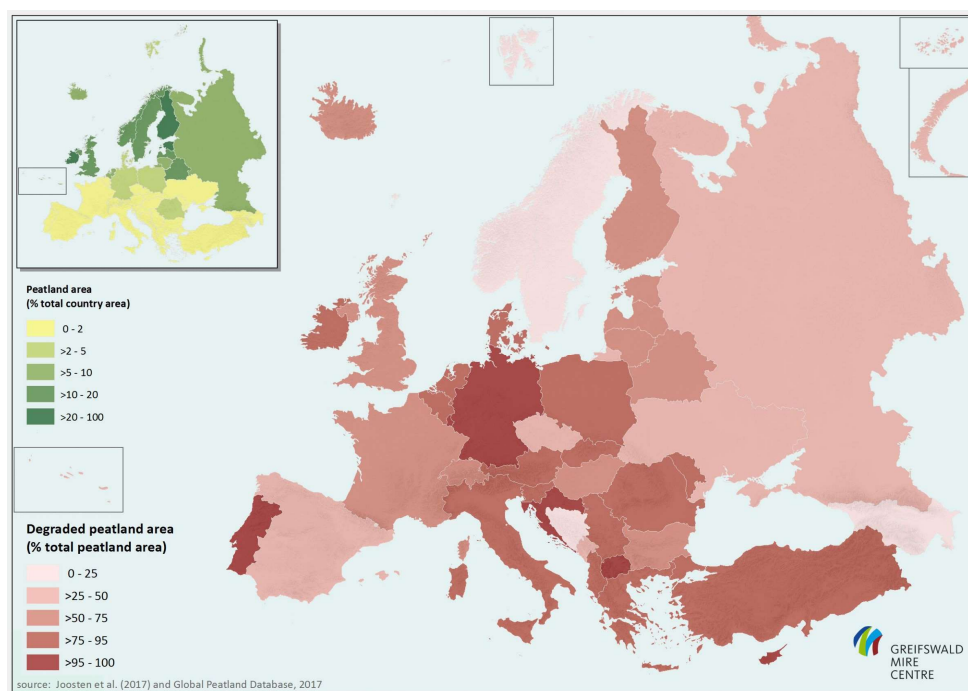
Figure 1.4 Proportion of degraded peatland area (large map) and proportion of peatland cover (small map) in Europe. The maps are based on the product made available by Greifswald Mire Centre with data from the Global Peatland Database 2017. (https://www.greifswaldmoor.de/global-peatland-database-en.html).

In Germany, Roßkopf et al. (2015) integrated legacy data, soil borehole databases, and detailed information on topography, hydrology, and geology to derive a detailed nationwide dataset on organic soils. This dataset revealed that organic soils cover an area of 15,682 km² (4.4% of Germany's total area) and contain an organic carbon pool of nearly 1.3 Gt (Gigaton). In the Federal State of Mecklenburg-Western Pomerania, different hydrogenetic mire types (HGMTs)

exhibit varying carbon storage due to stratigraphical distinctions. The three dominant HGMTs, namely percolation mire ("Durchströmungsmoor"; terms mentioned in **Figure 1.1**), terrestrialisation mire ("Verlandungsmoor"), and water-rise mire (mainly refers to "Hochmoor"), store approximately 430 Mt (Megaton) of organic carbon (Zauft et al., 2010). However, more than 90% of German peatlands have been degraded (Tanneberger et al., 2021). This includes more than 50% of peatlands used for agriculture in the Federal State of Brandenburg, which have been found to have a medium or high vulnerability to carbon loss in a specific evaluation of peatland carbon loss risk (Fell et al., 2016).

As environmental awareness grows, today's most controversial topic of climate change has drawn attention to the effects of peatland degradation (Tanneberger et al., 2021). There is no doubt that anthropogenic activities have a range of impacts on ecosystems. According to Evans et al. (2021), Tiemeyer et al. (2020), and Wilson et al. (2016), the drainage of peatlands results in substantial greenhouse gase (GHG) emissions, while managing the water table plays a crucial role in mitigating and balancing peatland GHG emissions at both national and international levels. Moreover, Glatzel et al. (2004) demonstrated that the alterations in CO_2 and CH_4 production potentials resulting from drainage, vegetation removal, and restoration have substantial implications for carbon cycling in peatlands. When these GHGs are released from degraded peat soils into the atmosphere, it directly diminishes the carbon storage capacity of peatlands (Waddington et al., 2010). Moreover, the inadequate water content in drained peatlands can expose organic-rich soil to the air, leading to mineralization and decomposition of peat. Degraded peatlands may thus struggle to perform the vital role of water storage and filtration, which can lead to ineffective regulators in the water cycle and poor water quality in adjacent areas (Lennartz et al., 2021). The continued loss and degradation of peatlands may eventually lead to the loss of special species and a decline in biodiversity (Parish et al., 2008).

1.2 Soil Properties and Processes of Peat

1.2.1 Soil physics and related studies on peatlands

The term "degraded peat" in our context refers to instances where peatlands experience a decline in quality due to human activities such as drainage. This process involves fundamental and diverse secondary pedogenetic phenomena, including aggregate formation, shrinkage cracks, earthification, and moorsh formation, significantly impacting soil properties (Mueller et al., 2007; Säurich et al., 2019; Zeitz and Velty, 2002). Maintaining good soil quality is essential for ecological balance as global climate problems intensify. The main determinants of soil sustainability are soil functions such as stable soil structure, functional soil water movement and solute transport, and sustainable access to water and nutrients by plant roots (Chapman et al., 2012;

Haj-Amor et al., 2023; Rabot et al., 2018; Schlüter et al., 2020). These are all relevant to soil physics, which plays an integral role across various disciplines, including environmental science, agronomy, climatology, hydrology, and geo-statistics (Shukla, 2013). As peatlands have received more attention in recent years, studies on the hydraulic and physical properties of peat soils have contributed significantly to understanding dynamic soil moisture, complex pore structure, diverse soil function, correlations among soil properties, and impacts by and on the environment in peatland ecosystems (Liu and Lennartz, 2019a; McCarter et al., 2020; Mueller et al., 2007; Oleszczuk and Truba, 2013; Truba and Oleszczuk, 2014; Rezanezhad et al., 2016; Wallor et al., 2018; Zeitz and Velty, 2002).

1.2.1.1 Peat soil physical and hydraulic properties

Peat soils are a three-phase system, like mineral soils, composed of water, air, and soil particles. However, unlike mineral soils, peat soils contain high levels of soil organic matter (SOM). This is because peat soils are organic materials formed through the incomplete decomposition of plant residues under waterlogged conditions (Grover and Baldock, 2013). In the field of peatland ecological science, three key processes—infilling, primary peat formation, and paludification—act together to shape peat soil formation, involving factors such as plant origin, climate, water table and flow, nutrient availability, and the biogeographical distribution of plant species (Rydin and Jeglum, 2006). Rydin and Jeglum (2006) described that infilling happens in stagnant water areas with constant heavy rainfall, where peat forms beneath plants like reeds, rushes, and sedges. Primary peat formation unfolds directly on fresh, wet mineral soil without prior standing water or sediment deposition. Paludification refers to peatland growth over previously less wet mineral ground, often featuring woody peat and stumps. Upslope paludification occurs as peat and the water table rise, affecting nearby uplands. Paludification can also start from pedogenic processes (soil development) causing reduced soil permeability and *Sphagnum* moss invasion.

The accumulation of partially decomposed plant material creates a unique pore structure, *i.e.*, a complex network of interconnected macropores, mesopores and micropores, contributing to the high porosity of peat soils. The high porosity of peat influences soil hydraulic properties, including water retention, hydraulic conductivity, as well as the availability and release of nutrients (Rezanezhad et al., 2016, 2012). The total porosity of peat can be exceptionally high, up to nearly 80 ~ 100 vol% (Liu and Lennartz, 2019a; Paavilainen and Päivänen, 1995; Oleszczuk and Truba, 2013). Another distinguishing characteristic of peat soil compared to mineral soil is their lower soil bulk density (BD/ρ_b; 0.01 to 0.76 g cm^{-3}), which can be well described by logarithmic or negative exponential models that show the negative correlation between bulk density and the SOM content of peat soils (Crnobrna et al., 2022; Grigal et al., 1989; Liu and Lennartz,

2019a). Earlier research on field samples from drained peatlands (peat-moorsh) in Poland indicated significant correlations among soil physical properties, such as a positive correlation between saturated water content and total porosity, a negative correlation between saturated water content and degree of decomposition, a negative correlation between bulk density and total porosity, and a positive correlation between bulk density and degree of decomposition (Oleszczuk and Truba, 2013). Moreover, the meta-study conducted by Liu and Lennartz (2019a) analyzed data from highly impactful publications on the hydro-physical properties of peat soils and further suggested that the bulk density of peat soils is negatively correlated with many soil hydro-physical properties (*e.g.*, macroporosity, saturated hydraulic conductivity, and van Genuchten model parameters), allowing trends in soil bulk density to indicate the degree of peatland degradation and highlighting the importance of soil physics research in peat soils and inspiring potential avenues for future investigation.

The flow of water in peat soils is controlled by their hydraulic and physical properties. A critical parameter is the saturated hydraulic conductivity (K_s), which represents the soil's capacity for water conduction under saturated conditions. Darcy's law is commonly utilized to determine the hydraulic conductivity (K) of soils, particularly the K_s in the case of peat soils, through the constant-head permeameter test (see Supplemental **Figure S3.1** in Supplemental Materials; Klute and Dirksen, 1986; Kruse et al., 2008; Liu et al., 2016), as given by Equation (1.1) to (1.2):

$$\frac{Q}{A_{cs}} = q = -K_s \cdot \frac{\Delta H}{L} \tag{1.1}$$

$$K_s = \frac{V_{water} \cdot L}{t \cdot A_{cs} \cdot \Delta H} \tag{1.2}$$

where Q describes the rate of water flow (cm^3 h^{-1}) through a certain cross-section area[1] (A_{cs}, cm^2), q is the water flux (cm h^{-1}), ΔH is the hydraulic head (cm), L is the length of the flow path (the length of soil samples; cm). The ratio of ΔH and L is the hydraulic gradient, which presents how much the hydraulic head changes over a certain distance along the flow path. V_{water} is the volume of water (cm^3) that flows through a soil sample over a specified period (t, h^{-1}). The range of K_s of peat soils can vary considerably depending on serval factors such as peat types, sampling depths, measurement method, peat decomposition/degradation degree, soil bulk density, disturbance and microtopography at the spatial scale, as well as pore size distribution and other factors at the pore scale (Liu and Lennartz, 2019a; Morris et al., 2022; Rezanezhad et al., 2016).

---

[1] Note: To avoid confusion with abbreviations, in the thesis, A_{cs} is used to represent the "cross-sectional area", while A represents the geostatistical model parameter "range".

Soil water retention curves (SWRCs) can characterize the water holding capacity and pore size distribution of peat soil by describing the relationship between soil moisture and soil water potential (Mueller et al., 2007). The pF box is usually used for measuring SWRCs in the laboratory, which involves placing the saturated soil column samples in a pressure chamber fitted with a porous ceramic plate or membrane (**Figure 1.5**; Richards, 1948). The pF box is subjected to increasing suction (pressure head, cm H_2O); at each level of suction, the amount of water remaining in the soil sample is measured by weighing the soil column samples, which can be further converted to a gravimetric water content (the mass of water per unit mass of dry soil; w, wt%). The more commonly used volumetric water content (the volume of water per unit volume of soil; θ, cm^3 cm^{-3}) can be obtained by multiplying the gravimetric water content by soil bulk density, allowing the SWRCs to be plotted as soil water content versus different suction pressure heads (ψ; cm H_2O or in pF unit). The van Genuchten model (VG) model is a well-known empirical model for describing SWRCs (van Genuchten, 1980), and it is based on the following Equation (1.3):

$$\theta(h) = \theta_r + \frac{\theta_s - \theta_r}{[1 + (\alpha|\psi|)^n]^m} \tag{1.3}$$

where volumetric water content (θ) at pressure head (h) is defined as the ratio of the volume of water to the total volume of the soil (cm^3 cm^{-3}), θ_r and θ_s are the residual and saturated volumetric water contents (cm^3 cm^{-3}), respectively. Empirical parameter α (cm^{-1}) expresses the inverse of the air entry pressure head and is related to the size of the largest pores in the soil. Empirical parameters n and m are associated with the pore size distribution and affect the slope of the retention function. Parameter n is a dimensionless shape parameter that controls the shape of the SWRCs, while m is related to n through the equation $m = 1 - 1/n$ (van Genuchten, 1980). These VG model parameters are determined empirically by fitting the VG model to experimental data, and they can vary widely depending on soil type, structure, and composition. In previous studies on peat soils, VG parameters θ_r and θ_s were usually fixed at zero and the total porosity, respectively (Liu and Lennartz, 2019a; Weiss et al., 1998).

Naturally intact and less decomposed peatlands are considered to have relatively high α values, indicating a lower air entry pressure and drain easily due to the presence of macropores (Kechavarzi et al., 2010; Liu and Lennartz, 2019a; Menberu et al., 2021). Nevertheless, heterogeneity in peat soils can lead to a complex pore structure consisting of a mixture of macropores, mesopores, and micropores, which contributes to a wider distribution of water retention properties, as reflected in the broader range of n values (Liu and Lennartz, 2019a). Steeper SWRCs with relatively large n values occur generally in more pristine peats, particularly with narrower pore size distributions (Dettmann and Bechtold, 2016; Liu and Lennartz, 2019a).
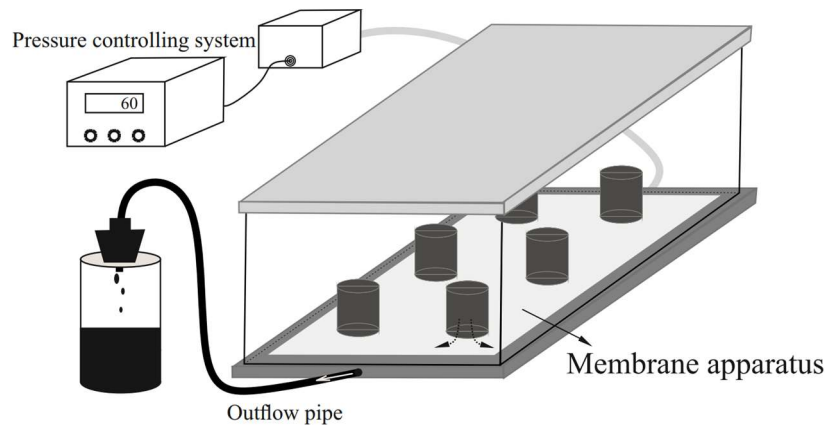
Figure 1.5 Experimental set up for soil water retention curves.

The impact of macropores on water movement and solute transport has received attention in peat soils, where macroporosity is a critical property with significant consequences for preferential flow (Baird, 1997; Holden, 2009; Ours et al., 1997). However, defining "macropores" can be challenging in soil science due to the ambiguity surrounding the pores size threshold (Giménez and Hirmas, 2016; Luxmoore, 1981; White, 1985). To quantitatively assess the abundance, size, and spatial distribution of macropores in soil, various *in-situ* techniques such as tracing and photographic methods can be utilized (Blodau and Moore, 2002; Logsdon et al., 1990). A better visualization of water flow and continuous macropores in peat soil can be achieved by dyes (*e.g.*, titanium oxide, TiO_2; Liu and Lennartz, 2015; Liu et al., 2016). In the laboratory, macroporosity can be quantified indirectly by measuring infiltration at different suctions or air permeability (Dettmann et al., 2014; Edwards et al., 1993). In addition, if complex pore structure (*e.g.*, pore size distribution and pore connectivity) are pursued in laboratory measurements, more advanced techniques (*e.g.*, X-ray and 3D image analysis) have also been applied to obtain a more accurate and comprehensive assessment of the characteristics of macropores in peat soils (Quinton et al., 2009; Rezanezhad et al., 2016, 2010).

1.2.1.2 Solute transport process of peat soils

Peat soils, as special porous media, have a dual-porosity structure, *i.e.*, they have open and connected (mobile), dead-ended (immobile), or isolated pores (McCarter et al., 2020; Rezanezhad et al., 2016). Advective water flow and solute transport occur mainly in the mobile porosity, while the immobile porosity does not contribute to advection, but only to diffusion of solutes between the two domains (**Figure 1.6**; McCarter et al., 2019, 2020). Solute transport through

pore networks in peat and their associated soil properties could shed light on the complex hydrological and biogeochemical cycles of this unique ecosystem (Gharedaghloo and Price, 2019; Liu et al., 2017; McCarter et al., 2019, 2018; Rezanezhad et al., 2016). However, solute transport in peat soils is a complex and multifaceted process related to a wide range of soil physical factors, including soil structure, pore size distribution, degradation, and hydrological conditions.
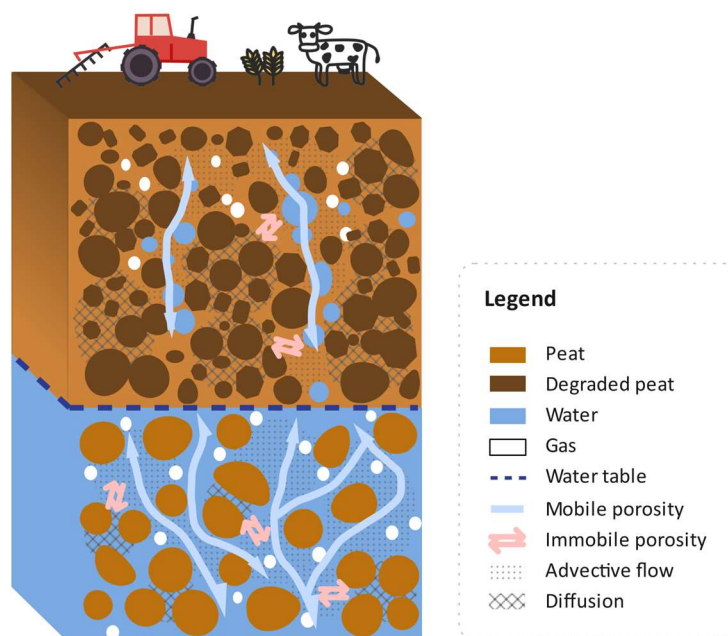
Figure 1.6 Simplified conceptual diagram summarizing the structure of undisturbed and degraded fen peat, comprised of larger pores (the mobile porosity) and smaller pores (the immobile porosity). (adapted from McCarter et al., 2020).

A fundamental approach to investigating solute transport in peat soil is to perform miscible displacement experiments using the flow-through reactors (FTRs) technique (see **Figure 3.1** in Chapter 3 and **Figure 4.2** in Chapter 4; Gosch et al., 2019; Kleimeier et al., 2017; Pallud et al., 2007). In FTRs, undisturbed peat soil columns are prepared with filters and end caps and can be supplied with a solution containing conservative tracers (*e.g.*, potassium bromide, KBr; Liu et al., 2017) or isotopes (*e.g.*, ^{18}O; Ronkanen and Kløve, 2007). Breakthrough curves (BTCs) can be generated by monitoring the solute (tracer) concentration in the outflow at regular intervals, and shape and parameters provide insights into solute transport mechanisms, including advection, dispersion, and nonequilibrium effects (Šimůnek et al., 2003; Šimůnek and Genuchten, 2008). Different solute transport models, such as classical equilibrium convection-dispersion equation (CDE; single porosity model; as given by Equation (1.4)) and physical nonequilibrium models (*e.g.*, dual-porosity models: mobile-immobile model, MIM; as given by Equation (1.5) to (1.7)), have been calibrated and validated in studies of peat soil using BTCs, aiming to enhance

our comprehension of the solute transport mechanisms in peat (Liu et al., 2017; Simhayov et al., 2018).

$$\frac{\partial C_e}{\partial T} = \frac{D}{R}\frac{\partial^2 C_e}{\partial X^2} - \frac{v}{R}\frac{\partial C_e}{\partial X} \tag{1.4}$$

$$\beta R\frac{\partial C_m}{\partial T} + (1-\beta)R\frac{\partial C_{im}}{\partial T} = \frac{1}{Pe}\frac{\partial^2 C_{im}}{\partial X^2} - \frac{\partial C_m}{\partial X} \tag{1.5}$$

$$(1-\beta)R\frac{\partial C_{im}}{\partial T} = \omega(C_e - C_{im}) \tag{1.6}$$

$$Pe = \frac{v_m L}{D_m} \tag{1.7}$$

where C_e is effluent concentration[2], T is dimensionless time, X is space coordinate, v is fluid average velocity (L T^{-1}). The retardation factor R is equal to 1 for a solute that does not react (Hoag and Price, 1997). D is the dispersion coefficient (L^2 T^{-1}), β is the fraction of the mobile soil water zone (dimensionless), D_m is the D of the mobile zone, ($D_m=D/\beta$; L^2 T^{-1}), ω is the mass transfer coefficient between the mobile and immobile regions (dimensionless). The Péclet number Pe expresses the ratio of advection to diffusion (dimensionless), where v_m is pore water velocity in the mobile zone (L T^{-1}) and L is length unit, typically indicating the spatial coordinate associated with the flow direction (L).

In Liu et al.'s (2017) study, the performance of equilibrium and non-equilibrium models for BTCs of fen peat samples with varying SOM content was investigated. However, the single porosity model could describe only 10% of the peat samples (with SOM content > 80%). The rest of the samples showed preferential flow behavior with early breakthrough and tailing in the BTCs, which were better fitted by a dual-porosity approach (*e.g.*, MIM model). In recent years, state-of-the-art applications of scanning electron microscope and X-ray micro-computed tomography have enabled the acquisition of high-resolution 3D images of pore structures in peat soils, thereby providing a powerful tool for assessing pore networks and various solute transport parameters (Gharedaghloo et al., 2018; McCarter et al., 2020). Notably, preferential flow pathways in peat soils can lead to preferential transport of pollutants and compounds through undecomposed plants, biological pores (*e.g.*, root channels), and other macropores to surrounding water bodies or groundwater, which may contribute to aquatic eutrophication (Forsmann and Kjaergaard, 2014; Ronkanen and Kløve, 2009). Hence, it is vital to understand

---

[2] Note: To avoid confusion with the abbreviations of spatial statistical parameter "nugget/sill ratio", the abbreviations for "the effluent concentration" and "the influent concentration" have been modified in this thesis to C_e and C_i, respectively, from the abbreviations (*C and C$_0$*) used in the corresponding publication of Chapter 3.

and model preferential flow in solute transport of peat for predicting and managing its environmental impacts.

1.2.1.3 The impact of peatland degradation on peat soil properties

The far-reaching effects of peatland degradation through drainage on the overall health and function of the ecosystem are manifested in a range of specific changes in soil properties, *i.e.*, alterations to soil physical, hydraulic, chemical, biological properties, and biogeochemical cycle (Kechavarzi et al., 2010; Liu and Lennartz, 2019a; McCarter et al., 2020; Zeitz and Velty, 2002). First and foremost is the change in soil structure. Peat soils become progressively more compacted after drainage, with an increase in the soil bulk density and a pronounced decrease in the porosity. A disturbed soil structure makes peatlands more vulnerable to erosion and drought. Based on the meta-analysis performed by Liu and Lennartz (2019a), **Figure 1.7** summarizes the correlation between the hydro-physical properties of peat soils and peatland degradation, thus enabling this thesis to further investigate the spatial variability of these properties in relation to peatland degradation within this context. Moreover, the still ambiguous aspects regarding the macroporosity of peat soils, as identified in Liu and Lennartz's (2019a) study, make it worthwhile to supplement new understanding through experimental data (Chapter 2).
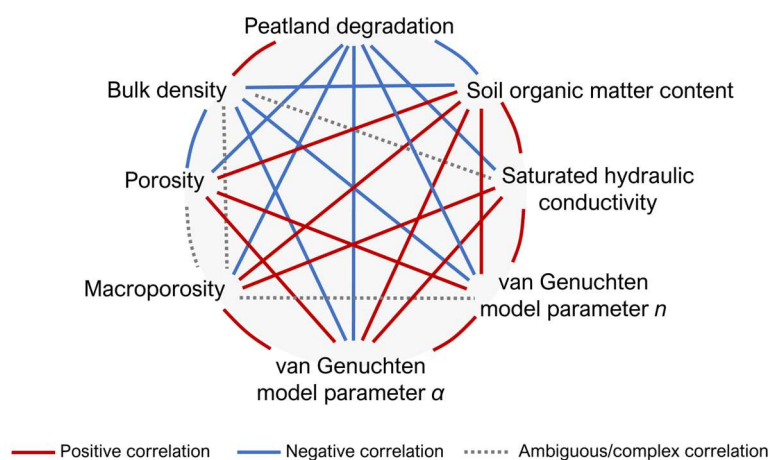
Figure 1.7 Statistically significant correlation among peat soil hydraulic and physical properties (Liu and Lennartz, 2019a).

Chemically, healthy *Sphagnum* bogs are usually acidic, with pH values ranging from 3.2 to 4.0 or < 5.5, while the pH of fen peat could be greater than 5.5 (Clymo et al., 1984; Solovey et al., 2021; Wheeler and Proctor, 2000). As peatlands are degraded, they may become more acidic (Maftu'ah et al., 2019). In addition, biogeochemical parameters reveal that peat degradation due to anthropogenic activities can lead to carbon loss (Krüger et al., 2015). Meanwhile, the stoichiometry of organic matter also varies with peat degradation (Leifeld et al., 2020). The loss of

organic matter further weakens the water and nutrient-holding capacity (Hudson, 1994; Sonon et al., 2014). The above changes can threaten the survival of plants and other organisms that depend on the unique habitat of the peatland, for instance, by forcing vegetation succession away from peat-forming plants and stimulating microbial decomposition (Andersson and Nilsson, 2001; Evans et al., 2012; Robroek et al., 2009). Thus, studying the soil properties of peatlands, particularly hydro-physical properties, is therefore crucial to understanding the complex effects of peatland degradation.

1.2.2 Anisotropic and heterogeneous behavior of peat soil properties

Peat soils are directionally dependent and non-uniform porous media (Baird et al., 2016; Beckwith et al., 2003; Gharedaghloo et al., 2018; Kruse et al., 2008; Liu et al., 2016; Morris et al., 2019). The anisotropy of soil physical properties can be mainly attributed to natural pedogenesis, anthropogenic factors and soil degradation (Beckwith et al., 2003; Liu et al., 2016; Peng, 2011). In the realm of soil hydraulic properties on peat soils, Beckwith and Heathwaite (2003) conducted a seminal study that examined the ratio in saturated hydraulic conductivity (K_s) between horizontal (K_{sh}) and vertical (K_{sv}) directions by conducting laboratory experiments on a substantial sample size. Due to the orientation and structure of the fibrous composition of peat soils, different investigations have confirmed that K_{sh} may exceed K_{sv} (Beckwith et al., 2003; Cunliffe et al., 2013; Lewis et al., 2012), while on other occasions, K_{sh} may be less than K_{sv} (Kruse et al., 2008; Liu et al., 2016; Surridge et al., 2005). The research undertaken by these researchers represents a pioneering contribution to the anisotropic character of hydraulic property of peat soil and potential patterns of water movement in peat soils. Further study is required to fully comprehend how anisotropy affects other soil physical processes (*i.e.*, solute transport).

The disturbance of peatlands due to anthropogenic or climatic factors severely affects peat soil properties. In addition to peat soil degradation due to land use of inland peatlands, the effects of microtopography and salinity on peat soil properties have also received attention as a result of the special geographical location of coastal peatlands, which are frequently subject to storm incursions (van Dijk et al., 2016; Gosch et al., 2018; Ahmad et al., 2020). Therefore, investigating the spatial heterogeneity of soil properties and developing spatial models are essential for customizing and assessing environmental sustainability and evaluating soil quality at different spatial scales (Ahmad et al., 2020; Negassa et al., 2019).

Geo-statistics is a commonly used tool to analyze the spatial variability of soil properties in soil science (Iqbal et al., 2005; Zhang et al., 2020). The semivariogram is a plot of semivariance as a mathematical function that can quantify the degree of spatial dependence of a soil property by measuring how the semivariance of this property changes as the distance between sampling

points increases (Matheron, 1963). The semivariance, $\gamma(h)$, is calculated as half the average squared difference between pairs of observations separated by a specific distance or lag (h), as given by Equation (1.8):

$$\gamma(h) = \frac{1}{2N(h)} \sum_{i=1}^{N(h)} [A_i(x_i) - A_i(x_i + h)]^2 \tag{1.8}$$

where $N(h)$ is the number of observations pairs, $A_i(x_i)$ and $A_i(x_i+h)$ are the measured soil property at spatial location i and $i+h$.
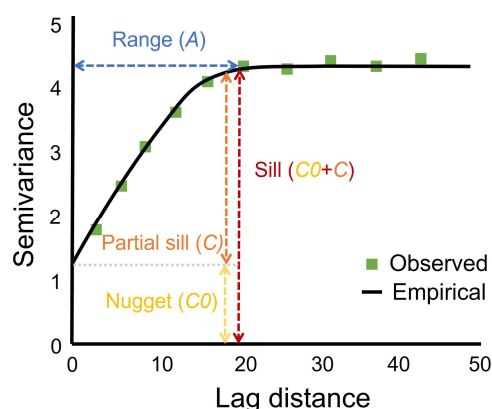
Figure 1.8 Typical semivariogram.

Moreover, semivariogram can provide a visual representation of the spatial autocorrelation of soil properties, which can be used to model the spatial distribution of these properties across the landscape. A typical semivariogram has three main components: the range (A), the sill ($C0+C$), and the nugget ($C0$; **Figure 1.8**). The x-axis displays the horizontal distance between pairs of observations, while the y-axis represents the semivariance. The degree of similarity between observations determines their position on the graph. For instance, the greater the similarity between observations, the higher they will be on the graph. The range (A) specifies the distance at which spatial dependence ceases to exist, indicating how far apart two sampling points become spatially independent. The sill is the maximum semivariance value, representing the total variability of the whole data set. The nugget is the semivariance value at zero distance, which reflects the variability occurring at distances smaller than the sampling interval or due to measurement error. The nugget effect occurs when the semivariogram does not always start from zero at zero distance, which can result from the presence of measurement error or random variation (Esri., n.d.; Lamorey and Jacobson, 1995).

The spatial variability of soil properties has been thoroughly investigated in soil science research, with a particular emphasis on SOM, bulk density, and hydraulic conductivity (Biswas

and Si, 2009; Bruland and Richardson, 2005; Gallardo, 2003; Sharma et al., 2011; Trangmar et al., 1987). In the context of peatlands, studies have mainly focused on the spatial variability of SOM (or soil organic carbon, SOC) and soil chemical properties (*e.g.*, soil stoichiometry), with limited exploration of the spatial dependence of hydraulic properties and other soil physical parameters in only a few studies (Ahmad et al., 2020; Negassa et al., 2022, 2019; Nkheloane et al., 2012). In addition, different types of peatlands are distinct ecosystems with unique characteristics and functions. Focusing solely on one type of peatland may not provide a comprehensive understanding of the heterogeneity of peatland and the spatial variability of soil properties. Significant changes in the spatial characteristics of soil properties resulting from either natural factors or human activities can alter the function of peatlands and affect their ability to provide ecosystem services (Negassa et al., 2022; Szumińska et al., 2023). Therefore, understanding the spatial patterns of soil properties is crucial for predicting the status of peatlands under different environmental conditions and management practices.

1.2.3 Nutrient and dissolved organic carbon (DOC) release in peatlands

Peatlands are not only a significant carbon sink, but also a potential source of nutrients, such as phosphorus and nitrogen (Hugelius et al., 2020; Schillereff et al., 2021). Drainage and grazing can accumulate nutrients in the soil due to natural and/or anthropogenic factors (*e.g.*, the decomposition of organic matter, commercial fertilizers, and residues of past agricultural vegetation and animal manure), putting surrounding water bodies at risk of nutrient exposure upon rewetting or flooding (Audet et al., 2020). For instance, in inland peatlands, phosphorus is likely to be transported primarily through preferential flow pathways and can accumulate in preferential flow path area (Forsmann and Kjaergaard, 2014; Ronkanen and Kløve, 2009). In coastal peatlands, the impact of salinity on nutrient release have received attention (Liu and Lennartz, 2019b; Pönisch et al., 2023). For instance, ammonium (NH_4^+) release is one of the most critical processes, since it may act as nutrient for algae and macrophytes, causing eutrophication at frequent N-limited conditions in marine systems (Bowen et al., 2020). Salinity has a considerable impact on NH_4^+ release from coastal peatland. The concentration of NH_4^+ leachate altered significantly during alternating fresh-brackish water cycles and could also be impacted by the salinity of the first flushing solution and soil texture (van Dijk et al., 2015; Liu and Lennartz, 2019b). To better understand the mechanism of NH_4^+ response to salinity, Servais et al. (2021) performed a mesocosms experiment in which NH_4^+ concentration increased with rising salinity under initial freshwater conditions, while it decreased with an ongoing increasing salinity under brackish water. Hence, understanding the nutrient responses to salinity is important for effective peatland management and protection of aquatic ecosystems.

Rewetting of peatlands can recreate carbon sinks (Zerbe et al., 2013), whereas dissolved organic carbon (DOC) release from the soil is an important but often ignored carbon loss pathway in ecosystems (Guo and Macdonald, 2006; Kindler et al., 2011). DOC is highly responsive to environmental changes, such as land use, hydrology, temperature, and geomorphological setting (Glatzel et al., 2003; Sheng et al., 2015). In addition, changes in salinity and pH may individually or collectively alter trends in soil water DOC concentrations due to shifts in biotic and abiotic processes (Chow et al., 2003; Kalbitz et al., 2000; Kreuzburg et al., 2020). For rewetted coastal peatlands, projecting the effects of rising salinity on DOC release is challenging as these factors may increase or decline DOC concentrations using different mechanisms (Herbert et al., 2015). Ardón et al. (2016) demonstrated that DOC concentrations in surface water of a mature and restored forested wetland in the coastal plain of North Carolina (USA) significantly dropped because of repeated saltwater intrusion (from ~40 to ~18 mg/L). Similarly, Liu and Lennartz (2019b) and Yang et al. (2018) also observed that DOC concentrations decreased with high salinity treatment. In contrast, Chambers et al. (2014) discovered that the saltwater inundated treatment had significantly higher pore water DOC than that of the control water level treatment in mangrove peat soils. Another nutrient leaching experiment conducted by Gosch et al. (2018) on inland marsh peats showed that elevated salinity in water increased DOC release. In addition, Weston et al. (2011) investigated that there was no significant difference in pore water DOC between saltwater-amended and freshwater-controlled soils in another coastal wetland ecosystem. Apparently, the interaction of numerous factors (*e.g.*, soil properties, geographical location, vegetation characteristics, atmospheric deposition, *etc.*) may locally and regionally influence DOC of surface and pore water (Camino-Serrano et al., 2016; Chambers et al., 2014). It is, thus, critical to investigate the response of DOC release to salinity in a specific coastal peatland, which is an important assessment of whether a seawater rewetting project can revert drained peatlands into carbon sinks.

Overall, **Figure 1.9** provides a simplified bibliometric mapping of the most important studies related to Chapter 1. The figure includes five themes: "soil hydraulic and properties", "solute transport", "spatial variability/anisotropy, heterogeneity", "impact of salinity", and "impact of land use". These keywords represent the main aspects of the research interests and focus of this thesis. These themes intersect to shape the research background of the three core chapters, considering a cross-disciplinary research approach to experimental design, aiming to address certain research gaps identified in previous studies and extend the conclusions to the application of peatland rewetting.
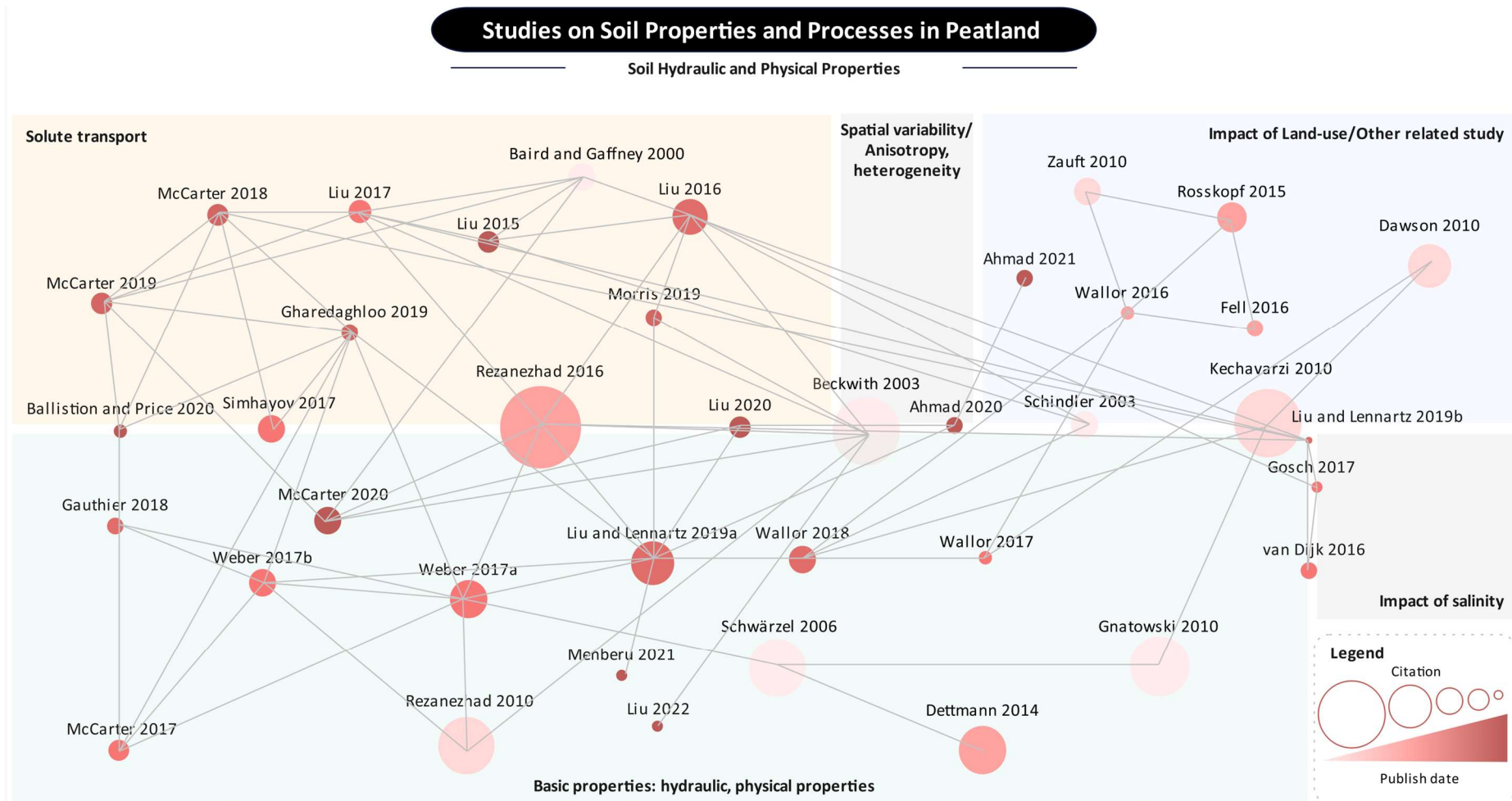
Figure 1.9 Simplified bibliometric mapping of the most important studies related to this thesis. (adapted from the searching result of "CONNECTED PAPERS").

1.3 Objectives and Outline of the Thesis

1.3.1 Objectives

The general research objective of this thesis is to assess the impact of human activities (*i.e.*, drainage and rewetting) on soil hydro-physical properties and the behavior of nutrient release in peatlands. To achieve this objective, this study conducted laboratory experiments on soil samples collected from five different peatlands in the Federal State of Mecklenburg-Western Pomerania in Northeastern Germany. The peatlands were selected based on their varying land uses and degradation stages, including a natural bog, a restored fen, two drained fens, and a coastal fen. By exploring the directional and spatial variations in peat soil hydro-physical properties and solute transport processes (*i.e.*, anisotropic and heterogenous behaviors), this research aims to provide new insights into land management and ecosystem restoration in peatlands.

With a sequential exploration of focal points progressing from different inland peatlands to a coastal peatland, the overarching research questioin of the is: By assessing the soil physical properties and their spatial characteristics, can we gain a better understanding and predict the outcomes of rewetting? Following the overarching research questioin, the specific objectives of this thesis were formulated as follows:

1) To assess the extent to which peat degradation affects the spatial heterogeneity of soil hydro-physical properties in inland peatlands.
2) To investigate the influence of the anisotropic nature of peat soil on solute transport in inland drained and restored peatlands.
3) To examine the effect of microtopography on the spatial heterogeneity of soil organic matter content and the potential nutrient release in a coastal peatland. In addition, to investigate the impact of salinity on nutrient release behavior upon rewetting.

1.3.2 Outline of the thesis

This thesis follows a cumulative structure and consists of five chapters, with chapters 2 to 4 dedicated to addressing the three specific objectives.

Chapter 1 introduces the background and motivation of this thesis. It begins by introducing the definition and classification of wetlands and peatlands and traces the historical development of research in this field, highlighting the varying research emphases across different periods. The importance of peatland ecological functions is also emphasized, along with examining the negative impacts of human disturbance on peatland soil. The chapter then concentrates on the hydraulic and physical properties of peat soils, which are essential for the assessment of peatland

soil quality and health, introducing and explaining several essential parameters. Additionally, the chapter focuses on the anisotropic and heterogeneous nature of soil properties, and geostatistical methods for studying spatial heterogeneity are introduced. It is emphasized that understanding the spatial characteristics of the hydraulic and physical properties of peat soils is of great significance for managing peatlands at small scale. Lastly, this chapter also provides a brief overview of the main objectives of the thesis.

Chapter 2 is an integrative assessment of soil hydro-physical properties of three peatlands in different degradation stages and provides a comprehensive description of the effect of peatland degradation on spatial heterogeneity of soil properties. It also highlights the importance of macroporosity for establishing the pedotransfer function for peat soils. This chapter has been published as an original research article entitled **"Small-scale spatial variability of hydro-physical properties of natural and degraded peat soils"** in *Geoderma* (Wang, M., Liu, H., Lennartz, B., 2021).

Chapter 3 focuses on the study of soil physical processes (water movement and solute transport) in terms of peat soil samples obtained from horizontal and vertical directions. It represents the difference in solute transport behavior between the two directions by using a 5% tracer mass arrival time to indicate the strength of preferential flow. This chapter has been published as an original research article entitled **"Effect of anisotropy on solute transport in degraded fen peat soils"** in *Hydrological Processes* (Wang, M., Liu, H., Zak, D., Lennartz, B., 2020).

Chapter 4 investigates the effects of microtopography on the spatial distribution of soil organic matter in a coastal peatland, revealing differences between coastal and inland peatlands due to the influence of marine systems. It further examines the impact of salinity on the potential nutrient release behavior when rewetting by brackish water and identifies the hotspot areas of nutrient release in the study site. This chapter has been submitted as an original manuscript entitled **"The influence of microtopography on soil carbon accumulation and nutrient release from a rewetted coastal peatland"** to *Geoderma* and published with minor revision (Wang, M., Liu, H., Rezanezhad, F., Zak, D., Lennartz, B., 2023).

Chapter 5 presents a concluding discussion that integrates the key findings from Chapters 2 to 4. It begins with an overview that concisely summarizes the main topics covered in Chapters 2 to 4. The synthesis section emphasizes the importance of soil properties, such as SOM, bulk density, water retention, and macroporosity, as indicators of peatland degradation and ecological functions. It also sheds light on the crucial factors explored in this thesis concerning the successful restoration of peatlands, particularly focusing on the challenges associated with nutrient leaching under a rewetting scenario. It further highlights the importance of increased

academic and societal attention to peatland restoration for successful outcomes, which is supported by a bibliometric analysis. Lastly, this chapter acknowledges the limitations and challenges encountered during the research, providing valuable considerations for further investigations and improvements in peatland conservation and restoration efforts.

It is important to note that the original publications in Chapters 2 and 3, as well as the submitted manuscript in Chapter 4, underwent formatting changes. These adjustments were made only to ensure consistency and coherence in the dissertation format, and underlying content of the studies remained unchanged. The main adjustments involved are: 1) modifications to abbreviations, 2) changes to arithmetic symbols, 3) re-numbering and repositioning of figures, tables, and equations, and 4) the use of consistent American Standard English spelling and Oxford comma.

In addition to the mentioned adjustments, three more modifications were implemented that 1) all references for the individual chapters were consolidated and formatted according to the format of the journal *Geoderma*, and they are placed as a unified reference list after Chapter 5; 2) the supplemental materials for each chapter were merged and placed after the reference list, but they are numbered according to their respective chapters; 3) a graphical abstract was newly added to Chapter 2, based on the original published paper.

2

Experimental Study 1

Small-Scale Spatial Variability of Hydro-Physical Properties of Natural and Degraded Peat Soils

Miaorun Wang[1], Haojie Liu[1]*, Bernd Lennartz[1]

[1]Faculty of Agricultural and Environmental Sciences, University of Rostock, Justus-von-Liebig-Weg 6, 18059 Rostock, Germany

*Corresponding author: Haojie Liu (email: haojie.liu@uni-rostock.de)

Graphical Abstract
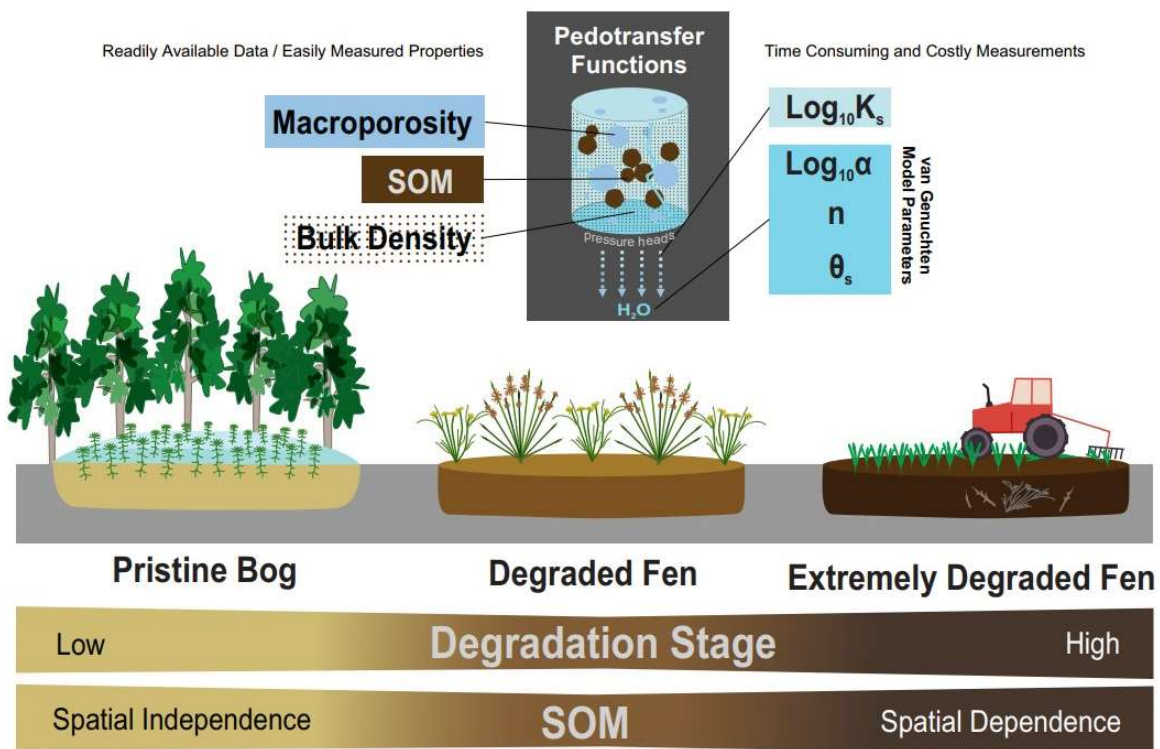
Abstract

The spatial variability of soil properties plays an important role in water and carbon cycles in peatlands. The objectives of this study were to analyze the spatial variation of hydro-physical properties of peat soils and to establish pedotransfer functions (PTFs) to estimate the hydraulic properties of peat using readily available soil properties. We selected three study sites, each representing a different state of peat degradation (natural, degraded and extremely degraded). At each site, 72 undisturbed soil cores were collected from 5 m by 5 m grid cells in an area of 35 m by 40 m. The saturated hydraulic conductivity (K_s), soil water retention curves, total porosity, macroporosity (pore diameter > 30 µm), bulk density and soil organic matter content (SOM) were determined for all sampling locations. The van Genuchten (VG) model parameters (θ_s, α, and n) were optimized using the RETC software package. A strong positive correlation between macroporosity and K_s was observed irrespective of the degradation stage of the peat. However, the relationships between macroporosity and K_s differed between the natural and the drained peatlands. Adding macroporosity to the PTFs substantially improves the prediction of K_s as well as VG parameters. Results show that the soil physical and hydraulic properties (*e.g.,* K_s and VG model parameters) exhibit different levels of spatial heterogeneity depending on the peat degradation stage. The geostatistical analysis suggests that the spatial dependence of soil hydro-physical properties varies depending on the considered property as well as land management (*e.g.,* drainage). Bulk density and SOM are spatially dependent, whereas K_s and macroporosity are spatially independent if the peat is severely degraded. In conclusion, the peat degradation stage plays an important role and should be generally considered in the spatial analysis of peatlands. The obtained semivariograms may serve as a basis for 2D and 3D hydrological modeling as well as peatland restoration studies.

2.1 Introduction

Peatlands cover approximately 3% of the Earth's land surface, but store ~21% of the global soil carbon and 10% of global freshwater (Joosten and Clarke, 2002; Leifeld and Menichetti, 2018; Limpens et al., 2008). Worldwide, approximately 15% of peatlands have been artificially drained mainly for cropland, grazing land, and forestry (Joosten et al., 2012). Land drainage damages ecosystem functions of peatlands, transforming them from long-term carbon sinks into sources due to the hydrologic alterations (Regan et al., 2019; Young et al., 2017). Peatland drainage causes land subsidence as well as organic carbon mineralization leading to changes in hydro-physical properties of peat (Kennedy and Price, 2005; Liu et al., 2020a; Morris et al., 2011; Price, 2003). However, the magnitude of the changes mainly depends on drainage type (deep or shallow; Stephens et al., 1984; Wallage and Holden, 2011), drainage history(Liu et al., 2020a; Pronger et al., 2014), land use (agriculture or forest; Hallema et al., 2015; Minkkinen and Laine, 1998), and peat types before drainage (bogs or fens; Hyväluoma et al., 2020; Kechavarzi et al., 2010). Compared with mineral soils, knowledge about hydraulic properties of peat is limited, particularly for variable saturation conditions (John et al., 2021; Wallor et al., 2018).

Peat soils as a porous medium are characterized by a strong heterogeneity and anisotropy (Beckwith et al., 2003; Wang et al., 2020), causing an enormous variability of the hydraulic properties (*e.g.*, saturated hydraulic conductivity, K_s). For instance, Cunliffe et al. (2013) observed a difference in K_s of three orders of magnitude in blanket peat on a decimeter scale. Lewis et al. (2012) determined the K_s of a blanket peat along a 210-meters transect and found that K_s ranged from 0.7×10^{-6} to 1.21×10^{-4} m s^{-1} with low K_s at the bog margins. The low-K_s margin phenomenon was also observed for raised bogs (Baird et al., 2008). However, such low-K_s margin was not confirmed in a shallow layer of a Swedish bog (Morris et al., 2015). The spatial variance of K_s of bogs is also strongly influenced by plant microhabitat type (hummocks and hollows, Baird et al., 2016; Morris et al., 2019). Baird (1997) observed that the K_s of peat (soil surface) varied from 8.2×10^{-5} to 4.3×10^{-3} m s^{-1} in one fen peatland. Liu et al. (2016) reported that the K_s of fen peat from the same horizon can change more than 2 orders of magnitude. For a same peat soil, K_s in vertical and horizontal directions may differ by two to three orders of magnitude (Beckwith et al., 2003; Cunliffe et al., 2013; Liu et al., 2016). The anisotropic behavior of K_s is related to the layered structure (Gharedaghloo et al., 2018) or to the distribution patterns of macropores in the peat (Liu et al., 2016).

The soil water retention curve is an essential hydraulic property for modeling water flow and solute transport under unsaturated conditions. The soil water retention curves (SWRCs) of peat

have been studied over the last two decades (John et al., 2021; Liu and Lennartz, 2019a; Schwärzel et al., 2006; Wallor et al., 2018; Weiss et al., 1998). In general, the well-known van Genuchten (VG; single domain) model seems suitable to describe the experimentally determined SWRCs. However, multi-models (*e.g.*, bimodal or trimodal models) are required to fully describe the SWRCs for specific peat types (*e.g.*, living *sphagnum*; Weber et al., 2017).

Direct measurements of hydraulic properties such as K_s and SWRCs are time consuming and costly (Wösten et al., 2001). Over the last several decades, pedotransfer functions (PTFs) have been increasingly employed to estimate the hydraulic parameters of mineral soils from easily measured soil properties such as soil organic matter content (SOM), bulk density and soil texture (Schaap et al., 2001; Vereecken et al., 2010; Wösten et al., 2001). In a few studies, PTFs have been developed for peat and organic soils (Liu and Lennartz, 2019a; Morris et al., 2015; Wallor et al., 2018; Weiss et al., 1998; Wösten et al., 1999). However, the performance of the PTFs for hydraulic properties is relatively low, especially if degraded peat soils are considered (Wallor et al., 2018; Liu and Lennartz, 2019a). One possible reason is that the K_s and VG parameters of highly degraded peat are less sensitive to readily available soil parameters such as SOM and bulk density. Therefore, additional parameters should be considered to be included into PTFs to improve their predictions.

Geostatistics (*i.e.*, kriging and semivariogram) has been proved as an important tool to investigate the spatial variation of soil hydraulic properties (Bevington et al., 2016; Iqbal et al., 2005; Nielsen and Wendroth, 2003; Vieira et al., 1981; Zhang et al., 2020). Kriging has been commonly considered as the best method to interpolate spatial data using a limited number of measurements. The semivariogram depicting the spatial dependence is the basis of kriging because kriging can only be applied if soil properties are spatially dependent. The spatial dependence of soil physical, chemical, and hydrological properties has been one focus of soil science over the last decades (Biswas and Si, 2009; Sharma et al., 2011; Trangmar et al., 1987; Tsegaye and Hill, 1998). In previous studies, a spatial dependence of different soil properties such as SOM, bulk density, K_s, and VG model parameters has been found for agricultural land, forests, and wetlands (Biswas and Si, 2009; Bruland and Richardson, 2005; Gallardo, 2003; Sharma et al., 2011). Compared to mineral soils, little information is available on the spatial dependence of soil properties of peat (Ahmad et al., 2020; Negassa et al., 2019; Tiemeyer et al., 2007) (Supplemental **Figure S2.1**). Proulx-McInnis et al. (2013) observed a strong spatial dependence of peat thickness in a Canadian peatland. Nkheloane et al. (2012)found that the soil organic carbon is strongly spatially dependent. Few studies on rewetted peatlands showed that the spatial dependence is strong for soil chemical, biochemical properties, as well as water quality (Negassa et al., 2019), but moderate for K_s (Ahmad et al., 2020). The impact of land drainage, known to

dramatically changing chemical as well as physical soil properties, on the spatial dependence of these properties remains uncovered.

This study aims at gaining insight into the small-scale spatial variability and dependence of hydro-physical properties of peat including bulk density, SOM, K_s, porosity, macroporosity, and VG model parameters at natural and drained peatlands. The specific objectives of this study were to: 1) establish PTFs to estimate hydraulic properties of peat, 2) to evaluate the spatial variability of hydro-physical properties, and 3) to quantify the spatial dependence of hydro-physical properties of natural and degraded peat.

2.2 Material and Methods

2.2.1 Study sites and soil sampling

One natural peatland (Site 1: Gresenhorst, 54°08'25.2"N, 12°27'10.7"E) and two artificially drained peatlands (Site 2: Knesse 54°07'58.2"N, 12°37'30.3"E; Site 3: Pölchow, 54°00'21.7"N, 12°06'59.5"E) in Mecklenburg-Western Pomerania, Germany were chosen for this study (**Figure 2.1**). Site 1 is a natural forest peatland without human disturbance (*e.g.*, land drainage or soil extraction), which can be considered as a pristine bog. The two degraded fen peatlands experienced their first drainage in the 16th (Site 2) and 13th (Site 3) centuries and were under agricultural usage as grassland since the second half of the 20th century. Site 3 shows a higher degree of degradation due to a long-term drainage history, causing more loss of soil organic matter than that at Site 2. The previous investigation suggests that the topsoil at Site 2 is a highly degraded peat with a bulk density ranging from 0.2 to 0.4 g cm^{-3} (Ahmad et al., 2020; Lennartz and Liu, 2019). The topsoil at Site 3 is an extremely degraded peat with a bulk density greater than 0.4 g cm^{-3} (Lennartz and Liu, 2019; Liu and Lennartz, 2015). The green and colourful *Sphagnum* (*S. magellanicum* and *S. Papillosum)* and *Sphagnetum magellanici* form the bog moss at Site 1. Peat rushes (*Juncus*) and sedges (*Cyperaceae*) are the main peat forming vegetation at Site 2. The peat at study Site 3 has formed from sedge (*Cyperaceae*) and alder (*Alnus*) and undecomposed woods.
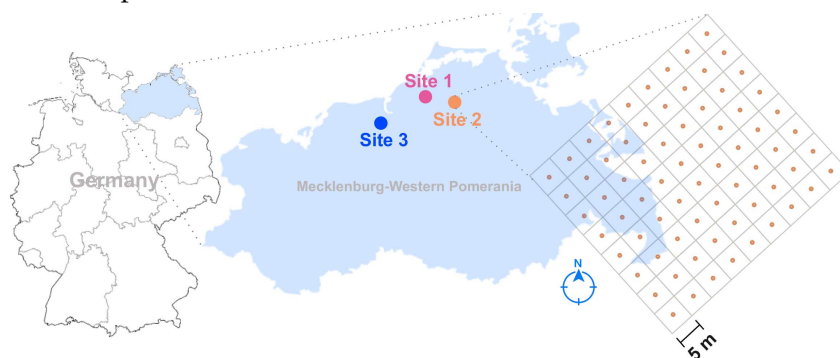
Figure 2.1 Three sampling sites in Mecklenburg-Western Pomerania, Germany. (right pane showing 72 sampling points at each site within a 35 m × 40 m plot).

From each study site, 72 undisturbed peat cores (5.6 cm in diameter and 4.0 cm in height) were collected from 5 m by 5 m grid cells within an area of 35 m × 40 m at a depth of 10 – 20 cm (**Figure 2.1**). All peat cores from two drained peatlands were taken by cutting soil with steel cylinders and a sharp knife (Liu and Lennartz, 2019b; Wang et al., 2020). In order to minimize the soil compaction during sampling, soil cores from the natural peatland were collected during winter when the soil was frozen. After soil sampling, both sides of the peat cores were covered with lids, and all cores were placed in freezer boxes and transported back to the laboratory.

2.2.3 Determination of hydro-physical properties of peat

Peat cores were saturated slowly using background solution for 7 days from the bottom upwards to avoid gas bubbles possibly blocking water flow (Skaggs et al., 2002). The background solution (sodium chloride) was prepared according to electrical conductivity (EC) and pH values of the groundwater in the field (Site 1: EC = 60 µS cm⁻¹, pH = 4.0; Site 2: EC = 800 µS cm⁻¹, pH = 6.5; Site 3: EC = 500 µS cm⁻¹, pH = 6.0). The pH of the background solution was adjusted using hydrochloric acid. The saturated hydraulic conductivity (K_s) of all peat cores were determined by a constant-head upward-flow method (Liu et al., 2016).

The soil water retention curves (SWRCs) were determined in the laboratory using a pressure membrane apparatus at different pressure heads: 0, –10, –30, –60, –100, –200 and –600 cm H_2O. In addition, volumetric soil water content at pF = 4.2 (–15850 cm H_2O) was determined for drained peat soils using a membrane apparatus (ceramic suction plates) equipped with a compressor unit for pF-value 4.2. For natural peatlands, the groundwater table is always near the ground surface. We assume that the chosen range of pressure heads[3] (ψ) applied to the pristine peat (from 0 to –600 cm H_2O) sufficiently reflects conditions how they prevail in natural peatlands. The VG model (van Genuchten, 1980; Equation (2.1)) was used to fit the measured SWRCs.

$$\theta(h) = \theta_r + \frac{\theta_s - \theta_r}{[1 + (\alpha|\psi|)^n]^m} \qquad (2.1)$$

where θ represents the volumetric water content (cm³ cm⁻³) at pressure head h (– cm), θ_r is the residual water content (cm³ cm⁻³), θ_s is the water content at saturation (cm³ cm⁻³). α, n, and m are empirical parameters ($m = 1–1/n$), where α is related to the inverse of the air entry pressure head (cm⁻¹) and n (>1) describes the pore size distribution affecting the slope of the retention function. In this study, θ_r was fixed at zero (Schwärzel et al., 2006); the parameters

---

[3] Note: To avoid confusion with abbreviation of spatial statistical parameters "lag distance", the abbreviation for "(suction) pressure heads" have been modified in this thesis to ψ from the abbreviation (h) used in the corresponding publication of Chapter 2.

θ_s, α, and n were optimized using the RETC software packages (van Genuchten et al., 1991). The parameter optimization procedure was recommended by Schwärzel et al. (2006).

After the determination of SWRCs, the soil samples were dried at 105°C to determine the soil dry bulk density. Although a relatively low temperate (50°C to 80°C) was suggested to determine the bulk density in a few studies (Lewis et al., 2012; Morris et al., 2019), a temperature of 105°C is commonly used for the determination of the bulk density of peat (Gnatowski et al., 2010; Kechavarzi et al., 2010; Schindler et al., 2003; Schwärzel et al., 2002). Soil organic matter content (SOM) was analyzed by the loss on ignition (LOI) method, burning samples at a temperature of 550°C for 4 hours (ISO 22476-3:2005).

The definition of macropore is ambiguous in soil science. The minimum equivalent diameter for macropores reported in the literature ranges between 30 and 3000 μm (Beven and Germann, 1982; Cameron and Buchan, 2016; Carter et al., 1994). In this study, we define macroporosity as pores with an equivalent cylindrical diameter greater than 30 μm (Cameron and Buchan, 2016). The pore size in soils can be estimated from the capillary rise equation (Bear, 1972; Equation (2.2)):

$$r = \frac{2\sigma \cos(\vartheta)}{\rho g H} \qquad (2.2)$$

where r is the pore radius (cm), σ is the surface tension of water (72.7 dyn cm^{-1}), ϑ is the soil liquid contact angle (°), ρ is the density of water (1.0 g cm^{-3}), g is the acceleration of gravity (980 cm s^{-2}) and H is water pressure head (– cm H$_2$O pressure head). The contact angle was reported to vary from 40° and 52° for moderately hydrophobic organic soils and peat (Bachmann et al., 2003; Carey et al., 2007; Gharedaghloo and Price, 2019). In this study, we set the contact angle to 52° for peat as recommended by Gharedaghloo and Price (2019). Thus, the macroporosity (> 30 μm) can be estimated as the difference between total porosity and the volumetric water content at around –60 cm H$_2$O pressure head (Schindler et al., 2003; Wallor et al., 2018).

2.2.3 Statistics analysis

In this study, the data of SOM, bulk density, porosity, macroporosity, and VG parameter n were normally distributed. The K_s and α values were log-normally distributed. Therefore, the K_s and α values were transformed to common logarithms (log$_{10}$) before further statistical and geostatistical analyses. Pearson's correlation coefficients were chosen to evaluate the strength of possible relationships between all hydro-physical properties and VG model parameters for each site.

A linear mixed-effect models (LMEMs) analysis was carried out to detect differences among sites with respect to hydro-physical properties of peat. The "site" was set as fixed effect while the "sampling location" was a random effect. The analysis was performed using R software with packages "lme4" and "lmerTest" (R Core Team, 2020). The pairwise comparison of LMEMs was performed using package "emmeans". The level of significance was set to 0.05 for all statistical tests.

The PTFs were derived to estimate the $\log_{10}K_s$ and VG parameters (θ_s, $\log_{10}\alpha$, and n) separately using physical properties (macroporosity, bulk density, and SOM). The best model was chosen according to a stepwise multiple regression analysis using SAS version 9.4 (SAS Institute Inc., 2013). Previous studies have used a similar approach to establish according PTFs (*e.g.*, Vereecken et al., 1989; Wösten et al., 1999).

The spatial variation (semivariance) of soil properties were analyzed with the geostatistical software GS+ package (version 10). In spatial statistics, the theoretical semivariance (γ) is a function of lag distance (h, spacing between samples). The γ is estimated by Equation (2.3) (Nielsen and Wendroth, 2003):

$$\gamma(h) = \frac{1}{2N(h)} \sum_{i=1}^{N(h)} [A_i(x_i) - A_i(x_i + h)]^2 \qquad (2.3)$$

where $\gamma(h)$ is the semivariance for the interval class h, $N(h)$ is the number of sample pairs separated by the lag distance. $A_i(xi)$ and $A_i(x_i+h)$ are the measured variable at spatial location i and $i+h$. In order to reduce the number of points in the empirical semivariogram, the pairs of locations are commonly grouped into lag bins based on their distance from one another (Lyon et al., 2006; Nielsen and Wendroth, 2003; Robertson, 2008). Semivariance calculations at each site were based on the half of maximum lag distance of 25.20 m as suggested by Englund and Sparks (1991). Linear, spherical, exponential, and Gaussian models were fitted to the experimental semivariograms in order to obtain the most suitable model as indicated by a high coefficient of determination (R^2) and low residual sum of squares (RSS). The chosen model selection procedure was recommended by Cambardella et al. (1994) and Gamma Design Software (Robertson, 2008).

2.3 Results

2.3.1 Hydro-physical properties of peat

Table 2.1 summarizes the hydro-physical properties of the investigated soils. The average value of the soil bulk density at sites 1, 2 and 3 were 0.08, 0.34 and 0.54 g cm^{-3}, respectively (**Table**

2.1). The macroporosity varied accordingly from 1.6 vol% to 62.1 vol%. The K_s of pristine peat ranged from 8.5×10^{-7} to 5.5×10^{-5} m s^{-1}, while the K_s of degraded peat varied from 7.6×10^{-8} to 9.3×10^{-5} m s^{-1}. In this study, the VG model appropriately described all the tested SWRCs with a fitting criterion of $R^2 > 0.95$. The VG parameter α ranged from 0.001 to 1.05 and n varied from 1.11 to 1.59. For SOM and macroporosity, the coefficient of variation (CV; **Table 2.1**) was smaller for natural than for degraded peatlands. However, the CV for VG model parameters is greater for natural than for degraded peatlands. The CV for K_s ranged from approximately 70% to 150%, with the highest value obtained for Site 2.

Table 2.1 Descriptive statistics of hydro-physical properties of investigated peat soils (N = 72): soil organic matter content, SOM; bulk density, BD; total porosity; macroporosity; saturated hydraulic conductivity, K_s; VG parameter, α, and VG parameter, n.

Property	Study site	Statistical parameter				
		Minimum	Maximum	Mean[b]	Standard deviation	Coefficient of variation (CV; %)
SOM (wt%)	1	92.11	99.78	97.73 a	0.98	0.99%
	2	53.61	79.37	69.11 b	4.13	5.93%
	3	10.70	45.08	30.44 c	7.05	23.00%
BD (g cm^{-3})	1	0.05	0.12	0.08 c	0.01	18.31%
	2	0.25	0.49	0.34 b	0.04	13.06%
	3	0.36	0.84	0.54 a	0.10	19.20%
Total porosity (vol%)	1	84.99	99.95	96.62 a	2.47	2.56%
	2	76.87	90.90	82.79 b	2.79	3.35%
	3	59.74	91.01	79.43 c	5.32	6.70%
Macroporosity[a] (vol%)	1	21.68	62.06	42.95 a	9.32	21.69%
	2	3.80	16.52	8.30 b	2.84	34.21%
	3	1.55	16.36	9.95 b	3.02	30.37%
K_s ($10^{-5} \cdot$ m s^{-1})	1	0.0851	5.53	1.28 a	1.14×10^{-5}	89.46%
	2	0.0076	9.27	1.24 b	1.85×10^{-5}	148.83%
	3	0.0779	4.00	1.01 a	7.04×10^{-5}	69.86%
α (cm^{-1})	1	0.0532	1.0494	0.1812 a	0.16	88.28%
	2	0.0008	0.0024	0.0012 b	2.98×10^{-4}	25.94%
	3	0.0006	0.0045	0.0014 b	5.54×10^{-4}	41.00%
n	1	1.11	1.41	1.23 c	0.07	5.43%
	2	1.35	1.63	1.49 a	0.05	3.65%
	3	1.27	1.59	1.45 b	0.07	4.58%

[a] Macroporosity was calculated by the difference between total porosity and volumetric soil water content at −60 cm H$_2$O pressure head.

[b] "a", "b", and "c" represent the significant difference from pairwise comparison of LMEMs. The significant difference of parameter "K_s" was determined with log-transformed K_s.

The results from the pairwise comparison of linear mixed-effect models (LMEMs; Supplemental **Table S2.1** and **S2.2**) indicated that the macroporosity of the pristine peat is significantly

greater than that of degraded peat soils ($p < 0.001$; **Table 2.1** and Supplemental **Table S2.2**). However, there is no significant difference in macroporosity between the two degraded peat soils ($p = 0.216$). The $\log_{10}K_s$ of peat at Site 2 is significantly lower than those values from Site 1 and Site 3 ($p < 0.001$) but there are no significant differences in $\log_{10}K_s$ between Site 1 and Site 3 ($p = 0.866$; Supplemental **Table S2.2**). In this study, the pristine peat has significant higher α and lower n values than the degraded peat soils ($p < 0.001$; **Table 2.1**), but, there is no significant difference in the VG model parameter α between the two degraded peat sites ($\log_{10}\alpha$: $p = 0.999$). In this study, the visual inspection confirms the general similar shape of the SWRCs for the two degraded peat soils (**Figure 2.2**). The high α and low n values indicate that pristine peat has a lower air-entry values and a steeper retention curve at high pressure heads (**Figure 2.2**). The 95% confidence intervals of the dataset for each pressure head and estimated VG model parameters are shown in Supplemental **Table S2.3** and **S2.4**.
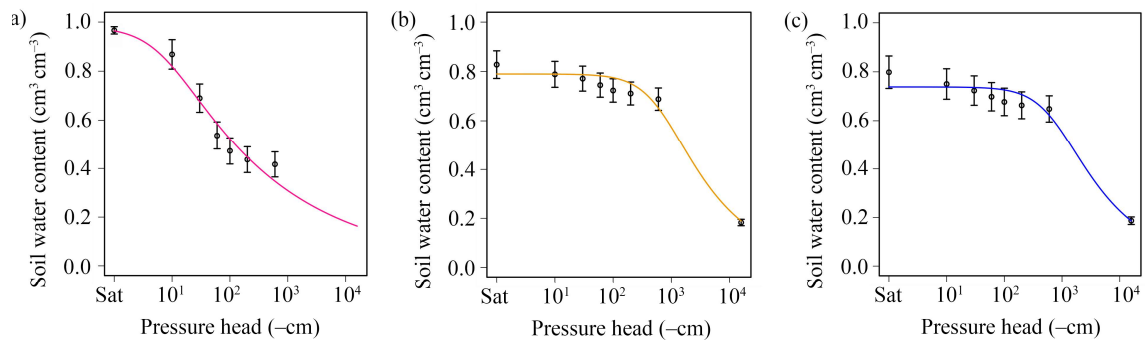
Figure 2.2 Plot of soil water retention curves (mean ± standard deviation, N = 72) of three study sites; (a) Site 1, natural peat; (b) Site 2, degraded peat; (c) Site 3, extremely degraded peat.
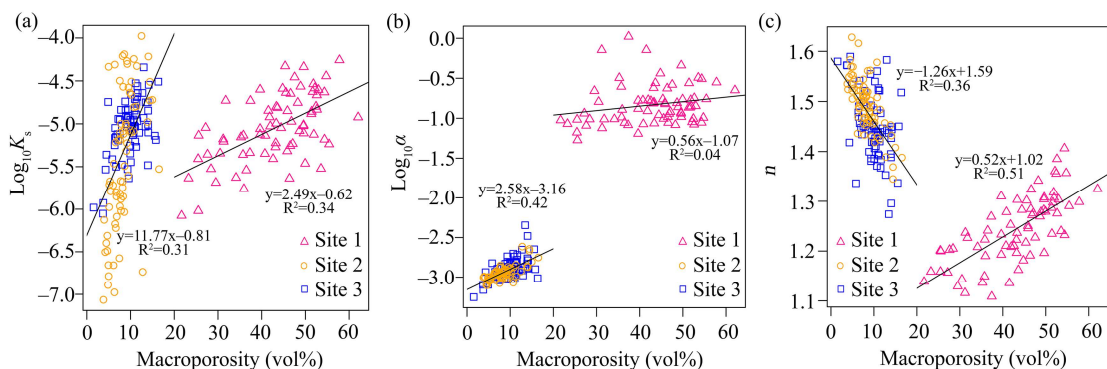
Figure 2.3 The relationship between (a) saturated hydraulic conductivity K_s ($\log_{10}K_s$) and macroporosity; (b) macroporosity and van Genuchten parameter α ($\log_{10}\alpha$); (c) macroporosity and van Genuchten parameter n of differently degraded peat. (pink: Site 1; orange: Site 2; blue: Site 3).

A moderate positive relationship was found between $\log_{10}K_s$ and macroporosity for all study sites (Pearson's correlation coefficient > 0.55; $p < 0.001$; Supplemental **Table S2.5**). The relationship between macroporosity and $\log_{10}K_s$, however, differed for pristine and degraded peat (**Figure 2.3a**). A moderately positive correlation was found in two degraded peatlands between

macroporosity and $\log_{10}\alpha$ (**Figure 2.3b**; Supplemental **Table S2.5**). In addition, a negative relationship between macroporosity and n was found for degraded peat (**Figure 2.3c**). Opposingly, a strong positive correlation between macroporosity and the VG parameter n was obtained for pristine peat (**Figure 2.3c**; Supplemental **Table S2.5**; Pearson's correlation coefficient of 0.71).

3.3.2 Pedotransfer functions (PTFs)

The PTFs for hydraulic parameters ($\log_{10}K_s$, θ_s, $\log_{10}\alpha$, and n) of natural and degraded peat soils were established based on soil physical properties (macroporosity, bulk density, and SOM). The best fitted multiple regression models with higher R^2 and lower MSE are given in **Table 2.2**. The results show that adding macroporosity to the PTFs substantially improved the prediction. For instance, the coefficient of determination increases by 0.2 for $\log_{10}K_s$ values if macroporosity is considered. The PTFs for $\log_{10}\alpha$ and n were acceptable for Site 2 with coefficients of determination of 0.51 and 0.62, respectively. For natural peatlands, the PTFs perform better for n than for $\log_{10}\alpha$. **Table 2.2** and Supplemental **Table S2.6** reveal a low performance of PTFs for n and $\log_{10}\alpha$ for extremely degraded peat (Site 3). **Figure 2.4** presents the measured and predicted values of the hydraulic parameters. A high correlation was observed between measured and estimated soil water content with a Lin's Concordance Correlation Coefficient of 0.96 if the total number of samples (1656) is considered (**Figure 2.5**).
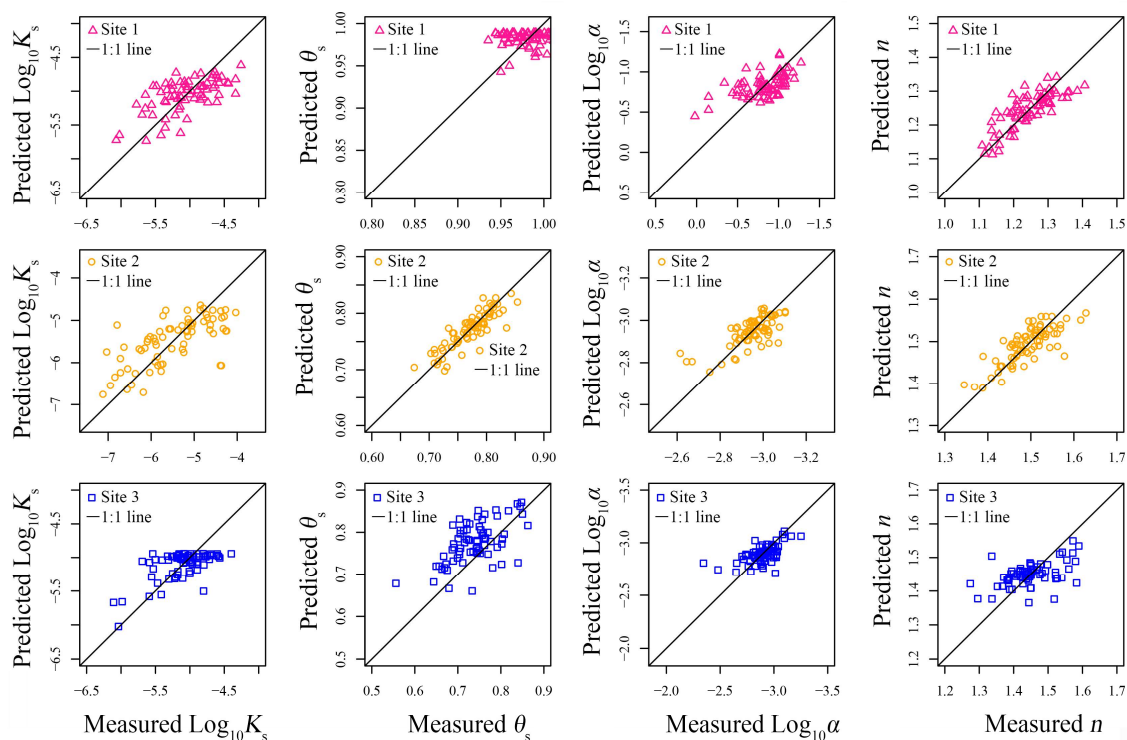
Figure 2.4 Relationship between measured and predicted hydraulic parameters ($\log_{10}K_s$, θ_s, $log_{10}\alpha$, and n) for different peat type (pink: Site 1; orange: Site 2; blue: Site 3).

Table 2.2 Results of the multiple regression analysis in which the hydraulic parameters ($log_{10}K_s$, θ_s, $log_{10}\alpha$, and n) were the dependent variables and the physical properties (macroporosity, MP, vol%; bulk density, BD, g cm^{-3}; organic matter content, SOM, wt%) were the explanatory variable.

Study site	Peat type	Parameter	Model[a][4]	R^2	RSE[b]	DF	MSE	P value
Site 1 (N = 72)	Natural peat	$Log_{10}K_s$	$-4.632 + 9.236 \cdot MP - 64.195 \cdot BD - 8.907 \cdot MP^2 + 368.711 \cdot BD^2$	0.40	0.318	67	0.094	<0.001
		θ_s	$0.767 + 5.610 \cdot BD - 35.390 \cdot BD^2$	0.11	0.027	69	0.001	0.019
		$Log_{10}\alpha$	$-2.611 + 1.868 \cdot MP + 12.994 \cdot BD$	0.32	0.210	69	0.042	<0.001
		n	$1.301 + 0.280 \cdot MP - 2.365 \cdot BD$	0.64	0.041	69	0.002	<0.001
Site 2 (N = 72)	Degraded peat	$Log_{10}K_s$	$-9.816 + 59.825 \cdot MP + 3.452 \cdot BD - 232.621 \cdot MP^2$	0.46	0.608	68	0.349	<0.001
		θ_s	$1.002 - 0.864 \cdot MP - 0.471 \cdot BD$	0.78	0.018	69	0.000	<0.001
		$Log_{10}\alpha$	$-3.147 \cdot 2.366 \cdot MP$	0.51	0.066	70	0.004	<0.001
		n	$1.736 - 1.368 \cdot MP - 0.385 \cdot BD$	0.62	0.034	69	0.001	<0.001
Site 3 (N = 72)	Extremely degraded peat	$Log_{10}K_s$	$-6.323 + 20.508 \cdot MP - 76.092 \cdot MP^2$	0.39	0.264	69	0.067	<0.001
		θ_s	$1.094 - 1.678 \cdot BD + 0.014 \cdot SOM + 1.183 \cdot BD^2 - 0.0002 \cdot SOM^2$	0.37	0.046	67	0.002	<0.001
		$Log_{10}\alpha$	$-3.308 + 2.868 \cdot MP + 0.238 \cdot BD$	0.36	0.113	69	0.012	<0.001
		n	$1.663 - 1.130 \cdot MP - 0.186 \cdot BD$	0.26	0.058	69	0.003	<0.001

[a] Abbreviations: MP, macroporosity; BD, bulk density; SOM, soil organic matter content; K_s, saturated hydraulic conductivity; θ_s, estimated water content at saturation (cm^3 cm^{-3}); α and n, empirical parameters.
[b] Abbreviations: R^2, the coefficient of determination; RSE, Residual standard error; DF, Degrees of freedom; MSE, Mean squared error.

[4] Note: In the original publication of Chapter 2, the symbol "×" in the formula denotes scalar multiplication, not vector multiplication. Thus, the dot symbol "·" is used in the thesis instead.
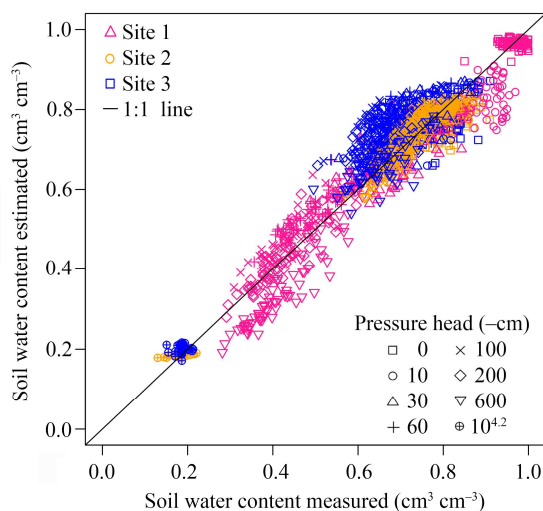
Figure 2.5 Relationship between measured and pedotransfer functions estimated soil water content for all investigated pressure heads.

2.3.3 Spatial variability of hydro-physical properties

Table 2.3 and **Figure 2.6** provide an overview of all optimized semivariogram parameters and the best-fitted model for hydro-physical properties of peat. The optimized models for auto-semivariograms differed between hydro-physical properties. For instance, the best model to depict the semivariogram of $\log_{10}\alpha$ (Site 3) was an exponential model, whereas the Gaussian model was suitable for the semivariogram of SOM (Site 3). The semivariogram models were also affected by soil degradation. For instance, the semivariograms of bulk density for the natural (Site 1) and the extremely degraded peat (Site 3) were best fitted using a linear and Gaussian model, respectively. The quality of fit varies among the various parameters and sites. The R^2 values of fitted models for macroporosity and $\log_{10}K_s$ for Site 3 and SOM at Site 1 are <0.1, while R^2 of other parameters ranged from 0.24 to 0.99 (**Table 2.3**).

A nugget to sill (nugget/sill) ratio of <25%, 25–75% and >75% reflects a strong, moderate, and weak spatial dependence, respectively (Cambardella et al., 1994). In this study, it was found that the SOM content of highly degraded peatlands is strongly spatially dependent according to the given classification scheme. The bulk density of all three peatlands falls into the class "moderately spatially dependent". The kriging analysis and the according 3D map shows that the bulk density varies greatly in space for all sites (Supplemental **Figure S2.2**). The bulk density was found to be high at one edge of the investigated plot, and gradually decreases in a certain direction at all investigated sites (Supplemental **Figure S2.2**). The range of the spatial dependence is, in general, less than 30 m for bulk density (**Table 2.3**). The porosity and macroporosity are only weakly spatially auto-correlated within the observation range.

Table 2.3 Semivariogram parameters of the best-fitted model for all hydro-physical properties.

Study site	Variable	Model[a]	Nugget $C0$	Total sill $C+C0$	Nugget/sill ratio $C0/(C+C0)\times100\%$	Spatial class[b]	Range	R^2	RSS[c]
Site 1	SOM	Lin.	7.81E–01	8.55E–01	91.39	W	25.20	0.086	3.45E–02
	Bulk density	Lin.	1.20E–04	2.00E–04	61.13	M	25.20	0.846	6.86E–10
	Porosity	Lin.	5.50E–04	6.40E–04	86.00	W	25.20	0.212	1.88E–08
	Macroporosity	Lin.	7.07E–03	9.40E–03	75.14	W	32.46	0.290	1.67E–06
	$Log_{10}K_s$	Lin.	1.28E–01	1.63E–01	78.54	W	25.20	0.593	5.24E–04
	$Log_{10}\alpha$	Lin.	4.08E–02	6.83E–02	59.72	M	26.09	0.691	2.29E–04
	n	Lin.	2.72E–03	4.74E–03	57.38	M	25.20	0.760	8.00E–07
Site 2	SOM	Lin.	1.31E+01	1.62E+01	80.56	W	25.20	0.391	9.61E+00
	Bulk density	Lin.	1.15E–03	1.95E–03	59.04	M	25.20	0.766	1.21E–07
	Porosity	Lin.	5.70E–04	7.50E–04	75.96	W	25.20	0.506	1.97E–08
	Macroporosity	Gau.	4.80E–04	7.87E–04	61.07	M	4.68	0.400	2.67E–08
	$Log_{10}K_s$	Exp.	5.00E–02	7.77E–01	6.43	S	3.44	0.450	6.32E–08
	$Log_{10}\alpha$	Lin.	6.58E–03	9.00E–03	73.11	M	25.20	0.414	5.13E–06
	n	Lin.	2.02E–03	2.99E–03	67.56	M	25.20	0.703	2.46E–07
Site 3	SOM	Gau.	8.70E+00	6.84E+01	12.72	S	36.56	0.995	9.36E+00
	Bulk density	Gau.	6.85E–03	1.59E–02	43.08	M	31.47	0.854	9.58E–06
	Porosity	Lin.	2.40E–03	2.80E–03	88.51	W	25.20	0.026	2.34E–06
	Macroporosity	Lin.	9.28E–04	9.55E–04	97.17	W	16.41	0.059	2.35E–09
	$Log_{10}K_s$	Lin.	1.07E–01	1.11E–01	96.40	W	30.50	0.044	2.42E–04
	$Log_{10}\alpha$	Exp.	1.27E–02	2.06E–02	61.78	M	6.07	0.780	8.25E–06
	n	Lin.	3.89E–03	4.62E–03	84.20	W	25.20	0.241	6.14E–07

[a] Abbreviations: Lin., Linear model; Gau., Gaussian model; Exp., Exponential model.
[b] A nugget/sill ratio of <25%, 25–75% and >75% reflects a strong, moderate, and weak spatial dependence, respectively (Cambardella et al., 1994).
[c] Abbreviations: R^2, the coefficient of determination; RSS, residual sum of squares.
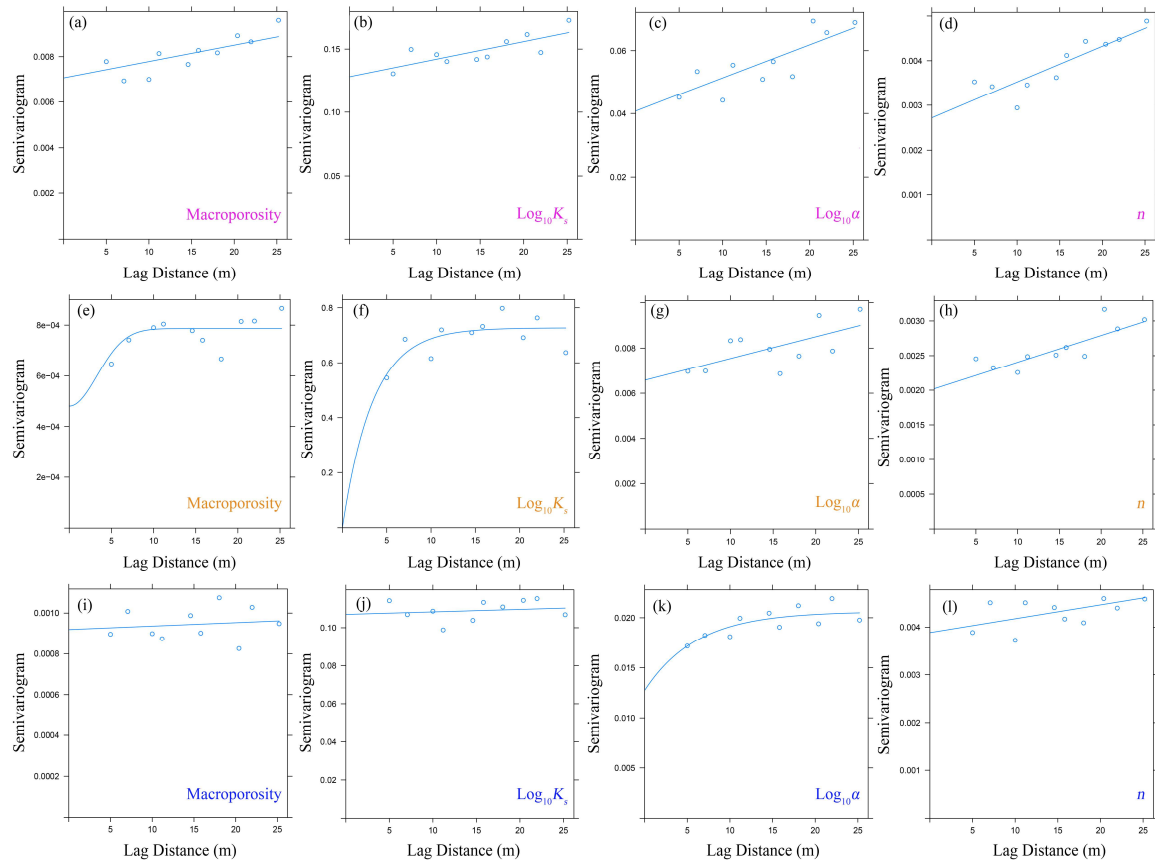
Figure 2.6 Semivariograms (symbols) and fitted model (solid lines) of selected hydro-physical properties (macroporosity, $\log_{10}K_s$, $\log_{10}\alpha$, and n) of three study sites. (pink: Site 1; orange: Site 2; blue: Site 3).

A spatial auto-correlation was observed for K_s and Site 2, but this spatial dependence was weak at the other sites. At extremely degraded peatlands, the high nugget effect for $\log_{10}K_s$ (>95%) suggests spatial independence. The ratio of nugget/sill of VG parameters α and n ranged from 57.38% to 84.20%, indicating that they are weakly to moderately spatially auto-correlated.

2.4 Discussion

2.4.1 Effect of peat degradation on hydro-physical properties

In this study, K_s of pristine peat (8.5×10^{-7} to 5.5×10^{-5} m s^{-1}) is lower than values reported for *Sphagnum* (10^{-3} to 10^{-5} m s^{-1}; Boelter, 1968; McCarter and Price, 2014; Price et al., 2008). However, the K_s of peat decreases substantially with increasing peat decomposition (Letts et al., 2000; McCarter et al., 2020). The peat at Site 1 is classified as hemic peat with values on the von Post scale of H4 – H5 (von Post, 1922). For the hemic peat, the range of K_s is reported to be 10^{-7} to 10^{-4} m s^{-1} (Irwin, 1968; Letts et al., 2000; Morris et al., 2019). The K_s values of peat at Site 2 and Site 3 (7.6×10^{-8} to 9.3×10^{-5} m s^{-1}) are comparable to previous studies for degraded fens (**Figure 2.7**; 10^{-8} to 10^{-5} m s^{-1}; Liu et al., 2016; Kechavarzi et al., 2010; Schwärzel et al., 2006).

40

The values for α and n we found in this study are within the range (although at the lower and upper limit) reported by Liu and Lennartz (2019a) and Wallor et al. (2018; **Figure 2.7**).
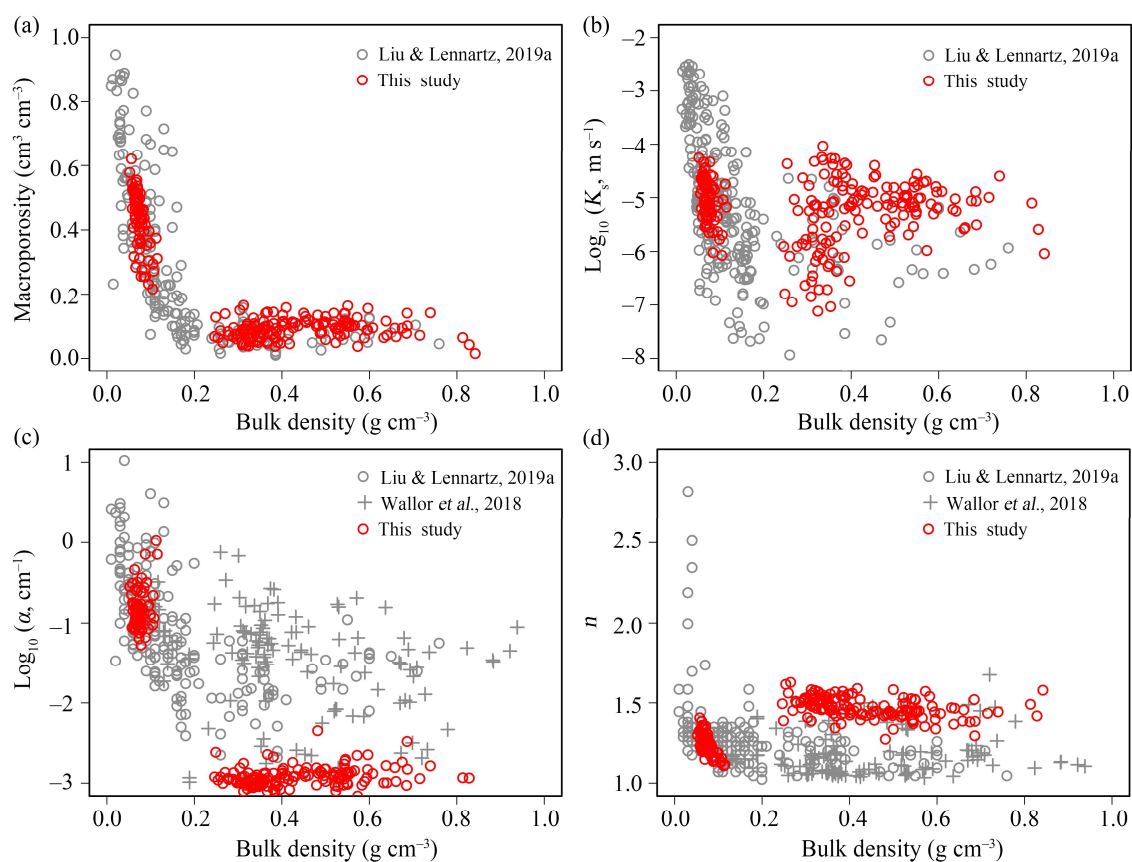
Figure 2.7 The relationship between (a) bulk density and macroporosity; (b) bulk density and $\log_{10}K_s$; (c) bulk density and van Genuchten parameter $\log_{10}\alpha$; (d) bulk density and van Genuchten parameter n. The grey cycles represent values from Liu and Lennartz (2019a) and the grey plus symbols are derived from Wallor et al. (2018) for topsoils (8–23 cm).

The observed low CV for SOM of natural peat matches the outcome of a study reported by Bruland and Richardson (2005), who found that the SOM of constructed and restored wetlands showed a greater spatial variability than that of a natural wetland. The CV values for $\log_{10}K_s$ at Site 1 and Site 3 (89% and 70%) are lower than the values reported for fen peat (98%; Baird, 1997). The high CV (149%) for $\log_{10}K_s$ at Site 2 is comparable to values of mineral soils (100% to 200%; Warrick and Nielsen, 1980). It is obvious that land use and management of peatlands enhance the spatial variability of soil properties, but the influence varies depending on the individual site.

Soil bulk density has been used as a proxy for peat decomposition and degradation (Frolking et al., 2010; Liu et al., 2020a). In this study, the relation between bulk density and macroporosity

as well as $\log_{10}K_s$ (**Figure 2.7**) follow functions reported earlier by Liu and Lennartz (2019a) and Liu et al. (2020a). The macroporosity decreases substantially with increasing bulk density from 0.01 to approximately 0.2 g cm^{-3}, and then remains almost constant with a further increase in bulk density (Liu and Lennartz, 2019a).

Although previous studies reported that the $\log_{10}K_s$ of bogs is strongly negatively correlated with bulk density (Liu and Lennartz, 2019a; Morris et al., 2019; Silins and Rothwell, 1998), only a moderate negative correlation (Pearson's correlation coefficient of 0.42, $p < 0.001$; Supplemental **Table S2.5**) was observed here (**Figure 2.7**). It is possible that microhabitats (*e.g.*, roots from vegetation/trees/shrub) play an important role in the permeability of peat (Morris et al., 2019). For both degraded sites, a very weak correlation was found between bulk density and $\log_{10}K_s$ (**Figure 2.7**; Supplemental **Table S2.5**), indicating that the permeability of degraded peat is not controlled by degradation processes once a threshold (bulk density > 0.2 g cm^{-3}) has been reached.

2.4.2 Macroporosity, K_s, and VG parameters

Macropores play a critical role in water flow and solute transport in peat soils (Holden et al., 2012; McCarter et al., 2020; Rezanezhad et al., 2016). However, the definition of macropore varies for peat. Baird (1997) and Holden et al. (2001) quantify the microporous volume and macropore flow from tension infiltrometer tests (–3 cm pressure head; pores with equivalent diameter > 1 mm). They observed that the macropore flow contributed 21% to 78% of the total surface water flow in peatlands. Liu et al. (2016) identified macropores (pore diameter > 0.1 mm) of peat from dye tracer experiments. Weber et al. (2017), McCarter et al. (2020), and Branham and Strack (2014) defined the macropore as pores with an equivalent diameter > 300 μm. They calculated the macroporosity as the differences between total porosity and water content at –10 cm H$_2$O pressure head. For *Sphagnum*, the microporous volume represents inter-plant pores (Weber et al., 2017). However, the reported definitions are mostly for natural or less decomposed (degraded) peat. For highly and extremely degraded peat (bulk density > 0.2 g cm^{-3}), the macroporosity is always estimated from the differences between total porosity and volumetric water content at –60 cm H$_2$O pressure head (Schwärzel et al., 2002; Schinlder et al., 2003; Wallor et al., 2018), corresponding to pores with an equivalent diameter > 30 μm (contact angle of 52°; Gharedaghloo and Price, 2019). One possible reason for diverging definitions is that values of macroporosity (pore diameter > 300 μm) are quite small for highly and extremely degraded peat (<1 vol%; Liu et al., 2020a) and are difficult to quantify.

The functional relations between macroporosity and $\log_{10}K_s$ differ between natural and drained peatlands, which is possibly linked to the origin and formation of macropores in peat. The

Sphagnum peat contains abundance of macropores due to the structure of *Sphagnum* plant and vascular plant roots (McCarter et al., 2020; Weber et al., 2017). The macropores are reported to be inter-connected (Quinton et al., 2009). However, the *Sphagnum* moss can alter the pore structure to suit its specific physiological growth (Goetz and Price, 2015), therefore, the pore size distribution varies greatly within the broad classification of *Sphagnum*. The hydraulic conductivity of *Sphagnum* is controlled by pore hydraulic radius (Quinton et al., 2008; Rezanezhad et al., 2010). Peatland drainage causes subsidence and carbon mineralization, which substantially decreases macroporosity and increases the micropore fraction (Silins and Rothwell, 1998; Rezanezhad et al., 2010; McCater et al., 2020; Liu et al., 2020a). Meantime, the pore tortuosity increases and pore connectivity declines (Rezanezhad et al., 2010). In contrast, the sedge-derived peat is more susceptible to decay than *Sphagnum* derived peat (Hájek et al., 2011). In degraded fen peat (Site 2 and Site 3), the peat forming plant materials (*e.g.*, Sedge) vanishes and the number of smaller pores, hence tortuosity, increases due to long-term drainage. In degraded peat soils, (secondary) bio-pores (roots and earthworm channels) and cracks are forming the macroporous network (Liu and Lennartz, 2015; Liu et al., 2016). Thus, the geometry of the macropores (*e.g.*, pore connectivity, pore throat diameter) differs between pristine and degraded peat, which may be the cause for differences in relationships between macroporosity and K_s.

Additionally, VG parameters are likewise affected by macroporosity. Interestingly, the VG parameter *n* presented an opposite correlation with macroporosity in degraded and natural peat soils in this study. It is possible that in degraded peat soils, a large fraction of small aggregates decreases the macroporosity but increases soil water retention, which corresponds to a greater *n* value (Guber et al., 2004). In contrast, the reason for a positive correlation between the macroporosity and the VG parameter *n* of the natural peat is unknown, we, however, assume that a more pronounced pore connectivity in pristine peat may have caused interrelations between macroporosity and the parameter *n*.

2.4.3 Pedotransfer functions

The performance of PTFs for K_s is low when only soil bulk density and SOM considered, especially for Site 2 and Site 3 ($R^2 < 0.2$; Supplemental **Table S2.7**). It seems that soil structure, known to strongly impact K_s, are insufficiently reflected by bulk density and SOM (Wagner et al., 2001), especially in the case of highly degraded peat soils (Liu and Lennartz, 2019a; Wallor et al., 2018). A continuous macroporous network (*e.g.*, cracks, earthworm holes or root channels) may have little impact on soil bulk density and SOM, but may substantially alter K_s (Beven and Germann, 1982; Holden, 2009; Liu et al., 2016).

We could show that the inclusion of macroporosity into the PTFs substantially improves the prediction of K_s (Supplemental **Table S2.7**). This finding indicates that soil macroporosity is a crucial driver of K_s, which has been overlooked in previous peatland studies (Liu and Lennartz, 2019a; Wallor et al., 2018; Wösten et al., 1999). Recent studies by Zhang et al. (2019) and Zhang et al. (2020) similarly indicate that adding macroporosity to PTFs substantially improves the prediction of hydraulic conductivity of mineral soils. It should be noted that the models developed in this study still have a relatively high RSE and low R^2 (<0.5). One possible reason for the comparable weak performance is that not only macroporosity but also pore connectivity and pore throats might have a strong control on water flow in soils (McCater et al., 2020; Liu et al., 2016; Rezanezhad et al., 2010; Schlüter et al., 2020).

The performance of PTFs for n is better than for α for pristine peat (**Table 2.2**). It should be, however, noted that the VG parameter α was more sensitive to large macropores (equivalent circular diameter of 300 µm) than to the macroporosity as defined in this study (> 30 µm; Supplemental **Figure S2.3**), because the air entry value refers to the minimum matric suction at which air starts to enter the largest pores in the soil (Nemati et al., 2002). This finding has been well documented in previous studies (Liu and Lennartz, 2019a; Thompson and Waddington, 2013). The performance of PTFs on VG parameters (α and n) declines with peat degradation. It is very likely that the mineral fraction of up to 70 wt% in extremely degraded peat plays an important role in soil pore size distribution. In future studies, additional information on the particle size distribution of the mineral fraction (Wösten et al., 1999) as well as the carbon to nitrogen ratio (Morris et al., 2015) shall be scrutinized to possibly improve the prediction power of PTFs for hydro-physical properties of peat.

2.4.3 Spatial dependence of hydro-physical properties

The nugget is the semivariance at a lag distance of zero, representing the measurement errors or microvariability of the variable over smaller distance than the sampling interval (Nielsen and Wendroth, 2003). The high nugget/sill ratio for SOM at Site 1 and Site 2 (> 80%), indicate that the microvariability of SOM cannot be detected at the scale of the sampling interval (5 m). The smallest nugget/sill ratio of SOM and bulk density was observed for Site 3 (extremely degraded peatland), indicating that sampling interval is suitable to analyze spatial variability of the two variables. The stronger spatial dependence of SOM and bulk density assists in generating a relatively accurate soil map or carbon storage map through kriging for extremely degraded peatlands. Recently, Negassa et al. (2019) observed a rather strong spatial dependency of SOM (nugget/sill ratio < 1%; topsoil) at a rewetted peatland. Given the fact that the rewetted peatland had a same development and drainage history as Site 2 of this study (Ahmad et al., 2021), it

seems that the land management (*e.g.*, rewetting) play an important role for the spatial distribution of soil properties.

The high nugget/sill ratio (> 75%) for K_s at Site 1 and Site 3, reveals that the microheterogeneity of K_s in the fields cannot be detected from the sampling interval as chosen in this study. A pure nugget effect (nugget/sill ratio > 95%; spatially independent) for K_s and macroporosity at Site 3 indicate a random distribution pattern (unpredictable) of the two variables (Webster and Oliver, 2001). The random distribution pattern (pure nugget effect) has also been reported for K_s of mineral soil at a scale of 6 m (Banton, 1993). It is interesting to note that the nugget/sill ratio of macroporosity and K_s are comparable for each individual site. We take this as a hint that the spatial distribution pattern of soil structure (*e.g.*, macroporosity) controls the spatial distribution pattern of K_s.

For all study sites, the nugget/sill ratio values for VG parameters are mostly less than 75%. This finding confirms results of Gnatowski et al. (1996), who studied drained peatlands in Poland and came up with nugget/sill ratios for VG parameters ranging from 46.4% to 77.1%. For mineral soils, as mentioned by Wang et al. (2015) and Biswas and Si (2009), a moderate or strong spatial dependence was found for both VG parameters α and n.

For mineral soils, the exponential or gaussian model have always been used to describe the semivariogram of K_s (Biswas and Si, 2009; Gwenzi et al., 2011; Iqbal et al., 2005; Zhang et al., 2020). However, we find the semivariograms of $\log_{10}K_s$ are depicted well by exponential model at Site 2 and linear model at Site 1 and Site 3. The linear model was also chosen to describe the semivariograms of $\log_{10}K_s$ by Gnatowski et al. (1996) for a drained peatland site.

2.5 Conclusions

Soil hydraulic and physical properties were determined on a grid basis for natural and drained peatlands. Pedotransfer functions were established to estimate saturated hydraulic conductivity and van Genuchten parameters using easily available soil properties. Spatial dependence of soil hydro-physical properties was investigated employing geo-statistical models. We found that the adding of soil structure information (macroporosity) to pedo-transfer-functions substantially improves the prediction of all hydro-physical parameters, especially for degraded peat. However, additional soil parameters such as the texture of the mineral fraction should be considered to even further improve the predictions in future studies. The hydro-physical properties of peat soils are weakly to strongly auto-correlated according to the nugget/sill ratio. The SOM content of highly degraded peat is strongly spatially dependent in opposite to other tested soil properties. It is possible that soil management produced, for instance, micro depressions, which conserved SOM longer than at other locations at the same site. From the data of this study, which

was collected at a meter to tens of meter scale, the stage of peat degradation impacts the spatial variability significantly. In order to better understand the overall functions of peatlands in hydrology and ecology, it is necessary to extend the work to a larger scale to get an in-depth knowledge of the hydraulic and physical properties of peatlands. With the so far obtained results, we are in a better position to more accurately parameterize spatially distributed (for instance 2D) hydrological models for peatlands. In addition, spatial patterns of soil properties may play an important role in peatland restoration projects. Thus, it is important in hydrological modeling and meta studies of peatland to take these spatial differences of soil properties into account as it appears that the human influence (*e.g.*, climate change, cultivation history) could significantly alter the inherent properties of the soil at a certain scale.

Data availability statement

Data available on request from the authors.

Competing interests

The authors declare that they have no competing interests.

Authors' contributions

MW and HL conceived the study, carried out the field work, and conducted laboratory experiments. MW analyzed the data and drafted the manuscript. HL edited the manuscript. BL provided funds and edited the manuscript. All authors read and approved the final manuscript.

Acknowledgements

3

Experimental Study 2

Effect of Anisotropy on Solute Transport in Degraded Fen Peat Soils

Miaorun Wang[1], Haojie Liu[1]*, Dominik Zak[2, 3], Bernd Lennartz[1]

[1]Faculty of Agricultural and Environmental Sciences, University of Rostock, Justus-von-Liebig-Weg 6, 18059 Rostock, Germany

[2]Department of Bioscience, Aarhus University, Silkeborg, 8600, Denmark

[3]Department of Chemical Analytics and Biogeochemistry, Leibniz-Institute of Freshwater Ecology and Inland Fisheries, Berlin, 12587, Germany

*Corresponding author: Haojie Liu (email: haojie.liu@uni-rostock.de)

Graphical Abstract
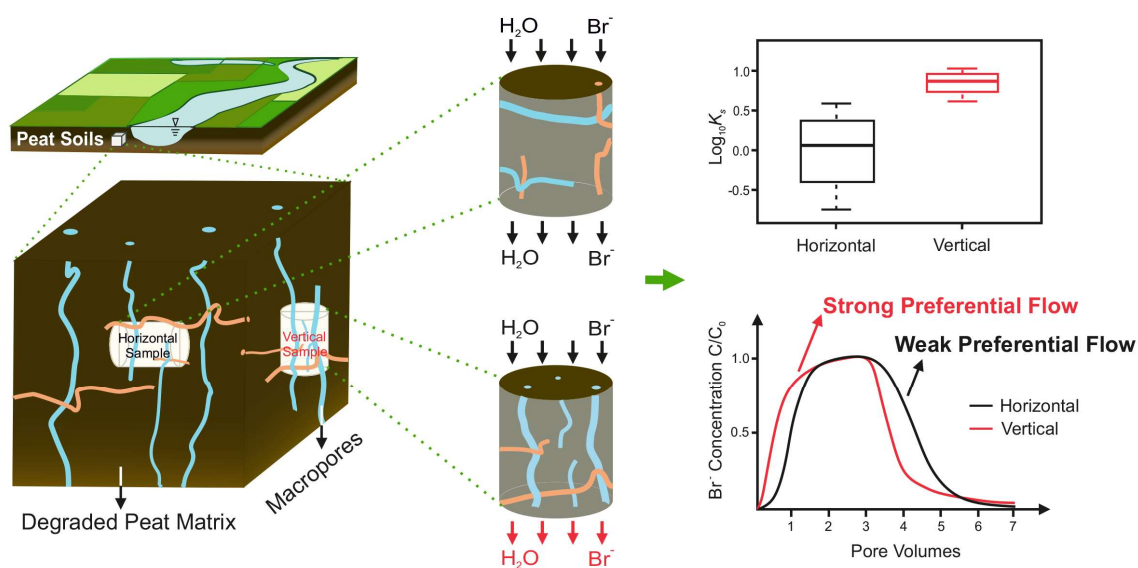
Abstract

Peat soils are heterogeneous and anisotropic porous media. Compared to mineral soils, there is still limited understanding of physical and solute transport properties of fen peat soils. In this study, we aimed to explore the effect of soil anisotropy on solute transport in degraded fen peat. Undisturbed soil cores, taken in vertical and horizontal direction, were collected from one drained and one restored fen peatland both in a comparable state of soil degradation. Saturated hydraulic conductivity (K_s) and chemical properties of peat were determined for all soil cores. Miscible displacement experiments were conducted under saturated steady state conditions using potassium bromide as a conservative tracer. The results showed that 1) the K_s in vertical direction (K_{sv}) was significantly higher than that in horizontal direction (K_{sh}), indicating that K_s of degraded fen peat behaves anisotropically; 2) pronounced preferential flow occurred in vertical direction with a higher immobile water fraction and a higher pore water velocity; 3) the 5% arrival time (a proxy for the strength of preferential flow) was affected by soil anisotropy as well as study site. A strong correlation was found between 5% arrival time and dispersivity, K_s and mobile water fraction; 4) phosphate release was observed from drained peat only. The impact of soil heterogeneity on phosphate leaching was more pronounced than soil anisotropy. The soil core with the strongest preferential flow released the highest amount of phosphate. We conclude that soil anisotropy is crucial in peatland hydrology, but additional research is required to fully understand anisotropic effects on solute transport.

3.1 Introduction

Peatlands cover only 3% of global land area, but store about 10% of global fresh water and play a major role in water purification (Rezanezhad et al., 2016; Xu et al., 2018). More than 40% of European peatlands have been anthropogenically altered and are degraded because of drainage and climate change, losing their ecosystem functions as water storage and water filter (Joosten, 2009; Lennartz and Liu, 2019). Several studies have been conducted on hydro-physical (Holden et al., 2004; Liu and Lennartz, 2019a), and solute transport properties (Liu et al., 2017; McCarter et al., 2019), as well as pore water chemistry (Tiemeyer et al., 2017; Zak and Gelbrecht, 2007) of degraded peat soils and their significant impact on carbon and nitrogen cycles could be demonstrated (Baird et al., 2009; Limpens et al., 2008; Liu et al., 2019). Water flow and solute transport in peat soils are controlled by soil physical properties (*e.g.,* soil organic matter content, pore structure), but are also affected by pore water chemistry (Kettridge and Binley, 2010; Ours et al., 1997).

Compared with mineral soils, peat has some unique features such as a high organic matter content and a low bulk density (Eggelsmann et al., 1993). The total porosity of peat could be as high as almost 100 vol% (Paavilainen and Päivänen, 1995). Peat soils exhibit highly heterogeneous and anisotropic properties. For instance, the saturated hydraulic conductivity (K_s) may range over about two orders of magnitude for a specific peat soil (Cunliffe et al., 2013; Liu and Lennartz, 2019a). The anisotropic behavior of K_s has been studied over the last two decades (Beckwith et al., 2003; Cunliffe et al., 2013; Gharedaghloo et al., 2018; Kruse et al., 2008; Lewis et al., 2012; Liu et al., 2016; Morris et al., 2019; Rosa and Larocque, 2008). Gharedaghloo et al. (2018) investigated the pore structure of bogs and found that K_s is isotropic locally at pore-scale, but becomes anisotropic after upscaling to core-scale because of the layered structure of the peat. Liu et al. (2016) conducted a dye tracer experiment for non-layered fens and the pore network indicated that the connected macropores are predominantly vertically or horizontally orientated depending on sampling site leading to an anisotropic K_s. In addition, the anisotropic nature of peat is highly affected by soil degradation (Liu et al., 2016). In more pristine peat, the dominant flow and transport direction depends on the peat forming process and how dying plants and decaying plant materials were deposited. With advancing peat degradation, the volume fraction of macropores and pore connectivity decrease significantly (Liu et al., 2016; Liu and Lennartz, 2019a) resulting in a relative isotropic structure of highly degraded peat soils (Kechavarzi et al., 2010; Liu et al., 2016). In addition, cracks occur in peat soils in dry summers, which may increase macroporosity of peat soils (Holden et al., 2001).

Tracer techniques provide useful tools to explore water flow and solute transport processes in soils (Leibundgut et al., 2009).Various forms of tracers such as isotope [18]O (Ronkanen and

Kløve, 2007), salt (Baird and Gaffney, 2000; Hoag and Price, 1997; Liu et al., 2017; McCarter et al., 2018), fluorescence (Ramirez et al., 2016), and dyes (Liu et al., 2016; Liu and Lennartz, 2015; Mooney et al., 1999) have been applied onto peat in the field or laboratory. All tracer experiments verify that preferential flow is a common phenomenon in peat soils. The occurrence of preferential flow is in accordance with the dual porosity structure of peat (active porosity and dead-end pores; Rezanezhad et al., 2016). Undecomposed plant material (*e.g.,* woody or *phragmites* structures) as well as biopores such as root channels may serve as preferential flow pathways in peat soils (Liu et al., 2016; Liu and Lennartz, 2015; Mooney et al., 1999). Recent studies indicated that pronounced preferential flow mainly occurs in highly degraded peat soils (Liu et al., 2017). In this study, we define preferential flow as all phenomena where water, solutes and colloids move along certain pathway, while bypassing a fraction of soil matrix (Hendrickx and Flury, 2001). In other words, the soil contains a fraction of dead-end pores and/or immobile water (Liu et al., 2017; Vanderborght and Vereecken, 2007).

The determination of solute transport properties and the identification of preferential flow also depend on the properties of applied tracers. Chloride as well as tritium tracers were retarded in less degraded peat soils (Liu et al., 2017; McCarter et al., 2018). The adsorption of chloride onto peat was found to be related to its concentration (*e.g.,* >500 mg L^{-1}, McCarter et al., 2018) and the soil organic matter content (Sheppard et al., 2009). Although there are several studies on solute transport in peat soils (Hoag and Price, 1997; Rezanezhad et al., 2012; Liu et al., 2017; McCarter et al., 2018), to our knowledge, there is no discussion on the effect of soil anisotropy on solute transport and strength of preferential flow in degraded fen peat soils in the existing literature.

Preferential flow pathways may enhance contaminant (*e.g.,* phosphate) transport to groundwater leading to eutrophication in adjacent water bodies (Forsmann and Kjaergaard, 2014; Ronkanen and Kløve, 2009). Macropores are likely the primary transport pathways for phosphorus (P) in soils (Geohring et al., 2001; Simard et al., 2000; Vidon and Cuadra, 2011). Previous studies also indicated the P accumulation along macropore flow pathways (Backnäs et al., 2012; Gächter et al., 1998; Ronkanen and Kløve, 2009). The P adsorption/desorption behavior was found to differ between soil material forming macropores (pore wall material) and the soil matrix (Hansen et al., 1999; Jensen et al., 2002). However, little is known about the effect of anisotropic soil structure on phosphate leaching in degraded fen peat. In this study, miscible displacement experiments were conducted on horizontally and vertically collected fen peat. The objectives of the study were to quantify the effect of peat anisotropy 1) on solute transport properties, 2) the preferential flow phenomenon, and 3) on the release of phosphate from degraded fen peat.

3.2 Material and Methods

3.2.1 Study sites and soil sampling

The two study sites are located at approximately 10 km south of the city of Rostock on either side of the Warnow River in Mecklenburg-Western Pomerania in Germany (Site 1, 54°00' N, 12°07' E; Site 2, 54°00' N, 12°08' E). The riparian fen peat soils at both sites have been artificially drained since the 19th century by ditches, which caused the mineralization of the organic matter predominantly of the upper few decimeters of soil horizons. The soil degradation process is accompanied by a loss of soil organic matter and an increase in soil bulk density. Both experimental sites have been under agricultural use mainly as grassland. Whereas Site 1 is still subject to agricultural use, Site 2 has been restored by blocking ditches and converted into a nature reserve (Ministry of the Environment Mecklenburg-Vorpommern, 2003) since the 1990s. The dominant botanical species forming the fen peat at both sites are sedge (*Cyperaceae*) and alder (*Alnus*). The fraction of wood-based material is approximately 30%. For each of the two study sites, an area of 8 m × 8 m was selected for sampling. Eight sampling profiles (0.5 m × 0.5 m) were randomly chosen within the area and excavated down to a depth of 0.4 m. Two samples (one vertical and one horizontal) were taken from each pit at 0.4 to 0.5 m depth. For the horizontal samples, the pit was first deepened down to 0.6 m in order to take the sample exactly from the same depth as the vertical sample.

All 32 undisturbed soil cores (diameter of 8 cm, length of 5 cm) from both sites were collected by cutting the soil with a sharp knife in front of cylinder, which was slowly inserted into the soil in either horizontal or vertical direction. Cylinders were then removed from the soil by excavating a large soil block, from which the cylinders were carefully removed (Liu and Lennartz, 2019b). The soil cores were sealed on both ends with lids and tape before being neatly placed in a cool box and transported back to the laboratory.

3.2.2 Hydro-physical properties

Before the determination of saturated hydraulic conductivity (K_s), all peat cores were slowly saturated upwards from the bottom with tap water; tap water was chosen because its electrical conductivity (EC, 650 µS cm^{-1}) is within the range of EC found for groundwater at the study sites (EC, 400 to 700 µS cm^{-1}). A previous study on samples from the same sites proved that the determination of K_s was not sensitive to water salinity and EC variations (Gosch et al., 2018). A constant-head upward-flow method was used to measure K_s in the laboratory at constant temperature of approximately 15°C (Supplemental **Figure S3.1**; Kruse et al., 2008; Liu et al., 2016). The chosen upward flow method allowed an exact adjustment of the hydraulic head and according to flow rates. Low flow rates are desired to avoid internal erosion and gas bubble

entrapment. The K_s values have always been standardized to 10°C employing the equation provided by Klute (1965; see also Kruse et al., 2008).

Soil dry bulk density was determined by oven-drying the samples at 105 °C for 24h. After drying, the soil mass was related to the volume of the sample cylinder. The organic matter content was measured in the laboratory by the loss on ignition (LOI) method (550 °C; ISO 22476-3:2005). Soil particle density was determined following standard measurements (ISO 17892-3:2004). Total porosity was estimated based on bulk density and particle density. Macroporosity was estimated by the differences between total porosity and volumetric water content at –60 cm H_2O pressure head assuming a contact angle of 0° for degraded fens (equivalent pore diameter of 50 μm; Liu and Lennartz, 2019a; Schindler et al., 2003). Recently, a contact angle of 51.7° was reported for bogs by Gharedaghloo and Price (2019). In this context[5], the macroporosity determined by our method corresponds to pores with an equivalent diameter >30 μm. However, differences in parent plant material as well as mineral content between bogs and fens do not allow to directly transfer the observation between peat types. The basic physical properties of the investigated peat are shown in **Table 3.1**.

Table 3.1 Physical properties of the peat soils investigated, mean (standard deviation), N = 8.

Study site	von Post	SOM content	Bulk density	Particle density	Total porosity	Macro-porosity[a]	Total phosphate content	Redox sensitive phosphate content
	–	wt%	g cm^{-3}	g cm^{-3}	vol%	vol%	mg g^{-1}	mg g^{-1}
Site 1	H5	81.2 (3.0)	0.19 (0.01)	1.56	87.8 (0.6)	10.16 (0.03)	0.78 (0.06)	0.03 (0.004)
Site 2	H5	88.1 (0.7)	0.19 (0.01)	1.51	87.4 (0.1)	4.34 (0.01)	0.44 (0.03)	0.01 (0.005)

[a] Macroporosity was calculated by the difference between total porosity and volumetric soil water content at –60 cm H_2O pressure head.

3.2.3 Miscible displacement experiments and strength of preferential flow

For each site, 6 soil cores (3 in vertical and 3 in horizontal direction) from 3 soil profiles were chosen to conduct the miscible displacement experiments. The chosen soil samples reflect the range of observed K_s values. Before the onset of the transport experiment, soil cores were saturated with background water (sodium chloride (NaCl) solution, EC = 500 μS cm^{-1}, pH = 6) using a peristaltic pump from bottom to top at a slow and constant flow rate of q = 0.1 cm h^{-1}

---

[5] Note: This sentence was added in this Chapter and did not appear in the corresponding published paper. To maintain methodological consistency throughout the thesis, the calculation of macroporosity in peat soils across all three experimental chapters followed the same approach. This decision was made due to the inherent ambiguity and complexity in defining the equivalent pore diameter for macropores in peat soils.

for 7 days to purge gas bubbles that may block flow (**Figure 3.1**; Skaggs et al., 2002). The background water was prepared using deionized water (Skaggs et al., 2002) with low gas content (2.3 mg O_2 L^{-1}; Gosch et al., 2018). Considering the low gas content in the background water, the effect of the dissolved gases on the experiment can be ignored. Thereafter, potassium bromide (KBr) tracer (KBr and NaCl solutions, concentration of Br 100 mg L^{-1}, EC=500 μS cm^{-1}, pH=6) was applied with a constant flux of q = 0.34 cm h^{-1} (within the range of observed K_s values) for 44 hours, which corresponds to three pore volumes (V/V_0; V, outflow volume; V_0, water-filled pore volume under fully water saturated conditions). Solute solution was collected by fraction samplers.

The experimental set-up is illustrated in **Figure 3.1**. Porous plates were placed onto both ends of the soil cores to ensure a homogenous distribution of the tracer. There is a small space above/below the porous plates, which enables mixing and homogenous entrance of the tracer into the column.
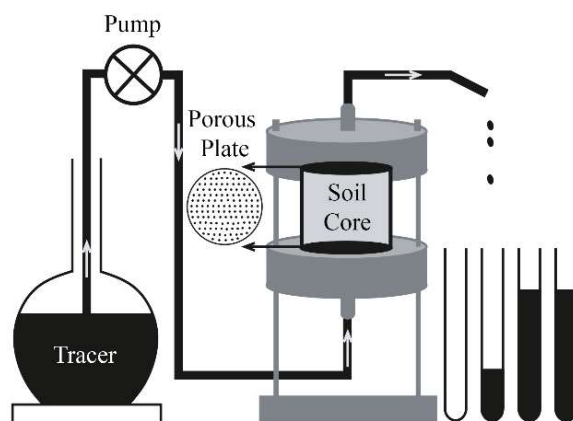
Figure 3.1 Set-up for miscible displacement experiments in intact peat soil samples.

The obtained bromide breakthrough curves (BTCs) were corrected by subtracting a blank-BTC (tracer experiment on the empty set-up), which removed the effect of dead volumes originating from tubes, porous plates *etc.* (Supplemental **Figure S3.2**; Rajendran et al., 2008; Rezanezhad et al., 2012). The corrected BTCs were plotted as relative concentration[6] (C_e/C_i; C_e, effluent concentration; C_i, influent concentration) against exchanged pore volumes (volume of peat soil core occupied by fluid). The well-established mobile-immobile model (MIM) was used to evaluate the obtained BTCs (van Genuchten and Wierenga, 1976). In the MIM model, according to the

---

[6] Note: As mentioned in Chatper 1, to avoid confusion with the abbreviations of spatial statistical parameters "nugget/sill ratio", the abbreviations for "the effluent concentration" and "the influent concentration" have been modified in this thesis to C_e and C_i, respectively, from the abbreviations (C and C_0) used in the corresponding publication of Chapter 3.

pore water flow velocity (v), two pore regions are distinguished: mobile region ($v_m > 0$) and immobile region ($v_{im} = 0$). In its dimensionless form, the solute transport in a dual porosity medium can be given as Equations (3.1) to (3.3):

$$\beta R \frac{\partial C_m}{\partial T} + (1 - \beta)R \frac{\partial C_{im}}{\partial T} = \frac{1}{Pe} \frac{\partial^2 C_{im}}{\partial X^2} - \frac{\partial C_m}{\partial X} \qquad (3.1)$$

$$(1 - \beta)R \frac{\partial C_{im}}{\partial T} = \omega(C_e - C_{im}) \qquad (3.2)$$

$$Pe = \frac{v_m L}{D_m} \qquad (3.3)$$

where T is dimensionless time, X is space coordinate, β is the fraction of the mobile soil water zone (dimensionless), ω is the mass transfer coefficient between the mobile and immobile regions (dimensionless). R is the retardation factor. The effluent concentration (C_e) was normalized with the influent concentration (C_i). The Péclet number expresses the ratio of advection to diffusion, where v_m is pore water velocity in the mobile zone, D_m is hydrodynamic dispersion coefficient of the mobile zone, ($D_m = D/\beta$; $L^2\ T^{-1}$). D is hydrodynamic dispersion coefficient for the entire sample (Radcliffe and Simunek, 2010; Skaggs et al., 2002; Toride et al., 1999).

In this study, the MIM model parameters (β, D, and ω) were calibrated using the nonlinear least-squares parameter optimization program CXTFIT (Toride et al., 1999) with R fixed at 1. The parameter v was fixed at the average pore water velocity (0.383 cm h^{-1}). During the optimization procedure, the parameters D, β, and ω were initially set to 1.0, 0.5 and 0.2, respectively (Toride et al., 1999) and thereafter several estimation trials were conducted with adjusting the initial values (van Genuchten et al., 2012). The upper and lower boundaries of the three fitted parameter values as obtained from the numerical inverse model are provided in the Supplemental **Table S3.1**. The parameters were eventually chosen based on the highest coefficient of determination and lowest mean square error.

Additionally, the strength of preferential flow was estimated based on the 5% bromide mass arrival time, when 5% of the applied bromide has been recovered in the effluent (Knudby and Carrera, 2005; Koestel et al., 2013, 2011; Norgaard et al., 2018; Soares et al., 2015). The lower the 5% arrival time, the stronger the preferential flow with limited residence time (Koestel et al., 2011; Soares et al., 2015).

3.2.4 Chemical and statistical analysis

For all collected effluent samples, bromide concentrations were determined by ion chromatography employing a Metrohm 930 Compact IC Flex. Soluble reactive phosphorus concentration in the outflowing water from soil cores, in following denoted as soil leachate, was analyzed after filtration with syringe filters (0.45 μm pore size) by using the molybdenum blue method (Cary IE; Varian, Darmstadt, Germany) according to Murphy and Riley (1962). For the determination of total phosphorus (TP), dried peat (60°C, 48 hours) was homogenized in a stainless-steel mill. The TP content of peat was determined as SRP after an acid digestion procedure (circa 10 mg dry sample + 2 mL 10 M H_2SO_4 + 4 mL 30% H_2O_2 + 20 mL deionized water at 160°C for 2 h). TP of sites 1 and 2 was 0.78 mg g^{-1} and 0.44 mg g^{-1}, respectively (N = 8, 40–50 cm depth). To determine the amount of P, which can be mobilized under anoxic conditions by redox processes, 10 g of fresh (*i.e.*, wet) peat were extracted with a 0.11 M bicarbonate-dithionite solution in accordance with Zak et al. (2008). The dissolved P in the filtered extract solution (syringe filters; 0.45 μm pore size) was analyzed with ICP-OES (Inductively coupled plasma - optical emission spectrometry).

A t-test was used to test the differences in K_s (as $\log_{10} K_s$) of peat between horizontal and vertical directions and the differences in total phosphate between sites. The effect of sites and sampling direction on 5% arrival time was tested using a general linear model. All the statistical analyses were performed using R (R Core Team, 2015) and the level of significance was set to 0.05.

3.3 Results and Discussion

3.3.1 The anisotropy of saturated hydraulic conductivity

The obtained K_s values of the investigated peat soils ranged over two orders of magnitude from 0.06 to 15.01 cm h^{-1}, which is within the previous reported range of values from 0.6 to 71.8 cm h^{-1} (Kruse et al., 2008; Liu and Lennartz, 2019a) of fen peat. The K_s values differed significantly between the two sites ($p<0.001$) although the peat of both sites is in a comparable degradation stage (*e.g.,* bulk density, von Post humification and organic matter content are within the same range). The geometric mean value of K_s of peat at Site 1 is 2.25 cm h^{-1}, which is significantly higher than that of the peat from Site 2 (geometric mean of K_s = 0.23 cm h^{-1}). The observed differences in K_s are most likely related to the macroporosity (equivalent pore diameter of >50μm; Schindler et al., 2003), which was found to be 0.13 ± 0.03 vol% (mean ± standard deviation) for Site 1 and 0.05 ± 0.01 vol% for Site 2 (**Table 3.1**). The finding indicates that the K_s of degraded peat is more sensitive to macroporosity rather than bulk density and von Post humification. The latter two properties did not differ between both sites (**Table 3.1**).
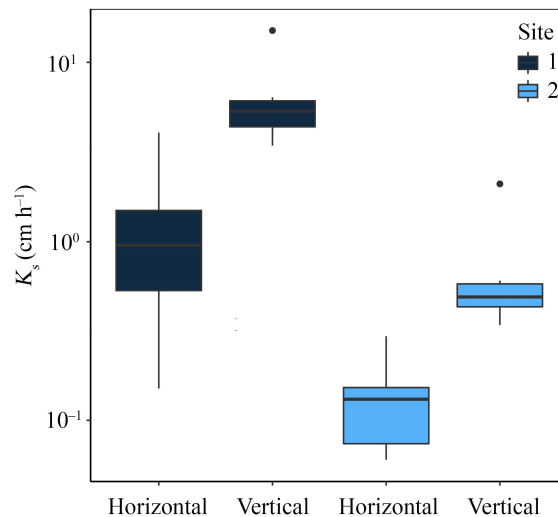
Figure 3.2 Boxplot of saturated hydraulic conductivity (K_s, cm h^{-1}) of peat soils in horizontal and vertical directions at Site 1 and Site 2.

At both sites, significant differences were observed in K_s between vertical (K_{sv}) and horizontal (K_{sh}) flow directions ($p < 0.01$), indicating that K_s is anisotropic in the case of the two investigated sites (**Figure 3.2**). The anisotropy ratio ($\log_{10}(K_{sh}/K_{sv})$); Beckwith et al., 2003; Liu et al., 2016) of sites 1 and 2 are −0.80 and −0.41, respectively, suggesting that K_{sv} was higher than K_{sh}. Previous studies on peat soils have reported that K_{sh} could be greater than K_{sv} (Beckwith et al., 2003; Lewis et al., 2012; Cunliffe et al., 2013), whereas the opposite results ($K_{sv} > K_{sh}$) were also obtained (Kruse et al., 2008; Liu et al., 2016; Surridge et al., 2005). The anisotropy ratio found in this study is within the earlier reported range of values from −1.1 to 2.4 (Beckwith et al., 2003; Kruse et al., 2008; Liu et al., 2016). The hydraulic anisotropy of peat soils is related to the orientation of undecomposed plant materials (Chason and Siegel, 1986; Liu et al., 2016; Surridge et al., 2005). At both investigated sites, undecomposed wood branches (alder) were predominantly vertically orientated (Liu et al., 2016; Liu and Lennartz, 2015), facilitating water movement in vertical direction.

3.3.2 Breakthrough curves

The measured and corrected BTCs are presented in **Figure 3.3**. For all the soil cores, the recovery of the applied tracer was greater than 95%, which is indicative for a negligible bromide adsorption (Kleimeier et al., 2014). All BTCs exhibited an early breakthrough with relative concentrations C_e/C_i of 0.5 occurring at less than one pore volume. Four BTCs of vertically collected peat samples (S1V2, S2V3, S2V1, and S2V3) had a much earlier breakthrough and a longer tailing than the other eight BTCs, indicating a strong preferential flow (Liu et al., 2017; Rezanezhad et al., 2012).
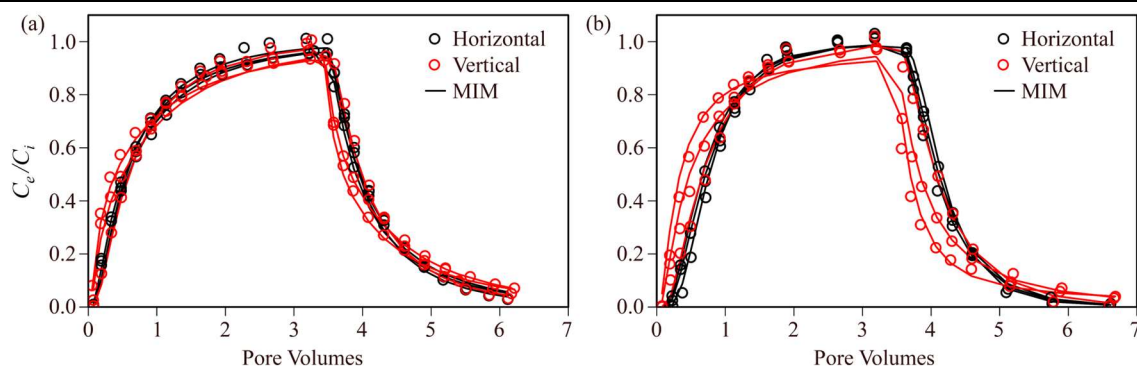
Figure 3.3 Corrected bromide breakthrough curves plotted as relative concentrations (C_e/C_i) against number of pore volumes: (a) Site 1; (b) Site 2. The solid lines show the mobile and immobile model (MIM).

In this study, both the CDE model (only D was fitted; Supplemental **Table S3.2**) and the MIM model (D, β, and ω were fitted) were employed to describe the measured BTCs (**Table 3.2**). The MIM model adequately described all BTCs with a higher fitting criterion of $R^2 > 0.99$ and smaller mean square error than those obtained with the CDE model (Supplemental **Table S3.3**), although for two BTCs the R^2 was above 0.99 using the CDE model. For most of the BTCs, the errors between simulated and observed values are normally distributed (Supplemental **Figure S3.3** and **Table S3.4**). The corrected Akaike information criterion (AICc; Burnham and Anderson, 2002); Supplemental **Table S3.3**) suggests that the MIM model did not over-fit the BTCs. The calibrated soil transport parameters of the MIM model, 95% confidence limits and the covariance matrix for fitted parameters of each sample are shown in **Table 3.2** and **Table 3.3** and Supplemental **Table S3.5**, respectively.

Table 3.2 Values of calibrated parameters from mobile-immobile model.

Study sites	Direction of Samples	Column	β^a –	ω –	v_m (cm h^{-1})	D_m (cm^2 h^{-1})	λ (cm)	R^2 –	MSE –
Site 1	Horizontal	S1H1	0.83	0.00^b	0.46	1.25	2.69	0.995	0.0008
		S1H2	0.94	0.00	0.41	1.36	3.34	0.995	0.0006
		S1H3	0.88	0.00	0.43	1.62	3.73	0.997	0.0004
	Vertical	S1V1	0.88	0.00	0.44	1.13	2.59	0.996	0.0006
		S1V2	0.48	1.69	0.80	3.30	4.10	0.993	0.0008
		S1V3	0.56	1.55	0.69	4.59	6.69	0.995	0.0005
Site 2	Horizontal	S2H1	0.86	0.02	0.44	0.35	0.78	0.995	0.0009
		S2H2	0.82	0.01	0.47	0.61	1.29	0.996	0.0007
		S2H3	0.86	0.01	0.44	0.53	1.20	0.998	0.0004
	Vertical	S2V1	0.83	0.03	0.46	1.92	4.15	0.986	0.0017
		S2V2	0.87	0.00	0.44	0.73	1.65	0.991	0.0014
		S2V3	0.52	0.14	0.74	2.52	3.42	0.982	0.0025

^{a} Abbreviations: β, mobile water fraction; ω, mass transfer coefficient; v_m, pore water velocity in mobile region; D_m, dispersion coefficient in mobile region; λ, dispersivity; R^2, the coefficient of determination; MSE, mean squared error.
^{b} The value of mass transfer coefficient with 0.00 means <1.00e−07.

Table 3.3 Upper and lower boundaries of the 95% confidence limits for fitted parameters (D, β, and ω) in mobile and immobile models.

Column	D [a] ($cm^2\,h^{-1}$)		β		ω	
	lower	upper	lower	upper	lower	upper
S1H1	0.83	1.23	0.77	0.88	0.10e−06	0.10e−06
S1H2	1.04	1.52	0.87	1.01	0.10e−06	0.10e−06
S1H3	1.23	1.64	0.83	0.93	0.10e−06	0.10e−06
S1V1	0.83	1.16	0.83	0.93	0.10e−06	0.10e−06
S1V2	1.07	2.07	0.33	0.62	0.50	2.90
S1V3	2.02	3.11	0.41	0.70	0.24	2.85
S2H1	0.22	0.38	0.82	0.91	0.00	0.07
S2H2	0.40	0.60	0.78	0.94	0.00	0.03
S2H3	0.40	0.53	0.83	0.89	0.00	0.03
S2V1	0.58	2.60	0.57	1.00	0.00	0.19
S2V2	0.46	0.81	0.80	0.93	0.10e−06	0.10e−06
S2V3	0.20	2.43	0.31	0.73	0.00	0.30

[a] Abbreviations: D, dispersion coefficient; β, mobile water fraction; ω, mass transfer coefficient.

The covariance matrix suggests that the transport parameters were not highly correlated in the majority of the samples. The calibrated D_m ranged from 0.34 to 4.59 $cm^2\,h^{-1}$ with a dispersivity (λ) ranging from 0.78 to 6.69 cm. The β value ranged from 0.48 to 0.94, indicating the presence of immobile water and preferential flow. The ω parameter was found to vary from 0 to 1.70. The ranges of all the optimized parameters (D, β, and ω) are within the span reported by Liu et al. (2017) for fen peat. The β values we found here generally smaller than those reported by Simhayov et al. (2018), who estimated that the values of β was almost equal to one but with a great variance. One possible reason for the differences in parameter values may be that the fen peat soils in their study were less degraded (bulk density of 0.12 $g\,cm^{-3}$) compared to soils in this study (bulk density of 0.20 $g\,cm^{-3}$). Larger variability of optimized parameters (*e.g.*, β and v_m) were observed for vertical samples, which is consistent with the results from Liu et al. (2017). In their study, transport properties (vertically collected) varied considerably as determined on samples collected from one depth. However, in our study here the variability of D, β, and ω for the horizontal samples are generally smaller than those reported by Liu et al. (2017) for highly degraded peat soils. The variability of calibrated parameter values is always greater for the vertical transport situation, which suggests that the spatial heterogeneity is greater in vertical direction than in horizontal direction. We take that as a hint that preferential flow is more likely to occur in vertical direction because of enhanced soil structure heterogeneity. In future studies, a range of velocities should be adjusted in flow-through experiments to derive definite conclusions.

In general, samples that were taken in vertical direction had a lower β, but higher v_m, ω, and D_m values than those of horizontal samples. Differences in solute transport properties between horizontal and vertical samples are more important than effects that are related to sampling sites. As mentioned above, four vertical samples from both sites (cores S1V2, S1V3, S2V1 and S2V3; **Table 3.1**) exhibit a pronounced preferential flow. The average value of β, as an indicator of the amount of mobile water, of these four soil cores was 0.60 ± 0.16 (mean ± standard deviation), which was significantly lower (stronger preferential transport) than that for the other eight soil with 0.87 ± 0.04 ($p<0.001$). As a consequence, these four vertical cores had a significantly higher pore water velocity of the mobile zone ($v_m = v/\beta$) than other soil cores ($p < 0.001$). The immobile water fraction of the mentioned four vertical cores was approximately 0.36 cm^3 cm^{-3}; this soil water volume is not participating in the convective transport of bromide.

For most soil cores, a low mass transfer coefficient ($\omega \approx 0$) was observed. In the MIM model, a small ω value (≈ 0) indicates that the immobile soil water region does not participate in transport and is not accessible for solutes (Radcliffe and Simunek, 2010). However, almost all β values are less than 0.9, which indicates that the tested peat soil is a dual porosity medium. Minor immobile water fractions ($\beta > 0.9$) may result from isolated pores or unavoidable experimental and calculation errors.

3.3.3 Strength of preferential flow

The 5% arrival time of bromide mass ranged from 6.15 to 10.28 hours. Significant differences in 5% arrival time were observed between sites ($p = 0.0095$; general linear model) and between soil sampling directions ($p = 0.024$). A significantly lower 5% bromide mass arrival time was observed for the samples from drained site (average of 7.58 hours) than those from the restored site (average of 9.46 hours). Moreover, a later 5% bromide mass arrival time was observed for horizontal samples (9.29 hours) than for vertical samples (7.75 hours). Thus, the strength of preferential flow is orientation-dependent and associated with land management. Given that no significant differences were observed in soil physical properties between sites and between orientations (*e.g.*, bulk density or von post humification), the 5% tracer mass arrival time or preferential flow respectively, is not predictable using physical properties of peat only.

The 5% arrival time has a strong negative linear relationship with dispersivity ($R^2 = 0.83$, $p < 0.001$; **Figure 3.4a**), moderate positive linear relationship with β ($R^2 = 0.39$, $p < 0.05$; **Figure 3.4b**) and moderate negative linear relationship with $\log_{10}K_s$ ($R^2 = 0.51$, $p < 0.01$; **Figure 3.4c**). These relationships generally point out that the assumption of the MIM is correct and that high dispersivity values and a large fraction of immobile water are in accordance with pronounced preferential transport situations.
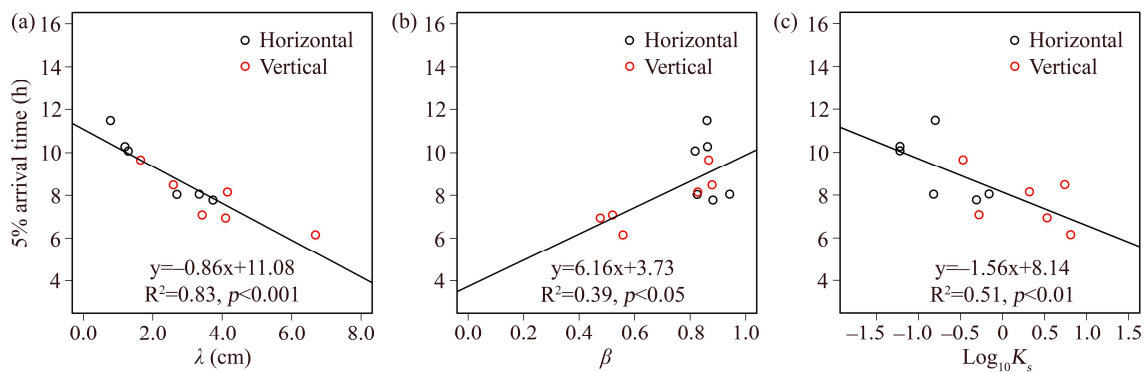
Figure 3.4 The correlation between 5% arrival time and (a) dispersivity (λ); (b) the fraction of mobile region (β); (c) saturated hydraulic conductivity ($\log_{10}K_s$).

The dispersivity may affect the values of 5% arrival time, however, it is hard to distinguish the effect of dispersivity on 5% arrival time when preferential flow occurs. For instance, in several soil cores (*e.g.,* S1V2, S1V3, and S2V3), the larger immobile water fraction suggests that pronounced preferential flow occurred although the soil dispersivity is high. Previous studies (*e.g.,* Koestel et al., 2011; Soares et al., 2015) have proved that 5% arrival time is the best indicator for the strength of preferential flow when preferential flow occurred. In this study, the corrected BTCs indicate that (strong/weak) preferential flow occurred in all soil cores. Therefore, the 5% arrival time was used to evaluate the BTCs. The results obtained here for peat soils for the first time are in consistence with observations made for mineral soils (Paradelo et al., 2013; Shaw et al., 2000; Soares et al., 2015; Vervoort et al., 1999). The occurrence of significant preferential flow in samples, which exhibit higher K_s and lower β values, suggests that a few macropores are active in solute transport and these macropores are, likewise, ensuring the water conductance under statured condition (Gonçalves et al., 2001).

Overall, solute transport in peat soils was affected by the anisotropic structure of peat. The effect of soil anisotropy on solute transport properties is not as clear as on K_s. The greater variability of the transport parameters and the lower 5% arrival time of vertical samples suggest that preferential flow is more likely to occur in vertical directions. It is more likely to encounter preferential transport situations in locations where K_s is high. In cases where K_s values are greater in horizontal than in vertical direction (Beckwith et al., 2003; Lewis et al., 2012), preferential flow can, likewise, be stronger in horizontal direction.

3.3.4 Phosphate leaching

Fertilization and ongoing soil organic matter mineralization of drained peatland results in a high TP content of the investigated peat soils (**Table 3.1**). This is also reflected in a high P release

61

rate from artificially drained peat soils. For most soil cores from the drained site, a high phosphate concentration (approximately 2 mg P L⁻¹; **Figure 3.5**) was observed in the leachate. The high P leaching concentrations are in consistent with recent studies by Parvage et al. (2015) and Riddle et al. (2018), who observed a range of phosphate concentrations in the effluent from 0.36 to 10.3 mg P L⁻¹ for organic soils. For the studied fen peat, the redox sensitive P accounts for only less than 4% of total P, which is a small fraction if compared to values reported in other studies (>15%; Forsmann and Kjaergaard, 2014). We assume that other more loosely-bound P fractions (*e.g.,* water-extractable P) dominated the released P of 3 to 18 mg during the relatively short experimental period of 3 days. The observed P concentrations in leachate from the drained and degraded peatland were 1000 times higher than the suggested threshold concentration of P (0.01 mg L⁻¹) to avoid eutrophication of surface waters. The strong preferential flow in vertical direction may enhance P release to surface or ground water.
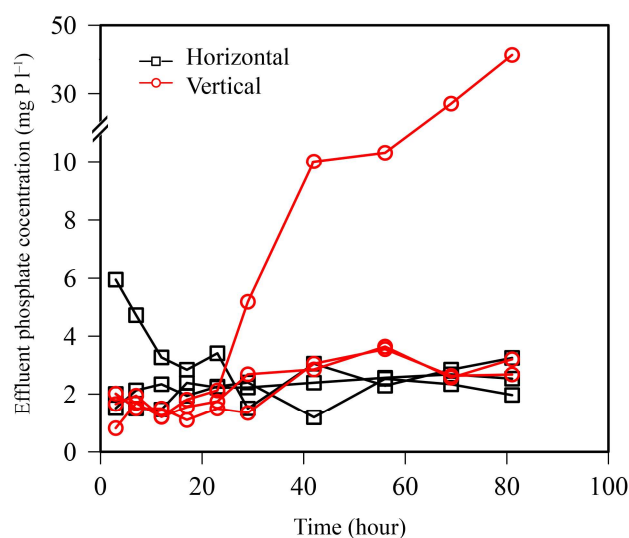
Figure 3.5 Effluent phosphate concentrations of peat soils in horizontal and vertical directions from drained peatland (Site 1).

There was no significant difference in the amount of released P between samples from the vertical and horizontal direction. A negative but statistically not significant correlation was observed between the mass of released P and 5% arrival time (Pearson's correlation coefficient of 0.76; *p* = 0.07). The very high P release rate as observed for one sample may be related to the P accumulation in preferential flow pathways. In cases where P content is high in the topsoil because of agricultural usage, it may be transported and enriched along preferential pathways (Backnäs et al., 2012; Gächter et al., 1998; Ronkanen and Kløve, 2009) and the preferential transport tracks enhanced P leaching (Backnäs et al., 2012; Fuchs et al., 2009; Gächter et al., 1998). In summary, the findings of this study provide evidence that solute transport and the

release of P are mainly related to soil heterogeneity and the effect of anisotropy needs more detailed consideration.

3.4 Conclusions

The effects of soil anisotropy on water flow and solute transport in degraded fen peat soils were explored. We assume that the more abundant vertically orientated macropores lead to a significantly higher K_s in the vertical than in the horizontal direction, whereas the solute transport properties as derived from breakthrough curves (BTCs) are moderately affected by soil anisotropy. The 5% arrival time as the indicator for the strength of preferential flow is influenced by soil anisotropy as well as the site management (drained versus restored). It is likely that the macroporous structure that facilitates water conductance also (rapidly) conveys dissolved compounds. The great variance of leached amount of phosphate indicates that phosphate transport is more determined by soil heterogeneity than anisotropy. In this study the solute transport behavior was investigated on samples that were either taken in horizontal or vertical direction. Both sample groups have their own heterogeneity, which may have overwritten the anisotropy effect. In future studies, an approach should be developed that allows for transport tests in various directions on the same sample. It should be likewise noted that soil anisotropy as well as preferential flow and compound release are scale-dependent and related to the degree of water saturation.

4

Experimental Study 3

The Influence of Microtopography on Soil Carbon Accumulation and Nutrient Release from a Rewetted Coastal Peatland

Miaorun Wang[1], Haojie Liu[1*], Fereidoun Rezanezhad[2], Dominik Zak[3,4], Bernd Lennartz[1]

[1]Faculty of Agricultural and Environmental Sciences, University of Rostock, Justus-von-Liebig-Weg 6, 18059 Rostock, Germany

[2]Ecohydrology Research Group, Department of Earth and Environmental Sciences and Water Institute, University of Waterloo, Waterloo, ON, Canada

[3]Department of Ecoscience, Aarhus University, Aarhus, Denmark

[4]Department of Ecohydrology and Biogeochemistry, Leibniz-Institute of Freshwater Ecology and Inland Fisheries, Berlin, Germany

 *Corresponding author: Haojie Liu (email: haojie.liu@uni-rostock.de)

Graphical Abstract
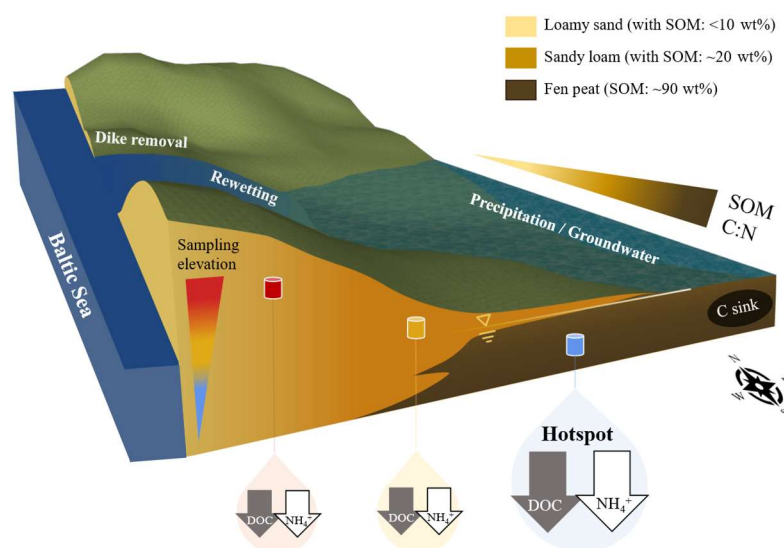
Abstract

Coastal peatlands have been frequently blocked from the sea and artificially drained for agriculture. With an increasing awareness of ecosystem functions, several of these coastal peatlands have been rewetted through dike removal, allowing sea water flooding. In this study, we investigated a recently rewetted peatland on the Baltic Sea coast with the aim to characterize the prevailing soils/sediments with respect to organic matter accumulation and the potential release of nutrients upon seawater flooding. Eighty disturbed soil samples were collected from two depths at different elevations (–0.90 to 0.97 m compared to sea level) and analyzed for soil organic matter (SOM) content and carbon:nitrogen (C:N) ratio. Additionally, nine undisturbed soil cores were collected from three distinct elevation groups and used in leaching experiments with alternating freshwater and Baltic Sea water. The results demonstrated a moderate to strong spatial dependence of surface elevation, SOM content, and C:N ratio. SOM content and C:N ratio were strongly negatively correlated with elevation, indicating that organic matter mineralization was restricted in low lying areas. The results also showed that the soils at low elevations release more dissolved organic carbon (DOC) and ammonium (NH_4^+) than soils at high elevations. For soils at low elevations, higher DOC concentrations were observed when flushing with freshwater, whereas higher NH_4^+ concentrations were found when flushing with brackish water. Recorded NH_4^+ concentrations in organic-rich peat reached 14.82 ± 9.25 mg L^{-1}, exceeding Baltic seawater (e.g., 0.03 mg L^{-1}) by two orders of magnitude. A potential sea level rise may increase the export of NH_4^+ from low-lying and rewetted peat soils to the sea, impacting adjacent marine ecosystems. Overall, in coastal peatlands, geochemical processes (e.g., C and N cycling and release) are closely linked to microtopography and related patterns of organic matter content of the soil and sediments.

4.1 Introduction

Coastal wetlands as "blue carbon" reservoirs only comprise 15% of the global natural wetland area but contribute substantially to global carbon sequestration (Davidson et al., 2018, 2019). The importance of soil properties and carbon pool has been acknowledged in the process of stabilizing and bolstering the coastal wetland ecosystem (Berkowitz et al., 2018), because the belowground soil carbon pool contains 50%–90% of the blue carbon stored in the various types of coastal wetlands (Howard et al., 2017). However, coastal wetlands have also been seriously disturbed by diking or drainage for industrial and agricultural purposes (Lemly et al., 2000; Newton et al., 2012). These anthropogenic activities have resulted in global as well as regional loss or degradation of coastal wetlands, thereby threatening water quality, emitting significant amounts of greenhouse gases (*e.g.*, carbon dioxide, CO_2) and reducing soil carbon accumulation (DeLaune and White, 2012; Zhao et al., 2016). Hence, more attention to minimizing greenhouse gas emission has heightened the need for wetland restoration and maintaining ecological safety (Zou et al., 2022).

Soil organic matter (SOM) and its stoichiometry, *e.g.*, the carbon:nitrogen (C:N) ratio, are used to estimate C and N stocks in soils, and in particular the C:N ratios are commonly used as a proxy of soil quality and/or greenhouse gas emission (*e.g.*, Yao et al., 2022). They also affect soil physical, hydrological, chemical, and biological properties, such as water retention capacity, cation exchange capacity (CEC), nutrient cycling, and pollutant absorption (Fließbach and Mäder, 2000; Klemedtsson et al., 2005; Ramos et al., 2018; Wattel-Koekkoek et al., 2001). It is unambiguous that inland mires as natural growing peatlands are characterized by high SOM content (> 30% of dry mass), low bulk density, large porosity and a high C:N ratio (Leifeld et al., 2020; Liu and Lennartz, 2019a; Rezanezhad et al., 2016), and changes in these parameters can provide insight into the peat degradation processes (Leifeld et al., 2020; Liu et al., 2019; Wallor et al., 2018; Wang et al., 2021) Nevertheless, coastal peatlands (*e.g.*, marshes and salt marshes), a subcategory of coastal wetlands, contain a considerable mineral fraction of sediment (Pratolongo et al., 2018). These so-called "peat" soils are occasionally also described as organogenic sediments formed primarily by freshwater plants growing in terrestrial ecosystems (peatlands) or marine systems with a high mineral content (Waller and Kirby, 2021). Research into soil properties in coastal wetlands including the peatlands is a complex task due to the high spatial heterogeneity formed by both marine and terrestrial processes.

The spatial distribution of the SOM content and the C:N ratio in different soil types has been effectively detected by geostatistical analysis and is now well established, as indicated by numerous studies undertaken at regional and ecosystem scale (Kumar et al., 2012; Mabit and Ber-

nard, 2010; Negassa et al., 2022; Watt and Palmer, 2012; Zhang et al., 2016). The above-mentioned studies have demonstrated that both SOM and C:N are pronouncedly spatially heterogeneous, being influenced by long-term (> 100–1000 years) predominant factors like topography, soil texture, hydrological regime, and natural vegetation and by short-term ecological disturbances such as land management in recent decades. In coastal wetlands, microtopography (*i.e.*, elevation), functioning as a crucial element of promoting ecosystem functions, has been found to be significantly associated with soil properties (Ahmad et al., 2020; Diamond et al., 2021; Osland et al., 2018; Saintilan and Rogers, 2013). For instance, a strong negative correlation between elevation and SOM was observed for a coastal wetland in Germany (Ahmad et al., 2020). However, in some other studies, the relation between elevation and organic C stock was positive or neutral because of other driving factors, *e.g.*, geomorphic setting and plant productivity (Hayes et al., 2017; Osland et al., 2018).

Regarding the influence of rewetting on both inland and coastal peatlands, numerous studies have focused on greenhouse gas emissions (Günther et al., 2020; Hahn et al., 2015; Liu et al., 2020b; Pönisch et al., 2023), microbial activities (Weil et al., 2020; Zak et al., 2019), soil parameters (Ahmad et al., 2020; Gosch et al., 2018), and the growth of vegetation (Batistel et al., 2022; Schwieger et al., 2022). However, only few studies exist investigating the effect on water quality of organic-rich coastal ecosystem (*e.g.*, coastal peatland) following rewetting with either salt or freshwater (Ardón et al., 2013; Liu and Lennartz, 2019b; Pönisch et al., 2023). It has been shown that the dissolved organic carbon (DOC) and ammonium (NH_4^+) release are critical processes to consider when rewetting coastal peatlands, where both can contribute positively and negatively to ecosystem services and are highly responsive to environmental changes (Audet et al., 2020; Bowen et al., 2020; Sheng et al., 2015; Tobias and Neubauer, 2009; Zerbe et al., 2013). It is challenging to project the effects of alternating salinity on DOC and NH_4^+ release as changes in water level, salinity or pH may individually or collectively alter trends in soil water DOC and NH_4^+ concentrations (Chow et al., 2003; Kalbitz et al., 2000; Kreuzburg et al., 2020; Liu and Lennartz, 2019b; van Dijk et al., 2015). However, the potential nutrient leaching from rewetted coastal peatlands that are substantially impacted by microtopography remains unknown.

In this study, we investigated a recently rewetted peatland located on the Baltic Sea coast, aiming to characterize the prevailing soils/sediments with respect to carbon accumulation and the potential release of DOC and NH_4^+ upon rewetting with brackish water. The specific objectives of this study are to: 1) investigate the relationship between SOM and microtopography (*i.e.*, elevation), 2) estimate the potential release of DOC and NH_4^+ upon rewetting with either brackish water or fresh water in areas with different elevations, and 3) evaluate the effect of microtopography on nutrient release.

4.2 Materials and Methods

4.2.1 Study sites and soil sampling

The "Polder Drammendorf" coastal fen peatland (54°22'23.4"N, 13°14'27.2"E) is located on the Rügen Island, Germany, situated 12 km from the center of Stralsund City in the Federal State of Mecklenburg-Western Pomerania (**Figure 4.1**). The study area covers approximately 14.6 ha, and the surface elevation ranges from approximately –1.2 m to 1.2 m relative to sea level. Historically, the area was created as a landscaped habitat on the coast, including watered areas, alternating wet-dry salt marshes, brackish reeds, and peatlands (Levermann, 2019). From 1962, the entire area has been protected from Baltic Sea floods by dikes, and a drainage system was developed. The areas were primarily used as agricultural land and grazing pasture for more than fifty years (Levermann, 2019). At the low-lying area, the groundwater level was close to the surface of the land (LUNG, 2006; Supplemental **Figure S4.1**). As a part of the coastal landscape transformation project "Renaturation Polder Drammendorf", the site was rewetted in winter of 2019 by removing the dikes and it is now completely flooded by Baltic Sea water.
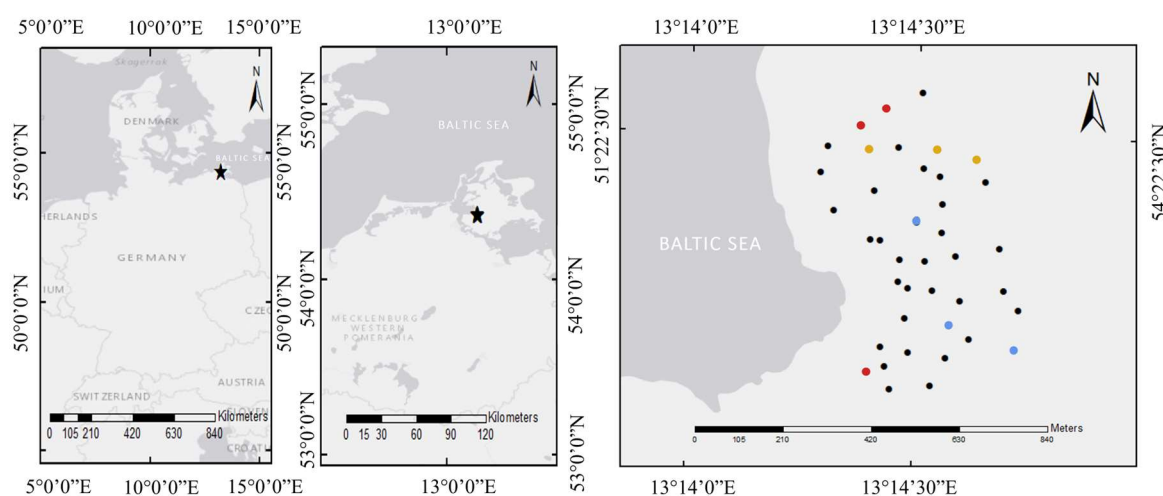
Figure 4.1 Location of the coastal peatland study site on the Rügen Island in Germany and the peat soil sampling areas. The undisturbed peat cores were collected from nine locations with three elevation group (Red dots: Group A; Yellow dots: Group B; Blue dots: Group C) and disturbed peat samples (black and colored dots) were collected from topsoil (10–15 cm depth) and subsoil (40–45 cm depth).

To conduct this study, a random sampling design was employed, resulting in the marking of 40 sampling locations within the study site. For accurate measurements, a microtopographic survey was carried out at each marked location, utilizing Real Time Kinematic (RTK) GPS technology (Leica GS14 GSM) to obtain precise surface elevation measurements. Subsequently, a total of 80 disturbed soil samples were collected from two different depths at each of the marked

locations. These soil samples were analyzed to investigate spatial heterogeneity and determine essential soil properties, such as SOM content and C:N ratios (**Figure 4.1**; 40 samples from 10–15 cm depth and the remaining from 40–45 cm depth). During the same sampling time, a total of 18 undisturbed soil cores were collected from 9 of 40 locations to determine soil hydraulic and physical properties. These soil cores (in Plexiglas rings of 5 cm length, 4.2 cm inside diameter and 5 cm outside diameter) were divided into three elevation groups based on surface elevation analysis (**Figure 4.1**; red dots: Group A, yellow dots: Group B; blue dots: Group C; topsoil sampling depth 10–15 cm, subsoil sampling depth 40–45 cm). From the 18 undisturbed soil cores, 9 of them were selected for nutrient leaching experiment (**Figure 4.2**) that considered sampling elevations with significant differences (Group A: elevation > 0.6 m, 10–15 cm depth; Group B: –0.1 < elevation < 0.1 m, 10–15 cm depth; Group C: elevation < –0.60 m, 40–45 cm depth). All collected soil samples were covered by lids and transported to the laboratory in a cool container.
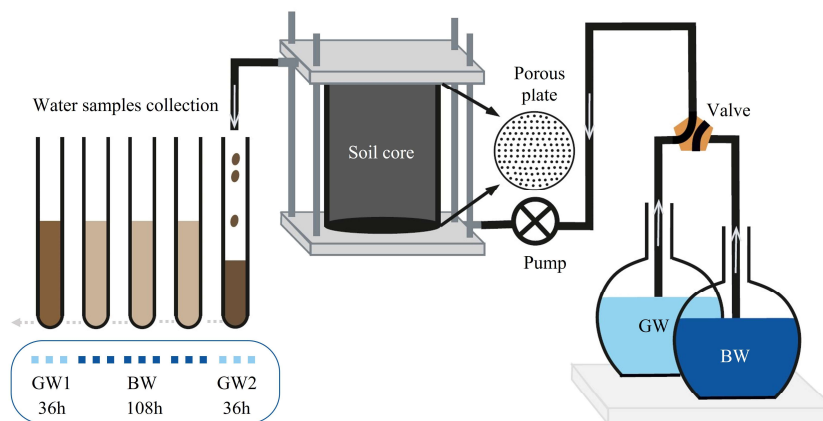
Figure 4.2 Schematic diagram of the flow-through reactor set-up for the leaching experiment. The experiment was conducted under three phases: GW1: groundwater; BW: Baltic seawater; GW2: groundwater (GW1 and GW2 are identical).

4.2.2 Nutrient leaching experiment

A flow-through reactor set-up (**Figure 4.2**) was used for a nutrient leaching experiment to measure the release of DOC and NH_4^+ from the undisturbed soil under environmental conditions (for more details about the flow-through reactor the readers are referred to Gosch et al., 2019; Kleimeier et al., 2017; Pallud et al., 2007). The reactor contained an undisturbed soil core with its Plexiglas ring. Positioned above and beneath the soil column are the 1 µm pore size glass fiber filters. The reactor is effectively sealed using polyvinyl chloride (PVC) plates and O-rings, secured tightly with stainless steel screws. A total of nine soil columns were divided into three rounds of leaching experiments, with three reactors being operated simultaneously in each round. The reactors were connected to a peristaltic pump via tubing with an inner diameter of

1.5 mm. The input solutions of artificial groundwater (GW) and brackish water (BW) were alternately supplied from the bottom to the top of the reactor column with a constant flux of 0.29 cm h^{-1} imposed by the peristaltic pump. Groundwater was mimicked by a sodium chloride (NaCl) solution made from demineralized water adjusted to an electrical conductivity (EC) of 2.55 mS cm^{-1}, a pH value of 4.7 and a low oxygen level of 2.3 mg O_2 L^{-1}, corresponding to the field groundwater chemical conditions. The brackish water was obtained from the Baltic Sea and its EC, pH and sodium (Na^+), chloride (Cl^-), sulfate (SO_4^{2-}), DOC, and NH_4^+ concentrations were 13.89 mS cm^{-1}, 4.5, 2282 mg L^{-1}, 4332 mg L^{-1}, 556.8 mg L^{-1}, 5.14 mg L^{-1}, 0.037 mg L^{-1}, respectively (Metrohm 930 Compact IC Flex; Herisau, Switzerland).

The soil columns were flushed first with GW for approximately 36 hours (phase: GW1) and then by BW for around 108 hours (phase: BW). The same GW flushing was repeated in the subsequent 36 hours (phase: GW2). Outflow samples were collected every 6 hours by a fraction collector and were analyzed for concentrations of DOC and NH_4^+. After filtering the outflow samples through a pre-washed cellulose mixed esters membrane (pore size: 0.45 μm), the DOC and NH_4^+ concentrations were measured using DIMATOC® 2000 (Dimatec Analysentechnik GmbH, Essen, Germany) and CFA Analysis (Continuous Flow Analyzer), respectively. In a separate supplementary leaching experiment, the average concentration of total iron released from a low elevation soil sample (SOM content of 85.7 wt%) were measured by Landwirtschaftliche Untersuchungs- und Forschungsanstalt of LMS Agrarberatung GmbH (LUFA Rostock) with concentration of 1.28 ± 0.24 mg L^{-1}and 1.84 ± 0.74 mg L^{-1} in GW1 and BW phases, respectively (using the standard DIN EN ISO 11885 (E 22): 2009-09).

4.2.3 Measurement of soil properties

Loss on ignition (LOI) method (ISO (2247)6−3:2005) was used to estimate the SOM content of all soil samples, involving burning of the samples at 550 °C for 4 hours. The C and N concentration of the soil samples was quantified by a Carbon/Nitrogen/Sulfur-Analyzer (Elementar PyroCube, Langenselbold, Germany) and C:N ratios were calculated. Soil water retention curves (SWRCs) and other selected soil hydro-physical properties such as total porosity, macroporosity, and dry bulk density were determined using the method reported of Wang et al. (2021). The van Genuchten (VG) model parameters, such as water content at saturation (θ_s), α, and n, were optimized using the RETC software packages (van Genuchten et al., 1991). Particle size distributions of soil samples from two sampling elevation groups A and B were measured by LUFA Rostock after pre-treatment of the samples to remove organic matter and salts (using the standard DIN ISO 11277:2002-08; **Table 4.1**).

Table 4.1 Practical size distribution of collected from different sampling elevation groups (A: loamy sand; B: sandy loam).

Elevation group	Soil depth (cm)	Sampling elevation (m)	SOM[a] (wt %)	Practical size distribution (mineral as 100%, wt %)								
				Sand			Sand	Silt			Silt	Clay
				C[b]	M	F		C	M	F		
A (High)	10–15	0.81±0.18	5.93±3.71	4.13	37.23	40.26	81.62	8.36	3.21	2.08	13.65	4.73
B (Middle)	10–15	−0.02±0.04	21.05±3.05	4.29	21.66	42.83	68.78	14.15	5.73	2.83	22.71	8.51
C (Low)	40–45	−0.69±0.01	87.63±3.95	-	-	-	-	-	-	-	-	-

[a] Abbreviations: SOM, soil organic matter content. The presence of high SOM in Group C is insufficient for measuring particle size distribution.

[b] Abbreviations: C, Coarse; M, Medium; F, Fine.

4.2.4 Statistical and geostatistical analysis

Descriptive statistics (mean, minimum, maximum, standard deviation, and coefficient of variance), regression analyses and Pearson correlation analyses were conducted using SAS software (Version 9.4) and the R package "stats" and "corrplot" (R Core Team, 2020) to evaluate the impact of elevation changes on the SOM content and C:N ratio. The significance of differences for the investigated parameters of soil core samples (*e.g.*, selected soil properties and the total amount of released nutrients) among three sampling elevation groups was implemented by ANOVA test, and then the Tukey-Kramer procedure (Tukey-HSD) was applied for post-hoc analysis in SAS. T-tests were used to determine the significance of the difference between the selected hydro-physical properties of the topsoil and subsoil samples.

The spatial variation (semivariance) of the parameters was estimated by semivariogram models with GS+ (Version 10; Gamma Design Software). The theoretical semivariance (γ) of normal distributed data was constructed by Equation (4.1) (Nielsen and Wendroth, 2003):

$$\gamma(h) = \frac{1}{2N(h)} \sum_{i=1}^{N(h)} [A_i(x_i) - A_i(x_i + h)]^2 \qquad (4.1)$$

where h is the spacing between sample xi and sample x_i+h, N(h) is the number of sample pairs separated by the lag distance. $A_i(x_i)$ and $A_i(x_i+h)$ are the measured variable at spatial location i and $i+h$. The active lag distance is set by default as half of the sample distance (347.1 m). The best semivariogram model was selected based on the highest coefficient of determination (R^2) and the smallest residual sum of squares (RSS). Semivariogram models are described by three key parameters: range (A), the sill ($C0+C$), and the nugget effect ($C0$). The range corresponds

to the distance at which the model tends to level off, while the sill represents the variance value attained at that range. The nugget effect refers to a non-zero variance observed at extremely close separation distances (Lamorey and Jacobson, 1995). Investigated soil properties were considered to be strongly, moderately and weakly spatially dependent when the ratio of nugget to sill *C0/(C0+C)* were <0.25, between 0.25 and 0.75, and >0.75, respectively (Cambardella et al., 1994).

A kriged estimate map for elevation and soil properties (SOM content and C:N ratio) were plotted using the ordinary kriging method with Equations (4.2) to (4.3) (Isaaks and Srivastava, 1989; Yao et al., 2013):

$$Z^*(x_0) = \sum_{i=1}^{j} \lambda_i \, Z(x_i) \tag{4.2}$$

$$\lambda_i = \frac{1/d_i^2}{\sum_{i=1}^{j} 1/d_i^2} \tag{4.3}$$

where $Z^*(x_o)$ is the predicted value at the unsampled point x_o, $Z(x_i)$ is the observed value at the sampled point x_i, λ_i is the weighting coefficient from x_i to x_o, j is the number of the closest sampled points within the neighborhood searching and d_i is the distance between the unsampled point and the sampled point. In this study, the ordinary kriging method was calculated using geostatistical analyst tool in ArcGIS (Version 10.5).

4.3 Results

4.3.1 Geostatistical analysis

The values of surface elevation, sampling elevation, the SOM content, and the C:N ratio of soil samples are summarized in **Table 4.2**. Soil sampling was performed over an elevation range from −0.90 m to 0.97 m. The topsoil samples exhibited a range of SOM contents from 1.7 wt% to 49.2 wt% and a C:N ratio from 9.6 to 17.0. Similarly, the subsoil samples showed a range of SOM content from 1.3 wt% to 91.0 wt% and a C:N ratio from 2.8 to 20.4. The values of the coefficient of variation (CV) of the C:N ratio of both topsoil and subsoil horizons (< 25%) indicated the low variability of the C:N ratio. The CV of the SOM content was much higher, especially for the subsoil (> 65%), indicating a strong variability of organic matter accumulation.

Table 4.2 The values of surface elevation, sampling elevation, the SOM content, and the C:N ratio of peat samples with their descriptive statistics.

Variable[a]	Soil depth	N	Minimum	Maximum	Mean	Standard deviation	Coefficient of variation (CV; %)[b]
Surface elevation (m)	-	40	−0.50	1.07	−0.11	0.39	--
Sampling elevation (m)	Topsoil (10–15 cm)	40	−0.60	0.97	−0.21	0.39	--
	Subsoil (40–45 cm)	40	−0.90	0.67	−0.51	0.39	--
SOM content (wt%)	Topsoil (10–15 cm)	40	1.65	49.19	28.71	12.50	43.53
	Subsoil (40–45 cm)	40	1.34	91.03	45.87	31.30	68.23
C:N ratio (-)	Topsoil (10–15 cm)	40	9.59	16.96	14.36	1.61	11.22
	Subsoil (40–45 cm)	40	2.77	20.44	15.27	3.37	22.05

[a] Abbreviations: SOM, soil organic matter; C:N ratio: the mass of carbon to the mass of nitrogen ratio.
[b] The CV will be negative, when the mean of the data is negative, which usually means that the CV is misleading. Introduction to SAS. UCLA: Statistical Consulting Group. From https://stats.oarc.ucla.edu/sas/modules/introduction-to-the-features-of-sas/ (accessed on August 22, 2021).

Table 4.3 and **Figure 4.3** summarize the geostatistical parameters and the semivariogram models of surface elevation, the SOM content, and the C:N ratio. Different models were selected as best fits for the different parameters, including exponential (SOM content of both top and subsoils) and Gaussian (surface elevation) models. The exponential model was the best fit for the semivariogram of C:N ratio of topsoil, whereas the linear model was the best fit for the C:N ratio of subsoil. At the study site, the surface elevation exhibited a moderate level of spatial dependence within a spatial autocorrelation range of 185.3 m. The nugget/sill ratio of the SOM content in the top and subsoil layers were 5% and 36%, respectively, suggesting a strongly or moderately spatial dependence of SOM distribution. In contrast, the C:N ratio demonstrated a very different spatial dependence between the two soil horizons. The magnitude of the range of the SOM content and the C:N ratio also showed a significant difference between topsoil and subsoil ($p < 0.05$). The SOM content was spatially dependent within a range of 72.9 m for topsoil and 486.3 m for subsoil, whereas the C:N ratio had a spatial autocorrelation range of 46.0 m for topsoil and 329.1 m for subsoil. The high nugget/sill ratio of 80% revealed that the C:N ratio in the deeper layer had less spatial heterogeneity, and the fit of its semivariance model was particularly weak ($R^2 = 0.047$).

Table 4.3 Semivariogram model parameters for surface elevation, SOM content, and C:N ratio for the topsoil and subsoil samples.

Parameter[a]	Model[b]	Nugget $C0$	Sill $C0+C$	$C0/C0+C$ (%)	Spatial dependence	Range (A; m)	R^2	RSS[c]
Surface elevation	Gau.	0.0613	0.133	46.229	Moderate	185.300	0.628	0.003
SOM topsoil	Exp.	8.000	157.700	5.073	Strong	72.900	0.394	9629
SOM subsoil	Exp.	528.000	1462.000	36.115	Moderate	486.300	0.557	127704
C:N topsoil	Exp.	0.302	2.368	12.753	Strong	46.000	0.284	3.02
C:N subsoil	Lin.	7.285	8.989	81.043	Weak	329.100	0.047	48.3

[a] Abbreviations: SOM, soil organic matter content; C:N: the mass of carbon to the mass of nitrogen ratio.
[b] Abbreviations: Gau, Gaussian model; Exp: exponential model; Lin, linear model.
[c] Abbreviations : R^2, the coefficient of determination; RSS, residual sum of squares.
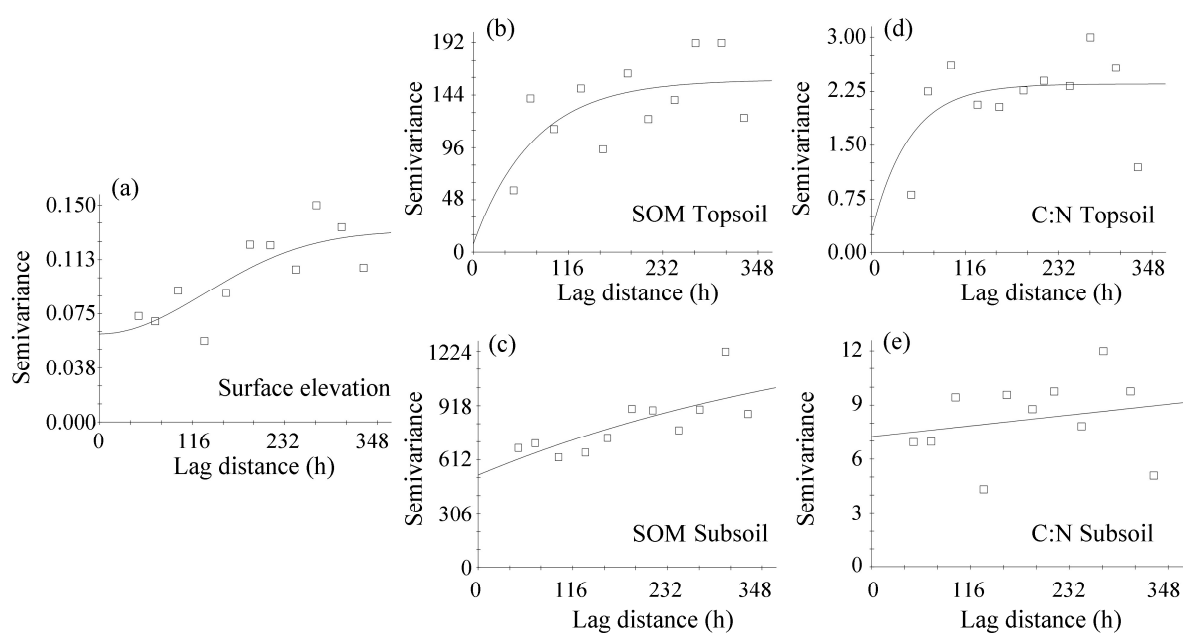
Figure 4.3 Semivariogram models showing the spatial dependence of surface elevation, soil organic matter content (SOM), and the mass of carbon to the mass of nitrogen ratio (C:N) of the topsoil and subsoil samples.

A computed kriging map of predicted surface elevation at the study site shows higher elevations in the northern and western areas (along the coast) than in the center and southeastern areas (**Figure 4.4a**). Thus, a surface elevation gradient was apparent across the study site. The spatial distribution of the SOM content and the C:N ratio are likewise presented in kriging maps in **Figure 4.4(b-e)**. The highest SOM content and C:N ratio were observed in the low-lying center, southern, and eastern areas of the study site, whereas the lowest values were distributed in the

northern area. Compared to the subsoil, the gradients of the SOM content and the C:N ratio in the topsoil were more variable **(Figure 4.4b and 4.4d)**.
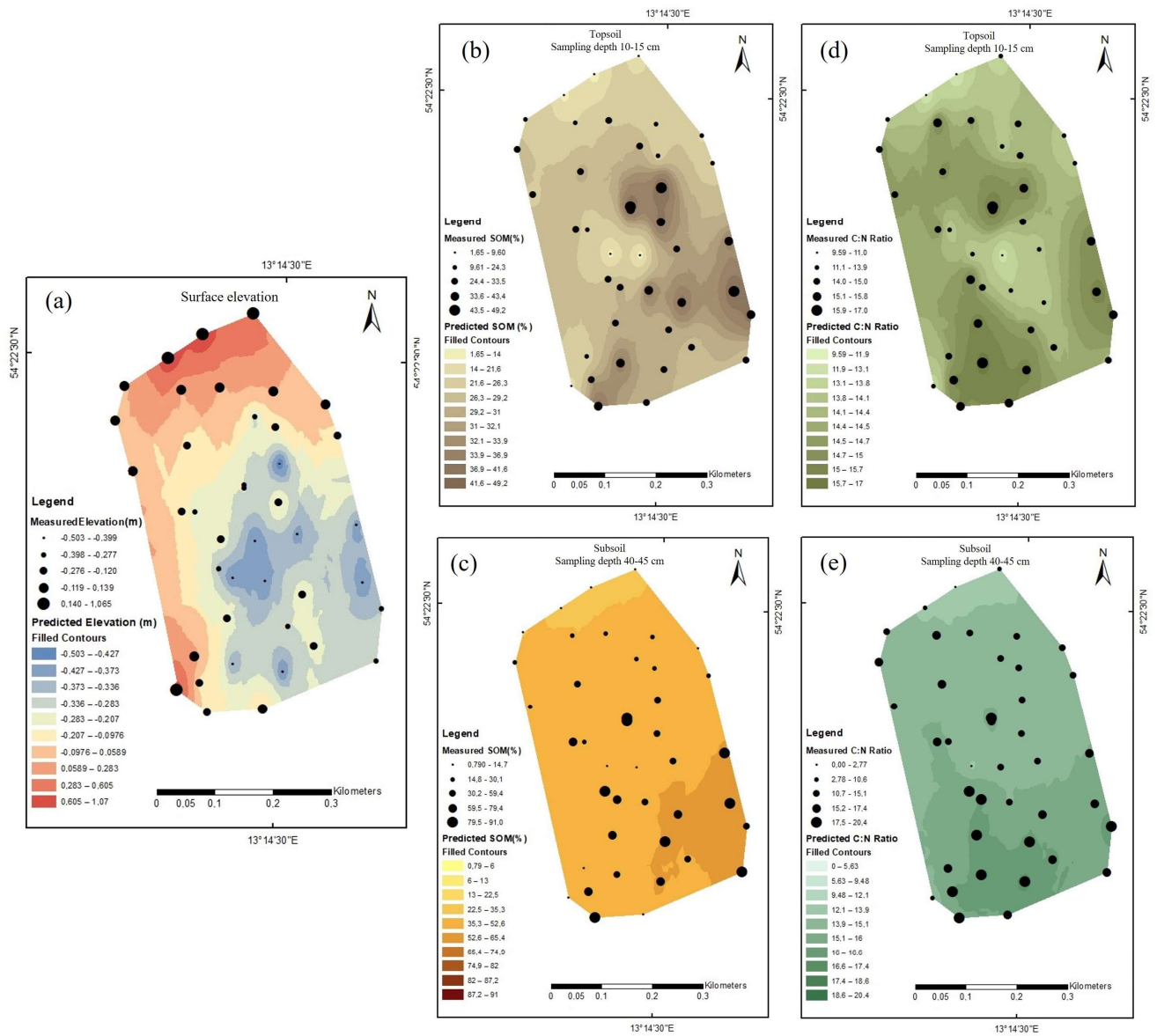
Figure 4.4 Kriged maps of surface elevation, soil organic matter (SOM) content, and the mass of carbon to the mass of nitrogen (C:N) ratio of the topsoil and subsoil samples.

4.3.2 Soil hydro-physical properties

The SOM content and the C:N ratio of both topsoil and subsoil samples were negatively correlated with the sampling location elevations (**Figure 4.5**). Regression analysis showed that the relationship between SOM content and sampling elevation was well modeled by exponential functions ($R^2 > 0.50$), while the C:N ratio was linearly correlated with sampling elevation ($R^2 >$

0.45). When considering the sampling elevations of all samples individually, the Pearson correlation coefficients showed significant associations between sampling elevation and the SOM content ($r = -0.64$, $p < 0.0001$), as well as the C:N ratio ($r = -0.70$, $p < 0.0001$) (Supplemental **Figure S4.2**). In both topsoil and subsoil samples, strong positive correlations between the SOM content and the C:N ratio were observed (topsoil: $r = 0.82$, subsoil: $r = 0.70$; both $p < 0.0001$).
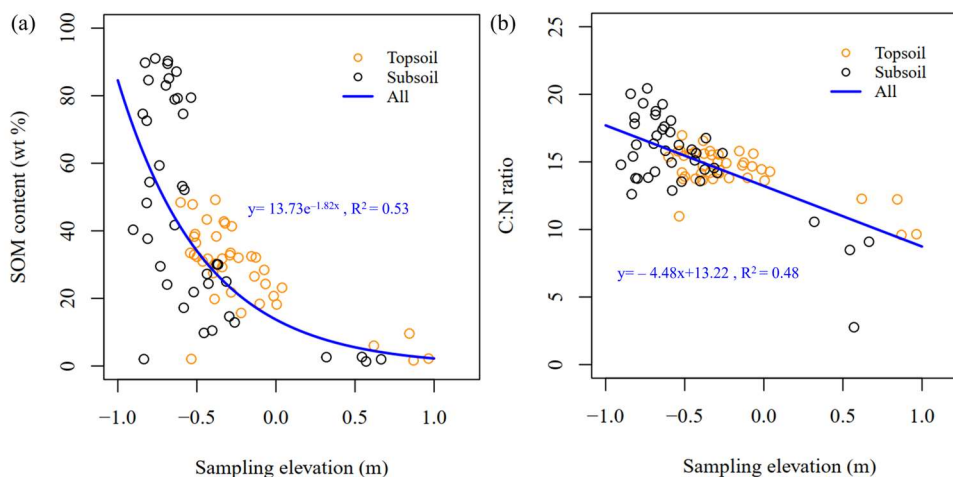
Figure 4.5 Best fit relationship between (a) elevation and soil organic matter (SOM) content; (b) elevation and the mass of carbon to the mass of nitrogen (C:N) ratio for all top and subsoil samples.

The hydraulic and physical properties of the selected soil cores are listed in **Table 4.4**. The bulk density of the samples from high and middle elevation (Groups A and B) were greater than 1 and 0.5, respectively, which was associated with a low SOM content and a high mineral content (**Table 4.1**). The SWRCs for the samples collected at three different elevations were presented in **Figure S4.3**[7]. The water retention capacity was observed to vary across different elevation groups, with the water content at saturation condition following the order of Group C > Group B > Group A (see also Supplementary **Table S4.1**). The values of VG model parameter α were all close to 1 cm^{-1} in Group C, while the other two groups demonstrated a wide range of values. The values of the model parameter n ranged from 1.031 to 1.087 (Supplemental **Table S4.1** and **Figure S4.3**).

The well-known correlation between SOM content and bulk density, saturated hydraulic conductivity (K_s) and macroporosity in peatlands was also confirmed in this study (Supplemental **Figure S4.4**; Liu and Lennartz, 2019a; Wang et al., 2021). In addition, bulk density rose with increasing elevation with a Pearson correlation coefficient of 0.836 ($p < 0.0001$), and total porosity as well as VG model parameter θ_s decreased with increasing elevation with Pearson cor-

---

[7] Note: This figure appears in the results section of the main text of the published paper.

relation coefficients of −0.812 and −0.811 ($p < 0.0001$), respectively. Contrastingly, macroporosity and the VG model parameter α were slightly negatively correlated with elevation, with Pearson correlation coefficients of −0.586 ($p = 0.011$) and −0.453 ($p = 0.059$), respectively (Supplemental **Figure S4.5**). The results of the ANOVA and post-hoc tests showed significant differences in sampling elevation between each pair of groups for both horizons ($p < 0.0001$). Significant differences were also found for SOM content, bulk density, total porosity, C:N ratio and VG model parameter θ_s among all three groups; however, not all the pairwise comparisons between groups showed significant differences (Supplemental **Figure S4.6**). The t-test results showed that only the difference in bulk density was statistically detectable between the two sampling depths of Group A ($p = 0.038$), as well as in Group C, the differences in bulk density and its related variables (SOM content and total porosity) were statistically noticeable between the two depths ($p <= 0.01$). However, in Group B, there were no significant differences between the two depths for any of the investigated soil physical parameters.

Table 4.4 The hydraulic and physical properties of collected peat cores from three sampling elevation groups.

Elevation group		No.	Surface elevation (m)	Sampling elevation (m)	K_s (×10⁻⁴, m s⁻¹)	Total porosity (vol%)	Macro-porosity (vol%)	SOM (wt%)	C:N Ratio (-)	Bulk density (g cm⁻³)
						Soil properties[a]				
A (high)	Topsoil	1	0.72	0.62	2.5	46.9	10.7	6.0	12.3	1.4
		2	1.07	0.84	1.3	40.5	7.1	2.2	9.6	1.4
		3	0.94	0.97	1.0	52.5	4.1	9.6	12.2	1.2
	Subsoil	1	0.72	0.32	0.3	34.0	5.9	2.6	10.6	1.7
		2	1.07	0.54	2.4	38.8	10.5	2.0	9.1	1.6
		3	0.94	0.67	0.2	40.7	5.1	2.7	8.5	1.6
B (middle)	Topsoil	1	0.11	−0.07	0.6	56.6	9.1	18.2	13.6	1.1
		2	0.09	−0.01	1.7	62.5	8.6	20.7	14.5	0.9
		3	0.03	0.01	0.1	66.9	3.5	24.3	15.6	0.8
	Subsoil	1	0.11	−0.37	0.5	44.5	3.3	14.7	14.2	1.3
		2	0.09	−0.31	2.3	67.6	13.9	25.0	14.6	0.7
		3	0.03	−0.30	0.7	75.9	14.7	30.0	16.8	0.5
C (low)	Topsoil	1	−0.28	−0.40	0.4	73.7	13.9	49.2	16.6	0.6
		2	−0.29	−0.39	0.6	69.2	17.0	30.3	15.8	0.7
		3	−0.30	−0.38	0.5	68.4	15.0	27.5	14.1	0.7
	Subsoil	1	−0.28	−0.70	0.6	83.6	20.5	90.3	18.8	0.3
		2	−0.29	−0.69	0.2	81.2	9.4	89.5	18.5	0.3
		3	−0.30	−0.68	0.5	78.3	12.7	83.1	16.4	0.3

[a] Abbreviations: K_s, saturated hydraulic conductivity; SOM, soil organic matter content; C:N ratio: the mass of carbon to the mass of nitrogen ratio.

4.3.3 Effect of elevation and salinity on DOC and NH_4^+ release

The soil types of the samples selected for the leaching test differed related to the elevation at which they were collected. The high elevation samples from Group A were primarily (loamy) sand with around 6% of SOM, the middle elevations samples from Group B were basically (sandy) loam with about 20% of SOM (**Table 4.1**), and samples from Group C at low elevations were predominantly fen peat with up to 90% of SOM (**Table 4.4**). The intrusion of brackish water caused a significant decrease in the pH of the leachate of soil cores from different elevations (Supplemental **Figure S4.7**). As the EC value of the background solution declined again to 4.25 mS cm^{-1}, the pH of the leachate increased considerably. The pH values of the leachates from the samples in the highest elevation Group A (ranged from 5.0 to 7.1) was generally higher than that of samples in the middle elevation Group B (range from 4.2 to 5.0) and the low elevation Group C (range from 3.9 to 5.5). EC responded differently to the intrusion of brackish water in the samples from the different elevation groups. Thus, the EC values in the leachates from Group B started to rise as soon as brackish water intruded, while they increased more slowly in Group C.

The concentration and amount of DOC released during the fresh-brackish water cycle are shown in **Figure 4.6**. Obviously, the water salinity in the GW and BW flushing solutions affected the leaching behavior of DOC. In Groups A and B, the impact of salinity on the leached DOC concentration was slightly detectable in the GW2 time phase. The DOC concentration in Group C was, however, very high at the beginning of the flush (GW1: 140 ~ 240 mg L^{-1}). DOC decreased significantly with leaching time and further dropped significantly to 25 ~ 55 mg L^{-1} with the addition of brackish water before an equilibrium was reached (BW; at about 60 hours; **Figure 4.6a**). However, the concentration of leached DOC increased sharply once salinity declined (GW2). In Groups A and C, the average amount leached per 36 hours was lower in the BW phase than during GW1 and GW2 (**Figure 4.6b**). The results of the ANOVA and post-hoc tests showed that the total amount of DOC released in Group C was significantly higher than in Groups A and B, but no significant difference appeared between Groups A and B ($p < 0.05$; **Figure 4.6c**). These results highlight that soil at low elevation acts as a hotspot of DOC release from the study site. During the entire process, the colored dissolved organic matter (CDOM) of all leachates was visually observed to change from dark to light and then dark again after the freshwater application (Supplemental **Figure S4.8**). Pearson correlation analysis indicated that the total DOC released was significantly correlated with various soil properties. It showed a negative correlation with sampling elevation and soil bulk density, but a positive correlation with SOM content, C:N ratio, total porosity, and macroporosity (Supplemental **Figure S4.9**).
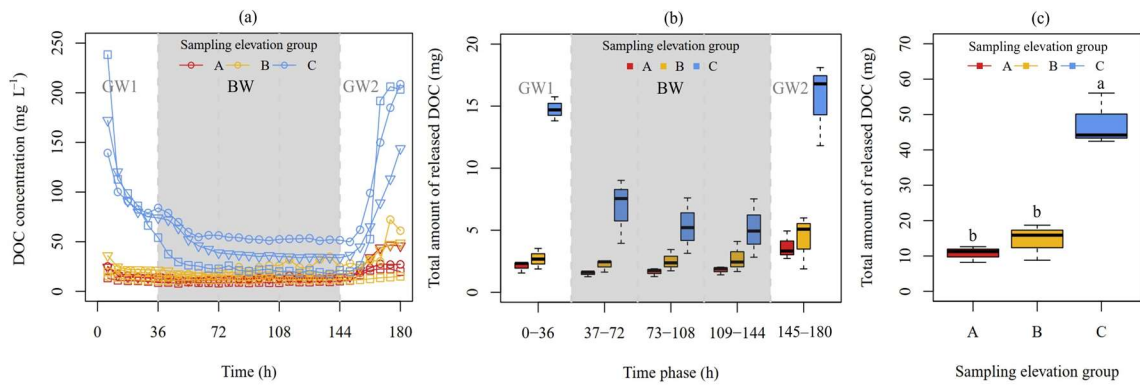
Figure 4.6 Leaching behavior of dissolved organic carbon (DOC); (a) Variation of DOC concentration over time during alternating freshwater and brackish water states for 9 soil core samples from 3 sampling elevation groups; (b) the amount of leached DOC for 36-hour intervals; (c) differences in ANOVA and post-hoc results of the total amount of leached DOC among three sampling elevation groups. (same GW solution was used for the GW1 and GW2 time phases; significant differences among the groups are indicated by the letters "a" and "b").
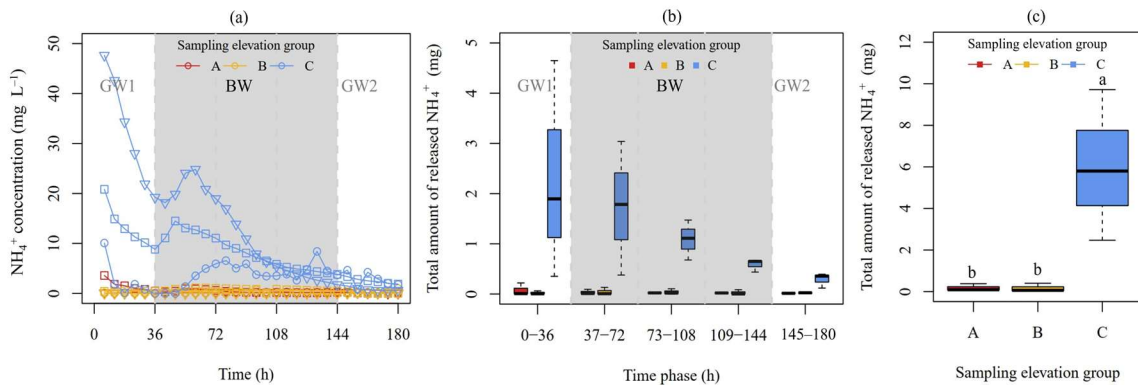
Figure 4.7 Leaching behavior of ammonium (NH_4^+); (a) Variation of NH_4^+ concentration over time during alternating freshwater and brackish water for 9 soil core samples from 3 sampling elevation groups; (b) the amount of leached NH_4^+ for 36-hour intervals; (c) differences in ANOVA and post-hoc results of the total amount of leached NH_4^+ among three sampling elevation groups. (same GW solution was used for GW1 and GW2 time phases; significant differences among the groups are indicated by the letters "a" and "b").

The variation of NH_4^+ concentrations with salinity fluctuations did not differ noticeably in Groups A and B (**Figure 4.7**), while the effect of salinity on NH_4^+ concentrations was clearly observed in the samples from Group C. Notably, the initial NH_4^+ concentration (GW1) in Group C (10.08 ~ 47.64 mg L^{-1}) was one order of magnitude higher than in the other two groups (0.00 ~ 3.58 mg L^{-1}). During GW1, the released NH_4^+ concentrations started to decrease relative to initial concentration, and with the switch from fresh to brackish water, the samples exhibited an abrupt increase in NH_4^+ concentrations, followed by a continued gradual decrease during BW. Once the samples were flushed by freshwater again (GW2), the NH_4^+ concentrations either fluctuated or continued to decline. Due to the very high initial concentration of leached NH_4^+ in Group C, the average release per 36 hours in the BW phase was not substantially higher than

in GW1 and GW2, but the release concentrations obviously rebounded during the salt flushing (**Figure 4.7a and b**). Likewise, the statistical tests indicated that the total amount of NH_4^+ leached from Group C was significantly different from those of Groups A and B, whereas there was no difference between Groups A and B (**Figure 4.7c**). Pearson correlation analysis revealed that the total amount of released NH_4^+ was negatively correlated with sampling elevation and soil bulk density, and positively correlated with SOM and total porosity ($p < 0.05$; Supplemental **Figure S4.9**).

4.4 Discussion

4.4.1 Small-scale spatial variability of soil/sediment properties

The CV values of topsoil and subsoil differed for both the SOM content and the C:N ratio, indicating a greater variability in values for subsoil than topsoil (**Table 4.2**). In this study, unlike previous research utilizing gaussian, spherical, and stable models for rewetted peatland (Ahmad et al., 2020; Negassa et al., 2019 and 2022), the spatial variation of the SOM was effectively represented by the exponential model. We assume that differences in the selection of the best model may be attributed to the distinct characteristics of individual study site and the investigated scale. The strength of spatial correlation for given variables was well indicated by the nugget/sill ratio (Cambardella et al., 1994; Iqbal et al., 2005). At the site of this study, the surface elevation was only moderately spatially dependent as the nugget/sill ratio ranged between 25% and 75%. In another coastal wetland in Germany, a stronger spatial dependence was observed with a nugget/sill ratio of 13% (Ahmad et al., 2020). The Kriging map gives an overview of the spatial distribution and prediction of surface elevation, which exhibited a pronounced spatial gradient from sea to land (**Figure 4.4**). Although the spatial distribution of these parameters was relatively more homogeneous in the subsoil than in the topsoil, both the SOM content and the C:N ratio of the topsoil samples were strongly spatially correlated with a low nugget/sill ratio (5.1% and 12.8%, respectively), and the spatial dependence was apparent at short ranges (**Table 4.3**). However, this finding differs from that of Ahmad et al. (2020), who found only a moderate spatial dependence of the SOM content of topsoil (at 10–15 cm depth).

Previous studies of inland peatlands have demonstrated a strong spatial dependence of the SOM content in highly degraded peatlands (nugget/sill = 12.72%) and rewetted peatlands (nugget/sill = 0.22%), while in a moderately degraded peatland, the spatial dependence of the SOM content was found to be weak or even absent (Negassa et al., 2019; Wang et al., 2021). In these inland peatlands, the spatial dependence of soil properties is influenced by the degree of peatland degradation and hydrological management (Negassa et al., 2022; Negassa et al., 2019; Wang et al., 2021). Coastal peatlands are, however, unique in that they are terrestrial habitats

that have a significant influence on and are influenced by marine environments. The strong spatial dependency of the topsoil SOM content with the C:N ratio is attributed to an intimate connection between the mineral sediment fraction and distance to the sea (**Table 4.1** and **Figure 4.1**). Previous studies have also found that intrinsic factors (*e.g.*, parent material/mineralogy) may significantly influence the spatial dependence of soil properties (Brady and Weil, 2000; Saleh, 2018). Therefore, spatial variability as influenced by soil texture must also be considered for coastal mires and peatlands because of a potential mineral sediment input during flooding events (Ahmad et al., 2020; Waller and Kirby, 2021).

4.4.2 Microtopography impacts the distribution and accumulation of organic matter

Microtopography influences a multitude of fundamental processes of coastal wetlands or peatlands. Our findings revealed that organic matter distribution and accumulation in coastal peatlands were influenced by microtopography (*i.e.*, the gradient in elevation), as an effect of the mineral sediment fraction and local hydrological situation. Low-lying peatlands are considered as organic matter-accumulating ecosystems. Both the SOM content and the C:N ratio were significantly negatively correlated with soil sampling elevations, as shown by the plotted models of regression analysis (**Figure 4.5**) and the kriging map (**Figure 4.4**). The kriging map predicts that the SOM values of the subsoil are highest in the southeastern area of the study site (low elevations) and decrease towards the dikes (high elevations). The high organic matter accumulation at low elevations is linked to a perennial groundwater table close to the soil surface. Lindsay and Andersen (2016) observed that local depressions can create wetter and thus more anaerobic conditions. Both field and laboratory experiments have demonstrated that the carbon mineralization rate may decline in anaerobic environments, which allows for the accumulation of organic matter (Ahmad et al., 2020; Blodau et al., 2004). Brust's (2019) research showed a relationship between the C:N ratio of organic nitrogen and its respective mineralization and immobilization rates. As the C:N ratio increases from 5 to 20, mineralization rates decrease gradually until an equilibrium between mineralization and immobilization is reached, whereas, for C:N ratios ranging from 30 to >50, the immobilization rates exhibit an increasing trend. In our study, the C:N ratios of the samples taken at the low elevations from the center and southeastern area are concentrated between approximately 15 and 20, indicating an equilibrium state between organic matter mineralization and immobilization. In comparison, areas with much lower C:N ratios along the coast and at high elevations were predominantly influenced by marine sedimentation.

Compared to the coastal fen peatland in this study, Whittle and Gallego-Sala (2016) drew a different conclusion in their study on bog peatland. The authors found that carbon accumulation increased with rising elevation in the range of 2–6 m and then decreased between 6–16 m. The

relevant reason for this observation is the effect of salinity on the vegetation communities of a growing bog, so carbon accumulation is lower in areas frequently affected by salinity. At our study site, it is apparent that the water table and sampling location have a greater impact on peat formation than salinity, since the Baltic Sea water is much less saline (~0.7 % of average salinity) than ocean water in general (~3.5%; Salinity, n.d.). Unlike inland peatlands, the main reason for the low SOM content at high elevations in the studied coastal peatland is the high percentage of sand (**Table 4.1**). Waller and Kirby (2021) suggested that SOM content is a crucial parameter to be precisely evaluated in coastal peatlands due to the influence of both marine and terrestrial environments. In this context, it is important to consider coastal "peat" as "organic sediment with a significant mineral fraction". Furthermore, the growth of organic-rich peat is bound to low-lying areas and influenced by the groundwater level and topography (Vis et al., 2015; Waller and Kirby, 2021). Despite the potential for sediment to be transported and deposited in low-lying areas because of wind-induced water level changes and storm surges along the Baltic Sea coast (Jurasinski et al., 2018), our study revealed a contrasting pattern. Considering the hydrological conditions of our study site, it is plausible to assume that vegetation was absent at lower elevations due to the high water table and that, conversely, (surviving) vegetation acting as sediment traps at higher elevations could promote sediment accumulation in these areas (Kretz et al., 2021).

Overall, microtopography is controlled by a variety of factors (*e.g.*, sediment supply, local hydrological variability, storm activity, and plant traits), and also responds to sea level rise and extreme weather events (flooding). In our study, we simulated the microtopography of a coastal peatland by measuring surface elevation at random locations. Our findings indicate that research on coastal peatlands is accompanied by a higher degree of uncertainty, primarily due to the influence of diverse microtopographical factors, in contrast to investigations conducted in inland peatlands. It should be noted that the elevations of soil samples collected in this study may not fully reflect the microtopographical factors of the original locations due to sampling artifacts introduced during the removal of soils (conducted to soil property measurements). Moreover, considering the constrained number of elevation measurement points achieved through the RTK method, future studies may benefit from integrating more sophisticated methods and techniques. Approaches such as light detection and ranging (LiDAR) survey or Structure-from-Motion and Multi-View-Stereo (SfM-MVS) using photos captured from unmanned aerial vehicles (UAVs) could significantly improve the accuracy of capturing and representing microtopographical effects in peatland ecosystems. These advanced techniques offer promising avenues to enhance the precision and comprehensiveness of data collection, leading to a more

in-depth understanding of peatland dynamics and processes (Mercer and Westbrook, 2016; Minasny et al., 2019). In this context, high resolution elevation maps can help to visually assess the possible effect of rewetting and soil carbon dynamics in coastal peatland restoration projects.

4.4.3 SOM content and hydro-physical properties

In inland peatlands, previous meta or experimental studies have explored the soil hydraulic-physical properties of peat with different types and degrees of degradation (Liu and Lennartz, 2019a; Rezanezhad et al., 2016; Wallor et al., 2018; Wang et al., 2021). Low bulk density (*e.g.*, < 0.76 g cm^{-3}), high organic matter content (*e.g.*, 83.2 ± 15.1 wt%) and high total porosity (*e.g.*, 71 ~ 95.1 vol%) are well-known as unique characteristics of inland peat soils (Liu and Lennartz, 2019a; Rezanezhad et al., 2016). Our study indicates that the influence of additional environmental factors (*e.g.*, soil texture), driven by microtopography, also needs to be considered when estimating soil hydro-physical properties in coastal peatlands. In this study, soil bulk density, total porosity, macroporosity, and VG model parameters had a pronounced to moderate correlation with sampling elevation. Apparently, the value of bulk density from the samples at high and middle elevations (Group A and B) reflected the circumstance that the low SOM content was affected by a high mineral (sand) content and not mainly by peat soil degradation. The values of K_s and VG model parameters (α and n) remained within the range reported by Liu and Lennartz (2019a) and Wallor et al. (2018) and were close to the range of natural peat soils reported by Wang et al. (2021). However, the estimated saturated water content (θ_s) of the samples from Group A (0.34 to 0.52 cm^3 cm^{-3}) was much lower than that of Groups B and C as well as in inland peat soils, indicating a weak water retention capacity of soils in high elevation areas (Supplementary **Figures S4.3** and **S4.5**).

The SOM content is an essential indicator of soil quality due to its influence on physical, chemical, and biological soil functions (Haynes, 2005), while alterations in soil properties, in turn, have an impact on SOM accumulation (Lal, 2011). In addition to the studies of the close linkage between bulk density and SOM content, there have also been several investigations correlating VG model parameters with SOM content, bulk density, macroporosity, and soil particle size distribution in both mineral and organic soils (Sonneveld et al., 2003; Wang et al., 2021; Zhang et al., 2019). The finding that the VG model parameter θ_s correlates with the sampling elevation was further validated by the analysis conducted in the present study (Supplemental **Figure S4.5**). Thus, the interaction among microtopography, SOM content, and soil hydro-physical properties further emphasizes the importance of microtopography on soil/sediment properties. The variability of soil hydro-physical properties in coastal peatlands has evidently implications for their restoration management. Thus, detailed information on soil physical patterns driven by microtopography must be obtained and considered prior restoration.

4.4.4 Microtopography and salinity impacts on pH, DOC, and NH_4^+ leaching

The pH values of leachates were lower (3.2 to 4.8) when the soil cores were flushed with brackish water than with freshwater (4.9 to 6.5). As reported in previous studies, if NaCl is introduced in high concentrations to raise water salinity, the Na^+ ions may replace the H^+ ions, lowering the pH of the effluent (Chambers et al., 2011; Gosch et al., 2019; Liu and Lennartz, 2019b; Tiemeyer et al., 2017). An increase in water salinity (*e.g.*, EC) from 0.1 to 1.0 mS cm^{-1} has been reported to result in a decrease in pH from 5.5 to 3.5 (Tiemeyer et al., 2017). Additionally, Liu and Lennartz (2019b) and Chambers et al. (2011) pointed out that the low pH might be a result of high SO_4^{2-} levels, which is consistent with the findings of this study.

High SOM accumulation in low-lying spots resulted in high DOC release rates in Group C samples in the early leaching stages (**Figure 4.6a**). Even in the same elevation group (Group C), spatial variability caused differences in DOC concentrations. Over the experimental period, the significant difference in the total DOC amount between Group C and the other two higher elevation groups suggests that the leaching behavior of DOC can be influenced by microtopography. Apparently, micro-topographically driven processes created high SOM in low-lying areas, forming a distinct pool of dissolved organic matter that can become major hotspots for DOC release. Our study also showed that soil bulk density was negatively correlated with DOC release (Supplemental **Figure S4.9**). However, our results appear to contradict those of Liu et al. (2019), who found higher bulk density in peat samples was related to higher DOC pore water concentrations. It should be noted that Liu et al. (2019) mainly compared peat samples with a gradient in bulk density created by land management and degradation stages, while our coastal peatland study included different soil types with a higher bulk density produced by mineral sediment fractions.

In addition, the leaching behavior of DOC in our study responded significantly to salinity changes (**Figure 4.6**). Chow et al. (2003) conducted a soil incubation experiment and revealed that increasing salinity reduced the DOC concentration; the same conclusion was drawn in the study by Liu and Lennartz (2019b). van Dijk et al. (2015) suggested that an enhanced salinity may reduce the desorption capacity of sediments due to the higher ionic strength in seawater than in wetland sediments. Meanwhile, as salinity increases, iron (Fe) and aluminum (Al) species are more receptive to forming hydroxides, and DOC may co-precipitate with hydroxides to form flocculation (Nierop et al., 2002). The soil Fe content of our study site seems to support the conclusion that DOC concentrations decrease under high salinity conditions. Thus, the restoration of coastal peatlands by rewetting with seawater will likely limit DOC leaching into the adjacent aquatic system. Nevertheless, higher DOC concentrations (> 200 mg L^{-1}) were observed again in the leachate of Group C when the freshwater replaced brackish water (GW2

phase). These high concentrations of released DOC from coastal peats are consistent with the findings in recent study undertaken by Liu and Lennartz (2019b), who observed DOC concentrations between 10 to 280 mg L^{-1} in effluent from the German Baltic coast during alternating inflow of seawater and freshwater. The result suggests that the release process of DOC is reversible, and considerable quantities of DOC might be released from rewetted sites to the marine ecosystem with low-saline groundwater or storm events with high precipitation (Liu and Lennartz, 2019b; Kreuzburg et al., 2020).

Since the Baltic Sea is a semi-enclosed brackish sea, the allochthonous (*e.g.*, terrestrial) input of DOC has been estimated to constitute as much as two-thirds of the total DOC input (Deutsch et al., 2012; Gustafsson et al., 2014; Lønborg et al., 2020). The leaching experiment in this study clearly demonstrated the occurrence of visible CDOM under low salinity conditions, while the turbidity was relatively low at high salinity conditions (Supplemental **Figure S4.8**). In several previous studies, increasing salinity has been proved to significantly decrease the CDOM absorption coefficient of light at various wavelengths (*e.g.*, a350 in Branco and Kremer, 2005; g440 in Harvey et al., 2015); and the existence of a positive correlation between DOC concentration and CDOM absorption coefficient is widely recognized (Ferrari et al., 1996; Fichot and Benner, 2011). Thus, the darkening of water caused by high concentrations of DOC reduces the amount of light passing through the water. However, the implications of this for the waters surrounding coastal peatlands are diverse. Water containing large amounts of CDOM have a preferential filtering effect on the light required for photosynthesis, and underwater light availability as an essential factor in the growth and abundance of primary producers in shallow water bodies is diminished (Nelson and Siegel, 2002). On the other hand, sunlight promotes the degradation of dissolved organic matter in marine ecosystems in a complex series of photochemical processes, which further converts CDOM into smaller organic compounds, carbon gases (*e.g.*, carbon monoxide (CO) and CO_2), and nutrients (*e.g.*, NH_4^+) (Lønborg et al., 2020; Moran and Zepp, 1997). As a result, heavy precipitation, and potential submarine groundwater discharge in the low-lying areas of study site are expected to result in considerable DOC leaching, eventually leading to carbon loss and adverse effects on aquatic organisms (Xenopoulos et al., 2021).

The NH_4^+ release behavior varied greatly among the different soil samples (**Figure 4.7**). The initial concentrations of NH_4^+ in Group C were significantly higher than in Groups A and B. The most considerable amount of NH_4^+ was also released by the soil cores from the low elevation group (**Figure 4.7c**). In other words, the low-lying areas of the study site could be considered hotspots of NH_4^+ release. NH_4^+ is frequently adsorbed to organo-mineral complexes and diffuses slightly in soil (Zheng et al., 2021). The soil/sediment from the high elevation locations (Groups A and B) contains a comparably low amount of organic matter and is, thus, more likely

to release nutrients because of a low holding capacity for nutrients and moisture (Hudson, 1994; Sonon et al., 2014).

Changes in the NH_4^+ concentration were observed under seawater-impacted conditions. In our study, more NH_4^+ was suddenly leached at the switching from fresh to brackish water. This phenomenon was observed not only for all the samples of Group C but also for individual samples from Groups A and B. The same findings were obtained by Liu and Lennartz (2019b), who found that the addition of seawater caused a rapid and substantial increase in the NH_4^+ concentration in the leachate. A possible explanation of this is that the Na^+ supplied by seawater competes with NH_4^+ for binding sites, causing NH_4^+ desorption from soil particles (Baldwin et al., 2006). A high SOM content can significantly increase the cation exchange capacity (CEC; Ramos et al., 2018). When seawater with high concentrations of Na^+ flush into organic-rich soils (*e.g.*, Group C), large amounts of NH_4^+ are released due to cation exchange (Liu and Lennartz, 2019b). In a recent field study conducted by Pönisch et al. (2023) at the same study site, following the rewetting of the peatland, a rapid and significant increase in NH_4^+ concentration was observed in the surface water of the recently flooded area, reaching levels as high as approximately 1.80 mg L^{-1} (equivalent to ~100 µmol L^{-1}). Concurrently, the NH_4^+ concentration in the surface water of the inner bay, located in front of the removed dike, exhibited corresponding changes and was significantly higher than that of the central Kubitzer Bodden. Remarkably, earlier studies have shown that NH_4^+ concentrations in the Baltic Sea ranged from 0 to 0.36 mg L^{-1} (*e.g.*, 0.03 mg L^{-1}, equivalent to 1.5 µmol L^{-1} in 2019 observed by Naumann et al., 2020; 0.36 mg L^{-1}, equivalent to 20 µmol L^{-1} recorded by Berg et al., 2015), but the initial and peak concentrations of NH_4^+ leached by peat samples from low elevation in our study ranged from 6.56 to 47.64 mg L^{-1}, which are two orders of magnitude higher than the level in the Baltic Sea water used in our leaching experiments (0.037 mg L^{-1}). This suggests that the risk of nutrient leaching at low elevations is exceptionally high when removing dikes for rewetting purposes and that the salt intrusion in coastal peatlands may provoke eutrophication of aquatic habitats, which poses a severe threat to the marine ecosystem (Pönisch et al., 2023).

The distribution of SOM driven by microtopography and its associated soil physical properties (*e.g.*, bulk density and total porosity) may influence the release of DOC and NH_4^+, also because organic matter plays the most important role in the nutrient storage capacity (Sonon et al., 2014; Weil and Magdoff, 2004). Overall, microtopography plays an essential role in rewetting coastal wetlands (especially peatlands) compared to inland peatlands due to the large spatial heterogeneity that is influenced by marine-terrestrial interactions, which also introduces uncertainty in the evaluation of rewetting outcomes.

4.5 Conclusions

Restoration of peatlands is regarded a fundamental action to mitigate climate change and help achieve sustainable development goals. In this context, this study provides support for the applicability of rewetting of coastal peatlands where the distribution of carbon and the potential of nutrient release are a function of microtopography.

The soil hydro-physical properties of coastal peatlands differ from those of inland peatlands as the low organic matter content in high elevation areas is not caused by degradation of peat soil but rather by the impact of the marine environment (*i.e.*, mineral sediment). In addition, our study showed that alternating salinity affected DOC and NH_4^+ release from the soil and that the release was also influenced by microtopography, *i.e.*, low elevation areas are hotspots of potential nutrient release. As peatlands are progressively submerged due to rewetting practices or sea level rise, coastal wetland systems gradually expand inland. Through elevated salinity of surface waters, low-lying areas have the potential to continue to accumulate carbon over time. However, the reversible process can cause a pronounced release of DOC with decreasing salinity, where high CDOM concentrations alter the watercolor and thereby, possibly limiting the photosynthesis in aquatic systems. Notably, enhanced salinity may cause low-lying areas with organic-rich soils/sediments to become major and direct exporters of NH_4^+ from land to adjacent waters. The high microtopography-driven spatial heterogeneity suggests that not all locations provide the same level of ecosystem services or show the same responses. Therefore, site-specific microtopography may contribute to the identification of success indicators for rewetting (*e.g.*, organic matter and water quality) to better monitor carbon sequestration and assess conservation effectiveness.

Data availability statement

Data available on request from the authors.

Competing interests

The authors declare that they have no competing interests.

Authors' contributions

MW conceived the study, carried out the field work and laboratory experiment, as well as analyzed the data and drafted the manuscript. HL conceived the study and edited the manuscript. FR and DZ provided the experiment devices and edited the manuscript. BL provided funds and edited the manuscript. All authors read and agreed to the published version of the manuscript.

Acknowledgements

5

Concluding Discussion

5.1 Overview

In recent years, there has been a growing recognition of the importance of conserving and sustainably managing peatlands, driven by their significant ecological value and the urgent need to address climate change. Peatland degradation caused by drainage and agricultural practices is acknowledged to pose a significant threat to the climate, in particular leading to considerable greenhouse gas emissions (Günther et al., 2020; Hahn et al., 2015; Liu et al., 2019). To address this issue, the restoration of drained peatlands through the implementation of rewetting measures has been widely promoted (Cris et al., 2014; Joosten, 2009; Tanneberger et al., 2021). This thesis asserts that, to effectively implement these measures and evaluate their effectiveness, a comprehensive understanding of the soil hydro-physical properties of peatlands as a fundamental approach is essential. It allows us to ascertain the condition of peatland ecosystems in response to human activities, such as drainage and rewetting.

The specific objectives proposed in Chapter 1.3.1 have been effectively accomplished. **Figure 5.1** provides a comprehensive overview of the key results and serves as a condensed representation of the main contributions of this thesis. The results from Chapter 2 confirmed that peatland degradation influenced the spatial variability of soil hydro-physical properties. For instance, the spatial dependence of the SOM content became stronger with increasing peatland degradation, underscoring the importance of incorporating spatial information to characterize the impact of land management on peatland functioning. The results further suggested that using spatial data can significantly enhance the assessment of peatland conservation status and restoration priorities (Manton et al., 2021). Additionally, this chapter emphasized the importance of considering soil structure, particularly macroporosity, in predicting hydro-physical parameters of peat soils, especially in degraded peatlands. These findings highlighted the importance of leveraging soil properties and their spatial information for making well-informed decisions in peatland conservation and restoration endeavors.
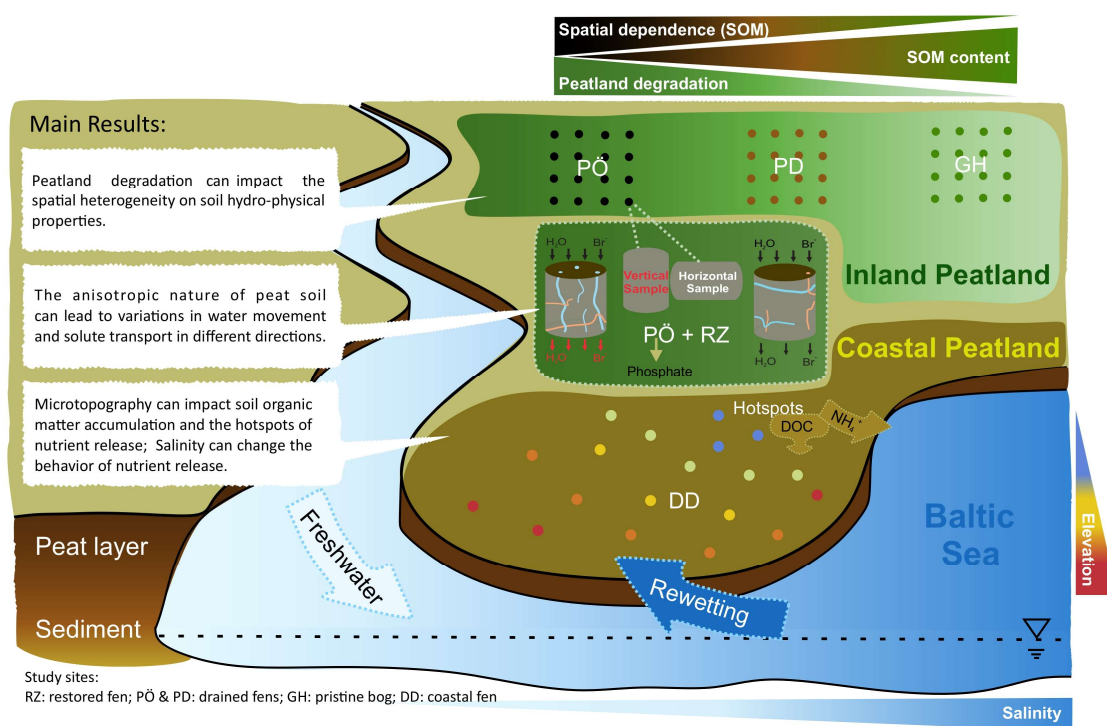
Figure 5.1 Integrated summary that visually and textually summarizes the main findings from chapter 2, 3, and 4 of this thesis.

Peat soils are anisotropic and heterogeneous porous media, where these characteristics influence water movement and solute transport. Chapter 3 demonstrated that the strength of preferential flow, which indicated the behavior of solute transport, displayed moderately higher in the vertical samples than in the horizontal samples. Indeed, the effects of heterogeneity on peatlands were more pronounced than those of anisotropy, as evidenced by the leaching behavior of phosphate in the drained site. As former agricultural land, degraded peatlands store large amounts of nutrients provided by farming activities. We concluded that the anisotropic nature of water movement and solute transport in peat soils could allow the transport and enrichment of phosphate along stronger preferential pathways (Backnäs et al., 2012; Gächter et al., 1998). Thereby, its impact on the surrounding water bodies should be given attention in peatland restoration practices (Zak et al., 2010).

The rewetting of peatlands has been carried out progressively in the Federal State of Mecklenburg-Western Pomerania (MV) in Germany. To simulate a post-rewetting scenario, soil column experiments were conducted with samples from a recently rewetted German coastal peatland (Supplemental **Figure S5.1**), which was the focus of Chapter 4. Considering the specific influence from the Baltic Sea, the site was studied as a distinct ecosystem, separated from inland

peatlands. The analysis of the soil physical properties (including particle size distributions) and RTK-GPS measurements showed that high elevation samples had low SOM content and high bulk density. This was mainly due to a greater proportion of mineral soils influenced by microtopography, rather than the typical degradation patterns observed in inland peatlands. Furthermore, the study revealed that a significant spatial heterogeneity in the distribution of potentially released DOC and NH_4^+, with low-lying areas acting as hotspots. However, the influence of salinity on the release behavior of different compounds posed additional challenges for the rewetting of coastal peatlands. These findings, therefore, emphasized the need to consider spatial heterogeneity, topographic factors, and coastal-land interactions when assessing the ecological functions of coastal peatlands and their responses to management practices (Ahmad et al., 2020; Pönisch et al., 2023).

5.2 Synthesis

5.2.1 Soil hydro-physical properties as indicators of peatland degradation and ecological functionality

The implications of soil physical properties for peatland restoration by rewetting are significant, influencing key aspects of the rewetting process and overall peatland ecosystem health. These properties serve as indicators not only for assessing the degradation of peatlands but also for evaluating the ecological functionality after rewetting. Soil physical properties, such as bulk density and porosity, reflect the water retention capacity and soil structure of peatlands. As indicators of peatland degradation, changes in these properties can signal the negative impact of human activities, such as drainage, on the stability of peatland ecosystem. Post-rewetting, monitoring these indicators becomes crucial to measure the success of restoration efforts. The ability of soil to retain water and maintain a healthy structure directly influences the re-establishment of native vegetation, nutrient cycling, and microbial communities. Therefore, recognizing these soil properties as dual indicators offers a comprehensive approach to understanding the dynamics of peatland ecosystems across different stages, from degradation assessment to post-rewetting ecological functionality.

5.2.1.1 SOM content and bulk density

The study of soil hydro-physical properties of peat soil can provide important information about the health and degradation of peatland ecosystems (Gabriel et al., 2018). Soil bulk density and the SOM stoichiometry are key indicators of peat soil quality that can be used to assess the extent of peatland degradation (Leifeld et al., 2020; Liu and Lennartz, 2019a). The high SOM content of natural peatlands undoubtedly plays an important role in the ecological function of peat soils, contributing to high carbon storage, good soil water retention capacity, and cation exchange

capacity (Sonon et al., 2014). This thesis demonstrated that the degradation and mineralization of peatlands result in a decrease in the SOM content and an increase in bulk density, as evidenced by the experimental data presented in **Figure 5.2**, which was consistent with previous research findings (Liu and Lennartz, 2019a). Apparently, in the discussion of Chapter 4, coastal "peat" should be considered to some extent as "organic sediment with significant mineral content". Thus, it can be inferred that considering both bulk density and the SOM content (including C:N ratio) simultaneously, rather than focusing solely on either one, allows for a more comprehensive assessment of peatland degradation or mineralization levels due to the inherent ecological variations among and within peatland ecosystems (**Figure 5.2**). In addition to these two parameters, the study by Sienkiewicz et al. (2019) concluded that the ratio of dissolved organic carbon to soil organic carbon (DOC/SOC ratio) could better represent the intensity of peat soil mineralization, as the loss of carbon (C) and nitrogen (N) in peat SOM occurs independently. However, the experimental design employed in this thesis may not substantiate this perspective.
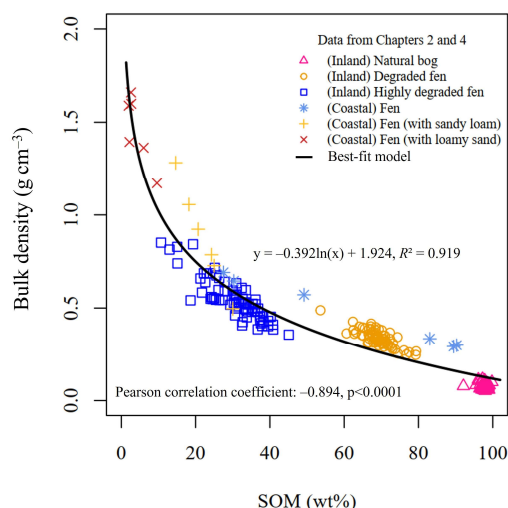
Figure 5.2 The correlation between bulk density (g cm^{-3}) and soil organic matter content (SOM, wt%) of all samples from Chapter 2 and 4 in this thesis.

5.2.1.2 Soil water content and macroporosity

Soil water content and soil structural information are other important indicators of peatland degradation. The water storage capacity of peatlands is influenced by their unique soil structure (Rezanezhad et al., 2016). Water content reflects the hydrological conditions of the peatland, where waterlogged anaerobic conditions due to high water levels are critical to peat formation as well as organic matter accumulation (Peatlands.org., n.d.). In turn, fluctuating water levels in peatlands inhibit *Sphagnum* growth and accelerate decomposition through fungal proliferation, thereby reducing the carbon sequestration potential of peatlands (Kim et al., 2021). **Figure 5.3a** showed that peatland degradation stages were closely linked to soil water content (or total

porosity). Compared to the degraded peatland, the inland pristine peatland investigated in this thesis exhibited a markedly higher macroporosity (**Figure 5.3b**), suggesting that changes in soil structure affected by peatland degradation can be significantly reflected by macroporosity.
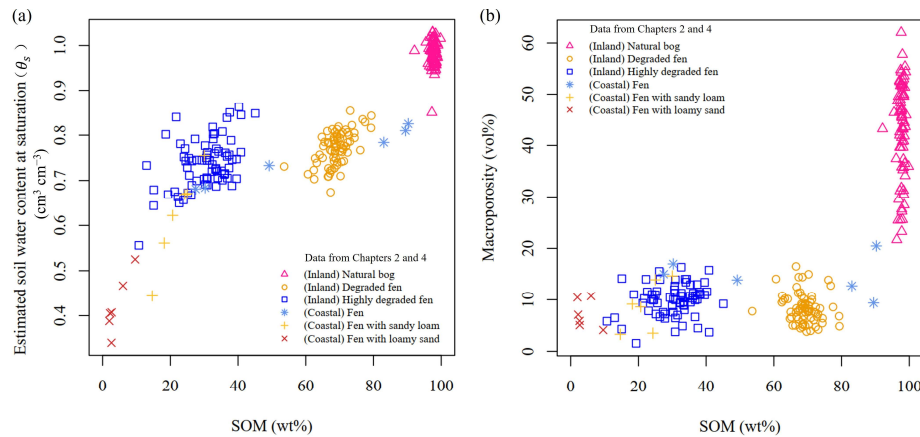
Figure 5.3 The relationship between soil organic matter content (SOM, wt%) and a) estimated soil water content at saturation (θ_s, cm^3 cm^{-3}); b) macroporosity (vol%) of all samples from Chapter 2 and 4 in this thesis.

Study on macroporosity is essential in peatlands because the large natural macropores in peatlands (*e.g.*, soil pipes in the English bogs) serve as a potential pathway for transporting substances among terrestrial, aquatic, and atmospheric systems (Dinsmore et al., 2011; Holden et al., 2012). Based on the variation in the origin and formation of macropores in peat, influenced by the type of peat/soil, different relationships were observed between macropores and other hydro-physical properties in the studied peatlands (**Figure 5.4** and Supplemental **Figure S5.2**). The macroporosity values of inland peat soils (bulk density < 0.8 g cm^{-3}) were within the range reported in Liu and Lennartz (2019a), while no significant correlation between macroporosity and bulk density was observed for soils sampled from the coastal peatland, especially for bulk density > 1.0 g cm^{-3} (**Figure 5.4**). Although Chapter 2 demonstrated the strong correlations between macroporosity and hydraulic properties, showing that incorporating macroporosity into pedotransfer functions can enhance the prediction of time-consuming hydraulic properties of inland peat soils using easily measurable parameters, the same approach might not be applicable for coastal peat soils. Similarly, the completely different correlations between macroporosity and VG model parameters illustrated that the study of coastal peatlands could not be directly extrapolated from environmental models of other single peatland types (Supplemental **Figure S5.2b and c**). In addition, compared to the "soil" of inland degraded fen and coastal fen, the natural peatland studied in this thesis was primarily formed by the growth of *Sphagnum*, and thus, their plant and vascular root structure contributed to their abundant macropores (McCarter et al., 2020; Weber et al., 2017). However, the high macroporosity observed in natural peatlands did not necessarily have higher K_s than in other study sites (Supplemental **Figure**

S5.2a). One possible reason for this is that multiple factors influence K_s, including soil depth, bulk density, the degree of peat humification, microtopography, peatland trophic type, and local climate conditions (Morris et al., 2022). Even if only pore structure is considered, the impact of factors such as pore connectivity on water movement should be taken into account (Gharedaghloo et al., 2018; McCarter et al., 2020).
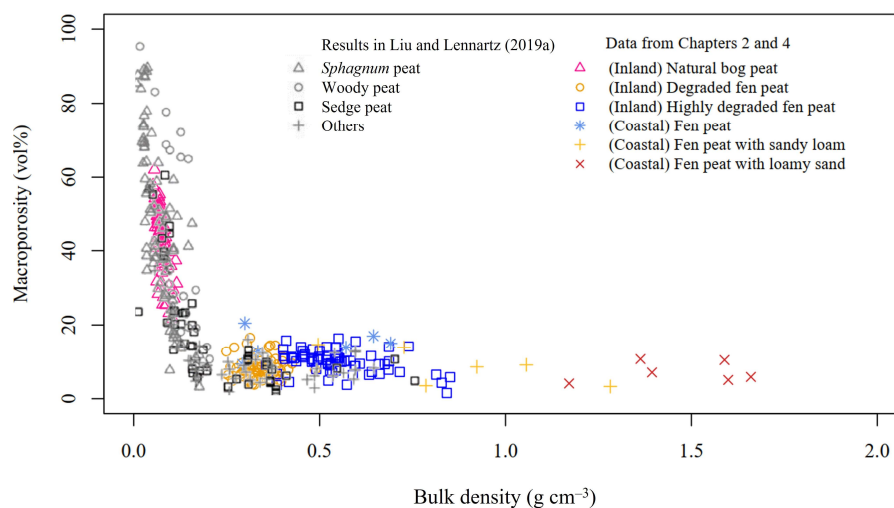
Figure 5.4 The relationship between soil bulk density (g cm⁻³) and macroporosity (vol%). Colored symbols represent the data of this thesis, while grey symbols represent values in the study of Liu and Lennartz (2019a).

Clearly, anthropogenic disturbance can lead to the collapse of peat soil structure and the loss of macropores, resulting in a decreased capacity to support vegetation and other ecosystem functions, and may also result in the loss of carbon stored in gaseous form (Chambers et al., 2019; Dinsmore et al., 2011; Kleimeier et al., 2017; Liu et al., 2016). A recent study reported that the hydrological regime and peat soil structure are not always fully restored, even after a decade of restoration efforts (Loisel and Gallego-Sala, 2022). In a case of restored *Sphagnum* bogs in Canada, Gauthier et al. (2018, 2022) proposed a possible reason that the hydrological connectivity was limited by the capillary barrier resulting from markedly different pore size distribution in degraded remnant cutover peat and regenerated *Sphagnum* moss. Based on their laboratory and field experiments, they suggested that mechanical compression could be a solution to the capillary barrier in the restored moss layer, although it would increase the bulk density and reduce the proportion of macropores. Their results proved an increased soil water retention and a higher average soil moisture content in compressed restored sites, ultimately facilitating the restoration of ecohydrological function in regenerated *Sphagnum* moss. It can therefore be assumed that by monitoring changes in water content and pore stucture, peatland restoration practitioners can assess the effectiveness of their restoration interventions and make informed decisions about future management strategies.

5.2.2 Important factors involved in this thesis on successful peatland restoration

Rewetting and effective management play crucial roles in peatland ecosystem restoration, offering multifaceted and essential implications. The restorative potential of rewetting extends to reviving ecological functions and mitigating GHG emissions in degraded peatlands (Evans et al., 2021; Tiemeyer et al., 2020; Wilson et al., 2016). Through rewetting, there is a likelihood of enhancing hydrological buffer function and potentially restoring a more favorable soil structure, which contributing to the mitigation of water table fluctuations and supporting the revival of native vegetation and promoting biodiversity (Ahmad et al., 2020). Moreover, the management of rewetted peatlands becomes instrumental in maintaining and enhancing these positive effects. In recent years, paludiculture cultivation, focusing on crops adapted to wetland conditions, has become a hot topic in the land use of rewetted peatlands (Tanneberger et al., 2022). Its crucial role in preventing the recurrence of degradation and ensuring the long-term sustainability of restored peatlands cannot be overstated. However, from a research perspective, rewetted peatlands still face some challenges that require ongoing attention and in-depth investigation.

5.2.2.1 Challenges of rewetting peatland

The peatland restoration process is intricate and involves numerous ecological, hydrological, and biogeochemical factors (Liu et al., 2020b; Monteverde et al., 2022). One of the primary challenges in evaluating the success of peatland restoration initiatives is the inherent heterogeneity of peatland ecosystems, which can affect the performance of different indicators employed to measure peatland characteristics and restoration success (*e.g.,* soil properties, local hydrology, and vegetation). However, not a lot of attention has been paid to this topic (Supplemental **Figure S5.3**).

Considering all forms of soil heterogeneity, including spatial heterogeneity (*e.g.*, spatial variability of soil properties) and more specific soil textural heterogeneity (*i.e.*, variations in soil type; McBratney and Minasny, 2007), is essential when planning a restoration practice in the field. The geostatistical analysis in Chapters 2 and 4 revealed differences in the autocorrelation of soil properties among different investigated peatland types. For instance, the spatially dependent range of the SOM content in the natural peatland was shorter than in the highly degraded peatland, indicating a more uniform distribution of the SOM content across the landscape than the highly degraded peatland (**Figure 5.5**). The spatial characteristics of the SOM content in inland peatlands, thus, can be inferred to assess the extent and severity of peatland degradation and restoration potential. Moreover, the coastal peatland studied showed the

strongest spatial autocorrelation in SOM of all sites due to the influence of factors such as microtopographic patterns and marine inputs (*e.g.*, the mineral sediment fraction). A comprehensive analysis of the spatial variation of SOM in highly heterogeneous peatland ecosystems, along with independent measurements, can enhance the understanding of carbon dynamics under rewetting scenarios.
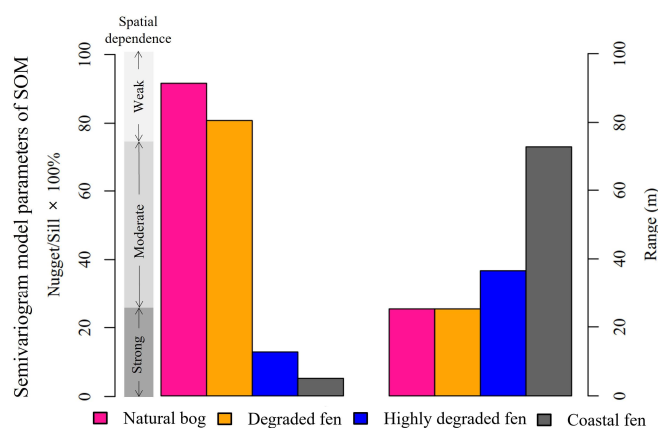
Figure 5.5 Semivarioagram parameters of the soil organic matter content (SOM) from Chapter 2 and 4. Links: level of spatial dependence (evaluated by nugget/sill ration of); right: range.

In addition, the spatial variability of the SOM content in peatlands can impact the effectiveness of rewetting efforts and pose certain environmental risks, such as the appearance of nutrient release "hotspots" (Chapter 4; Supplemental **Figure S5.4**). Long-term agricultural used peatlands can become "hotspots" for phosphate leaching when a rewetting project is applied to the site, which may lead to the eutrophication of groundwater and pose additional environmental risks to the peatland ecosystem (Tiemeyer et al., 2007; Zak et al., 2018). During the rewetting of a coastal peatland, low-lying areas with high SOM content are likely to remain "hotspots" for compounds (*e.g.*, NH_4^+) release and can export to adjacent marine systems (Pönisch et al., 2023). Meanwhile, seawater-rewetted areas that are potentially exposed to freshwater conditions (*e.g.*, storm, precipitation, and submarine groundwater discharge) have the possibility to lead to an increased DOC release from peatlands to waterbodies (Liu and Lennartz, 2019b).

On a global scale, boreal peatlands are the major contributors (~58%) of DOC export to surface waters (Rosset et al., 2022). Therefore, the dynamics of DOC concentrations should be taken into account in peatland restoration practices (Glatzel et al., 2003). Meanwhile, CDOM resulting from DOC release can increase turbidity and reduce transmissivity in the water, thereby impacting aquatic plant and animal communities (Branco and Kremer, 2005; Harvey et al., 2015; Lønborg et al., 2020; Moran and Zepp, 1997). Kreyling et al. (2021) pointed out that rewetted peatlands must be considered to be new ecosystems with potentially different functions. Thus,

when rewetting is approached as an effective way to recover the carbon sink function, side effects in this new ecosystem, such as high nutrient and DOC loss to adjacent aquatic systems due to altered soil characteristics and salinity changes in the wetted area, as well as salinity change-induced fluctuations in nutrient release, must be considered in order to better assess the potential impacts on the adjacent water quality.

5.2.2.2 The attention towards restoring peatland ecosystems

The restoration of peatlands, particularly through peatland rewetting, has received significant attention from the research community in recent years along with concerns about peatland degradation (**Figure S5.3**). To provide a better concluding discussion on the attention towards peatland restoration within the context of soil science, a bibliographic search was conducted in the Web of Science database (https://www.webofscience.com) on March 9, 2023, using the keywords "Peatland" AND "Soil properties" AND "Restoration" OR "Rewetting" in the "All field" category. This search yielded only a total of 108 articles. The earliest literature appeared in 2002 (1 article), and from 2015 onwards, the number of studies has notably increased, peaking at 20 articles per year in 2020 and 2022 (**Figure 5.6a**). An analysis of the geographic distribution of studies on the relevant topics revealed that Canada, Germany, and the United States were among the top three countries (**Figure 5.6b**). For instance, in Germany, comprehensive interdisciplinary studies have been conducted on degraded and rewetted peatlands to develop scientific principles for the sustainable and gentle management of these ecosystems, particularly through research projects, such as "BalticTRANSCOAST" and "WETSCAPES" (Jurasinski et al., 2020, 2018).
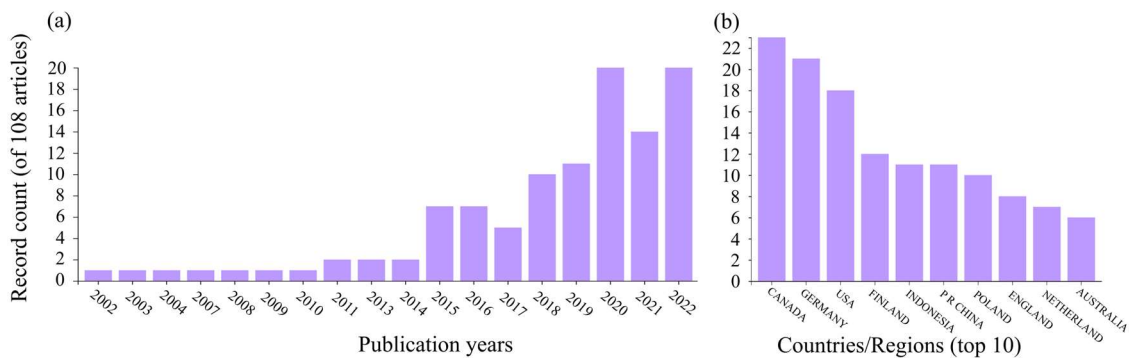
Figure 5.6 Results of (a) publication years; (b) countries/regions from the bliographic search in Web of Science database.

In addition to scientific aspects, successful peatland restoration requires engagement from multiple stakeholders, including policymakers, landowners, and local communities. For instance, the State Office for the Environment, Nature Conservation and Geology of the Federal State of

MV in Germany continuously disseminates information regarding the conservation and restoration of peatlands in the state, including an overview of the legal framework, goals, and measures related to peatland conservation and management, as well as examples of successful peatland restoration projects within the state. Additionally, raising public awareness can play a crucial role in promoting active participation among these stakeholders, facilitating the implementation of effective restoration practices, and ensuring the long-term success of peatland ecosystems.

Back to the scientific aspect, a bibliometric analysis[8] of these 108 articles was performed using VOSviewer Software (Apori et al., 2022; van Eck and Waltman, 2010), with a minimum co-occurrence threshold set at 6 (**Figure 5.7**).

Figure 5.7 Bibliometric analysis maps (co-occurrence network of keywords); (a) overlay visualization; (b) network visualization in 3 clusters.

---

[8] Note: The analytical methods used in this section were based on the approach described in Apori et al. (2022).

Overlay visualization analysis depicted a positive scenario in which the research priorities of peat soils have gradually shifted from examining soil (hydro-physical and chemical) properties to delving into the impact of rewetting on the environment over the last five years (**Figure 5.7a**). The emerging areas of interest also encompassed the challenges associated with rewetting peatlands, such as water quality (*i.e.*, keywords regarding different compounds and groundwater). The co-occurrence network of keywords identified three clusters, representing "hot" research focuses of the "soil properties" and "peatland restoration/rewetting" themes (**Figure 5.7b** and Supplemental **Table S5.1**). Network visualization analysis showed that cluster 3 ("land management"), which includes some methods of peatland restoration (*e.g.*, rewetting and revegetation), was closely linked to the other 2 clusters. It is also a good representation of the soil science community's approach to peatland restoration that takes full account of ecological, environmental, and applied aspects, and will guide more research involving these topics.

In particular, the keyword "water table" in the first cluster ("soil hydrology") can be a "bridge node" connecting different clusters and research communities (Supplemental **Figure S5.5**). By restoring proper water levels, the peatland rewetting process can reactivate vital processes such as peat accumulation, *sphagnum* growth, and nutrient cycling, which are essential for maintaining the unique biodiversity, carbon sequestration capacity, and hydrological regulation of peatlands. The integration of water table monitoring and management into peatland restoration efforts is, therefore, imperative to ensure these ecosystems' long-term success and resilience in the face of environmental challenges (Ahmad et al., 2021).

5.3 Limitations and Outlook

This thesis examined the soil physical properties of peatlands, achieving the proposed research objectives and providing valuable insights. It highlighted the ecological importance of peatlands and the risks associated with peatland degradation and discussed the role of soil physical properties in peatland degradation and ecosystem functions, as well as the factors that are essential for successful restoration of peatlands. The experimental sections offered guidance and tools for assessing and monitoring the condition and functionality of peatlands, including analysis of soil properties, mapping, and evaluation methods. The outcome and conclusions may contribute to advancing peatland research and provide practical support for sustainable peatland management and restoration.

However, there are still some limitations that cannot be ignored. For instance, in Chapter 2 the spatial dependence of SOM was strongly influenced by the degree of peatland degradation. However, the effect of this on other hydraulic and physical properties was not very significant. A possible reason for this is the small spatial scale or limited sample size, which may affect the

validity of the study results. On the one hand, although the measurement and analysis in Chapter 2 involved several types of peatlands that are typical in northeastern Germany, more data and factors from a larger scale (*e.g.*, national or global scale) are needed for analysis in order to develop more accurate models. Morris et al. (2022) demonstrated that their models could provide more accurate predictions of K_s of peat soils than in Chapter 2, because they accounted for some continuous and categorical predictors (*e.g.*, peatland trophic type, local surface microform, and climatic condition) that were overlooked by this thesis. On the other hand, it should be noted that spatial heterogeneity means that the effects of variables may differ in different sites or contexts, which may limit the generalizability of quantitative research results in different sites or contexts. Therefore, independent analysis of important variables is necessary for different study sites, especially inland and coastal peatlands.

In terms of the study design and methodology, the individual objectives and environmental constraints across the three studies led to differences in sampling depth and studied nutrients, potentially impacting result comparability and the overall coherence of the research. Additionally, reliance on traditional geostatistical methods in data analysis, such as semivariogram functions and Kriging interpolation, may be considered a limitation. The omission of more modern techniques, like digital elevation models (DEMs), in data visualization, could impact the depth of spatial analysis. Integrating advanced methods, including DEMs, is crucial for comprehensive spatial analysis in future peatland research. Furthermore, it is important to acknowledge another limitation associated with the linear mixed modeling analysis of spatially dependent data. The application of linear regression to non-independent samples suffers from theoretical shortcomings due to the presence of spatial autocorrelation, which poses a challenge in drawing reliable conclusions from the data. This limitation is reflected in the fitting accuracy of pedotransfer functions, which may not achieve the desired level of precision in predicting soil properties. Addressing this theoretical concern would require exploring alternative statistical approaches capable of handling spatially dependent data more effectively in future studies.

This thesis opens up several avenues for further research. One recommendation would be to conduct long-term experimental observations in rewetted peatlands to assess the dynamics of hydro-physical properties and their implication on peatland hydrology influenced by both marine and terrestrial systems on related ecosystems. In the field of macropore research, measurements of soil liquid contact angle should be conducted on intact and degraded peat soils to determine soil structure, including pore size distribution derived from soil water retention curves. Furthermore, attention should be given to the (peat) soil shrinkage characteristics. Another proposal is to investigate the correlation between greenhouse gas-related microbial activities and indicative soil properties of peatland degradation to reveal the mechanism of soil structure affecting greenhouse gas emissions (*e.g.*, methane production and ablution) and to provide

a more accurate and comprehensive reference for peatland management and protection. In addition, the inclusion of isotope labeling techniques in laboratory soil column experiments can more accurately explore the interaction between peat soil structure and biogeochemical cycles. Future research can certainly explore the use of novel techniques, such as remote sensing and machine learning to analyze the spatial variability of soil properties in peatlands. Lastly, it is essential to broaden our focus beyond rewetting as the sole method for restoring drained peatlands. As part of the restoration process, further investigation should be conducted on revegetation (*e.g.*, establishing growing *Sphagnum* moss; Glatzel and Rochefort, 2017). Specifically, the interactions between this approach and environmental responses need to be explored, taking into consideration soil physics aspects, such as pore structure.

Overall, the study of soil physics in peat soils is fundamental to the exploration of the structure, function, and composition of peatland ecosystems. A clear picture of peat soil hydraulic and physical properties and processes, thus, has important scientific significance and practical value, which is essential for the conservation and restoration of peatlands, as well as evaluating their response and contribution to global climate change.

References

Adam, P., 2016. Saltmarshes, in: Kennish, M.J. (Ed.), Encyclopedia of Estuaries. Encyclopedia of Earth Sciences Series. Springer, Dordrecht, pp. 515–535. https://doi.org/10.1007/978-94-017-8801-4_320

Ahmad, S., Liu, H., Alam, S., Günther, A., Jurasinski, G., Lennartz, B., 2021. Meteorological controls on water table dynamics in fen peatlands depend on management regimes. Front. Earth Sci. 9, 630469. https://doi.org/10.3389/feart.2021.630469

Ahmad, S., Liu, H., Beyer, F., Kløve, B., Lennartz, B., 2020. Spatial heterogeneity of soil properties in relation to microtopography in a non-tidal rewetted coastal mire. Mires Peat 26, article 04, 18pp. https://doi.org/10.19189/MaP.2019.GDC.StA.1779

Alongi, D.M., 2016. Mangroves, in: Kennish, M.J. (Ed.), Encyclopedia of Estuaries. Encyclopedia of Earth Sciences Series. Springer, Dordrecht, pp. 393–404. https://doi.org/10.1007/978-94-017-8801-4_3

Andersson, S., Nilsson, S.I., 2001. Influence of pH and temperature on microbial activity, substrate availability of soil-solution bacteria and leaching of dissolved organic carbon in a mor humus. Soil Biol. Biochem. 33, 1181–1191. https://doi.org/10.1016/S0038-0717(01)00022-0

Apori, S.O., Mcmillan, D., Giltrap, M., Tian, F., 2022. Mapping the restoration of degraded peatland as a research area: A scientometric review. Front Environ. Sci. 10. https://doi.org/10.3389/fenvs.2022.942788

Ardón, M., Helton, A.M., Bernhardt, E.S., 2016. Drought and saltwater incursion synergistically reduce dissolved organic carbon export from coastal freshwater wetlands. Biogeochemistry 127, 411–426. https://doi.org/10.1007/s10533-016-0189-5

Ardón, M., Morse, J.L., Colman, B.P., Bernhardt, E.S., 2013. Drought-induced saltwater incursion leads to increased wetland nitrogen export. Glob. Chang. Biol. 19, 2976–2985. https://doi.org/10.1111/gcb.12287

Audet, J., Zak, D., Bidstrup, J., Hoffmann, C.C., 2020. Nitrogen and phosphorus retention in Danish restored wetlands. Ambio 49, 324–336. https://doi.org/10.1007/s13280-019-01181-2

Bachmann, J., Woche, S.K., Goebel, M.-O., Kirkham, M.B., Horton, R., 2003. Extended methodology for determining wetting properties of porous media. Water. Resour. Res. 39, 1353. https://doi.org/10.1029/2003WR002143

Backnäs, S., Laine-Kaulio, H., Kløve, B., 2012. Phosphorus forms and related soil chemistry in preferential flow-paths and the soil matrix of a forested podzolic till soil profile. Geoderma 189–190, 50–64. https://doi.org/10.1016/j.geoderma.2012.04.016

Baird, A.J., 1997. Field estimation of macropore functioning and surface hydraulic conductivity in a fen peat. Hydrol. Process. 11, 287–295. https://doi.org/10.1002/(SICI)1099-1085(19970315)11:3<287::AID-HYP443>3.0.CO;2-L

Baird, A.J., Belyea, L.R., Comas, X., Reeve, A.S., Slater, L.D., 2009. Carbon Cycling in Northern Peatlands. American Geophysical Union, Washington, D. C. https://doi.org/10.1029/GM184

Baird, A.J., Eades, P.A., Surridge, B.W.J., 2008. The hydraulic structure of a raised bog and its implications for ecohydrological modelling of bog development. Ecohydrology 1, 289–298. https://doi.org/10.1002/eco.33

Baird, A.J., Gaffney, S.W., 2000. Solute movement in drained fen peat: a field tracer study in a Somerset (UK) wetland. Hydrol. Process. 14, 2489–2503. https://doi.org/10.1002/1099-1085(20001015)14:14<2489::AID-HYP110>3.0.CO;2-Q

Baird, A.J., Milner, A.M., Blundell, A., Swindles, G.T., Morris, P.J., 2016. Microform-scale variations in peatland permeability and their ecohydrological implications. J. Ecol. 104, 531–544. https://doi.org/10.1111/1365-2745.12530

Baldwin, D.S., Rees, G.N., Mitchell, A.M., Watson, G., Williams, J., 2006. The short-term effects of salinization on anaerobic nutrient cycling and microbial community structure in sediment from a freshwater wetland. Wetlands 26, 455–464. https://doi.org/10.1672/0277-5212(2006)26[455:TSEOSO]2.0.CO;2

Banton, O., 1993. Field- and laboratory-determined hydraulic conductivities considering anisotropy and core surface area. Soil Sci. Soc. Am. J. 57, 10–15. https://doi.org/10.2136/sssaj1993.03615995005700010003x

Batistel, C., Porsche, C., Jurasinski, G., Schubert, H., 2022. Responses of four peatland emergent macrophytes to salinity and short salinity pulses. Wetlands 42, 67. https://doi.org/10.1007/s13157-022-01592-0

Bear, J., 1972. Dynamics of fluids in porous media. Elsevier, New York.

Beckwith, C.W., Baird, A.J., Heathwaite, A.L., 2003. Anisotropy and depth-related heterogeneity of hydraulic conductivity in a bog peat. I: laboratory measurements. Hydrol. Process. 17, 89–101. https://doi.org/10.1002/hyp.1116

Berg, C., Vandieken, V., Thamdrup, B., Jürgens, K., 2015. Significance of archaeal nitrification in hypoxic waters of the Baltic Sea. ISME J. 9, 1319–1332. https://doi.org/10.1038/ismej.2014.218

Berkowitz, J.F., VanZomeren, C.M., Piercy, C.D., White, J.R., 2018. Evaluation of coastal wetland soil properties in a degrading marsh. Estuar. Coast. Shelf Sci. 212, 311–317. https://doi.org/10.1016/j.ecss.2018.07.021

Beven, K., Germann, P., 1982. Macropores and water flow in soils. Water Resour. Res. 18, 1311–1325. https://doi.org/10.1029/WR018i005p01311

Bevington, J., Piragnolo, D., Teatini, P., Vellidis, G., Morari, F., 2016. On the spatial variability of soil hydraulic properties in a Holocene coastal farmland. Geoderma 262, 294–305. https://doi.org/10.1016/j.geoderma.2015.08.025

Biswas, A., Si, B.C., 2009. Spatial relationship between soil hydraulic and soil physical properties in a farm field. Can. J. Soil. Sci. 89, 473–488. https://doi.org/10.4141/cjss08052

Blodau, C., Basiliko, N., Moore, T.R., 2004. Carbon turnover in peatland mesocosms exposed to different water table levels. Biogeochemistry 67, 331–351. https://doi.org/10.1023/B:BIOG.0000015788.30164.e2

Blodau, C., Moore, T.R., 2002. Macroporosity affects water movement and pore water sampling in peat soils. Soil Sci. 167, 98–109. https://doi.org/10.1097/00010694-200202000-00002

Boelter, D.H., 1968. Important physical properties of peat materials., in: Proceedings, Third International Peat Congress. Quebec, Canada.

Bowen, J.L., Giblin, A.E., Murphy, A.E., Bulseco, A.N., Deegan, L.A., Johnson, D.S., Nelson, J.A., Mozdzer, T.J., Sullivan, H.L., 2020. Not all nitrogen is created equal: Differential effects of nitrate and ammonium enrichment in coastal wetlands. Bioscience 70, 1108–1119. https://doi.org/10.1093/biosci/biaa140

Brady, N.C., Weil, R.R., 2000. Nature and properties of soils. Macmillan publishing company, New York.

Bragg, O., Lindsay, R., 2003. Strategy and Action Plan for Mire and Peatland Conservation in Central Europe. Wetlands International, Wageningen, The Netherlands.

Branco, A.B., Kremer, J.N., 2005. The relative importance of chlorophyll and colored dissolved organic matter (CDOM) to the prediction of the diffuse attenuation coefficient in shallow estuaries. Estuaries 28, 643–652. https://doi.org/10.1007/BF02732903

Branham, J.E., Strack, M., 2014. Saturated hydraulic conductivity in *Sphagnum* -dominated peatlands: Do microforms matter? Hydrol. Process. 28, 4352–4362. https://doi.org/10.1002/hyp.10228

Bruland, G.L., Richardson, C.J., 2005. Spatial variability of soil properties in created, restored, and paired natural wetlands. Soil Sci. Soc. Am. J. 69, 273–284. https://doi.org/10.2136/sssaj2005.0273a

Brust, G.E., 2019. Management strategies for organic vegetable fertility, in: Biswas, D., Micallef, S.A. (Eds.), Safety and Practice for Organic Food. Elsevier, pp. 193–212. https://doi.org/10.1016/B978-0-12-812060-6.00009-X

Burnham, K.P., Anderson, D.R., 2002. Model Selection and Multimodel Inference. Springer New York, New York, NY. https://doi.org/10.1007/b97636

Cambardella, C.A., Moorman, T.B., Novak, J.M., Parkin, T.B., Karlen, D.L., Turco, R.F., Konopka, A.E., 1994. Field-scale variability of soil properties in central Iowa soils. Soil Sci. Soc. Am. J. 58, 1501–1511. https://doi.org/10.2136/sssaj1994.03615995005800050033x

Cameron, K.C., Buchan, G.D., 2016. Porosity: Pore size distribution, in: Lal, R. (Ed.), Encyclopedia of Soil Science. CRC Press, Boca Raton, Florida.

Camino-Serrano, M., Graf Pannatier, E., Vicca, S., Luyssaert, S., Jonard, M., Ciais, P., Guenet, B., Gielen, B., Peñuelas, J., Sardans, J., Waldner, P., Etzold, S., Cecchini, G., Clarke, N., Galić, Z., Gandois, L., Hansen, K., Johnson, J., Klinck, U., Lachmanová, Z., Lindroos, A.-J., Meesenburg, H., Nieminen, T.M., Sanders, T.G.M., Sawicka, K., Seidling, W., Thimonier, A., Vanguelova, E., Verstraeten, A., Vesterdal, L., Janssens, I.A., 2016. Trends in soil solution dissolved organic carbon (DOC) concentrations across European forests. Biogeosciences 13, 5567–5585. https://doi.org/10.5194/bg-13-5567-2016

Carey, S.K., Quinton, W.L., Goeller, N.T., 2007. Field and laboratory estimates of pore size properties and hydraulic characteristics for subarctic organic soils. Hydrol Process 21, 2560–2571. https://doi.org/10.1002/hyp.6795

Carter, M.R., Kunelius, H.T., Angers, D.A., 1994. Soil structural form and stability, and organic matter under cool-season perennial grasses. Soil Sci. Soc. Am. J. 58, 1194–1199. https://doi.org/10.2136/sssaj1994.03615995005800040027x

REFERENCES

Chambers, L.G., Davis, S.E., Troxler, T., Boyer, J.N., Downey-Wall, A., Scinto, L.J., 2014. Biogeochemical effects of simulated sea level rise on carbon loss in an Everglades mangrove peat soil. Hydrobiologia 726, 195–211. https://doi.org/10.1007/s10750-013-1764-6

Chambers, L.G., Reddy, K.R., Osborne, T.Z., 2011. Short-term response of carbon cycling to salinity pulses in a freshwater wetland. Soil Sci. Soc. Am. J. 75, 2000–2007. https://doi.org/10.2136/sssaj2011.0026

Chambers, L.G., Steinmuller, H.E., Breithaupt, J.L., 2019. Toward a mechanistic understanding of "peat collapse" and its potential contribution to coastal wetland loss. Ecology 100. https://doi.org/10.1002/ecy.2720

Chapman, N., Miller, A.J., Lindsey, K., Whalley, W.R., 2012. Roots, water, and nutrient acquisition: Let's get physical. Trends Plant Sci. 17, 701–710. https://doi.org/10.1016/j.tplants.2012.08.001

Charman, D.J., 2009. Peat and peatlands, in: Encyclopedia of Inland Waters. Elsevier, pp. 541–548. https://doi.org/10.1016/B978-012370626-3.00061-2

Chason, D.B., Siegel, D.I., 1986. Hydraulic conductivity and related physical properties of peat, Lost River Peatland, northern Minnesota. Soil Sci. 142, 91–99. https://doi.org/10.1097/00010694-198608000-00005

Chow, A.T., Tanji, K.K., Gao, S., 2003. Production of dissolved organic carbon (DOC) and trihalomethane (THM) precursor from peat soils. Water Res. 37, 4475–4485. https://doi.org/10.1016/S0043-1354(03)00437-8

Clarke, D., Rieley, J., 2019. Strategy for responsible peatland management. International Peat Society, Jyväskylä, Finland, pp. 7–8.

Clymo, R.S., Kramer, J.R., Hammerton, D., 1984. *Sphagnum*-dominated peat bog: A naturally acid ecosystem. Philos. Trans. R. Soc. Lond. B. Biol. Sci. 305, 487–499.

Cowardin, L.M., Carter, V., Golet, F.C., LaRoe, E.T., 1979. Classification of wetlands and deepwater habitats of the United States. Washington, DC.

Craft, C., 2022. Peatlands, in: Creating and Restoring Wetlands. Elsevier, Georgia, USA, pp. 205–246. https://doi.org/10.1016/B978-0-12-823981-0.00012-5

Cris, R., Buckmaster, S., Reed, M.S., Bain, C., 2014. Global Peatland Restoration demonstrating success. Edinburgh.

Crnobrna, B., Llanqui, I.B., Cardenas, A.D., Panduro Pisco, G., 2022. Relationships between organic matter and bulk density in Amazonian peatland soils. Sustainability 14, 12070. https://doi.org/10.3390/su141912070

Cunliffe, A.M., Baird, A.J., Holden, J., 2013. Hydrological hotspots in blanket peatlands: Spatial variation in peat permeability around a natural soil pipe. Water Resour. Res. 49, 5342–5354. https://doi.org/10.1002/wrcr.20435

Dau, H.C., 1823. Neues Handbuch über den Torf, dressen Natur, Entstehung, und Wiedererzeugung. J. C. Hinrichshen Buchandlung, Leipzig.

Davidson, I.C., Cott, G.M., Devaney, J.L., Simkanin, C., 2018. Differential effects of biological invasions on coastal blue carbon: A global review and meta-analysis. Glob. Chang. Biol. 24, 5218–5230. https://doi.org/10.1111/gcb.14426

Davidson, N.C., van Dam, A.A., Finlayson, C.M., McInnes, R.J., 2019. Worth of wetlands: Revised global monetary values of coastal and inland wetland ecosystem services. Mar. Freshw. Res. 70, 1189. https://doi.org/10.1071/MF18391

Dawson, Q., Kechavarzi, C., Leeds-Harrison, P.B., Burton, R.G.O., 2010. Subsidence and degradation of agricultural peatlands in the Fenlands of Norfolk, UK. Geoderma 154, 181–187. https://doi.org/10.1016/j.geoderma.2009.09.017

Degner, J.H., 1729. Dissertatio physica de Turfis: Sistens historiam naturalem cespitum combustilium qui in multis Europae regionibus, & praecipue in Hollandia reperiuntur ac ligni loco usurpantur.

DeLaune, R.D., White, J.R., 2012. Will coastal wetlands continue to sequester carbon in response to an increase in global sea level?: A case study of the rapidly subsiding Mississippi river deltaic plain. Clim. Change. 110, 297–314. https://doi.org/10.1007/s10584-011-0089-6

Dettmann, U., Bechtold, M., 2016. Deriving effective soil water retention characteristics from shallow water table fluctuations in peatlands. Vadose Zone J. 15, vzj2016.04.0029. https://doi.org/10.2136/vzj2016.04.0029

Dettmann, U., Bechtold, M., Frahm, E., Tiemeyer, B., 2014. On the applicability of unimodal and bimodal van Genuchten–Mualem based models to peat and other organic soils under evaporation conditions. J. Hydrol. 515, 103–115. https://doi.org/10.1016/j.jhydrol.2014.04.047

Deutsch, B., Alling, V., Humborg, C., Korth, F., Mörth, C.M., 2012. Tracing inputs of terrestrial high molecular weight dissolved organic matter within the Baltic Sea ecosystem. Biogeosciences 9, 4465–4475. https://doi.org/10.5194/bg-9-4465-2012

Diamond, J.S., Epstein, J.M., Cohen, M.J., McLaughlin, D.L., Hsueh, Y., Keim, R.F., Duberstein, J.A., 2021. A little relief: Ecological functions and autogenesis of wetland microtopography. WIREs Water 8. https://doi.org/10.1002/wat2.1493

Dinsmore, K.J., Smart, R.P., Billett, M.F., Holden, J., Baird, A.J., Chapman, P.J., 2011. Greenhouse gas losses from peatland pipes: A major pathway for loss to the atmosphere? J. Geophys. Res. 116, G03041. https://doi.org/10.1029/2011JG001646

Du Rietz, E.G., 1954. Die Mineralbodenwasserzeigergrenze als Grundlage einer natürlichen Zweigliederung der nord- und mitteleuropäischen Moore. Vegetatio 5/6, 571–585.

Edwards, W.M., Shipitalo, M.J., Owens, L.B., 1993. Gas, water and solute transport in soils containing macropores: A review of methodology. Geoderma 57, 31–49. https://doi.org/10.1016/0016-7061(93)90146-C

Eggelsmann, R., Heathwaite, A.L., Grosse-Brauckmann, G., Kuster, E., Naucke, W., Schuch, M., Schweickle, V., 1993. Physical processes and properties of mires, in: Heathwaite, A.L. (Ed.), Mires: Process, Exploitation and Conservation. Wiley, Chicheste.

Englund, E., Sparks, A., 1991. GEO-EAS 1.2.1 geostatistical environmental assessment software: Users' guide. Las Vegas, Nevada.

Esri., n.d. Understanding a semivariogram: The range, sill, and nugget. ArcGIS Pro Documentation. Retrieved from https://pro.arcgis.com/en/pro-app/latest/help/analysis/geostatistical-analyst/understanding-a-semivariogram-the-range-sill-and-nugget.htm.

Evans, C.D., Jones, T.G., Burden, A., Ostle, N., Zieliński, P., Cooper, M.D.A., Peacock, M., Clark, J.M., Oulehle, F., Cooper, D., Freeman, C., 2012. Acidity controls on dissolved organic carbon mobility in organic soils. Glob. Chang. Biol. 18, 3317–3331. https://doi.org/10.1111/j.1365-2486.2012.02794.x

Evans, C.D., Peacock, M., Baird, A.J., Artz, R.R.E., Burden, A., Callaghan, N., Chapman, P.J., Cooper, H.M., Coyle, M., Craig, E., Cumming, A., Dixon, S., Gauci, V., Grayson, R.P., Helfter, C., Heppell, C.M., Holden, J., Jones, D.L., Kaduk, J., Levy, P., Matthews, R., McNamara, N.P., Misselbrook, T., Oakley, S., Page, S.E., Rayment, M., Ridley, L.M., Stanley, K.M., Williamson, J.L., Worrall, F., Morrison, R., 2021. Overriding water table control on managed peatland greenhouse gas emissions. Nature 593, 548–552. https://doi.org/10.1038/s41586-021-03523-1

Fell, H., Roßkopf, N., Bauriegel, A., Zeitz, J., 2016. Estimating vulnerability of agriculturally used peatlands in northeast Germany to carbon loss based on multi-temporal subsidence data analysis. Catena 137, 61–69. https://doi.org/10.1016/j.catena.2015.08.010

Ferrari, G.M., Dowell, M.D., Grossi, S., Targa, C., 1996. Relationship between the optical properties of chromophoric dissolved organic matter and total concentration of dissolved organic carbon in the southern Baltic Sea region. Mar. Chem. 55, 299–316. https://doi.org/10.1016/S0304-4203(96)00061-8

Fichot, C.G., Benner, R., 2011. A novel method to estimate DOC concentrations from CDOM absorption coefficients in coastal waters. Geophys. Res. Lett. 38, n/a-n/a. https://doi.org/10.1029/2010GL046152

Fließbach, A., Mäder, P., 2000. Microbial biomass and size-density fractions differ between soils of organic and conventional agricultural systems. Soil Biol. Biochem. 32, 757–768. https://doi.org/10.1016/S0038-0717(99)00197-2

Forsmann, D.M., Kjaergaard, C., 2014. Phosphorus release from anaerobic peat soils during convective discharge — Effect of soil Fe:P molar ratio and preferential flow. Geoderma 223–225, 21–32. https://doi.org/10.1016/j.geoderma.2014.01.025

Frolking, S., Roulet, N., Fuglestvedt, J., 2006. How northern peatlands influence the Earth's radiative budget: Sustained methane emission versus sustained carbon sequestration. J. Geophys. Res. 111, G01008. https://doi.org/10.1029/2005JG000091

Frolking, S., Roulet, N.T., Tuittila, E., Bubier, J.L., Quillet, A., Talbot, J., Richard, P.J.H., 2010. A new model of Holocene peatland net primary production, decomposition, water balance, and peat accumulation. Earth Syst. Dyn. 1, 1–21. https://doi.org/10.5194/esd-1-1-2010

Früh, J., Schröter, C., 1904. Die Moore der Schweiz. Stiftung Schnyder von Wartensee, Bern.

Fuchs, J.W., Fox, G.A., Storm, D.E., Penn, C.J., Brown, G.O., 2009. Subsurface transport of phosphorus in riparian floodplains: influence of preferential flow paths. J. Environ. Qual. 38, 473–484. https://doi.org/10.2134/jeq2008.0201

Gabriel, M., Toader, C., Faul, F., Roßkopf, N., Grundling, P., van Huyssteen, C., Grundling, A.T., Zeitz, J., 2018. Physical and hydrological properties of peat as proxies for degradation of South African peatlands: Implications for conservation and restoration. Mires Peat 21, article 23, 1–21. https://doi.org/https://doi.org/10.19189/MaP.2018.OMB.336

REFERENCES

Gächter, R., Ngatiah, J.M., Stamm, C., 1998. Transport of phosphate from soil to surface waters by preferential flow. Environ. Sci. Technol. 32, 1865–1869. https://doi.org/10.1021/es9707825

Gallardo, A., 2003. Spatial variability of soil properties in a floodplain forest in northwest Spain. Ecosystems 6, 564–576. https://doi.org/10.1007/s10021-003-0198-9

Gauthier, T.-L.J., Elliott, J.B., McCarter, C.P.R., Price, J.S., 2022. Field-scale compression of *Sphagnum* moss to improve water retention in a restored bog. J. Hydrol. 612, 128160. https://doi.org/10.1016/j.jhydrol.2022.128160

Gauthier, T.-L.J., McCarter, C.P.R., Price, J.S., 2018. The effect of compression on *Sphagnum* hydrophysical properties: Implications for increasing hydrological connectivity in restored cutover peatlands. Ecohydrology 11, e2020. https://doi.org/10.1002/eco.2020

Geohring, L.D., McHugh, O. V., Walter, M.T., Steenhuis, T.S., Akhtar, M.S., Walter, M.F., 2001. Phosphorus transport into subsurface drains by macropores after manure applications: Implications for best manure management practices. Soil Sci. 166, 896–909. https://doi.org/10.1097/00010694-200112000-00004

Gharedaghloo, B., Price, J.S., 2019. Characterizing the immiscible transport properties of diesel and water in peat soil. J. Contam. Hydrol. 221, 11–25. https://doi.org/10.1016/j.jconhyd.2018.12.005

Gharedaghloo, B., Price, J.S., Rezanezhad, F., Quinton, W.L., 2018. Evaluating the hydraulic and transport properties of peat soil using pore network modeling and X-ray micro computed tomography. J Hydrol. 561, 494–508. https://doi.org/10.1016/j.jhydrol.2018.04.007

Giménez, D., Hirmas, D., 2016. Macroporosity, in: Lal, R. (Ed.), The Encyclopedia of Soil Science. CRC Press, Boca Raton, FL, pp. 1388–1391.

Glatzel, S., Basiliko, N., Moore, T., 2004. Carbon dioxide and methane production potentials of peats from natural, harvested and restored sites, eastern Québec, Canada. Wetlands 24, 261–267. https://doi.org/10.1672/0277-5212(2004)024[0261:CDAMPP]2.0.CO;2

Glatzel, S., Kalbitz, K., Dalva, M., Moore, T. 2003. Dissolved organic matter properties and their relationship to carbon dioxide efflux from restored peat bogs. Geoderma 113, 397–411. https://doi.org/10.1016/S0016-7061(02)00372-5

Glatzel, S., Rochefort, L., 2017. Growing *sphagnum*: Foreword. Mires Peat 20, article 00, 1–4. https://doi.org/10.19189/MaP.2017.OMB.276

Gnatowski, T., Brandyk, T., Szatyłowicz, J., 1996. Ocena zmienności przestrzennej właściwości fizycznych i wodnych gleby w skali nawadnianej kwatery (in Eng. Spatial variability estimation of some soil properties at irrigated plot scale). Przegląd Naukowy Wydziału Melioracji i Inżynierii Środowiska 11, 129–136.

Gnatowski, T., Szatyłowicz, J., Brandyk, T., Kechavarzi, C., 2010. Hydraulic properties of fen peat soils in Poland. Geoderma 154, 188–195. https://doi.org/10.1016/j.geoderma.2009.02.021

Goetz, J.D., Price, J.S., 2015. Role of morphological structure and layering of *Sphagnum* and *Tomenthypnum* mosses on moss productivity and evaporation rates. Can. J. Soil. Sci. 95, 109–124. https://doi.org/10.4141/cjss-2014-092

Gonçalves, M.C., Leij, F.J., Schaap, M.G., 2001. Pedotransfer functions for solute transport parameters of Portuguese soils. Eur. J. Soil Sci. 52, 563–574. https://doi.org/10.1046/j.1365-2389.2001.00409.x

Gosch, L., Janssen, M., Lennartz, B., 2018. Impact of the water salinity on the hydraulic conductivity of fen peat. Hydrol. Process. 32, 1214–1222. https://doi.org/10.1002/hyp.11478

Gosch, L., Townsend, H., Kreuzburg, M., Janssen, M., Rezanezhad, F., Lennartz, B., 2019. Sulfate mobility in fen peat and its impact on the release of solutes. Front Environ Sci 7. https://doi.org/10.3389/fenvs.2019.00189

Greifswald Moor Centrum, 2019. Ein Drittel aller CO₂-Emissionen einzusparen ist möglich-schnelle Einstellung von Moor-Entwässerung für wirkungsvollen Klimaschutz nötig! Greifswald.

Grigal, D.F., Brovold, S.L., Nord, W.S., Ohmann, L.F., 1989. Bulk density of surface soils and peat in the North Central United States. Can J Soil Sci 69, 895–900. https://doi.org/10.4141/cjss89-092

Grover, S.P.P., Baldock, J.A., 2013. The link between peat hydrology and decomposition: Beyond von Post. J. Hydrol. 479, 130–138. https://doi.org/10.1016/j.jhydrol.2012.11.049

Guber, A., Pachepsky, Ya., Shein, E., Rawls, W.J., 2004. Soil aggregates and water retention, in: Pachepsky, Y., Rawls, W.J. (Eds.), Development of Pedotransfer Functions in Soil Hydrology, In Developments in Soil Science. pp. 143–151. https://doi.org/10.1016/S0166-2481(04)30008-5

Günther, A., Barthelmes, A., Huth, V., Joosten, H., Jurasinski, G., Koebsch, F., Couwenberg, J., 2020. Prompt rewetting of drained peatlands reduces climate warming despite methane emissions. Nat. Commun. 11, 1644. https://doi.org/10.1038/s41467-020-15499-z

Guo, L., Macdonald, R.W., 2006. Source and transport of terrigenous organic matter in the upper Yukon River: Evidence from isotope (δ^{13}C, Δ^{14}C, and δ^{15}N) composition of dissolved, colloidal, and particulate phases. Global Biogeochem. Cycles 20, n/a-n/a. https://doi.org/10.1029/2005GB002593

Gustafsson, E., Deutsch, B., Gustafsson, B.G., Humborg, C., Mörth, C.-M., 2014. Carbon cycling in the Baltic Sea — The fate of allochthonous organic carbon and its impact on air–sea CO_2 exchange. J. Mar. Syst. 129, 289–302. https://doi.org/10.1016/j.jmarsys.2013.07.005

Gwenzi, W., Hinz, C., Holmes, K., Phillips, I.R., Mullins, I.J., 2011. Field-scale spatial variability of saturated hydraulic conductivity on a recently constructed artificial ecosystem. Geoderma 166, 43–56. https://doi.org/10.1016/j.geoderma.2011.06.010

Hahn, J., Köhler, S., Glatzel, S., Jurasinski, G., 2015. Methane exchange in a coastal fen in the first year after flooding - A systems shift. PLoS One 10, e0140657. https://doi.org/10.1371/journal.pone.0140657

Haj-Amor, Z., Araya, T., Acharjee, T.K., Bouri, S., Anlauf, R., 2023. Soil-water modeling as a tool for sustainable soil resources management, in: Water, Land, and Forest Susceptibility and Sustainability, Volume 2. Elsevier, pp. 71–96. https://doi.org/10.1016/B978-0-443-15847-6.00001-X

Hájek, T., Ballance, S., Limpens, J., Zijlstra, M., Verhoeven, J.T.A., 2011. Cell-wall polysaccharides play an important role in decay resistance of *Sphagnum* and actively depressed decomposition in vitro. Biogeochemistry 103, 45–57. https://doi.org/10.1007/s10533-010-9444-3

Hallema, D.W., Périard, Y., Lafond, J.A., Gumiere, S.J., Caron, J., 2015. Characterization of water retention curves for a series of cultivated Histosols. Vadose Zone J. 14, vzj2014.10.0148. https://doi.org/10.2136/vzj2014.10.0148

Hansen, H.C.B., Hansen, P.E., Magid, J., 1999. Empirical modelling of the kinetics of phosphate sorption to macropore materials in aggregated subsoils. Eur. J. Soil. Sci. 50, 317–327. https://doi.org/10.1046/j.1365-2389.1999.00235.x

Harenda, K.M., Lamentowicz, M., Samson, M., Chojnicki, B.H., 2018. The role of peatlands and their carbon storage function in the context of climate change, in: Zielinski, T., Sagan, I., Surosz, W. (Eds.), Interdisciplinary Approaches for SustainableDevelopment Goals, GeoPlanet: Earth and Planetary Sciences. Springer, pp. 169–187. https://doi.org/10.1007/978-3-319-71788-3_12

Harvey, E.T., Kratzer, S., Andersson, A., 2015. Relationships between colored dissolved organic matter and dissolved organic carbon in different coastal gradients of the Baltic Sea. Ambio 44, 392–401. https://doi.org/10.1007/s13280-015-0658-4

Hayes, M.A., Jesse, A., Hawke, B., Baldock, J., Tabet, B., Lockington, D., Lovelock, C.E., 2017. Dynamics of sediment carbon stocks across intertidal wetland habitats of Moreton Bay, Australia. Glob. Chang. Biol. 23, 4222–4234. https://doi.org/10.1111/gcb.13722

Haynes, R.J., 2005. Labile organic matter fractions as central components of the quality of agricultural soils: an overview. Advances in Agronomy 85, 221–268. https://doi.org/10.1016/S0065-2113(04)85005-3

Hendrickx, J.M.H., Flury, M., 2001. Uniform and preferential flow mechanisms in the vadose zone, in: Conceptual Models of Flow and Transport in the Fractured Vadose Zone. The National Academies Press, Washington, D.C.

Herbert, E.R., Boon, P., Burgin, A.J., Neubauer, S.C., Franklin, R.B., Ardón, M., Hopfensperger, K.N., Lamers, L.P.M., Gell, P., 2015. A global perspective on wetland salinization: Ecological consequences of a growing threat to freshwater wetlands. Ecosphere 6, art206. https://doi.org/10.1890/ES14-00534.1

Hirschelmann, S., Tanneberger, F., Wichmann, S., Reichelt, F., Hohlbein, M., Couwenberg, J., Busse, S., Schröder, C., Nordt, A., 2020. Moore in Mecklenburg-Vorpommern im Kontext nationaler und internationaler Klimaschutzziele - Zustand und Entwicklungspotenzial (Faktensammlung). Greifswald.

Hoag, R.S., Price, J.S., 1997. The effects of matrix diffusion on solute transport and retardation in undisturbed peat in laboratory columns. J. Contam. Hydrol. 28, 193–205. https://doi.org/10.1016/S0169-7722(96)00085-X

Holden, J., 2009. Flow through macropores of different size classes in blanket peat. J. Hydrol. 364, 342–348. https://doi.org/10.1016/j.jhydrol.2008.11.010

Holden, J., Burt, T.P., Cox, N.J., 2001. Macroporosity and infiltration in blanket peat: The implications of tension disc infiltrometer measurements. Hydrol. Process. 15, 289–303. https://doi.org/10.1002/hyp.93

Holden, J., Chapman, P.J., Labadz, J.C., 2004. Artificial drainage of peatlands: Hydrological and hydrochemical process and wetland restoration. Progress in Physical Geography: Earth and Environment 28, 95–123. https://doi.org/10.1191/0309133304pp403ra

Holden, J., Smart, R.P., Dinsmore, K.J., Baird, A.J., Billett, M.F., Chapman, P.J., 2012. Morphological change of natural pipe outlets in blanket peat. Earth Surf. Process. Landf. 37, 109–118. https://doi.org/10.1002/esp.2239

REFERENCES

Holden, Joseph, Smart, R.P., Dinsmore, K.J., Baird, A.J., Billett, M.F., Chapman, P.J., 2012. Natural pipes in blanket peatlands: Major point sources for the release of carbon to the aquatic system. Glob. Chang. Biol. 18, 3568–3580. https://doi.org/10.1111/gcb.12004

Howard, J., Sutton-Grier, A., Herr, D., Kleypas, J., Landis, E., Mcleod, E., Pidgeon, E., Simpson, S., 2017. Clarifying the role of coastal and marine systems in climate mitigation. Front. Ecol. Environ. 15, 42–50. https://doi.org/10.1002/fee.1451

Hudson, B.D., 1994. Soil organic matter and available water capacity. J. Soil Water Conserv. 49, 189–194. https://doi.org/10.1201/9780429445552-36

Hugelius, G., Loisel, J., Chadburn, S., Jackson, R.B., Jones, M., MacDonald, G., Marushchak, M., Olefeldt, D., Packalen, M., Siewert, M.B., Treat, C., Turetsky, M., Voigt, C., Yu, Z., 2020. Large stocks of peatland carbon and nitrogen are vulnerable to permafrost thaw. Proc. Natl. Acad. Sci. U.S.A. 117, 20438–20446. https://doi.org/10.1073/pnas.1916387117

Hyväluoma, J., Räty, M., Kaseva, J., Keskinen, R., 2020. Changes over time in near-saturated hydraulic conductivity of peat soil following reclamation for agriculture. Hydrol. Process. 34, 237–243. https://doi.org/10.1002/hyp.13578

IPCC, 2014. 2013 supplement to the 2006 IPCC guidelines for national greenhouse gas inventories: Wetlands. IPCC, Switzerland.

IPS, n.d. What are peatlands? International Peatland Society. Retrieved from https://peatlands.org/peatlands/what-are-peatlands/.

Iqbal, J., Thomasson, J.A., Jenkins, J.N., Owens, P.R., Whisler, F.D., 2005. Spatial variability analysis of soil physical properties of alluvial soils. Soil Sci. Soc. Am. J. 69, 1338–1350. https://doi.org/10.2136/sssaj2004.0154

Irwin, R.W., 1968. Soil water characteristics of some (southern) Ontario peats, in: Proc. Third International Peat Congress. National Research Council of Canada, Quebec.

Isaaks, E.H., Srivastava, R.M., 1989. An Introduction to Applied Geostatistics. Oxford University Press, New York.

ISO 17892-3:2004, n.d. Geotechnical investigation and testing—Laboratory testing of soil—Part 3: Determination of particle density—Pycnometer method.

ISO 22476-3:2005, n.d. Methods of test for soils for civil engineering purposes. Chemical and electro-chemical tests.

Jensen, M.B., Hansen, H.C.B., Magid, J., 2002. Phosphate Sorption to Macropore Wall Materials and Bulk Soil. Water Air Soil Pollut. 137, 141–148. https://doi.org/10.1023/A:1015589011729

John, A., Fuentes, H.R., George, F., 2021. Characterization of the water retention curves of Everglades wetland soils. Geoderma 381, 114724. https://doi.org/10.1016/j.geoderma.2020.114724

Joosten, H., 2009. The Global Peatland CO_2 Picture: Peatland status and drainage related emissions in all countries of the world. Greifswald.

Joosten, H., Clarke, D., 2002. Wise Use of Mires and Peatlands: Background and principles including a framework for decision-making. International Mire Conservation Group.

Joosten, H., Couwenberg, J., Unger, M. von, 2016. International carbon policies as a new driver for peatland restoration, in: Peatland Restoration and Ecosystem Services. Cambridge University Press, pp. 291–313. https://doi.org/10.1017/CBO9781139177788.016

Joosten, H., Tanneberger, F., Moen, A., 2017. Mires and peatlands in Europe: Status, distribution and conservation. Schweizerbart Science Publishers, Stuttgart, Germany.

Joosten, H., Tapio-Biström, M.-L., Tol, S., 2012. Peatlands - guidance for climate change mitigation through conservation, rehabilitation and sustainable use. Rome.

Jurasinski, G., Ahmad, S., Anadon-Rosell, A., Berendt, J., Beyer, F., Bill, R., Blume-Werry, G., Couwenberg, J., Günther, A., Joosten, H., Koebsch, F., Köhn, D., Koldrack, N., Kreyling, J., Leinweber, P., Lennartz, B., Liu, H., Michaelis, D., Mrotzek, A., Negassa, W., Schenk, S., Schmacka, F., Schwieger, S., Smiljanić, M., Tanneberger, F., Teuber, L., Urich, T., Wang, H., Weil, M., Wilmking, M., Zak, D., Wrage-Mönnig, N., 2020. From understanding to sustainable use of peatlands: The WETSCAPES approach. Soil Syst. 4, 14. https://doi.org/10.3390/soilsystems4010014

Jurasinski, G., Janssen, M., Voss, M., Böttcher, M.E., Brede, M., Burchard, H., Forster, S., Gosch, L., Gräwe, U., Gründling-Pfaff, S., Haider, F., Ibenthal, M., Karow, N., Karsten, U., Kreuzburg, M., Lange, X., Leinweber, P., Massmann, G., Ptak, T., Rezanezhad, F., Rehder, G., Romoth, K., Schade, H., Schubert, H., Schulz-Vogt, H., Sokolova, I.M., Strehse, R., Unger, V., Westphal, J., Lennartz, B., 2018. Understanding the coastal ecocline: Assessing sea–land interactions at non-tidal, low-lying coasts through interdisciplinary research. Front. Mar. Sci. 5. https://doi.org/10.3389/fmars.2018.00342

Kalbitz, K., Solinger, S., Park, J.-H., Michalzik, B., Matzner, E., 2000. Controls on the dynamics of dissolved organic matter in soils: a review. Soil Sci. 165, 277–304. https://doi.org/10.1097/00010694-200004000-00001

Kechavarzi, C., Dawson, Q., Leeds-Harrison, P.B., 2010. Physical properties of low-lying agricultural peat soils in England. Geoderma 154, 196–202. https://doi.org/10.1016/j.geoderma.2009.08.018

Kennedy, G.W., Price, J.S., 2005. A conceptual model of volume-change controls on the hydrology of cutover peats. J. Hydrol. 302, 13–27. https://doi.org/10.1016/j.jhydrol.2004.06.024

Kettridge, N., Binley, A., 2010. Evaluating the effect of using artificial pore water on the quality of laboratory hydraulic conductivity measurements of peat. Hydrol. Process. 24, 2629–2640. https://doi.org/10.1002/hyp.7693

Kim, J., Rochefort, L., Hogue-Hugron, S., Alqulaiti, Z., Dunn, C., Pouliot, R., Jones, T.G., Freeman, C., Kang, H., 2021. Water table fluctuation in peatlands facilitates fungal proliferation, impedes *Sphagnum* growth and accelerates decomposition. Front. Earth Sci. 8. https://doi.org/10.3389/feart.2020.579329

Kindler, R., Siemens, J., Kaiser, K., Walmsley, D.C., Bernhofer, C., Buchmann, N., Cellier, P., Eugster, W., Gleixner, G., Grünwald, T., Heim, A., Ibrom, A., Jones, S.K., Jones, M., Klumpp, K., Kutsch, W., Larsen, K.S., Lehuger, S., Loubet, B., Mckenzie, R., Moors, E., Osborne, B., Pilegaard, K., Rebmann, C., Saunders, M., Schmidt, M.W.I., Schrumpf, M., Seyfferth, J., Skiba, U., Soussana, J.-F., Sutton, M.A., Tefs, C., Vowinckel, B., Zeeman, M.J., Kaupenjohann, M., 2011. Dissolved carbon leaching from soil is a crucial component of the net ecosystem carbon balance. Glob. Chang. Biol. 17, 1167–1185. https://doi.org/10.1111/j.1365-2486.2010.02282.x

Kleimeier, C., Karsten, U., Lennartz, B., 2014. Suitability of degraded peat for constructed wetlands — Hydraulic properties and nutrient flushing. Geoderma 228–229, 25–32. https://doi.org/10.1016/j.geoderma.2013.12.026

Kleimeier, C., Rezanezhad, F., Van Cappellen, P., Lennartz, B., 2017. Influence of pore structure on solute transport in degraded and undegraded fen peat soils. Mires Peat 19, article 18, 1–9. https://doi.org/10.19189/MaP.2017.OMB.282

Klemedtsson, L., Von Arnold, K., Weslien, P., Gundersen, P., 2005. Soil CN ratio as a scalar parameter to predict nitrous oxide emissions. Glob. Chang. Biol. 11, 1142–1147. https://doi.org/10.1111/j.1365-2486.2005.00973.x

Klute, A., Dirksen, C., 1986. Hydraulic Conductivity and Diffusivity: Laboratory Methods, in: Klute, Arnold (Ed.), Methods of Soil Analysis: Part 1—Physical and Mineralogical Methods. American Society of Agronomy, Inc. Soil Science Society of America, Inc., pp. 687–734. https://doi.org/10.2136/sssabookser5.1.2ed.c28

Knudby, C., Carrera, J., 2005. On the relationship between indicators of geostatistical, flow and transport connectivity. Adv. Water Resour. 28, 405–421. https://doi.org/10.1016/j.advwatres.2004.09.001

Koestel, J.K., Moeys, J., Jarvis, N.J., 2011. Evaluation of nonparametric shape measures for solute breakthrough curves. Vadose Zone J. 10, 1261–1275. https://doi.org/10.2136/vzj2011.0010

Koestel, J.K., Norgaard, T., Luong, N.M., Vendelboe, A.L., Moldrup, P., Jarvis, N.J., Lamandé, M., Iversen, B. V., Wollesen de Jonge, L., 2013. Links between soil properties and steady-state solute transport through cultivated topsoil at the field scale. Water Resour. Res. 49, 790–807. https://doi.org/10.1002/wrcr.20079

Kretz, L., Bondar-Kunze, E., Hein, T., Richter, R., Schulz-Zunkel, C., Seele-Dilbat, C., van der Plas, F., Vieweg, M., Wirth, C., 2021. Vegetation characteristics control local sediment and nutrient retention on but not underneath vegetation in floodplain meadows. PLoS One 16, e0252694. https://doi.org/10.1371/journal.pone.0252694

Kreuzburg, M., Rezanezhad, F., Milojevic, T., Voss, M., Gosch, L., Liebner, S., Van Cappellen, P., Rehder, G., 2020. Carbon release and transformation from coastal peat deposits controlled by submarine groundwater discharge: A column experiment study. Limnol. Oceanogr. 65, 1116–1135. https://doi.org/10.1002/lno.11438

Kreyling, J., Tanneberger, F., Jansen, F., van der Linden, S., Aggenbach, C., Blüml, V., Couwenberg, J., Emsens, W.-J., Joosten, H., Klimkowska, A., Kotowski, W., Kozub, L., Lennartz, B., Liczner, Y., Liu, H., Michaelis, D., Oehmke, C., Parakenings, K., Pleyl, E., Poyda, A., Raabe, S., Röhl, M., Rücker, K., Schneider, A., Schrautzer, J., Schröder, C., Schug, F., Seeber, E., Thiel, F., Thiele, S., Tiemeyer, B., Timmermann, T., Urich, T., van Diggelen, R., Vegelin, K., Verbruggen, E., Wilmking, M., Wrage-Mönnig, N., Wołejko, L., Zak, D., Jurasinski, G., 2021. Rewetting does not return drained fen peatlands to their old selves. Nat. Commun. 12, 5693. https://doi.org/10.1038/s41467-021-25619-y

Krüger, J.P., Leifeld, J., Glatzel, S., Szidat, S., Alewell, C., 2015. Biogeochemical indicators of peatland degradation – a case study of a temperate bog in northern Germany. Biogeosciences 12, 2861–2871. https://doi.org/10.5194/bg-12-2861-2015

Kruse, J., Lennartz, B., Leinweber, P., 2008. A modified method for measuring saturated hydraulic conductivity and anisotropy of fen peat samples. Wetlands 28, 527–531. https://doi.org/10.1672/07-153.1

REFERENCES

Kumar, S., Lal, R., Liu, D., 2012. A geographically weighted regression kriging approach for mapping soil organic carbon stock. Geoderma 189–190, 627–634. https://doi.org/10.1016/j.geoderma.2012.05.022

Lal, R., 2011. Organic matter, effects on soil physical properties and processes, in: Gliński, J., Horabik, J., Lipiec, J. (Eds.), Encyclopedia of Agrophysics. Encyclopedia of Earth Sciences Series. Springer, Dordrecht, pp. 528–534. https://doi.org/10.1007/978-90-481-3585-1_102

Lal, R., Smith, P., Jungkunst, H.F., Mitsch, W.J., Lehmann, J., Nair, P.K.R., McBratney, A.B., de Moraes Sá, J.C., Schneider, J., Zinn, Y.L., Skorupa, A.L.A., Zhang, H.-L., Minasny, B., Srinivasrao, C., Ravindranath, N.H., 2018. The carbon sequestration potential of terrestrial ecosystems. J. Soil Water Conserv. 73, 145A-152A. https://doi.org/10.2489/jswc.73.6.145A

Lamorey, G., Jacobson, E., 1995. Estimation of semivariogram parameters and evaluation of the effects of data sparsity. Math. Geol. 27, 327–358. https://doi.org/10.1007/BF02084606

Leibundgut, C., Maloszewski, P., Külls, C., 2009. Tracers in Hydrology. Wiley-Blackwell, Chichester, UK.

Leifeld, J., Klein, K., Wüst-Galley, C., 2020. Soil organic matter stoichiometry as indicator for peatland degradation. Sci. Rep. 10, 7634. https://doi.org/10.1038/s41598-020-64275-y

Leifeld, J., Menichetti, L., 2018. The underappreciated potential of peatlands in global climate change mitigation strategies. Nat Commun 9, 1071. https://doi.org/10.1038/s41467-018-03406-6

Lemly, A.D., Kingsford, R.T., Thompson, J.R., 2000. Irrigated agriculture and wildlife conservation: conflict on a global scale. Environ. Manage. 25, 485–512. https://doi.org/10.1007/s002679910039

Lennartz, B., Liu, H., 2019. Hydraulic functions of peat soils and ecosystem service. Front. Environ. Sci. 7. https://doi.org/10.3389/fenvs.2019.00092

Lennartz, B., Liu, H., Tanneberger, F., 2021. Peatlands regulate the water cycle in our landscapes.

Letts, M.G., Roulet, N.T., Comer, N.T., Skarupa, M.R., Verseghy, D.L., 2000. Parametrization of peatland hydraulic properties for the Canadian land surface scheme. Atmosphere-Ocean. 38, 141–160. https://doi.org/10.1080/07055900.2000.9649643

Levermann, F., 2019. Renaturierung am Kubitzer Bodden. Report from official website of municipality Rambin in the Vorpommern-Rügen district of Germany. https://www.rambin.de/2019/08/12/renaturierung-am-kubitzer-bodden/

Lewis, C., Albertson, J., Xu, X., Kiely, G., 2012. Spatial variability of hydraulic conductivity and bulk density along a blanket peatland hillslope. Hydrol. Process. 26, 1527–1537. https://doi.org/10.1002/hyp.8252

Limpens, J., Berendse, F., Blodau, C., Canadell, J.G., Freeman, C., Holden, J., Roulet, N., Rydin, H., Schaepman-Strub, G., 2008. Peatlands and the carbon cycle: from local processes to global implications – a synthesis. Biogeosciences 5, 1475–1491. https://doi.org/10.5194/bg-5-1475-2008

Lindsay, R., 2018. Peatland Classification, in: The Wetland Book. Springer Netherlands, Dordrecht, pp. 1515–1528. https://doi.org/10.1007/978-90-481-9659-3_341

Lindsay, R., Andersen, R., 2016. Peat, in: Finlayson, C.M., Milton, G.R., Prentice, R.C., Davidson, N.C. (Eds.), The Wetland Book II: Distribution, Description and Conservation. Springer Netherlands, Dordrecht.

Liu, H., Forsmann, D.M., Kjaergaard, C., Saki, H., Lennartz, B., 2017. Solute transport properties of fen peat differing in organic matter content. J. Environ. Qual. 46, 1106–1113. https://doi.org/10.2134/jeq2017.01.0031

Liu, H., Janssen, M., Lennartz, B., 2016. Changes in flow and transport patterns in fen peat following soil degradation. Eur. J. Soil Sci. 67, 763–772. https://doi.org/10.1111/ejss.12380

Liu, H., Lennartz, B., 2019a. Hydraulic properties of peat soils along a bulk density gradient-A meta study. Hydrol Process 33, 101–114. https://doi.org/10.1002/hyp.13314

Liu, H., Lennartz, B., 2019b. Short term effects of salinization on compound release from drained and restored coastal wetlands. Water 11, 1549. https://doi.org/10.3390/w11081549

Liu, H., Lennartz, B., 2015. Visualization of flow pathways in degraded peat soils using titanium dioxide. Soil Sci. Soc. Am. J. 79, 757–765. https://doi.org/10.2136/sssaj2014.04.0153

Liu, H., Price, J., Rezanezhad, F., Lennartz, B., 2020a. Centennial-scale shifts in hydrophysical properties of peat induced by drainage. Water Resour. Res. 56. https://doi.org/10.1029/2020WR027538

Liu, H., Wrage-Mönnig, N., Lennartz, B., 2020b. Rewetting strategies to reduce nitrous oxide emissions from European peatlands. Commun. Earth Environ. 1, 17. https://doi.org/10.1038/s43247-020-00017-2

Liu, H., Zak, D., Rezanezhad, F., Lennartz, B., 2019. Soil degradation determines release of nitrous oxide and dissolved organic carbon from peatlands. Environ. Res. Lett. 14, 094009. https://doi.org/10.1088/1748-9326/ab3947

Logsdon, S.D., Allmaras, R.R., Wu, L., Swan, J.B., Randall, G.W., 1990. Macroporosity and its relation to saturated hydraulic conductivity under different tillage practices. Soil Sci. Soc. Am. J. 54, 1096–1101.

Loisel, J., Gallego-Sala, A., 2022. Ecological resilience of restored peatlands to climate change. Commun. Earth Environ. 3, 208. https://doi.org/10.1038/s43247-022-00547-x

Lønborg, C., Carreira, C., Jickells, T., Álvarez-Salgado, X.A., 2020. Impacts of global change on ocean dissolved organic carbon (DOC) cycling. Front. Mar. Sci. 7. https://doi.org/10.3389/fmars.2020.00466

Luxmoore, R.J., 1981. Micro-, meso-, and macroporosity of soil. Soil Sci. Soc. Am. J. 45, 671–672. https://doi.org/10.2136/sssaj1981.03615995004500030051x

Lyon, S.W., Lembo, A.J., Walter, M.T., Steenhuis, T.S., 2006. Defining probability of saturation with indicator kriging on hard and soft data. Adv. Water Resour. 29, 181–193. https://doi.org/10.1016/j.advwatres.2005.02.012

Mabit, L., Bernard, C., 2010. Spatial distribution and content of soil organic matter in an agricultural field in eastern Canada, as estimated from geostatistical tools. Earth Surf. Process. Landf. 35, 278–283. https://doi.org/10.1002/esp.1907

Maftu'ah, E., Fahmi, A., Hayati, A., 2019. Changes in degraded peat land characteristic using FTIR-spectrocopy. IOP Conf. Ser. Earth Environ. Sci. 393, 012091. https://doi.org/10.1088/1755-1315/393/1/012091

Manton, M., Makrickas, E., Banaszuk, P., Kołos, A., Kamocki, A., Grygoruk, M., Stachowicz, M., Jarašius, L., Zableckis, N., Sendžikaitė, J., Peters, J., Napreenko, M., Wichtmann, W., Angelstam, P., 2021. Assessment and spatial planning for peatland conservation and restoration: Europe's trans-border Neman River basin as a case study. Land 10, 174. https://doi.org/10.3390/land10020174

Matheron, G., 1963. Principles of geostatistics. Economic Geology 58, 1246–1266. https://doi.org/10.2113/gsecongeo.58.8.1246

McBratney, A., Minasny, B., 2007. On measuring pedodiversity. Geoderma 141, 149–154. https://doi.org/10.1016/j.geoderma.2007.05.012

McCarter, C.P.R., Price, J.S., 2014. Ecohydrology of *Sphagnum* moss hummocks: Mechanisms of capitula water supply and simulated effects of evaporation. Ecohydrology 7, 33–44. https://doi.org/10.1002/eco.1313

McCarter, C.P.R., Rezanezhad, F., Gharedaghloo, B., Price, J.S., Van Cappellen, P., 2019. Transport of chloride and deuterated water in peat: The role of anion exclusion, diffusion, and anion adsorption in a dual porosity organic media. J. Contam. Hydrol. 225, 103497. https://doi.org/10.1016/j.jconhyd.2019.103497

McCarter, C.P.R., Rezanezhad, F., Quinton, W.L., Gharedaghloo, B., Lennartz, B., Price, J., Connon, R., Van Cappellen, P., 2020. Pore-scale controls on hydrological and geochemical processes in peat: Implications on interacting processes. Earth Sci. Rev. 207, 103227. https://doi.org/10.1016/j.earscirev.2020.103227

McCarter, C.P.R., Weber, T.K.D., Price, J.S., 2018. Competitive transport processes of chloride, sodium, potassium, and ammonium in fen peat. J Contam Hydrol 217, 17–31. https://doi.org/10.1016/j.jconhyd.2018.08.004

Menberu, M.W., Marttila, H., Ronkanen, A., Haghighi, A.T., Kløve, B., 2021. Hydraulic and physical properties of managed and intact peatlands: application of the van Genuchten-Mualem models to peat soils. Water Resour. Res. 57. https://doi.org/10.1029/2020WR028624

Mercer, J. J., Westbrook, C. J., 2016. Ultrahigh-resolution mapping of peatland microform using ground-based structure from motion with multiview stereo. Journal of Geophysical Research: Biogeosciences, 121(11), 2901–2916. https://doi.org/10.1002/2016JG003478

Minasny, B., Berglund, Ö., Connolly, J., Hedley, C., de Vries, F., Gimona, A., Kempen, B., Kidd, D., Lilja, H., Malone, B., McBratney, A., Roudier, P., O'Rourke, S., Rudiyanto, Padarian, J., Poggio, L., ten Caten, A., Thompson, D., Tuve, C., Widyatmanti, W. 2019. Digital mapping of peatlands – A critical review. Earth-Science Reviews. https://doi.org/10.1016/j.earscirev.2019.05.014

Ministry of the Environment Mecklenburg-Vorpommern, 2003. Umweltministerium Mecklenburg-Vorpommern (Hrsg.): Unteres Recknitztal 210 in: Die Naturschutzgebiete in Mecklenburg-Vorpommern. Schwerin.

Minkkinen, K., Laine, J., 1998. Long-term effect of forest drainage on the peat carbon stores of pine mires in Finland. Can. J. For. Res. 28, 1267–1275. https://doi.org/10.1139/x98-104

Mitsch, W.J., Gosselink, J.G., 1986. Wetlands, 1st ed. John Wiley & Sons, Inc., Hoboken.

Mitsch, W.J., Gosselink, J.G., 2007. Wetlands, 4th ed. John Wiley & Sons, Inc., Hoboken.

Monteverde, S., Healy, M.G., O'Leary, D., Daly, E., Callery, O., 2022. Management and rehabilitation of peatlands: The role of water chemistry, hydrology, policy, and emerging monitoring methods to ensure informed decision making. Ecol. Inform. 69, 101638. https://doi.org/10.1016/j.ecoinf.2022.101638

Mooney, S.J., Holden, N.M., Ward, S.M., Collins, J.F., 1999. Morphological observations of dye tracer infiltration and by-pass flow in milled peat. Plant Soil 208, 167–178. https://doi.org/10.1023/A:1004538207229

Moore, P.D., Bellamy, D., 1974. Peatlands. Elek Science, London, England.

REFERENCES

Moran, M.A., Zepp, R.G., 1997. Role of photoreactions in the formation of biologically labile compounds from dissolved organic matter. Limnol. Oceanogr. 42, 1307–1316. https://doi.org/10.4319/lo.1997.42.6.1307

Morris, P.J., Baird, A.J., Belyea, L.R., 2015. Bridging the gap between models and measurements of peat hydraulic conductivity. Water Resour. Res. 51, 5353–5364. https://doi.org/10.1002/2015WR017264

Morris, P.J., Baird, A.J., Eades, P.A., Surridge, B.W.J., 2019. Controls on near-surface hydraulic conductivity in a raised bog. Water Resour. Res. 55, 1531–1543. https://doi.org/10.1029/2018WR024566

Morris, P.J., Davies, M.L., Baird, A.J., Balliston, N., Bourgault, M. -A., Clymo, R.S., Fewster, R.E., Furukawa, A.K., Holden, J., Kessel, E., Ketcheson, S.J., Kløve, B., Larocque, M., Marttila, H., Menberu, M.W., Moore, P.A., Price, J.S., Ronkanen, A. -K., Rosa, E., Strack, M., Surridge, B.W.J., Waddington, J.M., Whittington, P., Wilkinson, S.L., 2022. Saturated hydraulic conductivity in northern peats inferred from other measurements. Water Resour. Res. 58. https://doi.org/10.1029/2022WR033181

Morris, P.J., Waddington, J.M., Benscoter, B.W., Turetsky, M.R., 2011. Conceptual frameworks in peatland ecohydrology: looking beyond the two-layered (acrotelm-catotelm) model. Ecohydrology 4, 1–11. https://doi.org/10.1002/eco.191

Mueller, L., Schindler, U., Behrendt, A., Shepherd, T.G., Eulenstein, F., 2007. Implications of soil substrate and land use for properties of fen soils in North-East Germany Part II: Aspects of structure in the peat soil landscape, Archives of Agronomy and Soil Science, 53:2, 127-136. http://dx.doi.org/10.1080/03650340701223916

Murphy, J., Riley, J.P., 1962. A modified single solution method for the determination of phosphate in natural waters. Anal. Chim. Acta. 27, 31–36. https://doi.org/10.1016/S0003-2670(00)88444-5

Naumann, M., Gräwe, U., Mohrholz, V., Kuss, J., Kanwischer, M., Feistel, S., Hand, I., Waniek, J.J., Schulz-Bull, D.E., 2020. Hydrographic-hydrochemical assessment of the Baltic Sea 2019, Meereswiss. Ber., Warnemünde. Warnemünde. https://doi.org/10.12754/msr-2020-0114

Negassa, W., Baum, C., Beyer, F., Leinweber, P., 2022. Spatial variability of selected soil properties in long-term drained and restored peatlands. Front. Environ. Sci. 10. https://doi.org/10.3389/fenvs.2022.804041

Negassa, W., Baum, C., Schlichting, A., Müller, J., Leinweber, P., 2019. Small-scale spatial variability of soil chemical and biochemical properties in a rewetted degraded peatland. Front. Environ. Sci. 7. https://doi.org/10.3389/fenvs.2019.00116

Nelson, N.B., Siegel, D.A., 2002. Chapter 11- Chromophoric DOM in the open ocean, in: Hansell, D.A., Carlson, C.A. (Eds.), Biogeochemistry of Marine Dissolved Organic Matter. Biogeochemistry Academic Press, San Diego.

Nemati, M.R., Caron, J., Gallichand, J., 2002. Predicting hydraulic conductivity changes from aggregate mean weight diameter. Water Resour. Res. 38, 9-1-9-11. https://doi.org/10.1029/2001WR000625

Newton, A., Carruthers, T.J.B., Icely, J., 2012. The coastal syndromes and hotspots on the coast. Estuar. Coast Shelf Sci. 96, 39–47. https://doi.org/10.1016/j.ecss.2011.07.012

Nielsen, D.R., Wendroth, O., 2003. Spatial and temporal statistics: Sampling field soils and their vegetation. Catena Verlag, Reiskirchen, Germany.

Nieminen, M., Ahti, E., Nousiainen, H., Joensuu, S., Vuollekoski, M., 2005. Capacity of riparian buffer zones to reduce sediment concentrations in discharge from peatlands drained for forestry. Silva Fenn. 39. https://doi.org/10.14214/sf.371

Nierop, K.G.J.J., Jansen, B., Verstraten, J.M., 2002. Dissolved organic matter, aluminium and iron interactions: precipitation induced by metal/carbon ratio, pH and competition. Sci. Total Environ. 300, 201–211. https://doi.org/10.1016/S0048-9697(02)00254-1

Nkheloane, T., Olaleye, A.O., Mating, R., 2012. Spatial heterogeneity of soil physico-chemical properties in contrasting wetland soils in two agro-ecological zones of Lesotho. Soil Res. 50, 579. https://doi.org/10.1071/SR12145

Norgaard, T., Paradelo, M., Moldrup, P., Katuwal, S., de Jonge, L.W., 2018. Particle leaching rates from a loamy soil are controlled by the mineral fines content and the degree of preferential flow. J. Environ. Qual. 47, 1538–1545. https://doi.org/10.2134/jeq2018.02.0065

Oleszczuk, R., Truba, M., 2013. The analysis of some physical properties of drained peat-moorsh layers. Ann. Warsaw Univ. of Life Sci.– SGGW, Land Reclam. 45(1): 41–48. https://doi.org/10.2478/sggw-2013-0004

Osland, M.J., Gabler, C.A., Grace, J.B., Day, R.H., McCoy, M.L., McLeod, J.L., From, A.S., Enwright, N.M., Feher, L.C., Stagg, C.L., Hartley, S.B., 2018. Climate and plant controls on soil organic matter in coastal wetlands. Glob. Chang Biol. 24, 5361–5379. https://doi.org/10.1111/gcb.14376

Ours, D.P., Siegel, D.I., H. Glaser, P., 1997. Chemical dilation and the dual porosity of humified bog peat. J. Hydrol. 196, 348–360. https://doi.org/10.1016/S0022-1694(96)03247-7

Paavilainen, E., Päivänen, J., 1995. Peatland Forestry: Ecology and Principles. Springer-Verlag, Berlin, Heidelberg, New York.

Pallud, C., Meile, C., Laverman, A.M., Abell, J., Van Cappellen, P., 2007. The use of flow-through sediment reactors in biogeochemical kinetics: Methodology and examples of applications. Mar. Chem. 106, 256–271. https://doi.org/10.1016/j.marchem.2006.12.011

Paradelo, M., Moldrup, P., Arthur, E., Naveed, M., Holmstrup, M., López-Periago, J.E., de Jonge, L.W., 2013. Effects of past copper contamination and soil structure on copper leaching from soil. J. Environ. Qual. 42, 1852–1862. https://doi.org/10.2134/jeq2013.05.0209

Parish, F., Sirin, A., Charman, D., Joosten, H., Minayeva, T., Silvius, M., Stringer, L., 2008. Assessment on Peatlands, Biodiversity and Climate Change: Main Report. Wageningen.

Parvage, M.M., Ulén, B., Kirchmann, H., 2015. Nutrient leaching from manure-amended topsoils (Cambisols and Histosols) in Sweden. Geoderma Reg. 5, 209–214. https://doi.org/10.1016/j.geodrs.2015.08.003

Peatlands.org., n.d. Peat Formation. Retrieved from https://peatlands.org/peat/peat-formation/.

Peng, X., 2011. Anisotropy of Soil Physical Properties, in: Encyclopedia of Agrophysics. Encyclopedia of Earth Sciences Series. Springer, Dordrecht, pp. 55–57. https://doi.org/10.1007/978-90-481-3585-1_15

Phragmites peat, n.d. The Columbia Electronic Encyclopedia®. (2013). Retrieved from https://encyclopedia2.thefreedictionary.com/Phragmites+peat.

Pönisch, D.L., Breznikar, A., Gutekunst, C.N., Jurasinski, G., Voss, M., Rehder, G., 2023. Nutrient release and flux dynamics of CO_2, CH_4, and N_2O in a coastal peatland driven by actively induced rewetting with brackish water from the Baltic Sea. Biogeosciences 20, 295–323. https://doi.org/10.5194/bg-20-295-2023

Pratolongo, P., Leonardi, N., Kirby, J.R., Plater, A., 2018. Temperate coastal wetlands: morphology, sediment processes, and plant communities, in: Perillo, G.M.E., Wolanski, E., Cahoon, D.R., Hopkinson, C.S. (Eds.), Coastal Wetlands, an Integrated Ecosystem Approach. Elsevier, Amsterdam, pp. 105–152. https://doi.org/10.1016/B978-0-444-63893-9.00003-4

Price, J., Evans, C., Evans, Martin, Allott, Tim, Shuttleworth, E., 2016. Peatland restoration and hydrology, in: Bonn, A., Allott, T, Evans, M, Joosten, H., Stoneman, R. (Eds.), Peatland Restoration and Ecosystem Services: Science, Policy and Practice. Cambridge University Press, pp. 77–94. https://doi.org/10.1017/CBO9781139177788.006

Price, J.S., 2003. Role and character of seasonal peat soil deformation on the hydrology of undisturbed and cutover peatlands. Water Resour. Res. 39. https://doi.org/10.1029/2002WR001302

Price, J.S., Whittington, P.N., Elrick, D.E., Strack, M., Brunet, N., Faux, E., 2008. A method to determine unsaturated hydraulic conductivity in living and undecomposed *Sphagnum* moss. Soil Sci. Soc. Am. J. 72, 487–491. https://doi.org/10.2136/sssaj2007.0111N

Pronger, J., Schipper, L.A., Hill, R.B., Campbell, D.I., McLeod, M., 2014. Subsidence rates of drained agricultural peatlands in New Zealand and the relationship with time since drainage. J. Environ. Qual. 43, 1442–1449. https://doi.org/10.2134/jeq2013.12.0505

Proulx-McInnis, S., St-Hilaire, A., Rousseau, A.N., Jutras, S., 2013. A review of ground-penetrating radar studies related to peatland stratigraphy with a case study on the determination of peat thickness in a northern boreal fen in Quebec, Canada. Prog. Phys. Geogr: Earth and Environment 37, 767–786. https://doi.org/10.1177/0309133313501106

Quinton, W.L., Elliot, T., Price, J.S., Rezanezhad, F., Heck, R., 2009. Measuring physical and hydraulic properties of peat from X-ray tomography. Geoderma 153, 269–277. https://doi.org/10.1016/j.geoderma.2009.08.010

Quinton, W.L., Hayashi, M., Carey, S.K., 2008. Peat hydraulic conductivity in cold regions and its relation to pore size and geometry. Hydrol. Process. 22, 2829–2837. https://doi.org/10.1002/hyp.7027

R Core Team, 2020. R: A language and environment for statistical computing. Retrieved from https://www.r-project.org/index.html.

R Core Team, 2015. R: A language and environment for statistical computing. Retrieved from https://www.r-project.org.

Rabot, E., Wiesmeier, M., Schlüter, S., Vogel, H.-J., 2018. Soil structure as an indicator of soil functions: A review. Geoderma 314, 122–137. https://doi.org/10.1016/j.geoderma.2017.11.009

Radcliffe, D.E., Simunek, J., 2010. Soil Physics with HYDRUS. CRC Press, Boca Raton. https://doi.org/10.1201/9781315275666

Rajendran, A., Kariwala, V., Farooq, S., 2008. Correction procedures for extra-column effects in dynamic column breakthrough experiments. Chem. Eng. Sci. 63, 2696–2706. https://doi.org/10.1016/j.ces.2008.02.023

REFERENCES

Ramirez, J.A., Baird, A.J., Coulthard, T.J., 2016. The effect of pore structure on ebullition from peat. J. Geophys. Res. Biogeosci. 121, 1646–1656. https://doi.org/10.1002/2015JG003289

Ramos, F.T., Dores, E.F. de C., Weber, O.L. dos S., Beber, D.C., Campelo, J.H., Maia, J.C. de S., 2018. Soil organic matter doubles the cation exchange capacity of tropical soil under no-till farming in Brazil. J. Sci. Food Agric. 98, 3595–3602. https://doi.org/10.1002/jsfa.8881

Ramsar, 1971. The Ramsar convention. Ramsar, Iran.

Regan, S., Flynn, R., Gill, L., Naughton, O., Johnston, P., 2019. Impacts of groundwater drainage on peatland subsidence and its ecological implications on an Atlantic raised bog. Water Resour. Res. 55, 6153–6168. https://doi.org/10.1029/2019WR024937

Rennie, R., 1810. Essays on the natural history and origin of peat moss. Edinburgh.

Rezanezhad, F., Price, J.S., Craig, J.R., 2012. The effects of dual porosity on transport and retardation in peat: A laboratory experiment. Can. J. Soil. Sci. 92, 723–732. https://doi.org/10.4141/cjss2011-050

Rezanezhad, F., Price, J.S., Quinton, W.L., Lennartz, B., Milojevic, T., Van Cappellen, P., 2016. Structure of peat soils and implications for water storage, flow and solute transport: A review update for geochemists. Chem. Geol. 429, 75–84. https://doi.org/10.1016/j.chemgeo.2016.03.010

Rezanezhad, F., Quinton, W.L., Price, J.S., Elliot, T.R., Elrick, D., Shook, K.R., 2010. Influence of pore size and geometry on peat unsaturated hydraulic conductivity computed from 3D computed tomography image analysis. Hydrol. Process. 24, 2983–2994. https://doi.org/10.1002/hyp.7709

Richards, L.A., 1948. Porous plate apparatus for measuring moisture retention and transmission by soil. Soil. Sci. 66, 105–110. https://doi.org/10.1097/00010694-194808000-00003

Riddle, M., Bergström, L., Schmieder, F., Kirchmann, H., Condron, L., Aronsson, H., 2018. Phosphorus leaching from an organic and a mineral arable soil in a rainfall simulation study. J. Environ. Qual. 47, 487–495. https://doi.org/10.2134/jeq2018.01.0037

Robertson, G.P., 2008. GS+: Geostatistics for the Environmental Sciences.

Robroek, B.J.M., van Ruijven, J., Schouten, M.G.C., Breeuwer, A., Crushell, P.H., Berendse, F., Limpens, J., 2009. *Sphagnum* re-introduction in degraded peatlands: The effects of aggregation, species identity and water table. Basic Appl. Ecol. 10, 697–706. https://doi.org/10.1016/j.baae.2009.04.005

Ronkanen, A.-K., Kløve, B., 2009. Long-term phosphorus and nitrogen removal processes and preferential flow paths in Northern constructed peatlands. Ecol. Eng. 35, 843–855. https://doi.org/10.1016/j.ecoleng.2008.12.007

Ronkanen, A.-K., Kløve, B., 2007. Use of stabile isotopes and tracers to detect preferential flow patterns in a peatland treating municipal wastewater. J. Hydrol. 347, 418–429. https://doi.org/10.1016/j.jhydrol.2007.09.029

Rosa, E., Larocque, M., 2008. Investigating peat hydrological properties using field and laboratory methods: Application to the Lanoraie peatland complex (southern Quebec, Canada). Hydrol. Process. 22, 1866–1875. https://doi.org/10.1002/hyp.6771

Rosset, T., Binet, S., Rigal, F., Gandois, L., 2022. Peatland dissolved organic carbon export to surface waters: Global significance and effects of anthropogenic disturbance. Geophys. Res. Lett. 49. https://doi.org/10.1029/2021GL096616

Rydin, H., Jeglum, J.K., 2006. Peatland succession and development. In The Biology of Peatlands. Oxford Scholarship Online. https://doi.org/10.1093/acprof:oso/9780198528722.003.0007

Roßkopf, N., Fell, H., Zeitz, J., 2015. Organic soils in Germany, their distribution and carbon stocks. Catena 133, 157–170. https://doi.org/10.1016/j.catena.2015.05.004

Saintilan, N., Rogers, K., 2013. The significance and vulnerability of Australian saltmarshes: implications for management in a changing climate. Mar Freshw Res 64, 66. https://doi.org/10.1071/MF12212

Saleh, A.M., 2018. Spatial variability mapping of some soil properties in Jadwal Al_Amir Project/Babylon/Iraq. Journal of the Indian Society of Remote Sensing 46, 1481–1495. https://doi.org/10.1007/s12524-018-0795-x

Salinity, n.d. Marine Finland. Retrieved from https://www.marinefinland.fi/en-US/The_Baltic_Sea_now/Water_quality/Salinity.

SAS Institute Inc., 2013. SAS Language.

Säurich, A., Tiemeyer, B., Don, A., Fiedler, S., Bechtold, M., Amelung, W., Freibauer, A., 2019. Drained organic soils under agriculture — The more degraded the soil the higher the specific basal respiration. Geoderma, 355, 113911. https://doi.org/10.1016/j.geoderma.2019.113911

Schaap, M.G., Leij, F.J., van Genuchten, M.Th., 2001. ROSETTA: A computer program for estimating soil hydraulic parameters with hierarchical pedotransfer functions. J. Hydrol. 251, 163–176. https://doi.org/10.1016/S0022-1694(01)00466-8

Schillereff, D.N., Chiverrell, R.C., Sjöström, J.K., Kylander, M.E., Boyle, J.F., Davies, J.A.C., Toberman, H., Tipping, E., 2021. Phosphorus supply affects long-term carbon accumulation in mid-latitude ombrotrophic peatlands. Commun. Earth Environ. 2, 241. https://doi.org/10.1038/s43247-021-00316-2

Schindler, U., Behrendt, A., Müller, L., 2003. Change of soil hydrological properties of fens as a result of soil development. J. Plant Nutr. Soil Sci. 166, 357–363. https://doi.org/10.1002/jpln.200390055

Schlüter, S., Sammartino, S., Koestel, J., 2020. Exploring the relationship between soil structure and soil functions via pore-scale imaging. Geoderma 370, 114370. https://doi.org/10.1016/j.geoderma.2020.114370

Schoock, M., 1658. Tractatus de turffis, ceu cespitibus bituminosis. Joh. Collenu.

Schumann, M., Joosten, H., 2008. Global Peatland Restoration Manual. Greifswald.

Schwärzel, K., Renger, M., Sauerbrey, R., Wessolek, G., 2002. Soil physical characteristics of peat soils. J. Plant Nutr. Soil Sci. J 165, 479. https://doi.org/10.1002/1522-2624(200208)165:4<479::AID-JPLN479>3.0.CO;2-8

Schwärzel, K., Šimůnek, J., Stoffregen, H., Wessolek, G., van Genuchten, M.Th., 2006. Estimation of the unsaturated hydraulic conductivity of peat soils: Laboratory versus field data. Vadose Zone J. 5, 628–640. https://doi.org/10.2136/vzj2005.0061

Schwieger, S., Kreyling, J., Peters, B., Gillert, A., Freiherr von Lukas, U., Jurasinski, G., Köhn, D., Blume-Werry, G., 2022. Rewetting prolongs root growing season in minerotrophic peatlands and mitigates negative drought effects. J. Appl. Ecol. 59, 2106–2116. https://doi.org/10.1111/1365-2664.14222

Scott, D.A., Jones, T.A., 1995. Classification and inventory of wetlands: A global overview. Vegetatio 118, 3–16. https://doi.org/10.1007/BF00045186

Servais, S., Kominoski, J.S., Fernandez, M., Morales, K., 2021. Saltwater and phosphorus drive unique soil biogeochemical processes in freshwater and brackish wetland mesocosms. Ecosphere 12. https://doi.org/10.1002/ecs2.3704

Sharma, P., Shukla, M.K., Mexal, J.G., 2011. Spatial variability of soil properties in agricultural fields of southern New Mexico. Soil Sci. 176, 288–302. https://doi.org/10.1097/SS.0b013e31821codab

Shaw, J.N., West, L.T., Radcliffe, D.E., Bosch, D.D., 2000. Preferential flow and pedotransfer functions for transport properties in sandy Kandiudults. Soil Sci. Soc. Am. J. 64, 670–678. https://doi.org/10.2136/sssaj2000.642670x

Sheng, H., Zhou, P., Zhang, Y., Kuzyakov, Y., Zhou, Q., Ge, T., Wang, C., 2015. Loss of labile organic carbon from subsoil due to land-use changes in subtropical China. Soil Biol. Biochem. 88, 148–157. https://doi.org/10.1016/j.soilbio.2015.05.015

Sheppard, S., Long, J., Sanipelli, B., Sohlenius, G., 2009. Solid/liquid partition coefficients (Kd) for selected soils and sediments at Forsmark and Laxemar-Simpevarp. SKB Report R-09-27. Stockholm, Sweden.

Short, F., Carruthers, T., Dennison, W., Waycott, M., 2007. Global seagrass distribution and diversity: A bioregional model. J. Exp. Mar. Biol. Ecol. 350, 3–20. https://doi.org/10.1016/j.jembe.2007.06.012

Shukla, M.K., 2013. Soil Physics: An Introduction. CRC Press.

Sienkiewicz, J., Porębska, G., Ostrowska, A., Gozdowski, D., 2019. Indicators of peat soil degradation in the Biebrza valley, Poland. Environmental Protection and Natural Resources 30, 41–51. https://doi.org/https://doi.org/10.2478/oszn-2019-0009

Silins, U., Rothwell, R.L., 1998. Forest peatland drainage and subsidence affect soil water retention and transport properties in an Alberta peatland. Soil Sci. Soc. Am. J. 62, 1048–1056. https://doi.org/10.2136/sssaj1998.03615995006200040028x

Simard, R.R., Beauchemin, S., Haygarth, P.M., 2000. Potential for preferential pathways of phosphorus transport. J. Environ. Qual. 29, 97–105. https://doi.org/10.2134/jeq2000.00472425002900010012x

Simhayov, R.B., Weber, T.K.D., Price, J.S., 2018. Saturated and unsaturated salt transport in peat from a constructed fen. SOIL 4, 63–81. https://doi.org/10.5194/soil-4-63-2018

Šimůnek, J., Genuchten, M.Th., 2008. Modeling nonequilibrium flow and transport processes ssing HYDRUS. Vadose Zone J. 7, 782–797. https://doi.org/10.2136/vzj2007.0074

Šimůnek, J., Jarvis, N.J., van Genuchten, M.Th., Gärdenäs, A., 2003. Review and comparison of models for describing non-equilibrium and preferential flow and transport in the vadose zone. J. Hydrol. 272, 14–35. https://doi.org/10.1016/S0022-1694(02)00252-4

Sjörs, H., 1980. Peat on Earth: Multiple Use or Conservation? Ambio 9, 303–308.

Skaggs, T.H., Jaynes, D.B., Kachanoski, R.G., Shouse, P.J., Ward, A.L., 2002. Solute transport: data analysis and parameter estimation, in: Methods of Soil Analysis: Part 4 Physical Methods (First Version). Soil Science

REFERENCES

Society of America, Inc., Madison, Wisconsin, USA, pp. 1412–1413. https://doi.org/10.2136/sssabookser5.4.c58

Soares, A., Moldrup, P., Vendelboe, A.L., Katuwal, S., Norgaard, T., Delerue-Matos, C., Tuller, M., de Jonge, L.W., 2015. Effects of soil compaction and organic carbon content on preferential flow in loamy field soils. Soil Sci. 180, 10–20. https://doi.org/10.1097/SS.0000000000000105

Solovey, T., Wojewódka-Przybył, M., Janica, R., 2021. Hydrochemical indicators of water source and contamination in fen peatlands of varying hydrogeomorphic settings in northern and central Poland. Ecol. Indic. 129, 107944. https://doi.org/10.1016/j.ecolind.2021.107944

Sonneveld, M.P.W., Backx, M.A.H.M., Bouma, J., 2003. Simulation of soil water regimes including pedotransfer functions and land-use related preferential flow. Geoderma 112, 97–110. https://doi.org/10.1016/S0016-7061(02)00298-7

Sonon, L.S., Kissel, D.E., Saha, U., 2014. Cation exchange capacity and base saturation. University of Georgia, Extension, Circular 1040.

Stephens, J.C., Allen, L.H., Chen, E., 1984. Organic soil subsidence, in: Man-Induced Land Subsidence, Reviews in Engineering Geology. Geological Society of America, Inc., pp. 107–122. https://doi.org/10.1130/REG6-p107

Succow, M., Joosten, H., 2001. Landschaftsökologische Moorkunde. Schweizerbart Science Publishers, Stuttgart, Germany.

Surridge, B.W.J., Baird, A.J., Heathwaite, A.L., 2005. Evaluating the quality of hydraulic conductivity estimates from piezometer slug tests in peat. Hydrol. Process. 19, 1227–1244. https://doi.org/10.1002/hyp.5653

Szumińska, D., Czapiewski, S., Sewerniak, P., 2023. Natural and anthropogenic factors influencing changes in peatland management in Poland. Reg. Environ. Change 23, 5. https://doi.org/10.1007/s10113-022-02001-2

Tanneberger, F., Appulo, L., Ewert, S., Lakner, S., Ó Brolcháin, N., Peters, J., Wichtmann, W., 2021. The Power of Nature-Based Solutions: How Peatlands Can Help Us to Achieve Key EU Sustainability Objectives. Adv. Sustain. Syst. 5, 2000146. https://doi.org/10.1002/adsu.202000146

Tanneberger, F., Birr, F., Couwenberg, J., Kaiser, M., Luthardt, V., Nerger, M., Pfister, S., Oppermann, R., Zeitz, J., Beyer, C., van der Linden, S., Wichtmann, W., Närmann, F., 2022. Saving soil carbon, greenhouse gas emissions, biodiversity and the economy: paludiculture as sustainable land use option in German fen peatlands. Reg Environ Change 22, 69. https://doi.org/10.1007/s10113-022-01900-8

Tanneberger, F., Wichtmann, W., Steiner, A., Tsalko, V., Merck, J., 2011. Carbon Credits from Peatland Rewetting: Climate - Biodiversity - Land Use. Schweizerbart Science Publishers.

Thompson, D.K., Waddington, J.M., 2013. Peat properties and water retention in boreal forested peatlands subject to wildfire. Water Resour. Res. 49, 3651–3658. https://doi.org/10.1002/wrcr.20278

Tiemeyer, B., Frings, J., Kahle, P., Köhne, S., Lennartz, B., 2007. A comprehensive study of nutrient losses, soil properties and groundwater concentrations in a degraded peatland used as an intensive meadow – Implications for re-wetting. J. Hydrol. 345, 80–101. https://doi.org/10.1016/j.jhydrol.2007.08.002

Tiemeyer, B., Freibauer, A., Borraz, E.A., Augustin, J., Bechtold, M., Beetz, S., Beyer, C., Ebli, M., Eickenscheidt, T., Fiedler, S., Förster, C., Gensior, A., Giebels, M., Glatzel, S., Heinichen, J., Hoffmann, M., Höper, H., Jurasinski, G., Laggner, A., Leiber-Sauheitl, K., Peichl-Brak, M., Drösler, M., 2020. A new methodology for organic soils in national greenhouse gas inventories: Data synthesis, derivation and application. Ecological Indicators, 109, 105838. https://doi.org/10.1016/j.ecolind.2019.105838

Tiemeyer, B., Pfaffner, N., Frank, S., Kaiser, K., Fiedler, S., 2017. Pore water velocity and ionic strength effects on DOC release from peat-sand mixtures: Results from laboratory and field experiments. Geoderma 296, 86–97. https://doi.org/10.1016/j.geoderma.2017.02.024

Tobias, C., Neubauer, S.C., 2009. Salt marsh biogeochemistry-an overview, in: Perillo, G.M.E., Wolanski, E., Cahoon, D.R., Brinson, M.M. (Eds.), Coastal Wetlands: An Integrated Ecosystem Approach. Elsevier, pp. 445–492.

Toride, N., Leij, F.J., van Genuchten, M.Th., 1999. The CXTFIT code for estimating transport parameters from laboratory or field tracer experiments. Version 2.1, Research Report No. 137. Riverside, CA.

Trangmar, B.B., Yost, R.S., Wade, M.K., Uehara, G., Sudjadi, M., 1987. Spatial variation of soil properties and rice yield on recently cleared land. Soil Sci. Soc. Am. J. 51, 668–674. https://doi.org/10.2136/sssaj1987.03615995005100030021x

Truba, M., Oleszczuk, R., 2014. An analysis of some basic chemical and physical properties of drained fen peat and moorsh soil layers. Ann. Warsaw Univ. of Life Sci.– SGGW, Land Reclam. 46 (1), 69–78. http://doi.org/10.2478/sggw-2014-0006

Tsegaye, T., Hill, R.L., 1998. Intensive tillage effects on spatial variability of soil physical properties. Soil Sci. 163, 143–154. https://doi.org/10.1097/00010694-199802000-00008

USDA, 1999. Soil Taxonomy. Agricultural Handbook No. 436. U.S. Government Printing Office, Washington, DC.

USDA, NRCS, 2003. Field Indicators of Hydric Soils in the United States, Version 5.01. USDA, NRCS in cooperation with the National Technical Committee for Hydric Soils, Fort Worth, TX.

Väänänen, R., Nieminen, M., Vuollekoski, M., Nousiainen, H., Sallantaus, T., Tuittila, E.-S., Ilvesniemi, H., 2008. Retention of phosphorus in peatland buffer zones at six forested catchments in southern Finland. Silva Fenn. 42. https://doi.org/10.14214/sf.253

van Dijk, G., Smolders, A.J.P., Loeb, R., Bout, A., Roelofs, J.G.M., Lamers, L.P.M., 2015. Salinization of coastal fresh-water wetlands; effects of constant versus fluctuating salinity on sediment biogeochemistry. Biogeochemistry 126, 71–84. https://doi.org/10.1007/s10533-015-0140-1

van Eck, N.J., Waltman, L., 2010. VOSViewer: Visualizing Scientific Landscapes [Software].

van Genuchten, M.Th., 1980. A Closed-form equation for predicting the hydraulic conductivity of unsaturated soils. Soil Sci. Soc. Am. J. 44, 892–898. https://doi.org/10.2136/sssaj1980.03615995004400050002x

van Genuchten, M.Th., Leij, F.J., Yates, S.R., 1991. The RETC code for quantifying the hydraulic functions of unsaturated soils. Riverside, California.

van Genuchten, M.Th., Šimůnek, J., Leij, F.J., Toride, N., Šejna, M., 2012. STANMOD: Model use, calibration, and validation. Trans ASABE 55, 1355–1368. https://doi.org/10.13031/2013.42247

van Genuchten, M.Th., Wierenga, P.J., 1976. Mass transfer studies in sorbing porous media I. Analytical solutions. Soil Sci. Soc. Am. J. 40, 473–480. https://doi.org/10.2136/sssaj1976.03615995004000040011x

Vanderborght, J., Vereecken, H., 2007. Review of dispersivities for transport modeling in soils. Vadose Zone J. 6, 29–52. https://doi.org/10.2136/vzj2006.0096

Vereecken, H., Maes, J., Feyen, J., Darius, P., 1989. Estimating the soil moisture retention characteristic from texture, bulk density, and carbon content. Soil Sci. 148, 389–403. https://doi.org/10.1097/00010694-198912000-00001

Vereecken, H., Weynants, M., Javaux, M., Pachepsky, Y., Schaap, M.G., van Genuchten, M.Th., 2010. Using pedo-transfer functions to estimate the van Genuchten-Mualem soil hydraulic properties: a review. Vadose Zone J. 9, 795–820. https://doi.org/10.2136/vzj2010.0045

Vervoort, R.W., Radcliffe, D.E., West, L.T., 1999. Soil structure development and preferential solute flow. Water Resour. Res. 35, 913–928. https://doi.org/10.1029/98WR02289

Vidon, P., Cuadra, P.E., 2011. Phosphorus dynamics in tile-drain flow during storms in the US Midwest. Agric. Water Manag. 98, 532–540. https://doi.org/10.1016/j.agwat.2010.09.010

Vieira, S.R., Nielsen, D.R., Biggar, J.W., 1981. Spatial variability of field-measured infiltration rate. Soil Sci. Soc. Am. J. 45, 1040–1048. https://doi.org/10.2136/sssaj1981.03615995004500060007x

Vikman, A., Sarkkola, S., Koivusalo, H., Sallantaus, T., Laine, J., Silvan, N., Nousiainen, H., Nieminen, M., 2010. Nitrogen retention by peatland buffer areas at six forested catchments in southern and central Finland. Hydrobiologia 641, 171–183. https://doi.org/10.1007/s10750-009-0079-0

Vis, G.-J., Cohen, K.M., Westerhoff, W.E., Veen, J.H. Ten, Hijma, M.P., van der Spek, A.J.F., Vos, P.C., 2015. Paleogeography, in: Handbook of Sea-Level Research. John Wiley & Sons, Ltd, Chichester, UK, pp. 514–535. https://doi.org/10.1002/9781118452547.ch33

Vitt, D.H., 2013. Peatlands, in: Encyclopedia of Ecology. Elsevier, pp. 557–566. https://doi.org/10.1016/B978-0-12-409548-9.00741-7

von Post, L., 1922. Sveriges Geologiska Undersöknings torvinventering och några av dess hittills vunna resultat.

Waddington, J.M., Strack, M., Greenwood, M.J., 2010. Toward restoring the net carbon sink function of degraded peatlands: Short-term response in CO_2 exchange to ecosystem-scale restoration. J. Geophys. Res. 115, G01008. https://doi.org/10.1029/2009JG001090

Wagner, B., Tarnawski, V.R., Hennings, V., Müller, U., Wessolek, G., Plagge, R., 2001. Evaluation of pedo-transfer functions for unsaturated soil hydraulic conductivity using an independent data set. Geoderma 102, 275–297. https://doi.org/10.1016/S0016-7061(01)00037-4

Wallage, Z.E., Holden, J., 2011. Near-surface macropore flow and saturated hydraulic conductivity in drained and restored blanket peatlands. Soil Use Manag. 27, 247–254. https://doi.org/10.1111/j.1475-2743.2011.00336.x

Waller, M., Kirby, J., 2021. Coastal peat-beds and peatlands of the southern North Sea: Their past, present and future. Biological Reviews 96, 408–432. https://doi.org/10.1111/brv.12662

REFERENCES

Wallor, E., Rosskopf, N., Zeitz, J., 2018. Hydraulic properties of drained and cultivated fen soils part I - Horizon-based evaluation of van Genuchten parameters considering the state of moorsh-forming process. Geoderma 313, 69–81. https://doi.org/10.1016/j.geoderma.2017.10.026

Wang, M., Liu, H., Lennartz, B., 2021. Small-scale spatial variability of hydro-physical properties of natural and degraded peat soils. Geoderma 399, 115123. https://doi.org/10.1016/j.geoderma.2021.115123

Wang, M., Liu, H., Zak, D., Lennartz, B., 2020. Effect of anisotropy on solute transport in degraded fen peat soils. Hydrol. Process. 34, 2128–2138. https://doi.org/10.1002/hyp.13717

Wang, Y., Shao, M., Han, X., Liu, Z., 2015. Spatial variability of soil parameters of the van Genuchten model at a regional scale. Clean 43, 271–278. https://doi.org/10.1002/clen.201300903

Warrick, A.W., Nielsen, D.R., 1980. Spatial variability of soil physical properties in the field, in: Hillel, D. (Ed.), Applications of Soil Physics. Elsevier Academic Press, New York, pp. 319–344. https://doi.org/10.1016/B978-0-12-348580-9.50018-3

Watt, M.S., Palmer, D.J., 2012. Use of regression kriging to develop a Carbon: Nitrogen ratio surface for New Zealand. Geoderma 183–184, 49–57. https://doi.org/10.1016/j.geoderma.2012.03.013

Wattel-Koekkoek, E.J.W., van Genuchten, P.P.L., Buurman, P., van Lagen, B., 2001. Amount and composition of clay-associated soil organic matter in a range of kaolinitic and smectitic soils. Geoderma 99, 27–49. https://doi.org/10.1016/S0016-7061(00)00062-8

Weber, C.A., 1907. Die grundlegenden Begriffe der Moorkunde. Zeitschrift für Moorkultur und Torfverwertung 5, 258–289.

Weber, T.K.D., Iden, S.C., Durner, W., 2017. Unsaturated hydraulic properties of *Sphagnum* moss and peat reveal trimodal pore-size distributions. Water Resour. Res. 53, 415–434. https://doi.org/10.1002/2016WR019707

Webster, R., Oliver, M., 2001. Geostatistics for Environmental Scientists. John Wiley & Sons, Ltd., Chichester.

Weil, M., Wang, H., Bengtsson, M., Köhn, D., Günther, A., Jurasinski, G., Couwenberg, J., Negassa, W., Zak, D., Urich, T., 2020. Long-term rewetting of three formerly drained peatlands drives congruent compositional changes in pro- and eukaryotic soil microbiomes through environmental filtering. Microorganisms 8, 550. https://doi.org/10.3390/microorganisms8040550

Weil, R., Magdoff, Fred, 2004. Significance of soil organic matter to soil quality and health, in: Magdoff, F., Weil, R.R. (Eds.), Soil Organic Matter in Sustainable Agriculture. CRC Press, Boca Raton, pp. 1–43. https://doi.org/10.1201/9780203496374.ch1

Weiss, R., Alm, J., Laiho, R., Laine, J., 1998. Modeling moisture retention in peat soils. Soil Sci. Soc. Am. J. 62, 305. https://doi.org/10.2136/sssaj1998.03615995006200020002x

Weston, N.B., Vile, M.A., Neubauer, S.C., Velinsky, D.J., 2011. Accelerated microbial organic matter mineralization following salt-water intrusion into tidal freshwater marsh soils. Biogeochemistry 102, 135–151. https://doi.org/10.1007/s10533-010-9427-4

Wheeler, B.D., Proctor, M.C.F., 2000. Ecological gradients, subdivisions and terminology of north-west European mires. J. Ecol. 88, 187–203. https://doi.org/10.1046/j.1365-2745.2000.00455.x

White, R.E., 1985. The influence of macropores on the transport of dissolved and suspended matter through soil, in: Stewart, B.A. (Ed.), Advances in Soil Science. Springer, New York, pp. 95–120. https://doi.org/10.1007/978-1-4612-5090-6_3

Whittaker, R.H., Likens, G.E., 1973. Carbon in the biota, in: Woodwell, G.M., Pecan, E. V (Eds.), Carbon and the Biosphere. Technical Information Center, Springfield, Virginia, pp. 281–302.

Whittle, A., Gallego-Sala, A. V., 2016. Vulnerability of the peatland carbon sink to sea-level rise. Sci. Rep. 6, 28758. https://doi.org/10.1038/srep28758

Wilson, D., Farrell, C. A., Fallon, D., Moser, G., Müller, C., & Renou-Wilson, F., 2016. Multiyear greenhouse gas balances at a rewetted temperate peatland. Global Change Biology, 22, 4080–4095. https://doi.org/10.1111/gcb.13325

Wösten, J.H.M., Lilly, A., Nemes, A., Le Bas, C., 1999. Development and use of a database of hydraulic properties of European soils. Geoderma 90, 169–185. https://doi.org/10.1016/S0016-7061(98)00132-3

Wösten, J.H.M., Pachepsky, Ya.A., Rawls, W.J., 2001. Pedotransfer functions: Bridging the gap between available basic soil data and missing soil hydraulic characteristics. J. Hydrol. 251, 123–150. https://doi.org/10.1016/S0022-1694(01)00464-4

Xenopoulos, M.A., Barnes, R.T., Boodoo, K.S., Butman, D., Catalán, N., D'Amario, S.C., Fasching, C., Kothawala, D.N., Pisani, O., Solomon, C.T., Spencer, R.G.M., Williams, C.J., Wilson, H.F., 2021. How humans alter dissolved organic matter composition in freshwater: Relevance for the Earth's biogeochemistry. Biogeochemistry 154, 323–348. https://doi.org/10.1007/s10533-021-00753-3

120

Xu, J., Morris, P.J., Liu, J., Holden, J., 2018. Hotspots of peatland-derived potable water use identified by global analysis. Nat. Sustain. 1, 246–253. https://doi.org/10.1038/s41893-018-0064-6

Yang, J., Zhan, C., Li, Y., Zhou, D., Yu, Y., Yu, J., 2018. Effect of salinity on soil respiration in relation to dissolved organic carbon and microbial characteristics of a wetland in the Liaohe River estuary, Northeast China. Sci. Total Environ. 642, 946–953. https://doi.org/10.1016/j.scitotenv.2018.06.121

Yao, X., Fu, B., Lü, Y., Sun, F., Wang, S., Liu, M., 2013. Comparison of four spatial interpolation methods for estimating soil moisture in a complex terrain catchment. PLoS One 8, e54660. https://doi.org/10.1371/journal.pone.0054660

Yao, Z., Yan, G., Ma, L., Wang, Yan, Zhang, H., Zheng, X., Wang, R., Liu, C., Wang, Yanqiang, Zhu, B., Zhou, M., Rahimi, J., Butterbach-Bahl, K., 2022. Soil C/N ratio is the dominant control of annual N_2O fluxes from organic soils of natural and semi-natural ecosystems. Agric. For. Meteorol. 327, 109198. https://doi.org/10.1016/j.agrformet.2022.109198

Young, D.M., Baird, A.J., Morris, P.J., Holden, J., 2017. Simulating the long-term impacts of drainage and restoration on the ecohydrology of peatlands. Water Resour. Res. 53, 6510–6522. https://doi.org/10.1002/2016WR019898

Zak, D., Gelbrecht, J., 2007. The mobilisation of phosphorus, organic carbon and ammonium in the initial stage of fen rewetting (a case study from NE Germany). Biogeochemistry 85, 141–151. https://doi.org/10.1007/s10533-007-9122-2

Zak, D., Gelbrecht, J., Wagner, C., Steinberg, C.E.W., 2008. Evaluation of phosphorus mobilization potential in rewetted fens by an improved sequential chemical extraction procedure. Eur. J. Soil Sci. 59, 1191–1201. https://doi.org/10.1111/j.1365-2389.2008.01081.x

Zak, D., McInnes, R.J., Gelbrecht, J., 2018. Managing phosphorus release from restored minerotrophic peatlands, in: The Wetland Book. Springer Netherlands, Dordrecht, pp. 1321–1327. https://doi.org/10.1007/978-90-481-9659-3_223

Zak, D., Roth, C., Unger, V., Goldhammer, T., Fenner, N., Freeman, C., Jurasinski, G., 2019. Unraveling the importance of polyphenols for microbial carbon mineralization in rewetted riparian peatlands. Front. Environ. Sci. 7. https://doi.org/10.3389/fenvs.2019.00147

Zak, D., Wagner, C., Payer, B., Augustin, J., Gelbrecht, J., 2010. Phosphorus mobilization in rewetted fens: The effect of altered peat properties and implications for their restoration. Ecol. Appl. 20, 1336–1349. https://doi.org/10.1890/08-2053.1

Zauft, M., Fell, H., Glaßer, F., Rosskopf, N., Zeitz, J., 2010. Carbon storage in the peatlands of Mecklenburg-Western Pomerania, north-east Germany. Mires Peat 6, article 04, 1–12.

Zeitz, J., Velty, S., 2002. Soil properties of drained and rewetted fen soils. J. Plant Nutr. Soil Sci. 165, 618–626. https://doi.org/10.1002/1522-2624(200210)165:5<618::AID-JPLN618>3.0.CO;2-W

Zerbe, S., Steffenhagen, P., Parakenings, K., Timmermann, T., Frick, A., Gelbrecht, J., Zak, D., 2013. Ecosystem service restoration after 10 years of rewetting peatlands in NE Germany. Environ. Manage 51, 1194–1209. https://doi.org/10.1007/s00267-013-0048-2

Zhang, S., Yan, L., Huang, J., Mu, L., Huang, Y., Zhang, X., Sun, Y., 2016. Spatial heterogeneity of soil C:N Ratio in a Mollisol watershed of northeast China. Land Degrad. Dev. 27, 295–304. https://doi.org/10.1002/ldr.2427

Zhang, X., Wendroth, O., Matocha, C., Zhu, J., Reyes, J., 2020. Assessing field-scale variability of soil hydraulic conductivity at and near saturation. Catena 187, 104335. https://doi.org/10.1016/j.catena.2019.104335

Zhang, X., Zhu, J., Wendroth, O., Matocha, C., Edwards, D., 2019. Effect of macroporosity on pedotransfer function estimates at the field scale. Vadose Zone J. 18, 1–15. https://doi.org/10.2136/vzj2018.08.0151

Zhao, Q., Bai, J., Huang, L., Gu, B., Lu, Q., Gao, Z., 2016. A review of methodologies and success indicators for coastal wetland restoration. Ecol. Indic. 60, 442–452. https://doi.org/10.1016/j.ecolind.2015.07.003

Zheng, X., Liu, Q., Ji, X., Cao, M., Zhang, Y., Jiang, J., 2021. How do natural soil NH_4^+, NO_3^- and N_2O interact in response to nitrogen input in different climatic zones? A global meta-analysis. Eur. J. Soil Sci. 72, 2231–2245. https://doi.org/10.1111/ejss.13131

Zou, J., Ziegler, A.D., Chen, D., McNicol, G., Ciais, P., Jiang, X., Zheng, C., Wu, Jie, Wu, Jin, Lin, Z., He, X., Brown, L.E., Holden, J., Zhang, Z., Ramchunder, S.J., Chen, A., Zeng, Z., 2022. Rewetting global wetlands effectively reduces major greenhouse gas emissions. Nat. Geosci. 15, 627–632. https://doi.org/10.1038/s41561-022-00989-0

Supplemental Materials

Supplemental Materials to Chapter 2
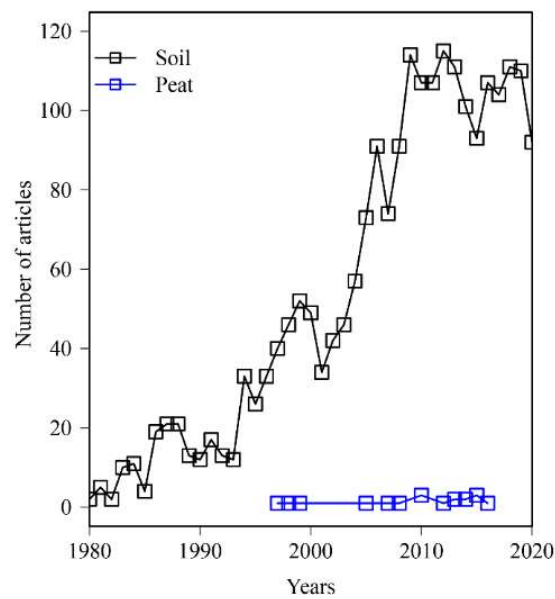
Figure S2.1 Numbers of publications per year found from a SCOPUS database search combining the search terms "Soil" and "Semivariogram" or "Variogram"; "Peat" and "Semivariogram" or "Variogram". The results also indicate *Geoderma* published the highest number of articles on this topic.
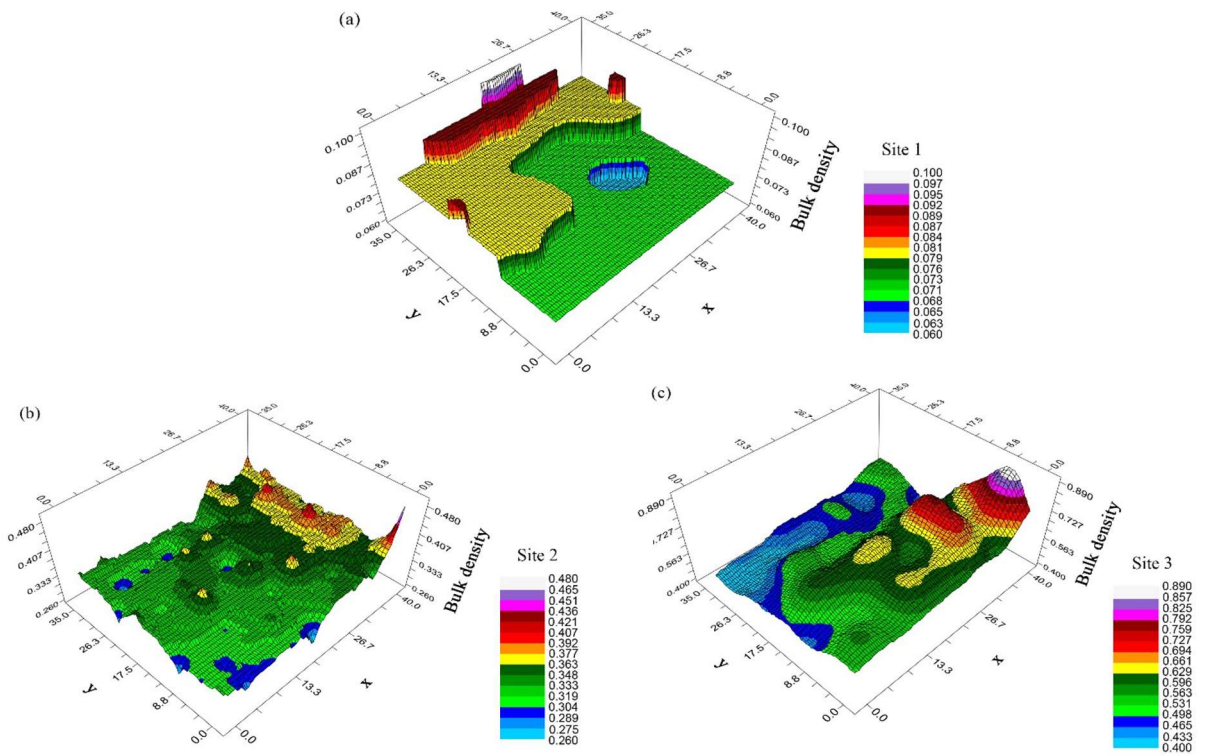
Figure S2.2 Kriging interpolation map of estimated bulk density for three study sites.

Figure S2.3 The relationship between $\text{Log}_{10}\alpha$ and macroporosity at Site 1 (natural peat). Macroporosity is calculated by the difference between total porosity and water content at −10 cm H_2O pressure head.

Table S2.1 Summary of linear mixed-effect model (LMEM) fit by REML in "R" Software with "lme4" and "lmerTest" package. (fixed effect: "site"; random effect: "sampling location").

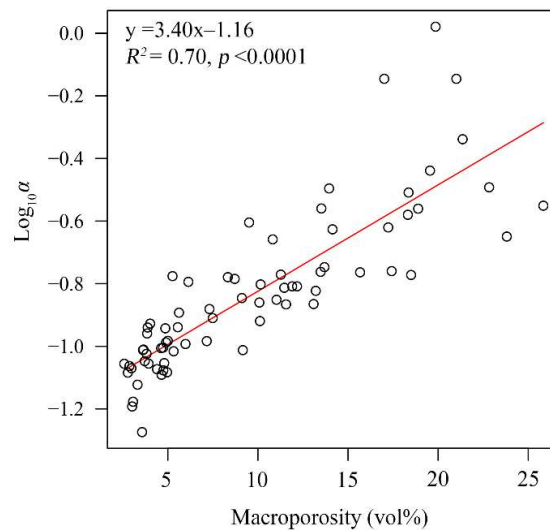| Parameter[a]	Criterion at convergence	Fixed effect ("site")						Random effect ("location")			
			Estimate	SE[c]	DF	t-value	Pr(>|t|)[d]	Groups	Name	Variance	SD
SOM (wt%)	1279.6	(Intercept)	97.7300	0.5598	209.92	174.58	<0.0001 ***	location	(Intercept)	1.932	1.390
		siteSite2	−28.6190	0.7570	142.00	−37.80	<0.0001 ***	Residual		20.632	4.542
		siteSite3	−67.2921	0.7570	142.00	−88.89	<0.0001 ***	Number of obs: 216, groups: location, 72			
BD (g cm^{-3})	−543.8	(Intercept)	0.0752	0.0077	211.60	9.726	<0.0001 ***	location	(Intercept)	0.0002	0.0157
		siteSite2	0.2623	0.0106	142.00	24.709	<0.0001 ***	Residual		0.0041	0.0637
		siteSite3	0.4675	0.0106	142.00	44.029	<0.0001 ***	Number of obs: 216, groups: location, 72			
Total porosity (vol%)	−782.9	(Intercept)	0.9662	0.0044	209.88	218.57	<0.0001 ***	location	(Intercept)	0.0001	0.0110
		siteSite2	−0.1383	0.0060	142.00	−23.14	<0.0001 ***	Residual		0.0013	0.0359
		siteSite3	−0.1718	0.0060	142.00	−28.75	<0.0001 ***	Number of obs: 216, groups: location, 72			
Macro-Porosity[b] (vol%)	−589.2	(Intercept)	0.4295	0.0069	213.00	61.90	<0.0001 ***	location	(Intercept)	0.0000	0.0000
		siteSite2	−0.3465	0.0098	213.00	−35.31	<0.0001 ***	Residual		0.0035	0.0589
		siteSite3	−0.3300	0.0098	213.00	−33.63	<0.0001 ***	Number of obs: 216, groups: location, 72			
Log$_{10}K_s$	367.6	(Intercept)	−5.0573	0.0656	212.65	−77.08	<0.0001 ***	location	(Intercept)	0.0089	0.0942
		siteSite2	−0.4158	0.0915	142.00	−4.55	<0.0001 ***	Residual		0.3011	0.5487
		siteSite3	−0.0467	0.0915	142.00	−0.51	0.6110	Number of obs: 216, groups: location, 72			
α (cm^{-1})	−397.5	(Intercept)	0.1812	0.0109	213.00	16.65	<0.0001 ***	location	(Intercept)	1.685e−05	0.0041
		siteSite2	−0.1801	0.0154	142.00	−11.71	<0.0001 ***	Residual		8.512e−03	0.0923
		siteSite3	−0.1798	0.0154	142.00	−11.70	<0.0001 ***	Number of obs: 216, groups: location, 72			
n	−562.6	(Intercept)	1.2440	0.0074	207.10	167.22	<0.0001 ***	location	(Intercept)	0.0005	0.0218
		siteSite2	0.2492	0.0099	142.00	25.24	<0.0001 ***	Residual		0.0035	0.0592
		siteSite3	0.2058	0.0099	142.00	20.85	<0.0001 ***	Number of obs: 216, groups: location, 72			

[a] Abbreviations: SOM, soil organic matter content; BD, bulk density; K_s, saturated hydraulic conductivity; θ_s, estimated water content at saturation (cm^3 cm^{-3}); α and n, empirical parameters.

[b] The linear mixed-effect models of "macroporosity" result in singular fits, which indicated that the random effects are very small.

[c] Abbreviations: SE, standard error; SD, standard deviation; DF, degrees of freedom.

[d] Significance codes: 0, "***"; 0.001, "**"; 0.01, "*".

Table S2.2 Summary of pairwise comparison of linear mixed-effect models (LMEMs) in "R" Soft-ware with "em-mean" package. Tukey method for comparing a family of 3 estimates for *p*-value adjustment.

Parameter[a]	Pairwise difference of "Site"					
	Pairwise	Estimate	Standard error	DF[b]	t-ratio	*p*-value[c]
SOM (wt%)	Site 1 – Site 2	28.600	0.757	142	37.804	<0.0001[***]
	Site 1 – Site 3	67.300	0.757	142	88.889	<0.0001[***]
	Site 2 – Site 3	38.700	0.757	142	51.058	<0.0001[***]
BD (g cm^{-3})	Site 1 – Site 2	−0.262	0.011	142	−24.709	<0.0001[***]
	Site 1 – Site 3	−0.467	0.011	142	−44.029	<0.0001[***]
	Site 2 – Site 3	−0.205	0.011	142	−19.320	<0.0001[***]
Total porosity (vol%)	Site 1 – Site 2	0.138	0.006	142	23.138	<0.0001[***]
	Site 1 – Site 3	0.172	0.006	142	28.751	<0.0001[***]
	Site 2 – Site 3	0.034	0.006	142	5.613	<0.0001[***]
Macroporosity (vol%)	Site 1 – Site 2	0.347	0.010	142	35.310	<0.0001[***]
	Site 1 – Site 3	0.330	0.010	142	33.629	<0.0001[***]
	Site 2 – Site 3	−0.017	0.010	142	−1.680	0.2163
Log$_{10}K_s$	Site 1 – Site 2	0.035	0.217	142	0.159	<0.0001[***]
	Site 1 – Site 3	0.268	0.217	142	1.237	0.8664
	Site 2 – Site 3	0.234	0.217	142	1.078	0.0003[***]
α (cm^{-1})	Site 1 – Site 2	0.180	0.015	142	11.709	<0.0001[***]
	Site 1 – Site 3	0.180	0.015	142	11.696	<0.0001[***]
	Site 2 – Site 3	−0.0002	0.015	142	−0.013	0.9999
n	Site 1 – Site 2	−0.249	0.010	142	−25.241	<0.0001[***]
	Site 1 – Site 3	−0.206	0.010	142	−20.848	<0.0001[***]
	Site 2 – Site 3	0.043	0.010	142	4.394	0.0001[***]

[a] Abbreviations: SOM, soil organic matter content; BD, bulk density; K_s, saturated hydraulic conductivity; α and *n,* empirical parameters.
[b] Abbreviation: DF, degrees of freedom.
[c] Significance codes: 0, "***"; 0.001, "**"; 0.01, "*".

Table S2.3 Mean, standard deviation and 95% confidence intervals of water contents at different pressure heads in the soil water retention curves (SWRCs). (Site 1: natural peatland; Site 2: degraded peatland; Site 3: extremely degraded peatland).

Pressure head (−cm H₂O)	Site	Mean	Standard deviation	95% confidence intervals	
				Lower limit	Upper limit
At saturation	1	0.97	0.02	0.960	0.972
	2	0.83	0.03	0.821	0.835
	3	0.80	0.06	0.785	0.812
10	1	0.87	0.07	0.852	0.884
	2	0.79	0.04	0.779	0.798
	3	0.75	0.06	0.736	0.764
30	1	0.69	0.09	0.670	0.709
	2	0.77	0.04	0.762	0.781
	3	0.72	0.06	0.710	0.737
60	1	0.54	0.10	0.515	0.559
	2	0.74	0.04	0.736	0.754
	3	0.70	0.06	0.684	0.712
100	1	0.47	0.09	0.452	0.493
	2	0.72	0.04	0.714	0.733
	3	0.68	0.06	0.663	0.691
200	1	0.44	0.08	0.418	0.455
	2	0.71	0.04	0.702	0.720
	3	0.66	0.06	0.649	0.677
600	1	0.42	0.08	0.399	0.435
	2	0.69	0.04	0.679	0.697
	3	0.65	0.06	0.634	0.662
15850	1	-	-	-	-
	2	0.18	0.01	0.181	0.185
	3	0.19	0.01	0.184	0.189

Table S2.4 Mean, standard deviation and 95% confidence intervals of van Genuchten model parameters. (Site 1: natural peatland; Site 2: degraded peatland; Site 3: extremely degraded peatland).

Parameter[a]	Site	Mean	Standard deviation	95% confidence intervals	
				Lower limit	Upper limit
θ_s (cm³ cm⁻³)	1	0.98	0.03	0.976	0.989
	2	0.77	0.04	0.763	0.780
	3	0.74	0.06	0.725	0.751
α (cm⁻¹)	1	0.18	0.16	0.144	0.218
	2	1.15×10^{-3}	2.98×10^{-4}	1.08×10^{-3}	1.22×10^{-3}
	3	1.35×10^{-3}	5.54×10^{-4}	1.22×10^{-3}	1.48×10^{-3}
n	1	1.24	0.07	1.230	1.260
	2	1.49	0.05	1.480	1.510
	3	1.45	0.07	1.430	1.460

[a] Abbreviations: θ_s, estimated water content at saturation (cm³ cm⁻³); α and n, empirical parameters.

Table S2.5 Pearson correlation coefficient between different hydro-physical properties of three study sites (site 1: natural peatland; site 2: degraded peatland; site 3: highly degraded peatland).

		SOM[a]	BD	Total porosity	Macro-porosity	$Log_{10}K_s$	θ_s	$Log_{10}\alpha$	n
SOM		-							
BD	Site 1	−0.121[b]	-						
	Site 2	−0.792***							
	Site 3	−0.861***							
Total Porosity	Site 1	−0.040	−0.004	-					
	Site 2	0.665***	−0.788***						
	Site 3	0.528***	−0.821***						
Macro-porosity	Site 1	0.046	−.678***	0.045	-				
	Site 2	−0.171	0.033	−0.205					
	Site 3	0.204	−0.336*	0.218					
$Log_{10}K_s$	Site 1	0.018	−0.424**	−0.073	0.581***	-			
	Site 2	−0.255	0.244*	−0.477***	0.573***				
	Site 3	0.182	−0.237*	0.128	0.553***				
θ_s	Site 1	0.007	−0.107	0.941***	0.070	−0.063	-		
	Site 2	0.573***	−0.584***	0.852***	−0.679***	−0.678***			
	Site 3	0.484***	−0.676***	0.840***	−0.003	0.068			
$Log_{10}\alpha$	Site 1	−0.123	0.245	−0.232*	0.208	0.182	−0.469***	-	
	Site 2	−0.113	−0.021	−0.045	0.715***	0.159	−0.364*		
	Site 3	−0.046	0.032	−0.168	0.575***	0.350	−0.385		
n	Site 1	0.098	−0.745***	0.078	0.714***	0.458***	0.289*	−0.476***	-
	Site 2	0.435**	−0.337*	0.381**	−0.722***	−0.327*	0.629***	−0.820***	
	Site 3	0.152	−0.236*	0.434**	−0.431**	−0.246*	0.666***	−0.884***	

[a] Abbreviations: SOM, soil organic matter content; BD, bulk density; K_s, saturated hydraulic conductivity; θ_s, estimated water content at saturation (cm^3 cm^{-3}); α and n, empirical parameters.

[b] Significance codes: 0, "***"; 0.001, "**"; 0.01, "*".

Table S2.6 Summary of the multiple regression models fitted to the hydraulic parameters.

Study site	Peat type	Parameters	Descriptor[a]	Coefficient	Standard error	t-value	Significance[b]
Site 1	Natural peat	$\text{Log}_{10}K_s$	MP	9.236	3.519	2.624	<0.001***
			BD	−64.195	29.286	−2.192	0.010*
			MP²	−8.907	4.366	−2.040	0.032*
			BD²	368.711	172.292	2.140	0.036*
		θ_s	BD	5.611	2.140	2.622	0.011*
			BD²	−35.390	12.928	−2.737	0.007**
		$\text{Log}_{10}\alpha$	MP	1.868	0.364	5.126	<0.001***
			BD	12.994	2.458	5.289	<0.001***
		n	MP	0.280	0.072	3.905	<0.001***
			BD	−2.364	0.483	−4.897	<0.001***
Site 2	Degraded peat	$\text{Log}_{10}K_s$	MP	59.825	13.228	4.523	<0.001***
			BD	3.452	1.638	2.107	0.039*
			MP²	−232.621	69.026	−3.370	0.001**
		θ_s	MP	−0.864	0.075	−11.587	<0.001***
			BD	−0.471	0.048	−9.874	<0.001***
		$\text{Log}_{10}\alpha$	MP	2.366	0.276	8.562	<0.001***
		n	MP	−1.368	0.143	−9.587	<0.001***
			BD	−0.385	0.091	−4.222	<0.001***
Site 3	Extremely degraded peat	$\text{Log}_{10}K_s$	MP	20.508	4.776	4.294	<0.001***
			MP²	−76.092	24.74	−3.075	0.003**
		θ_s	BD	−1.678	0.614	−2.732	0.008**
			SOM	0.014	0.006	2.252	0.028*
			BD²	1.183	0.497	2.380	0.020*
			SOM²	−0.0002	0.0001	−2.112	0.038*
		$\text{Log}_{10}\alpha$	MP	2.868	0.461	6.221	<0.001***
			BD	0.238	0.134	1.771	0.081.
		n	MP	−1.130	0.237	−4.771	<0.001***
			BD	−0.186	0.069	−2.702	0.009**

[a] Abbreviations: MP, macroporosity; BD, bulk density; SOM, soil organic matter content; K_s, saturated hydraulic conductivity; θ_s, estimated water content at saturation (cm³ cm⁻³); α and n, empirical parameters.

[b] Significance codes: 0, "***"; 0.001, "**"; 0.01, "*"; 0.05, ".".

Table S2.7 Comparison of fitted multiple regression model with the predictor "macroporosity (MP)" and without "macroporosity".

Study site	Peat type	Parameter	Predictor with macroporosity[a] (MP)				Predictor without macroporosity (MP)			
			R^2	RSE[b]	P value	AIC	R^2	RSE	P value	AIC
Site 1 (N=72)	Natural peat	$Log_{10}K_s$	0.40	0.318	<0.001	−160.22	0.23	0.355	<0.001	−146.41
		θ_s	0.11	0.027	0.019	−519.74	0.11	0.027	0.019	−519.74
		$Log_{10}\alpha$	0.32	0.210	<0.001	−221.52	0.23	0.229	0.003	−206.72
		n	0.64	0.041	<0.001	−455.78	0.56	0.045	<0.001	−443.41
Site 2 (N=72)	Degraded peat	$Log_{10}K_s$	0.46	0.608	<0.001	−67.73	0.07	0.790	0.025	−32.05
		θ_s	0.78	0.018	<0.001	−576.87	0.37	0.030	<0.001	−502.72
		$Log_{10}\alpha$	0.51	0.066	<0.001	−389.17	0.14	0.089	0.019	−344.02
		n	0.62	0.034	<0.001	−483.51	0.19	0.049	<0.001	−430.96
Site 3 (N=72)	Extremely de-graded peat	$Log_{10}K_s$	0.39	0.264	<0.001	−331.68	0.14	0.319	0.0356	−159.81
		θ_s	0.37	0.046	<0.001	−437.91	0.37	0.046	<0.001	−437.91
		$Log_{10}\alpha$	0.36	0.113	<0.001	−311.68	0.10	0.135	0.111	−283.58
		n	0.26	0.058	<0.001	−407.62	0.16	0.063	0.020	−393.92

[a] Macroporosity was calculated by the difference between total porosity and volumetric soil water content at −60 cm H_2O pressure head.
[b] Abbreviations: R^2, the coefficient of determination; RSE, Residual standard error; AIC, Akaike information criterion.

Supplemental Materials to Chapter 3
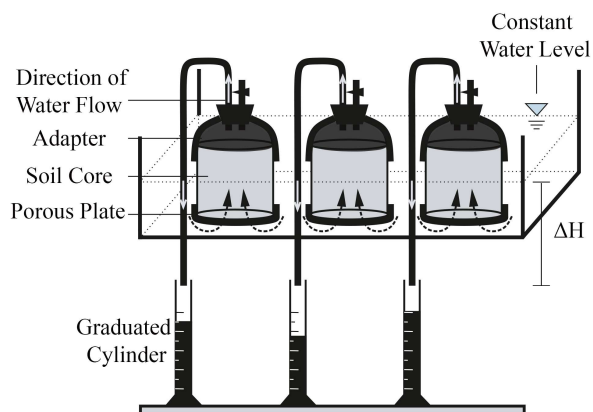
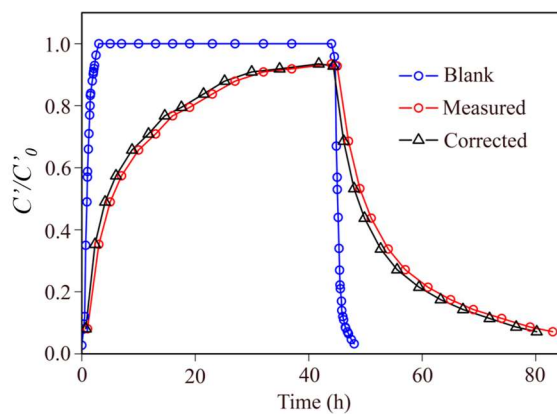**Figure S3.1** Set up for saturated hydraulic conductivity measurement.

Figure S3.2 Bromide breakthrough curves (*e.g.*, column S1V3) where corrected data are fitted using the two-region non-equilibrium transport model in CXTFIT.
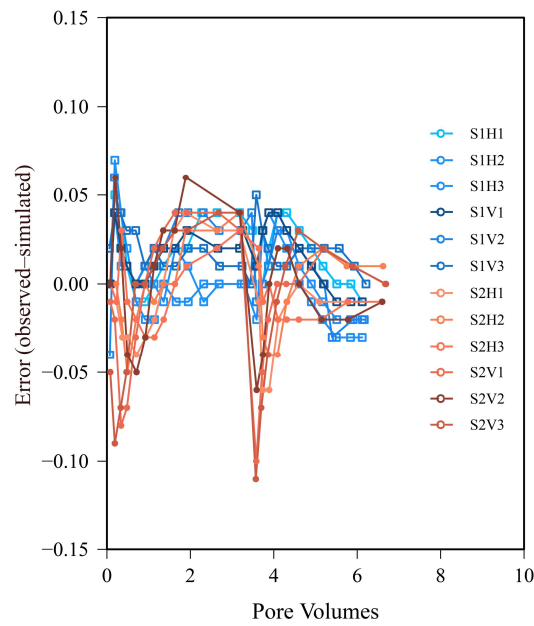
Figure S3.3 Plot of the error (observed – fitted) against pore volume from mobile-immobile model.

Table S3.1 Upper and lower boundaries of fitted parameters (D, β, and ω) in the numerical inverse model.

D [a] (cm² h⁻¹)		β		ω	
lower	upper	lower	upper	lower	upper
0.01	100	0.01	0.99	0.10e−07	100

[a] Abbreviations: D, dispersion coefficient; β, mobile water fraction; ω, mass transfer coefficient.

Table S3.2 Values of optimized parameters from CDE model (only parameter D was fitted).

Column	D[a] (cm² h⁻¹)	R^2	MSE
S1H1	1.45	0.984	0.0020
S1H2	1.41	0.994	0.0007
S1H3	1.76	0.994	0.0007
S1V1	1.19	0.989	0.0014
S1V2	2.46	0.982	0.0018
S1V3	3.41	0.989	0.0011
S2H1	0.49	0.981	0.0031
S2H2	0.82	0.978	0.0031
S2H3	0.67	0.986	0.0020
S2V1	2.24	0.983	0.0019
S2V2	0.88	0.981	0.0024
S2V3	4.11	0.972	0.0035

[a] Abbreviations: D, dispersion coefficient; R^2, the coefficient of determination; MSE, mean squared error.

Table S3.3 The R square (R^2) for regression of observed vs fitted value and corrected Akaike information criterion (AICc) of convection-dispersion equation (CDE) model and mobile-immobile (MIM) model.

Column	CDE			MIM		
	R^2	AICc	MSE	R^2	AICc	MSE
S1H1	0.984	−153.63	0.0020	0.995	−175.89	0.0008
S1H2	0.994	−180.04	0.0007	0.995	−180.19	0.0006
S1H3	0.994	−179.68	0.0007	0.997	−195.18	0.0004
S1V1	0.989	−156.47	0.0014	0.996	−176.54	0.0006
S1V2	0.982	−156.22	0.0018	0.993	−174.39	0.0008
S1V3	0.989	−147.00	0.0011	0.995	−184.90	0.0005
S2H1	0.981	−120.45	0.0031	0.995	−143.34	0.0009
S2H2	0.978	−119.95	0.0031	0.996	−149.81	0.0007
S2H3	0.986	−129.76	0.0020	0.998	−161.79	0.0004
S2V1	0.983	−129.81	0.0019	0.986	−129.83	0.0017
S2V2	0.981	−119.22	0.0024	0.991	−128.90	0.0014
S2V3	0.972	−117.80	0.0035	0.982	−122.59	0.0025

[a] Abbreviations: R^2, the coefficient of determination; MSE, mean squared error.

$$AIC_c = N ln \left(\frac{SSE}{N} \right) + 2k + \frac{2k(k+1)}{N-k-1}$$

where N is the number of the observed data for each BTC; SSE is the sum of squared error between observed and predicted values; k is the number of estimated parameters.

Table S3.4 Tests of Normality (Shapiro-Wilk) of variable "Error (observed – fitted)" from the UNIVARIATE Procedure of SAS.

Column	Statistic	N	P Value (Pr<W)
S1H1	0.942	25	0.163
S1H2	0.922	25	0.056
S1H3	0.949	25	0.235
S1V1	0.957	24	0.384
S1V2	0.977	25	0.815
S1V3	0.955	25	0.326
S2H1	0.969	21	0.707
S2H2	0.986	21	0.983
S2H3	0.924	21	0.104
S2V1	0.927	21	0.120
S2V2	0.976	20	0.881
S2V3	0.903	21	0.040

[a] Abbreviations: N, number of data points used in the test.

Table S3.5 The covariance matrix for fitted parameters of each sample.

Column		D (cm² h⁻¹)	β	ω
S1H1	D^a	1		
	β	0.767	1	
	ω	−0.578	−0.437	1
S1H2	D	1		
	β	0.815	1	
	ω	−0.636	−0.494	1
S1H3	D	1		
	β	0.831	1	
	ω	−0.623	−0.507	1
S1V1	D	1		
	β	0.764	1	
	ω	−0.562	−0.400	1
S1V2	D	1		
	β	0.527	1	
	ω	0.566	−0.306	1
S1V3	D	1		
	β	0.327	1	
	ω	0.528	−0.537	1
S2H1	D	1		
	β	0.749	1	
	ω	−0.690	−0.606	1
S2H2	D	1		
	β	0.704	1	
	ω	−0.619	−0.429	1
S2H3	D	1		
	β	0.717	1	
	ω	−0.646	0.485	1
S2V1	D	1		
	β	0.964	1	
	ω	−0.870	−0.883	1
S2V2	D	1		
	β	0.706	1	
	ω	−0.567	−0.334	1
S2V3	D	1		
	β	0.956	1	
	ω	−0.799	−0.855	1

[a] Abbreviations: D, dispersion coefficient; β, mobile water fraction; ω, mass transfer coefficient.

Supplemental Materials to Chapter 4
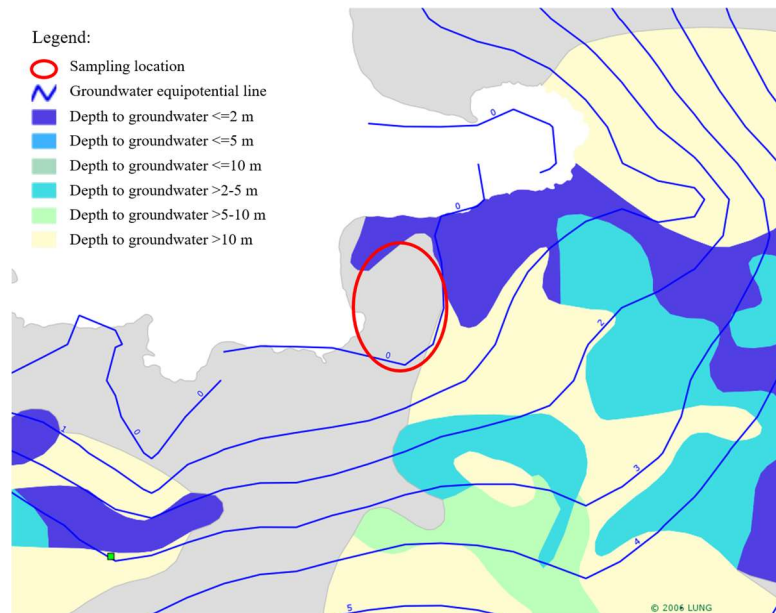
Figure S4.1 The local hydrological regime of the coastal peatland study site. (based on data from LUNG 2006, Kartenportal Umwelt Mecklenburg-Vorpommern, Landesamt für Umwelt, Naturschutz und Geologie, https://www.umweltkarten.mv-regierung.de).
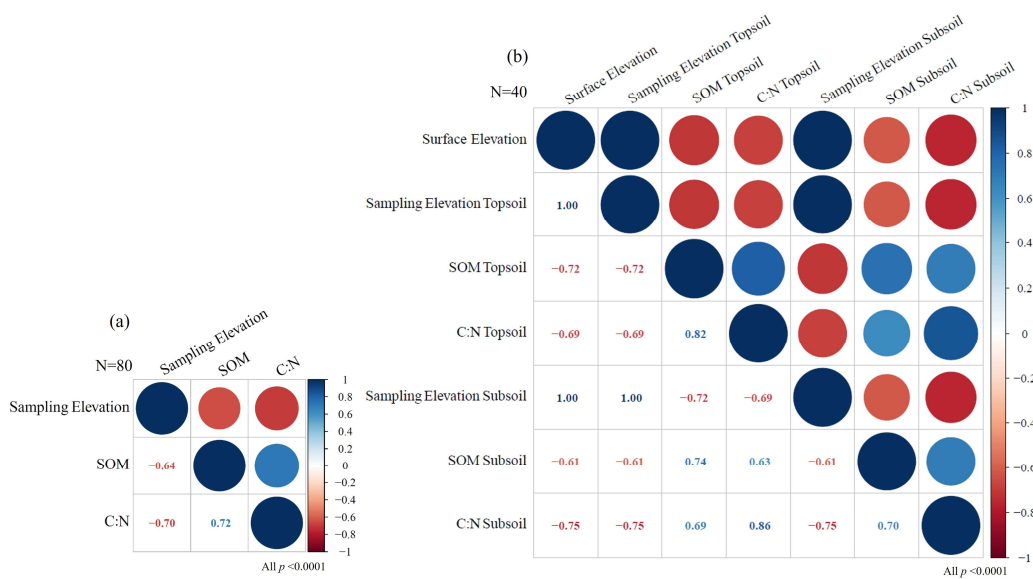
Figure S4.2 Pearson correlation coefficients among elevations, soil organic matter content (SOM) and carbon:nitrogen ratio (C:N) of disturbed soil samples; (a) N = 80 for all samples; (b) N = 40 for top and subsoil horizon.
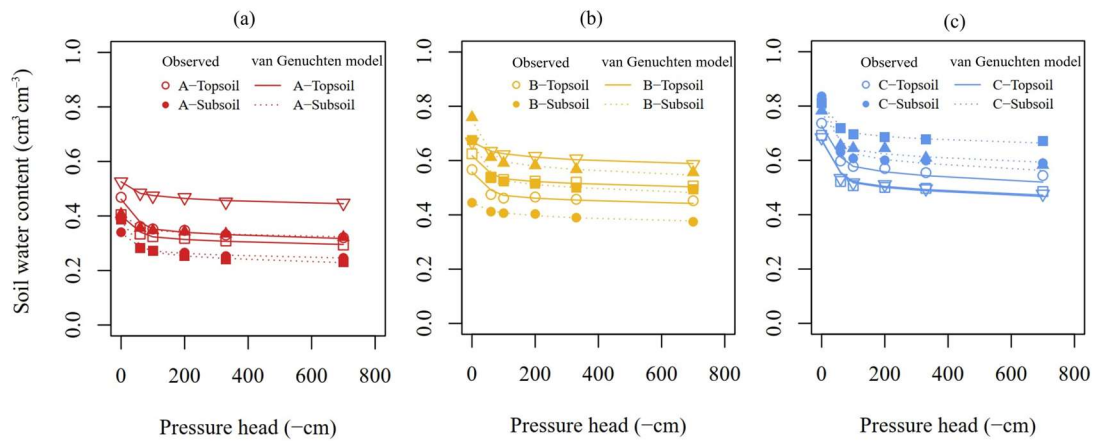
Figure S4.3 Soil water retention curves for eighteen undisturbed soil core samples from three different sampling elevation groups; (a) Group A; (b) Group B; (c) Group C.
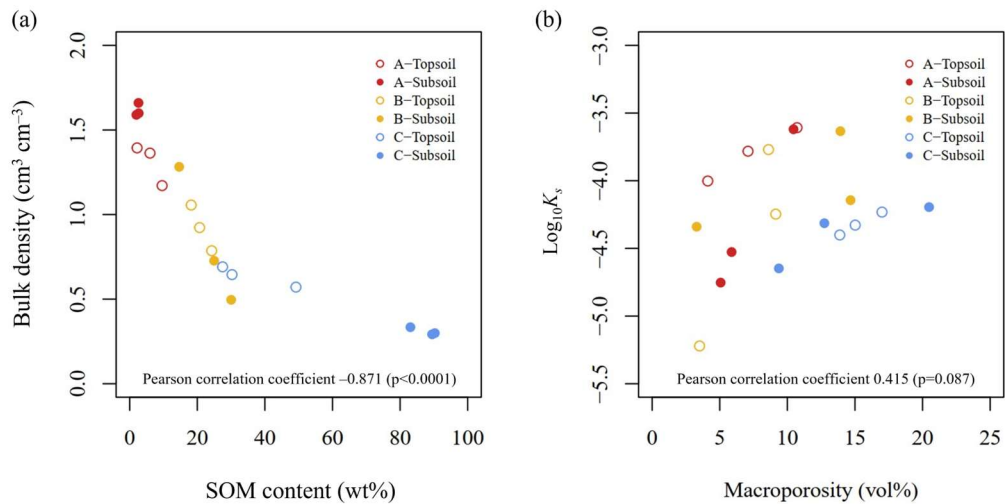
Figure S4.4 Correlation between (a) soil organic matter (SOM) content (wt%) and bulk density (g cm^{-3}); (b) macroporosity (vol%) and log-transformed saturated hydraulic conductivity (Log$_{10}K_s$).

135
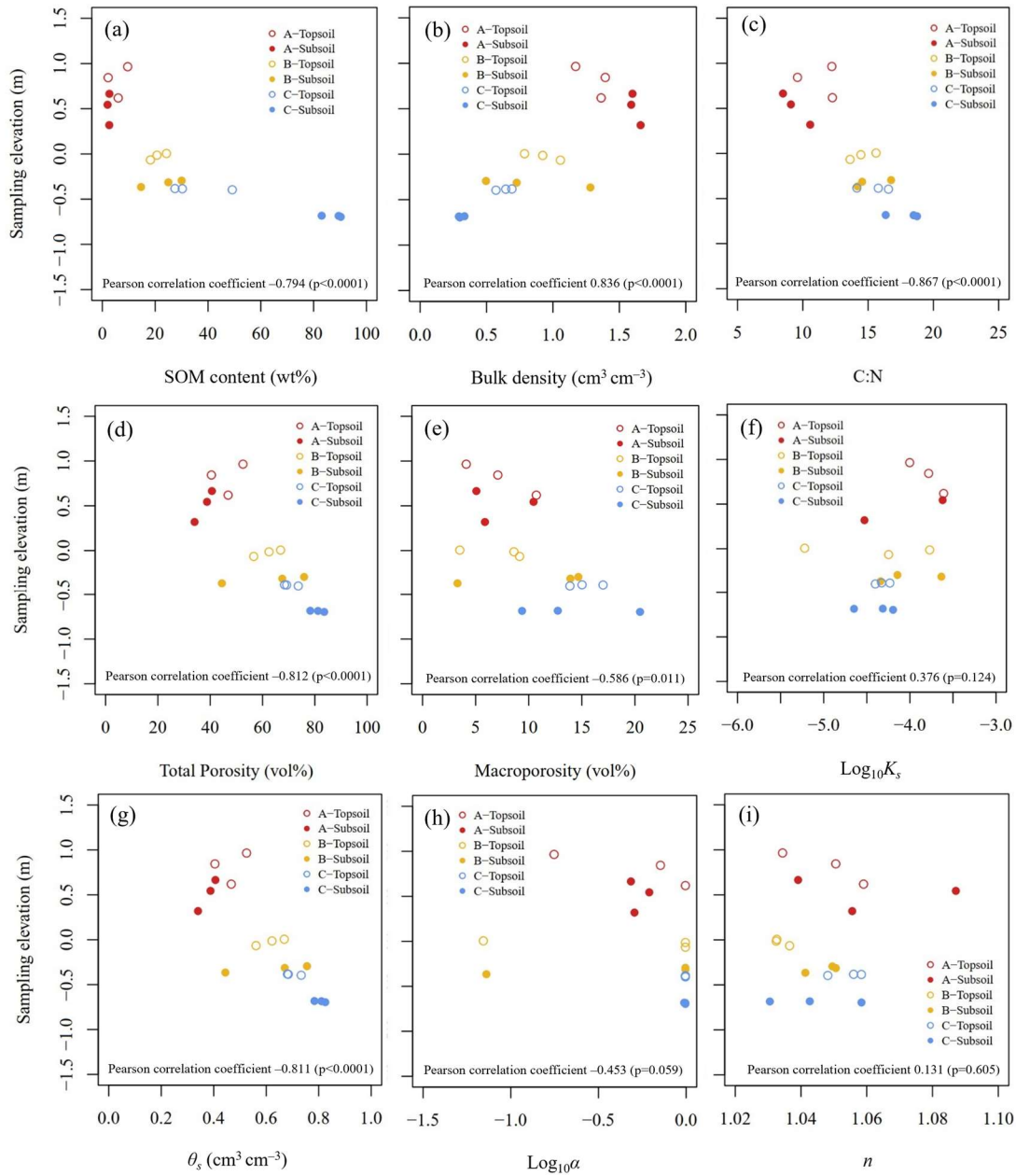
Figure S4.5 Correlation between sampling elevation and selected soil hydro-physical properties (N = 18); (a) soil organic matter content (SOM, wt%); (b) bulk density; (c) carbon:nitrogen ratio (C:N); (d) total porosity (vol%); (e) macroporosity (vol%); (f) log-transformed saturated hydraulic conductivity (Log$_{10}K_s$); (g) van Genuchten (VG) model parameter θ_s; (h) log-transformed VG model parameter α; (i) VG model parameter n.
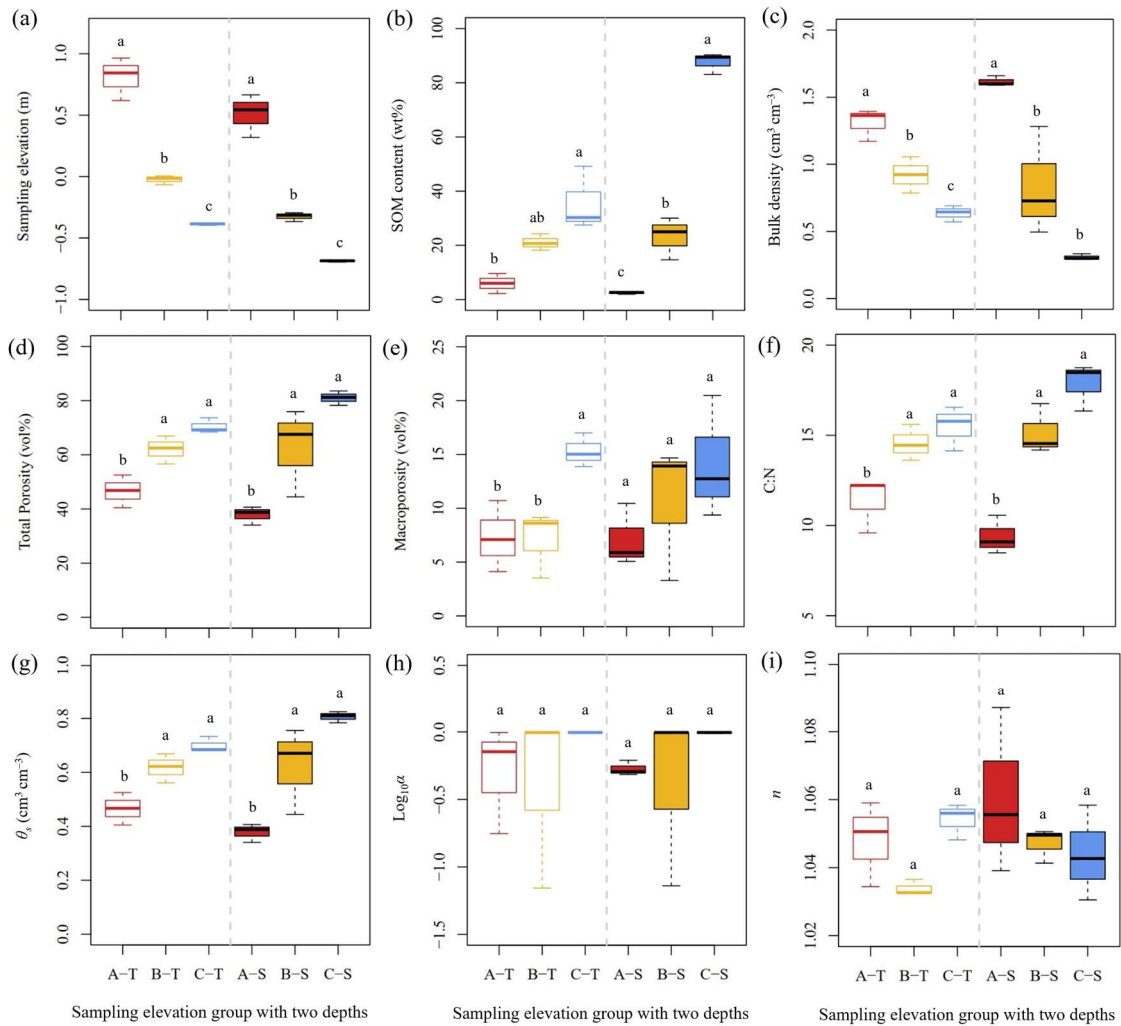
Figure S4.6 ANOVA tests of selected soil hydro-physical properties between different elevation groups at two sampling horizons (N = 3); (a) sampling elevation (m); (b) soil organic matter content (SOM, wt%); (c) bulk density; (d) total porosity (vol%); (e) macroporosity (vol%);(f) carbon:nitrogen ratio (C:N); (g) van Genuchten (VG) model parameter θ_s; (h) log-transformed VG model parameter α; (i) VG model parameter n.
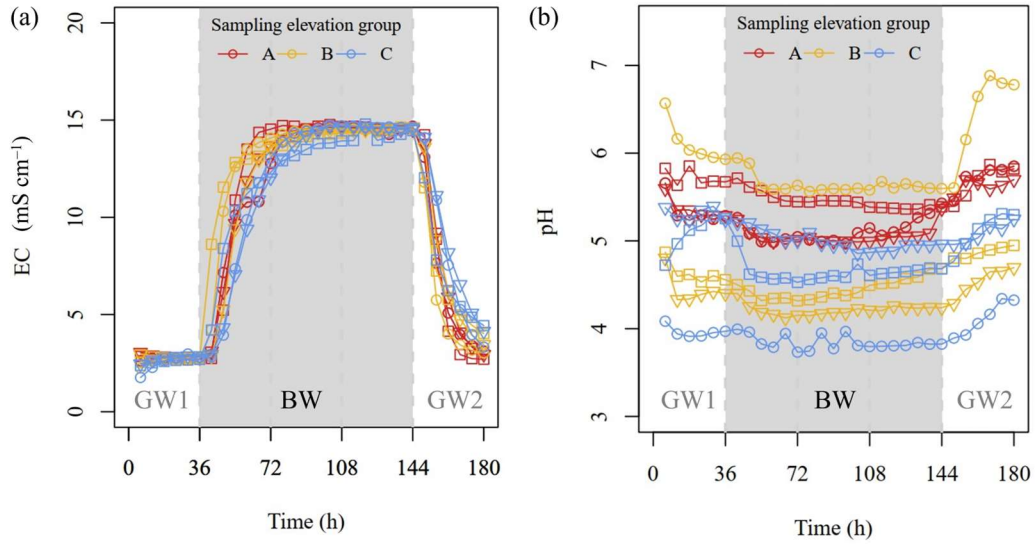
Figure S4.7 Variation of (a) electrical conductivity (EC); (b) pH over time during alternating freshwater and brackish water. (same GW solution was used for GW1 and GW2 time phases).
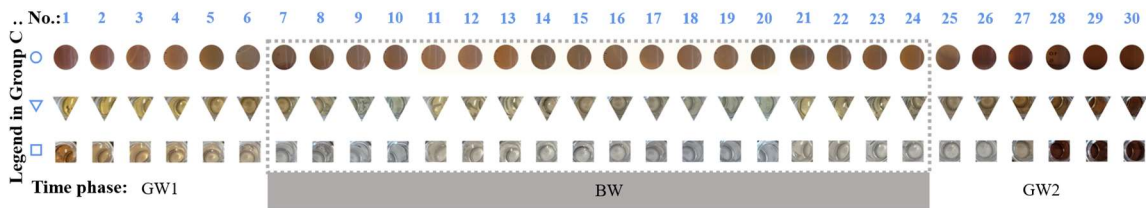
Figure S4.8 Visualization of leachate color of samples from sampling elevation group C.
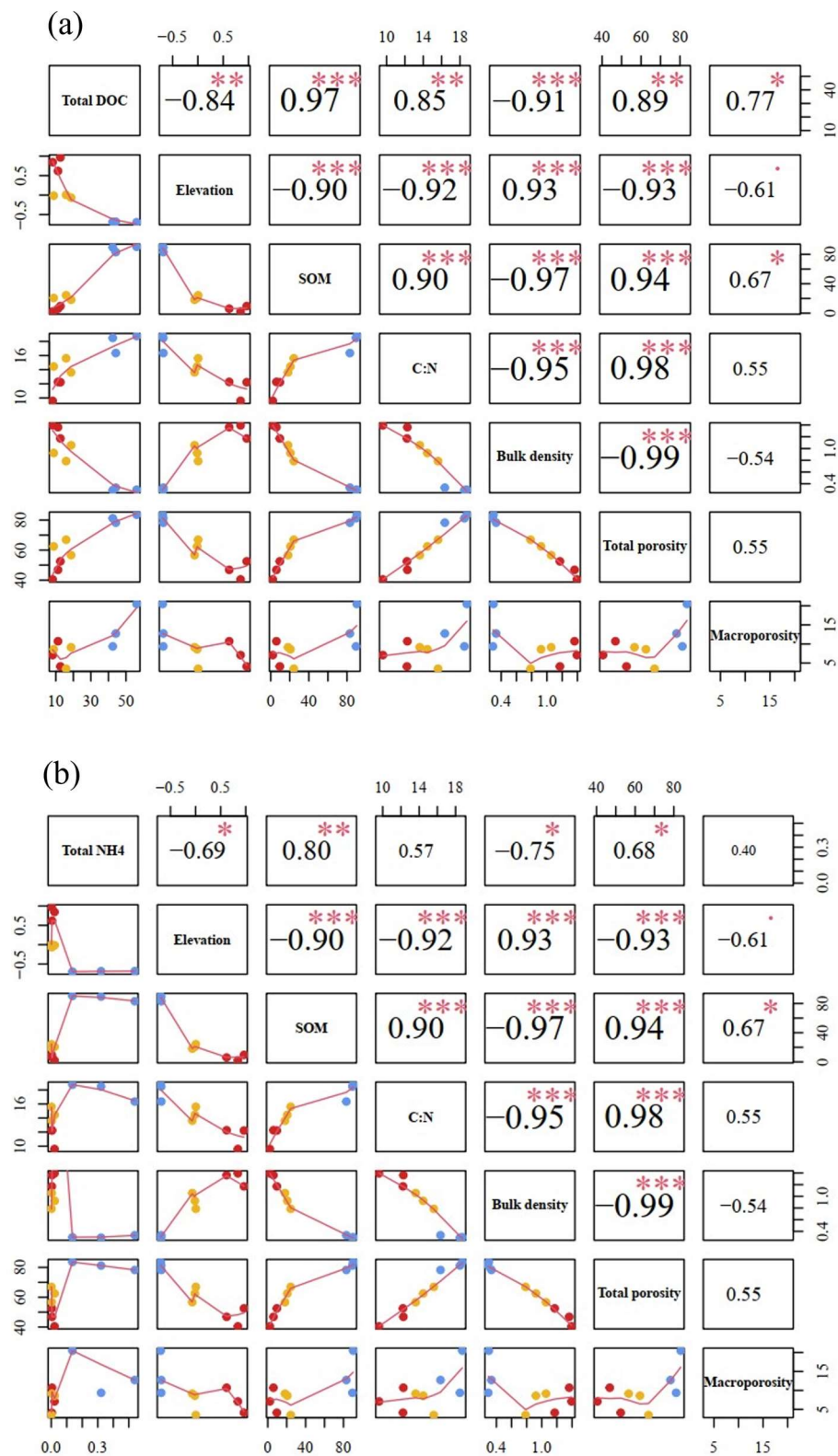
Figure S4.9 Pearson correlation coefficient among total amount of released nutrient and selected soil properties; (a) the total amount of DOC; (b) the total amount of NH_4^+. (significance codes: <0.001, "***"; <0.01, "**"; <0.05, "*"; <0.1, ".").

Table S4.1 Summary of van Genuchten (VG) model parameters of undisturbed soil core samples.

Elevation group	Soil horizon	No.	θ_s (cm³ cm⁻³)	α	n	R^2	SSD[b]
A	Topsoil	1	0.467	0.990	1.059	0.994	8.64E–05
		2	0.405	0.713	1.051	0.998	1.86E–05
		3	0.525	0.176	1.034	0.988	4.89E–05
	Subsoil	1	0.340	0.507	1.056	0.997	1.86E–05
		2	0.388	0.616	1.087	0.999	1.15E–05
		3	0.407	0.484	1.039	0.997	1.39E–05
B	Topsoil	1	0.561	0.990	1.037	0.959	3.86E–04
		2	0.622	0.990	1.032	0.988	1.11E–04
		3	0.669	0.070	1.033	0.989	4.32E–05
	Subsoil	1	0.444	0.073	1.041	0.978	6.07E–05
		2	0.671	0.990	1.051	0.985	3.39E–04
		3	0.755	0.990	1.050	0.991	2.45E–04
C	Topsoil	1	0.733	0.990	1.048	0.981	2.15E–03
		2	0.684	0.990	1.058	0.967	1.00E–03
		3	0.681	0.990	1.056	0.993	1.93E–04
	Subsoil	1	0.825	0.990	1.058	0.959	1.88E–03
		2	0.810	0.990	1.031	0.989	1.54E–04
		3	0.784	0.974	1.043	0.980	4.88E–04

[a] Abbreviations: θ_s, estimated water content at saturation (cm³ cm⁻³); α and n, empirical parameters.
[b] Abbreviations: R^2, the coefficient of determination; SSD, sum of the squared deviations.

Supplemental Materials to Chapter 5

Figure S5.1 The "wayback" images of the coastal study site visually presents the spatial changes over time. The figure was generated by using an ArcGIS license from the Technical University of Civil Engineering Bucharest (Prof. Ana Cornelia Badea, EU-CONEXUS PhD Campus) and produced from the website: https://livingatlas.arcgis.com/wayback/#active=57965&ext=13.22126,54.36619,13.26117,54.37899&s-lected=46399,32645&animationSpeed=1.5.
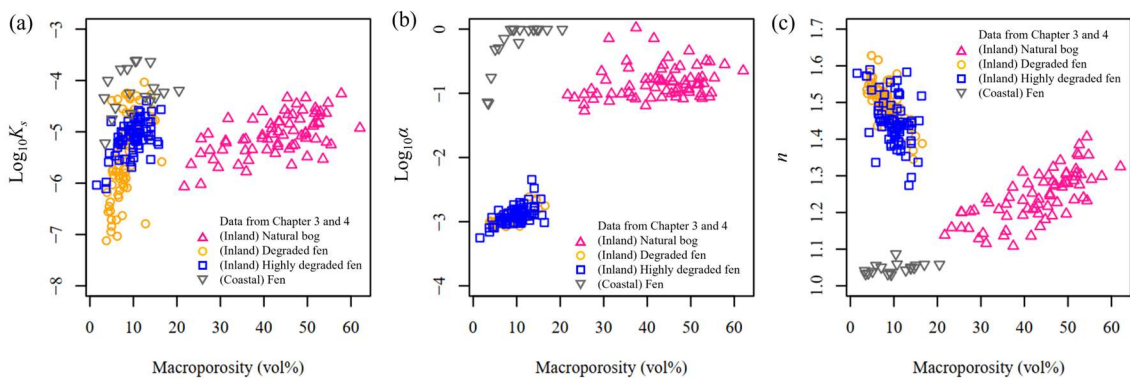
Figure S5.2 The relationship between (a) saturated hydraulic conductivity K_s ($\log_{10}K_s$) and macroporosity; (b) macroporosity and van Genuchten (VG) model parameter α ($\log_{10}\alpha$); (c) macroporosity and VG model parameter n of differently degraded peat (pink: inland natural bog; orange: inland degraded fen; blue: inland highly degraded fen; grey: coastal fen).
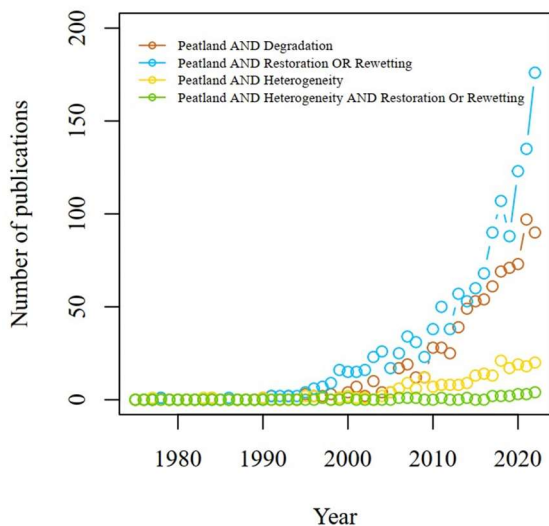
Figure S5.3 Numbers of publications per year found from a Web of Science database search combining the different search terms.
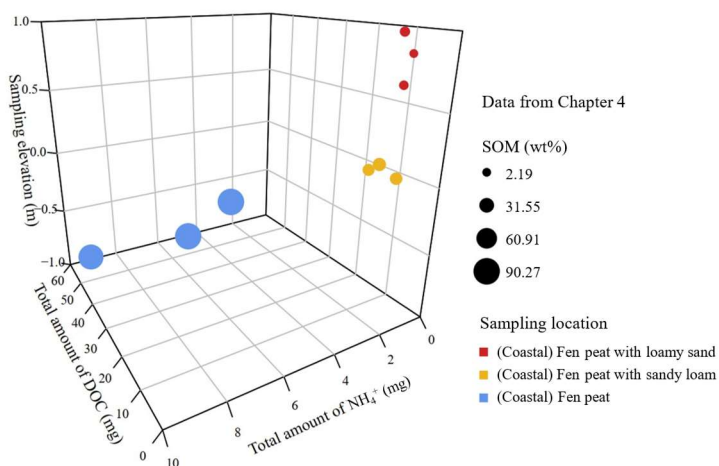
Figure S5.4 Total amount of compound release (DOC and NH_4^+) from samples with different soil organic matter content (SOM, wt%) during entire leaching phases. (data from Chapter 4).
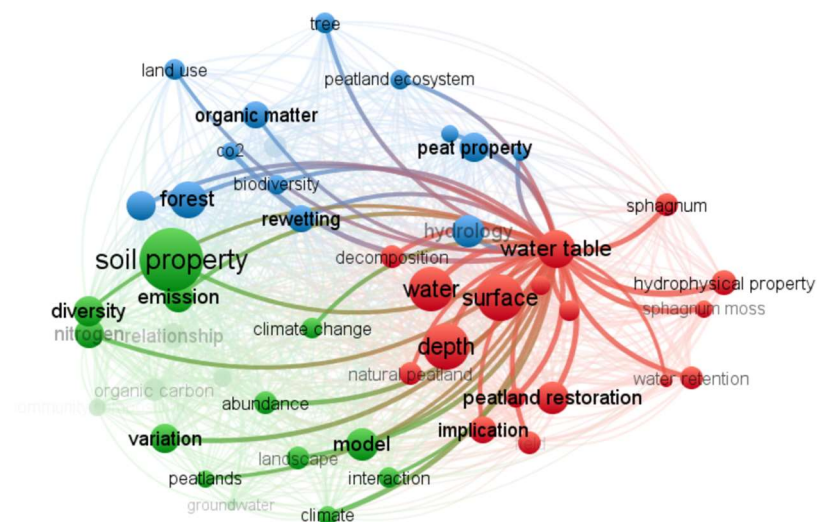
Figure S5.5 Network visualization from bibliometric analysis with highlighted keyword "water table".

Table S5.1 Summary of 3 clusters in bibliometric analysis that express different research focus in the "soil properties" and "peatland restoration/rewetting" themes.

Cluster	Items	Keywords[a]
Cluster 1	17	"decomposition", "depth", "field", "growth", "hydraulic conductivity", "hydrophysical property", "implication", "natural peatland", "northern peatland", "peatland restoration", "soil moisture", "sphagnum", "sphagnum moss", "surface", "water", "water retention", "water table"
Cluster 2	17	"abundance", "climate", "climate change", "community composition", "diversity", "emission", "groundwater", "interaction", "landscape", "model", "nitrogen", "organic carbon", "peatlands", "phosphorus", "relationship", "soil property", "variation"
Cluster 3	14	"biodiversity", "characteristic", "chemical property", "co2", "forest", "hydrology", "land use", "organic matter", "peat extraction", "peat property", "peatland ecosystem", "revegetation", "rewetting", "tree"

[a] The keywords are consistent with the presentation in the figure, all in lowercase letters and without any font formatting (such as italics, capitalization, or specific chemical nomenclature).

Acknowledgements

When I look back on the past few years, I feel a great deal of gratitude. Therefore, I would like to extend my sincere thanks to the following people and organizations that contributed to making this thesis possible:

Prof. Dr. Dominik Zak and Prof. Dr. Fereidoun Rezanezhad: for their valuable support in the publications.

Ms. Evelyn Bolzmann and Dr. Stefan Köhler: for their professional laboratory measurements.

Ms. Diana Werner and Mr. Matthias Naumann: for their kind assistance with technical measurements.

Dr. Lennart Gosch and Dr. Sate Ahmad: for their helpful discussions about the project's progress.

Team of Documentary Film "Maritimes Erbe: Die deutsche Ostseeküste" and the director Mr. Mathias Haentjes: for their professional and artistic documentation, which provided precious images of my fieldwork.

Graduiertenakademie and EU-CONEXUS: for their financial support enabling me to participate in numerous PhD courses.

DFG Ph.D. Training Program "BalticTRANSCOAST" and the project coordinator Dr. Martin Sperling: for their excellent organizational efforts that contributed to the success of our project.

Prof. Dr. Bärbel Gerowitt and Dr. Sabine Andert: for their encouragement and flexibility in accommodating my transition into a new role.

Last but certainly not least, I would like to thank all my dear friends from "BalticTRANSCOAST", Dr. Cheryl Batistel, Erwin Don Racasa, and Dr. Simeon Choo. Their support and encouragement throughout my study have been instrumental in my PhD journey. The power of friendship in scientific research has made me braver and stronger.

Above all, I would like to express my heartfelt appreciation to my parents, my parents-in-law, and my husband, Zekun Pi. Their boundless love and unwavering belief in me were the cornerstones of my success in completing this study.

Thank all supporters for their extraordinary effort during this global difficult time. Also, I would like to thank myself for embracing academia as an art and approaching it with passion and creativity. This journey has been immensely rewarding, enabling me to acquire valuable knowledge, enhance my skills, and experience remarkable personal growth. With these valuable experiences in scientific research, I will look positively into the future.

Scientific Curriculum Vitae

Personal Information

Surname, First Name:	Wang, Miaorun
Full Name in Chinese:	王苗润 (Wáng Miáo Rùn)
Gender:	Female
Date of Birth:	December 06, 1992
Place of Birth:	Luoyang City, Henan Province, P. R. China
Nationality:	Chinese
Marital Status:	Married, no children
Languages:	Chinese, English, German
Email:	miaorun.wang@uni-rostock.de; miaorunwang@gmail.com
RG profile:	https://www.researchgate.net/profile/Miaorun-Wang
ORCID:	https://orcid.org/0000-0002-1401-9920

Education and Research Experience

06/2023 onwards	Scientific Researcher	Crop Health, Faculty of Agricultural and Environmental Sciences, University of Rostock, Germany
	Project	"MAPS" (Landwirte-Netzwerk: Mehrjahres-Analyse der Pflanzenschutz-Strategien)
02/2019 – 12/2023	PhD Student	Faculty of Agricultural and Environmental Sciences, University of Rostock, Germany
	Major	Soil Physics
02/2019 – 08/2022	Scientific Researcher	Soil Physics, Faculty of Agricultural and Environmental Sciences, University of Rostock, Germany
	Project	DFG-Research Project "BalticTRANSCOAST"
04/2017 – 01/2019	Master	Faculty of Agricultural and Environmental Sciences, University of Rostock, Germany
	Major	Crop Production and Environment
02/2018 – 10/2018	Scientific Assistant	Faculty of Agricultural and Environmental Sciences, University of Rostock, Germany
	Project	ESF-Research Project "WETSCAPES"
11/2015 – 01/2016	Intern	Department of Coleoptera, Zoologisches Forschungsmuseum Alexander König, Germany
09/2011 – 06/2015	Bachelor	College of Plant Protection, Nanjing Agricultural University, China
	Major	Plant Protection

Research and Technical Skills

Text and images processing:	Microsoft Word │ Excel │ PowerPoint │ BI; CorelDRAW; LATEX(Overleaf)
Programming languages:	R (*e.g.*, dplyr, stats, lmerTest, tidyverse, ggplot2, scatterplot3d); SAS (*e.g.*, t-test, one-way ANOVA, correlation); Python (numpy, pandas, matplotlib)
Geo-statistics:	ArcGIS; QGIS; GS+
Others:	RETC (soil water retention modeling); STANMOD (solute transport modeling); VOSviewer (bibliometric analysis)

Academic Activities

<u>Conferences:</u>

04/2019 EGU General Assembly | Session HS10.8 -- Peatland Hydrology (PICO Presentation)
"Effect of anisotropy on solute transport in degraded fen peat soils"

09/2019 WETSCAPES Conference (Poster Presentation)
"Effect of anisotropy on solute transport and phosphate release in peatlands"

04/2020 EGU General Assembly | Session HS10.6 -- Peatland Hydrology (Virtual Poster Presentation)
"Small-scale spatial variability of hydraulic properties of degraded peatland"

04/2021 EGU General Assembly | Session HS10.8 -- Peatland Hydrology (Virtual PICO Presentation)
"Effect of macroporosity on physical property estimates for peat soils"

05/2021 16th International Peatland Congress (iPoster)
"Small-scale spatial variability of hydro-physical properties of natural and degraded peat soils"

12/2021 AGU Fall Meeting | Session B086 --
Wetlands and Peatlands in a Changing Climate: Science and Management (iPoster)
"Micro-topography effects on carbon accumulation and nutrient release from rewetted coastal wetlands"

<u>Workshops and Summer Schools:</u>

03/2019 HYDRUS short course
Czech University of Life Sciences Prague | Czech Republic

09/2019 Peatland research summer/autumn school
Hyytiälä Forestry Field Station | Finland

06/2020 Academic Writing
Graduate Academy | University of Rostock | Germany

08/2020 Publishing Journal Articles: Strategies for Success
Graduate Academy | University of Rostock | Germany

11/2020 NatureMasterclasses – Part 3: Writing and publishing a review paper
BalticTRANSCOAST (DFG) | University of Rostock & IOW | Germany

11/2020 Introduction to Python for Data Science
Graduate Academy | University of Rostock | Germany

08/2021 EU-CONEXUS -- 1st Online Research Summer Camp in Future Use and Protection of Coasts
University of Rostock | Germany

10/2021 Concept, Design and Presentation of Academic Posters
Graduate Academy | University of Rostock | Germany

06/2022 Einführung in die Statistik-Software R
Graduate Academy | University of Rostock | Germany

07/2022 EU-CONEXUS -- 2nd PhD Summer School in Open Science
Catholic University of Valencia | Spain

09/2022 Grundlagen der Betriebswirtschaft in Finanzen und Controlling für Wissenschaftler*innen
Graduate Academy | University of Rostock | Germany

05/2023 PhD Transversal and SmUCS -- Geographic Information Systems & Data Science Research Methods
EU-CONEXUS | Smart Campus

Peer-reviewed Journal Articles

<u>Publications for the thesis:</u>

1 Wang et al. (2020). Effect of anisotropy on solute transport in degraded fen peat soils. *Hydrological Processes*, 34(9). DOI: 10.1002/hyp.13717

2 Wang et al. (2021). Small-scale spatial variability of hydro-physical properties of natural and degraded peat soils. *Geoderma*, 399(04):115123. DOI: 10.1016/j.geoderma.2021.115123

3 Wang et al. (2023). The influence of microtopography on soil carbon accumulation and nutrient release from a rewetted coastal peatland. *Geoderma*, 438:116637. DOI: 10.1016/j.geoderma.2023.116637
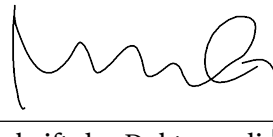
<u>Publication about another research:</u>

1 Yang et al. (2020). Effects of ocean acidification and microplastics on microflora community composition in the digestive tract of the thick shell mussel *Mytilus coruscus* through 16S RNA gene sequencing. *Bulletin of Environmental Contamination and Toxicology*, 107(13):1-10. DOI: 10.1007/s00128-020-03022-5

Eidesstattliche Erklärung

Hiermit bestätige ich, dass ich die vorliegende Arbeit selbstständig verfasst und keine anderen als die angegebenen Hilfsmittel benutzt habe. Die Stelle der Arbeit, die dem Wortlaut oder dem Sinn nach anderen Werken entnommen sind, wurden unter Angabe der Quelle kenntlich gemacht. Die Dissertation ist in dieser Form noch keiner anderen Prüfungsbehörde vorgelegt worden.

Rostock, 23.12.2023

_____

Ort, Datum

_____

Unterschrift der Doktorandin/des Doktoranden